Dynamique de la méthylation d'ADN et sa caractérisation fonctionnelle durant les phases précoces de la tumorigénèse intestinale

Marco Bruschi

Collège Doctoral Languedoc-Roussillon

Délivré par

THÈSE

Pour obtenir le grade de Docteur

l'Université de Montpellier

Préparée au sein de l'école doctorale CBS2
Et de l'unité de recherche UMR5203-U1191-UM

Spécialité : BIOLOGIE SANTE

Présentée par Marco BRUSCHI

DNA METHYLATION DYNAMICS AND ITS FUNCTIONAL IMPACT DURING THE EARLY STAGES OF INTESTINAL TUMORIGENESIS

Soutenue le 04 Novembre 2016 devant le jury composé de

Mme Florence CAMMAS, CR1, IRCM	Examinateur
M Pierre CORDELIER, DR2, CRCT Toulouse	Rapporteur
Mme Silvia FRE, CR1, Institut Curie, Paris	Rapporteur
M Philippe JAY, DR2, IGF	Directeur de thèse

UNIVERSITÉ MONTPELLIER

It is not knowledge, but the act of learning, not possession but the act of getting there, which grants the greatest enjoyment. When I have clarified and exhausted a subject, then I turn away from it, in order to go into darkness again; the never-satisfied man is so strange: if he has completed a structure, then it is not in order to dwell in it peacefully, but in order to begin another. I imagine the world conqueror must feel thus, who, after one kingdom is scarcely conquered, stretches out his arms for others.

C.F. Gauss

Take a sad song and make it better !

The Beatles

REMERCIEMENTS/AKNOWLEDGMENTS/RINGRAZIAMENTI

Ce travail a été réalisé au sein de l'équipe « auto-renouvellement et différenciation des epithélia », dans le département de biologie du cancer de l'institut de génomique fonctionnelle.

Je tiens à remercier mon directeur de thèse, Philippe, pour m'avoir confié des projets ambitieux et m'avoir permis de développer mes intérêts de manière autonome, tout en gardant la porte de ton bureau toujours ouverte à des nouvelles discussions. J'ai beaucoup appris de toi, de ta façon de voir le scientifique comme un vrai explorateur. J'ai surtout appris que la bonne science est fille des bonnes questions, qu'il ne faut jamais avoir peur de se poser.

Je souhaite apporter un grand remerciement aux docteurs Pierre Cordelier et Florence Cammas, pour avoir accepté de suivre mon travail tout au long de ces 4 ans en faisant partie de mon comité de thèse et de mon jury, tout aussi bien comme le docteur Silvia Fre ayant accepté d'être rapportrice de cette thèse.

Je remercie toutes les personnes qui ont fait partie de l'équipe depuis mon arrivée. François, qui a été pour moi un exemple de pragmatisme scientifique, mais aussi quelqu'un avec qui discuter de foot pendant les pauses café. Catherine Legreverand, pour avoir été une figure bienveillante pendant les premières phases de ma thèse, mais aussi pour sa rigueur et sa bonne humeur. Salima, la première des collègues à avoir aussi été une amie. Stanislas, qui a conçu et commencé le projet susceptibilité épigénétique. Pierre, un chapitre de cette thèse ne suffirait pas pour raconter ce que nous avons partagé pendant ces 4 ans, ni pour te remercier assez. Si je partirai de l'IGF en parlant 3 mots de français ce sera surtout grâce à toi, mais je te dois beaucoup plus que cela et je suis ravi d'avoir partagé ce bureau avec toi. Manue, amie bien avant que collègue, ne t'inquiète pas : tu vas devoir me supporter bien au-delà de la fin de mon parcours à l'IGF. Laure, Pistache, Stachepie, ton arrivée dans l'équipe a été pire qu'une bourrasque, et je ne peux que te remercier de l'énergie, de ta bonne humeur et de l'énorme apport que tu as donné à ce travail. Nathalie, toujours à l'écoute, je me fais ici un pense-bête pour te souhaiter bon anniversaire le jour de la soutenance. Laetitia, la super-stagiaire qui m'a initié aux secrets du microtome (qui pourtant reste toujours un objet assez mystérieux pour moi). Miloud, pour tes magnifiques ISH mais surtout pour ta curiosité vivace que j'ai beaucoup apprécié. Sarah, pour avoir fortement voulu travailler sur ce projet et avoir contribué

aux résultats. Tous les autres stagiaires que j'ai vu passer dans l'équipe: Amandine, Alison, Greg, Remy.
Les collaborateurs pour leur investissement et leur disponibilité: Michael Helmrath et Max Mahe, pour avoir rendu possible la chirurgie qui nous a compliqué la vie pendant deux ans (n'est-ce pas Pierre ?), et Michael Weber pour les analyses RRBS et les conseils techniques.
Je tiens à remercier l'ensemble de l'IGF, en commençant par son Directeur, Jean-Philippe Pin, pour son investissement pour le bien-être collectif et surtout des jeunes chercheurs comme nous. Anne Chabannes et Carmen pour la disponibilité et pour leur travail pour le fonctionnement de l'Institut, et Catherine Augé, pour l'aide quotidienne dans les démarches administratives.
Tous les chercheurs avec qui j'ai eu l'occasion d'interagir et discuter, et qui ont contribué à ma formation, surtout ceux qui font partie du département cancer biology, parmi lesquels je tiens à remercier Julie Pannequin, Tristan Bouschet, Laurent Journot, Anne Le Digarcher, Annie Varrault, Fred Bienvenu, Alexandre David, Jean-Marc Pascussi, Chris Planque, Françoise Macari, Armelle Chouquet entre autres, qui ont tous répondu plusieurs fois à mes questions.
Tous les doctorants que j'ai rencontré à l'Institut pendant ces 4 ans, parmi lesquels je dois citer Leila, Hélène, Julie, Laura (source constante de bruit dans notre couloir, mais aussi la maman qui m'a souvent écouté râler et sauvé plusieurs fois quand j'avais oublié de préparer à manger pour le midi), Fanny, et ceux qui font partie de l'asso SPIN pour la belle réussite dans l'animation de la vie à l'Institut.
Toutes les personnes qui travaillent dans les services communs et qui ont toujours montré une grande disponibilité. Parmi ces personnes je dois remercier de manière spéciale Céline Garnier et Jacqueline Siméoni, qui ont été adorables avec moi bien avant que j'apprenne leur langue pour pouvoir les remercier comme il faut.
Toutes les personnes qui travaillent à l'animalerie IGH/IGF pour leur gentillesse et leur disponibilité envers moi (voir les sorties d'animaux toujours à la dernière minute), parmi lesquelles je dois un très grand merci à Fred Gallardo pour son aide et sa professionnalité, Luc Forichon, Denis Greuet et Elodie Gavois… Et merci Ségolène Debiesse pour les milliers de génotypes !
Les doctorants de l'asso CBS2, qui a représenté pour moi une très belle expérience pendant mes trois premières années de thèse.

Amélie Sarrizin de la plateforme MRI, pour m'avoir formé au moins 5 fois à la cytométrie de base, Christophe Duperray et Emilie Dufourq pour la compétence et la bonne humeur que j'ai connu et apprecié dans les interminables après-midi au FACS.
Et bien sûr je vais remercier tous les copains que je me suis fait à Montpellier pour les bons souvenirs, les soirées, les sorties, les voyages : Pedro, le tout premier copain à l'IGF, je n'ai pas oublié la première fois où on s'est parlé comme si on se connaissait depuis des années. Laura Sgnappi Ceola, la grande sœur dont j'avais besoin ici. Manue, Laura Y., Filippo, Serena Capozi (mental coach), Mattia (alèalèalè oh !), Gaspard, Serena Vegna, Geoffrey, Max, Nico de Laura, Peppe, Etienne, Nico Romanò, Sophie, Nico de Sophie, Teresita, Ivana, Ségolène, Benjamin, Karsten, Romain, Simona, Andrés, Marianne, Girish.
Les amis plus loins (mais seulement géographiquement parlant): Enrica Montalban (i 6 kilometri a piedi che m'hai fatto fare alle 3 di notte a Parigi la prima volta ancora non me li sono scordati), Claudia, Francesco, Giulia, Ylenia, Glauco, Caterina, Stefano, Luca, Marco, Marcolino: la distanza è un'invenzione…
Saint-Gély-du-Fesc et place de la Comedie, pour les promesses de 4h qui m'ont tenu et me tiennent éveillé bien plus tard que 4h.

Pour finir, je veux surtout remercier ma famille, sans laquelle rien de tout ce que je viens d'écrire n'aurait pu être possible. Aucune distance ne me fera oublier l'arbre duquel je suis tombé. Tutto ciò che ho avuto e avrò lo devo solo a voi: grazie!

SUMMARY

INTRODUCTION

1. General anatomy of the intestine and functions of the intestinal epithelium

The mammalian intestine is organized into two anatomical portions sharing the same basic structure but accounting for different functions: the small and the large intestine (or colon). Both of these portions are organized in multiple layers of tissues consisting in an external smooth muscle layer (muscularis externa) responsible for peristaltism, a dense irregular connective tissue (submucosa), a thin lamina of muscle outside the lamina propria and a an internal mucosa constituted by a lose cell-rich connective tissue accounting for myofibroblast, lymphocites, plasma cells, mast cells and macrophages and rich in capillaries (Slomianka and Lutz, 2009). The inner mucosal surface of the intestine is covered by a monolayer of different epithelial cells representing the largest surface of interaction of the organism with the external world (about 250m^2 in humans) and which is constantly renewed by the stem and proliferative compartment. Newborn cells are incessantly generated by cell division in the proliferative compartment and migrate upward to differentiate and eventually die by anoikis before they are shed into the intestinal lumen. The homeostatic self-renewal is accomplished within 3 to 5 days. The intestinal epithelia exert at least 4 main functions:

- Absorption: after the initial degradation in the stomach, the chow enters the luminal flow through the pyloric valve and is forced in its progression toward the distal intestine by the peristaltic contractions. All along the small intestine the content is continuously degraded by the populations of commensal bacteria hosted in the lumen (microflora or microbiota), and is then absorbed by the epithelial cells. The molecules that are absorbed are then distributed to the whole body by the blood supply.
- Endocrine function: the epithelial layer accounts for a specialized cell type (enteroendocrine cells) responsible for the secretion of hormones in the blood such as the serotonine, the glucagon-like peptide (GLP), the gastric-inhibitory peptide (GIP), that regulate the secretion of insulin and the digestion.
- The barrier function: the intestinal epithelium constitutes a physical barrier allowing the selective entry of small molecules in the blood. The epithelial cells are connected by different type of junctions: tight junctions, adherent junctions, GAP junctions and desmosomes allowing cell-to-cell adhesion, communication and

selective permeability (figure 1). This selective filter can be modulated by signaling molecules that can alter the organization of the junctions (Tsukita, Furuse, and Itoh 2001). A supplemental physical layer is represented by the mucus secreted by specialized cells (goblet cells) and is constituted by mucines, polysaccharides and antimicrobial peptides having the role of embedding trillions of bacteria and pathogens impeding their contact with epithelial cells. The mucus also contains secreted antimicrobial molecules such as the resistin-like molecules (RELM) and antibodies like the Immunoglobulin-A. The density, composition and bacterial load of the mucus varies along the intestinal portions and its elimination and renewal is permitted by the peristaltic contractions of the intestine.

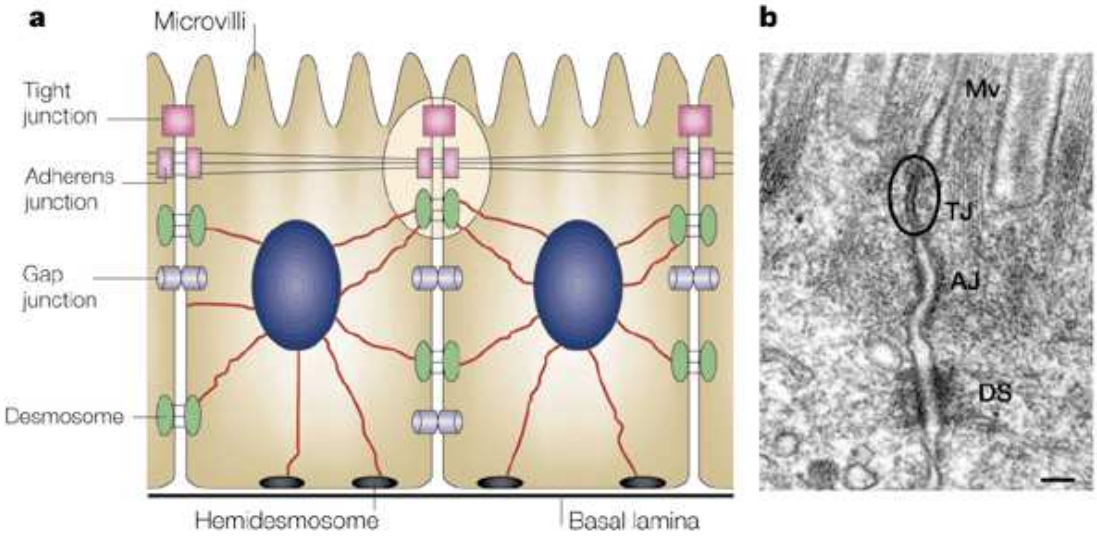

Figure 1: A) Schematic illustration of epithelial cell-cell junctions. B) Electon micrograph of the junctional complex of mouse intestinal epithelia (Mv: microvilli; TJ: tight junction; AJ: adherens junction; DS: desmosomes). Adapted from Tsukita, Furuse, and Itoh 2001.

- Immune function: as mentioned, the intestine represents the largest surface of contact with the external world represented by the luminal content. The intestinal mucosa constantly interacts with trillions of commensal microorganisms and is periodically challenged by the presence of different pathogens. Several immune mechanisms participate to protect the host from the infection with enteric bacteria and shape the composition of the commensal microbiota(figure 2) (Perez-Lopez et al. 2016). The sensing of pathogens associated molecular patterns (PAMPs) occur via different classes of pattern recognition receptors (PRRs) expressed at the

membrane or in the intracellular compartments of epithelial cells (Akira et al., 2006). Toll like receptors (TLRs) and NOD-like receptors (NLRs) can sense the microorganisms and trigger downstream signaling pathways leading to the activation of mechanisms of innate and adaptive immune response (Zheng et al. 2008; Behnsen et al. 2014). Pathogen recognition leads to the production of pro-inflammatory cytokines that can induce activation of the IL23-Th17 immune cell axis and the secretion of antimicrobial proteins and defensins (Zheng et al. 2008; Behnsen et al. 2014). In addition, activation of the mucosal adaptive immunity involves the production of specific antibodies like immunoglobulin A (IgA), which is an antibody class unique to the mucosa and produced by the plasma B-cells residing in the lamina propria (Cerutti and Rescigno 2008; McPherson et al. 2008). These mechanisms also control the normal composition of the intestinal commensal microbiota which, in turn, participates to the protection to infection with pathogens, both directly through the competition for nutrients and indirectly through the modulation of mucosal immunity.

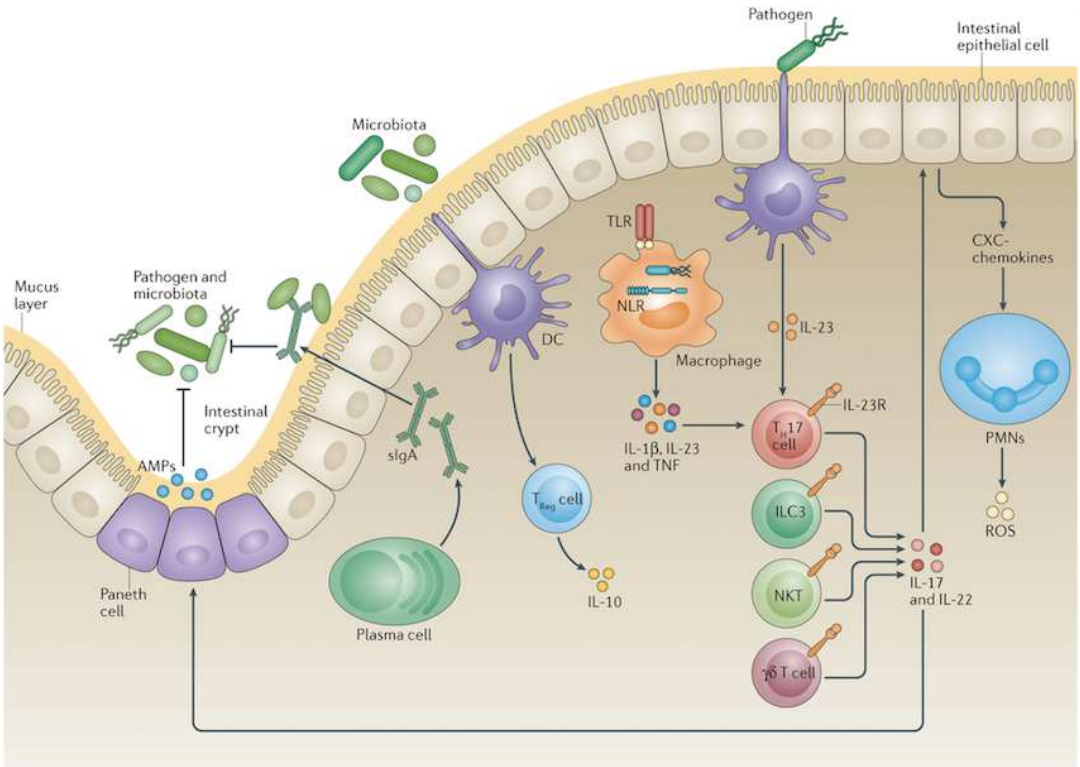

Figure 2: schematic illustration of the major mechanisms involved in the sensing of pathogen and microbiota and immune response. Dendritic cells (DC) sample the intestinal content and induce the activation of regulatory T (T_{reg}) cells to produce IL10 and stimulate the activity of several other cell types like T_h17, ILC3, NK and γδ cells. Plasma cells contribute in controlling the intestinal flora by producing

secretory IgA. IL17 and IL22 induce the production of antimicrobial peptides (AMP) secreted by Paneth cells. (IL23-R: IL23 receptor; NLRs: NOD-like receptors; PMSs: polymorphonuclear cells; ROS: reactive oxygen species; TLR: toll-like receptors; TNF: tumor necrosis factor). Figure adapted from Perez-Lopez et al., 2016.

1.1. The small intestine

The epithelium in the portion of the intestine located between the stomach and the cecum (i.e. the small intestine) is organized in two different compartments that constitute the crypt-villus unit (figure 3). Villi are finger-like protrusions that project into the lumen to increase the surface of absorption and are covered by a monolayer of post-mitotic epithelial cells. The apical (luminal) surface of each epithelial cell is covered by protrusions, the microvilli, which serve to further increase the luminal epithelial surface. Lymph vessels and capillaries located in the lamina propria of each villus mediate the transport of absorbed nutrients to the whole body. Each villus is surrounded at its base by multiple epithelial invaginations, the crypts of Lieberkühn that constitute the proliferative compartment of intestinal epithelia. Multiple intestinal stem cells are located at the very bottom of each crypt where they are intermingled between terminally differentiated Paneth cells. The intestinal epithelium accounts for 6 differentiated cell types with absorptive or secretory functions: enterocytes, goblet cells, enteroendocrine cells, Paneth cells, tuft cells and M-cells (figure 4) (van der Flier and Clevers 2009). The genetic interactions driving the specification and the functions of these lineages are further described later in the text.

Follicular structures named Peyer's patches are found in the small intestine, which are found at higher density in the distal small intestine. These structures are rich in B and T-lymphocytes and are lined by a simple monolayer of epithelial cells containing specialized M-cells.

The absorption of nutrients, vitamins and ions occurs in the small intestine that can be anatomically divided in 3 portions: the duodenum, the jejunum and the ileum. The duodenum represents the most proximal and the shortest portion of the small intestine starting at the exit of the pyloric valve of the stomach, and in anatomical contact with the pancreas. In this portion the lenght of villi is maximal, providing the largest surface of absorption. Absorptive cells in this portion express the proteins forming the channels for the absorption of iron. The jejunum represent the medial portion of the intestine, followed by the ileum which is characterized by shorter villi and smaller proliferative compartment in which, however, the Paneth cells are more abundant.

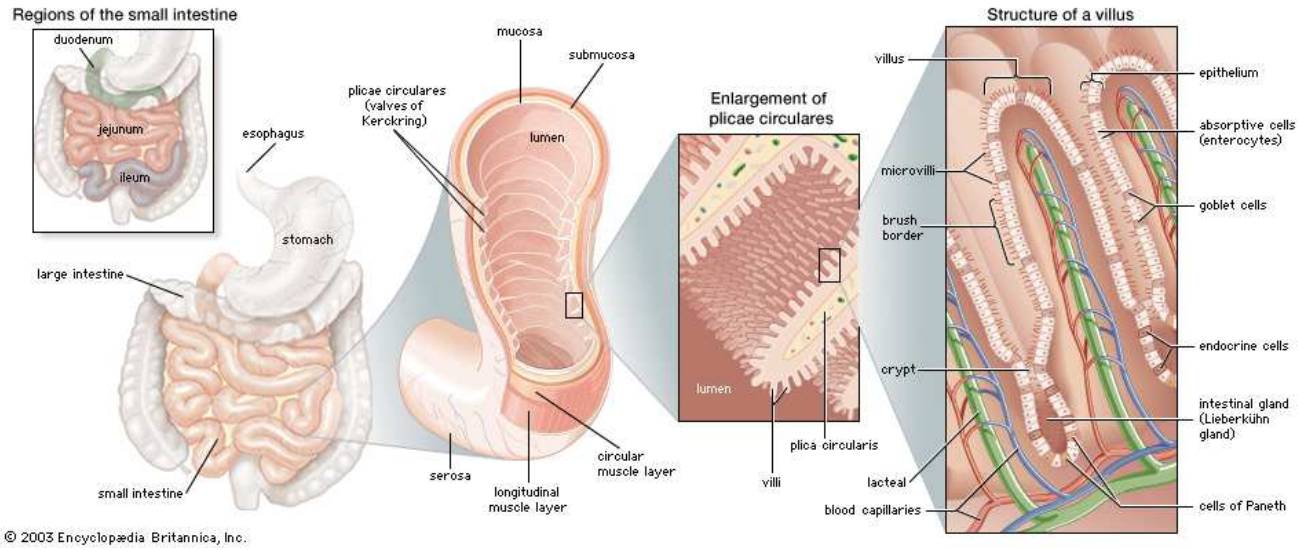

Figure 3: illustration of the human small intestinal regions and architecture. (Encyclopaedia Britannica, 2003)

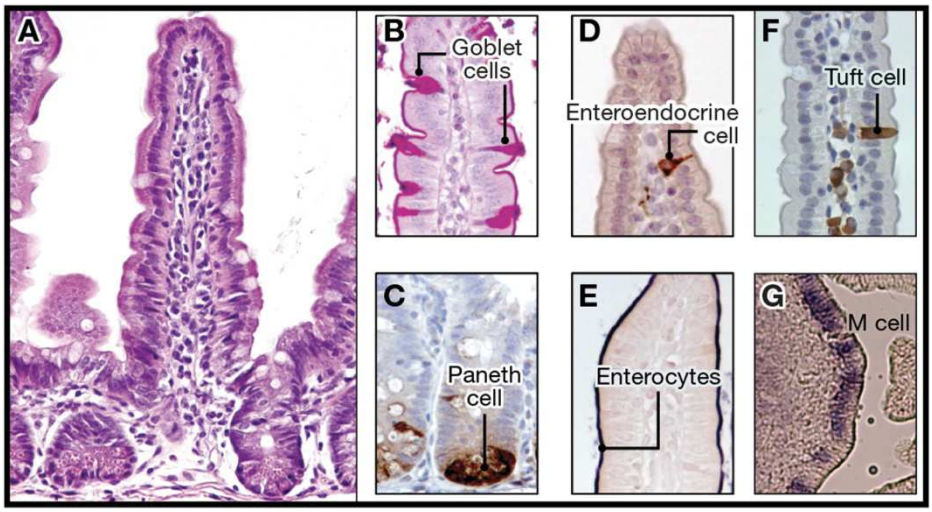

Figure 4 : intestinal epithelial cells types. A) crypt-villus axis visualized via hematoxylin-eosin staining. B) Goblet cells by PAS staining. C) Paneth cells revealed by lyzozyme immunostaining. D) Enteroendocrine cells revealed by Chromogranin A immunostaining. G) Enterocytes revealed by F) Tuft cells expressing the DCLK1 marker. G) M-cells expressing Spi-B. Picture from H. Clevers, 2013.

1.2. The large intestine

The large intestine, or colon, represents the portion of the intestine located between the cecum and the rectum (figure 5). The human colon accounts for different anatomical portions. The epithelium is organized in crypts, resembling to those found in the small intestine and

accounting for the proliferative cells but they lack Paneth cells. Villi are replaced by a flat epithelial layer, mainly constituted by colonocytes. The flow of the intestinal content is accompanied by the absorption of water and sodium.

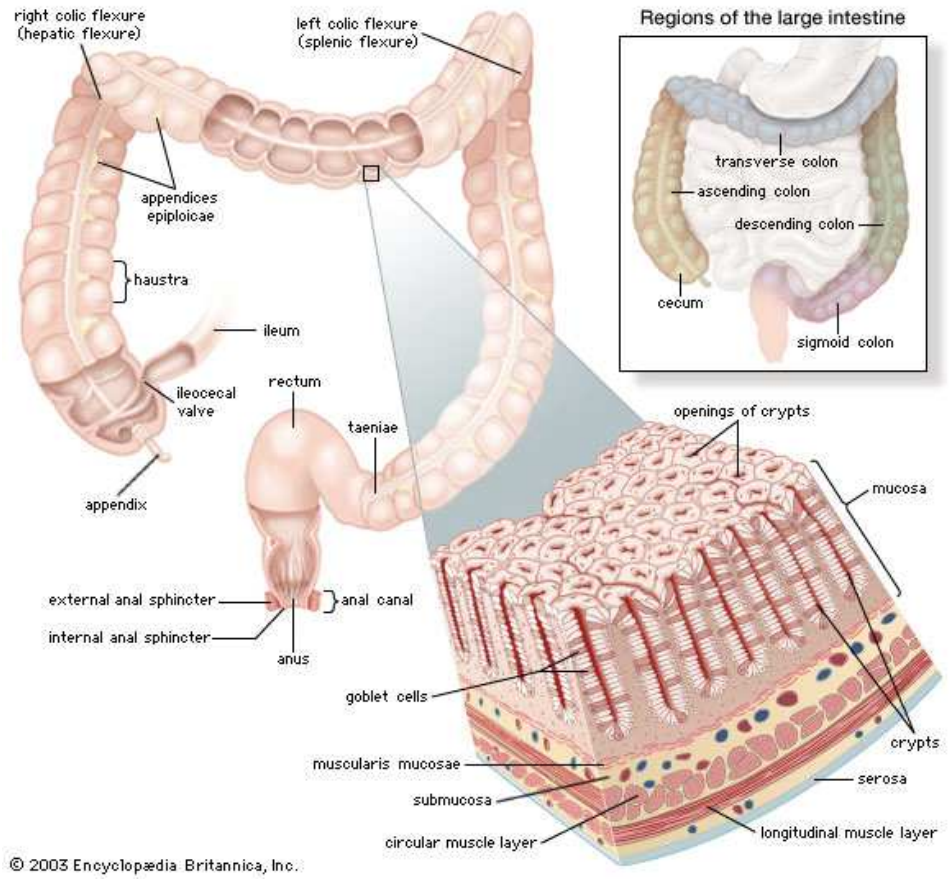

Figure 5: illustration of the architecture of the human large intestine (colon). (Encyclopaedia Britannica, 2003)

1.3. Epithelial lineages: specification and functions

The intestinal epithelium accounts for six differentiated lineages whose functional identity is either absorptive (enterocytes) or secretory (goblets cells, Paneth cells, enteroendocrine cells, tuft cells and M-cells) (figure 6). The intestinal stem cell compartment lying at the bottom of the crypt represents the common origin of all these lineages (H. Clevers 2013). Epithelial cell fates are commonly believed to be set just above the stem cell compartment at the position +5 in the crypt, which is considered as the origin of differentiation of the progenitors representing the immediate progeny of intestinal stem cells. The molecular circuit governing the choice between absorptive and secretory fate consists in the relatively simple genetic interaction

between two helix-loop-helix transcription factors: Math1 and Hes1. *Math1* represents the master gene responsible for the secretory fate decision. Its deletion results in the complete loss of all secretory cell types, whereas its overexpression can force progenitors into a secretory fate (Yang et al. 2001; Shroyer et al. 2007; VanDussen and Samuelson 2010). The expression of *Math1* is negatively regulated by Hes1, a transcriptional target of the Notch signaling pathway in epithelial cells. The deletion of *Hes1* leads to the depletion of enterocytes and increased number of secretory cells (Jensen et al. 2000). Downstream to this genetic interaction, specific transcription factors (or combinations of these) are responsible for the differentiation of each specialized cell type.

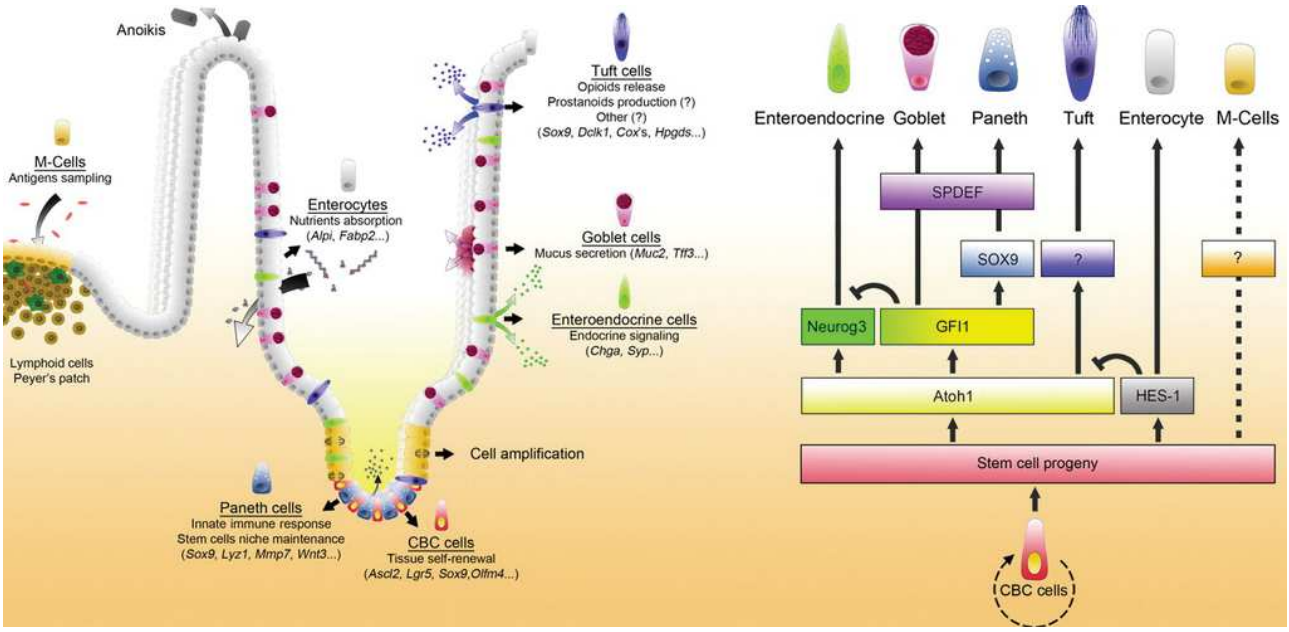

Figure 6: epithelial specification and function. Left: schematic representation of the different epithelial cell types according to their position in the crypt-villus axis. Right: Molecular program driving the specification of the different mature cell types.

1.3.1. The Intestinal stem cell compartment

The intestinal epithelium is completely renewed every 3-5 days throughout the entire lifetime. This outstanding capacity is conferred by the proliferating crypts representing the real engine of the epithelial self-renewal process, as Stevens and Leblond showed in the landmark study they published in 1947 (Leblond and Stevens 1948). This work showed for the first time that the life span of most cells in the intestinal epithelium is in the order of days, and the high rate of production of newborn cells is continuously balanced by the elimination of cells that migrate upward from the crypt, before they are ejected as soon as they reach the tip of the

villus. Such a dynamic turnover implies the existence of one or multiple populations of cells capable to give rise to the different cell types populating the intestinal epithelium (multipotency) and maintain their own pool throughout the entire life (self-renewal), a dual ability that correspond to the definition of adult stem cell. More than a century back, Bizzozero showed that, in homeostatic conditions, cell divisions only occur in the intestinal crypts in which cells with stem properties were already suspected to reside (Bizzozero, 1893 (M. Bjerknes and Cheng 1981). The following decades of work have lead to the formulation of the stem cell zone model according to which intestinal stem cells reside, together with Paneth cells, in a permissive environment at the very bottom of the crypts allowing self-renewal capacities. These cells are identified as crypt base columnar cells (CBC). As soon as newborn cells exit this location and pass through the position +5 (above the uppermost Paneth cell) they start their maturation toward precise differentiated cell lineages.

1.3.1.1. Lgr5, a robust marker of intestinal stem cells

One of the key challenges in the field of stem cell biology consists in the capacity of investigators to identify exquisite reliable markers that can serve to discriminate cells with self-renewal ability from their non-stem progeny. Such markers have long remained elusive in the case of intestinal stem cells, making the quantification and the characterization of these cells only speculative. By analyzing a list of genes that are part of a common genetic program shared by colon cancer cells and intestinal crypts Barker and collaborators were able to identify the first robust maker of intestinal stem cells, the leucine-reach repeat containing G-protein coupled receptor 5 (*Lgr5*)(Barker et al. 2007). This gene encodes a serpentine receptor which is a facultative component of the Wnt complex. The generation of a knock-in mouse model in which the expression of the recombinase Cre is driven by the *Lgr5* promoter ($Lgr5^{EGFP\text{-}Ires\text{-}CreERT2}$) crossed with the Rosa26R-LacZ reporter allowed the formal demonstration of the capacity of *Lgr5*-positive cells to permanently replenish the entire epithelial compartment giving rise to all differentiated cell types within 5 days. All $Lgr5^{GFP+}$ cells were invariably found to divide each day and to be in physical contact with Paneth cells. Apart from the intestine, Lgr5 was found to represent a bona fide marker for stem cells of other organs including the stomach, the hair follicle, the prostate and the kidney.

The opportunity to isolate GFP positive cells in the $Lgr5^{EGFP\text{-}Ires\text{-}CreERT2}$ model by fluorescent activated cell sorting allowed the further identification and the functional analysis of additional stem cell markers with different cellular localization and functions (figure 7), such

as the transcription factor Ascl2 representing a master regulator of the intestinal stem cells genetic program, Olfm4 and Smoc2 (van der Flier, Haegebarth, et al. 2009; van der Flier, van Gijn, et al. 2009; Muñoz et al. 2012). Other markers were identified although their expression is shared with cells in the non-stem transit amplifying compartment, such as CD133, Musashi1 and Hunk among the others (Zhu et al., 2009; Munoz et al., 2012). These non-specific markers are often used in combination as an alternative to the few mentioned *bona fide* intestinal stem cells markers in order to evaluate the stem genetic program exhibited by cells in different experimental conditions.

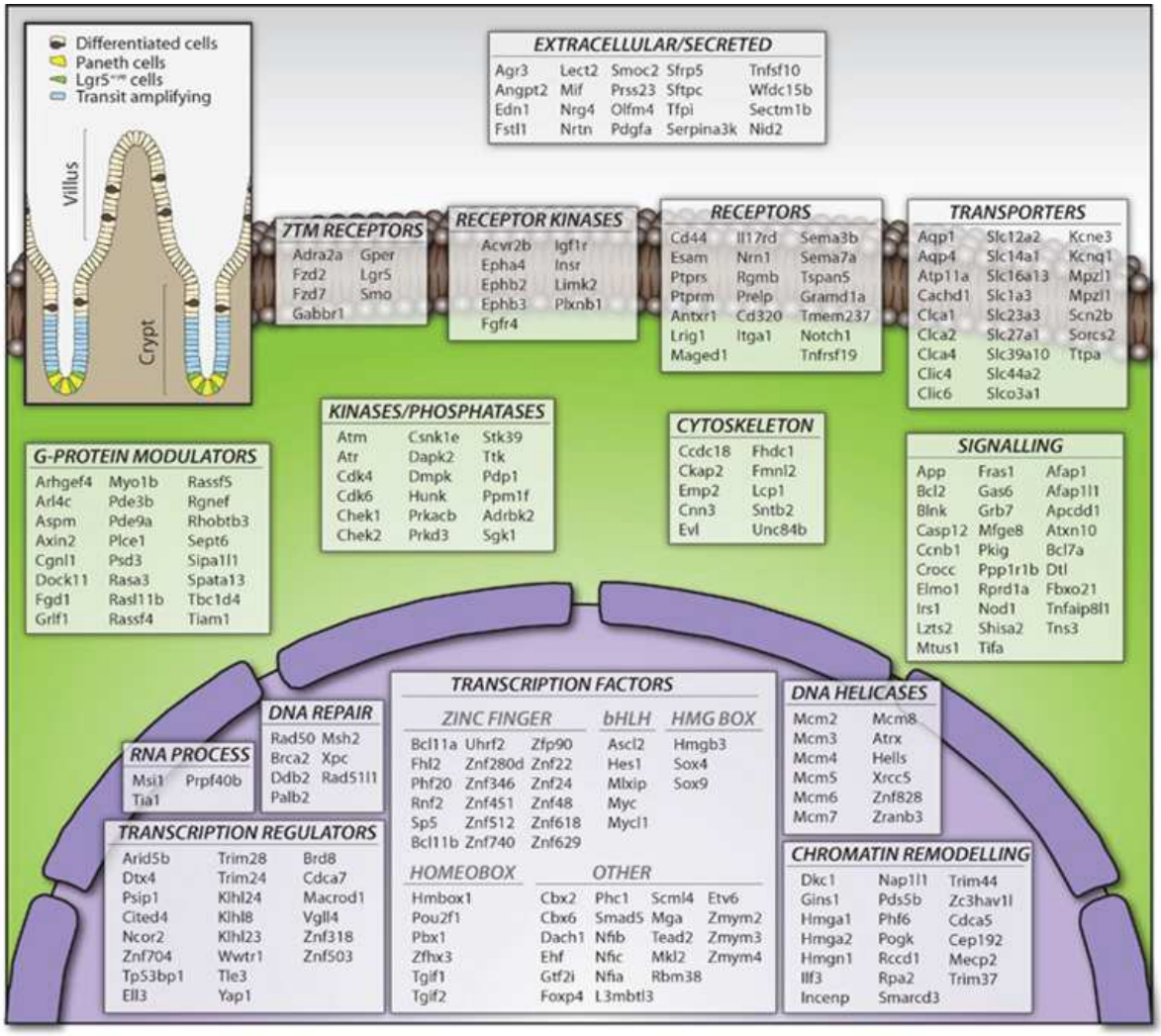

Figure 7: Functional classification of genes up-regulated in *Lgr5^{high}* intestinal stem cells. Genes are assigned to different functional classes according to their gene ontology molecular function with PANTHER. The figure presents 279 genes for some of the most relevant functional categories, selected in a list of 510 genes found to be enriched in Lgr5^{high} cells. Muñoz et al. 2012.

1.3.1.2. The +4 stem cells model

During the recent years some studies have revealed the existence of a multipotent *Lgr5*-negative population located at the position +4, just above the uppermost Paneth cells. These cells express the *Bmi1* proto-oncogen marker (Sangiorgi and Capecchi 2008). Tian and colleagues elegantly showed that *Lgr5*$^{+}$ cells are dispensable to the maintenance of the intestinal homeostasis during a couple of days (Tian et al. 2011). The authors made use of a genetic model in which the expression of the diphteria toxin receptor is driven by the *Lgr5* promoter resulting in the ablation of *Lgr5*-positive cells after the administration of diphtheria toxin to the mice. They also performed a genetic tracing model in which the expression of the recombinase Cre under the control of the *Bmi1* promoter is combined with the R26R-LacZ reporter locus to demonstrate that the ablation of the *Lgr5*$^{+}$ cells can be obviated by the capacity of crypt *Lgr5*$^{-}$-*Bmi*$^{+}$ cells to repopulate the intestine. These observations led the authors to speculate that Lgr5^{+} compartment may represent the unique or prevalent source of stem cells in normal homeostasis and that the Bmi1^{+} population deriving from Lgr5^{+} cells might be recruited to take on the role of their in the case of injury and depletion of the *Lgr5*$^{+}$ compartment.

1.3.1.3. Crypt plasticity and self-renewal

The possibility that population of cells capable of self-renewal might be organized in a hierarchical fashion prompted the investigators in the field of stem cell biology to further focus the attention on the plasticity of non-stem intestinal precursors and their capacity to regain stemness.

The first lineage tracing study to report the potential reversion of progenitor cells to stemness during tissue regeneration concerned the *Lgr5*$^{-}$;*Dll1*$^{+}$ population, which normally represent a subset of goblet and Paneth progenitors (van Es et al. 2012). In 2013 Buczacki and colleagues showed that non dividing short-lived *Lgr5*$^{+}$ Paneth/enteroendocrine precursors disappear over time as a result of terminal differentiation in healthy mice whereas they are able to dedifferentiate and repopulate the other epithelial lineages upon damage (Buczacki et al. 2013). Another very recent work from Tetteh and colleagues has shown that upon Lgr5-expressing stem cells depletion, short-lived *Alpi*$^{+}$ enterocyte precursors may serve as a reservoir of potential stem cells by dedifferentiating to replenish the damaged *Lgr5*$^{+}$ compartment (Tetteh et al., 2016).

These studies showing an unexpected degree of plasticity of committed progenitors has prompted the scientific community to reconsider the role of cellular reprogramming in the intestinal homeostasis. The molecular program driving such plasticity has not been extensively investigated yet, but one recent study based on an innovative algorithm for the analysis of transcriptional heterogeneity in a given cell population provided clues for an attempting some speculations. By making use of this methodology the authors were able to detect previously unidentified sub-types of enteroendocrine cell types (Grün et al. 2015). The application of such a tool to investigate the heterogeneity existing within the *Lgr5*$^{+}$-*GFP*^{high} compartment showed that these bona fide stem cells represent a heterogeneous population mixed with rare *Lgr5*-positive early secretory cell types. One possible interpretation of these evidences may be that *Lgr5*$^{+}$ cells undergo commitment toward defined secretory fates very early in the crypt and then they gradually lose their self-renewal ability later during migration.

1.3.2. Enterocytes

Enterocytes (or colonocytes in the colon) are the most abundant cell types in the small and large intestines. Their primary function consists in the absorption of nutrients and vitamins at the apical surface and in the export of these nutrients to the blood supply. Enterocytes were recently showed to be capable of secreting mucines that serve to protect the epithelium from the contact with pathogens. Their differentiation depends on the expression of Hes1 and on the inhibition of the secretory fate played by the Notch signaling through the repression of Math1 (see above) (Kazanjian et al. 2010; T.-H. Kim and Shivdasani 2011). *Ptk6* deficient mice display delayed maturation of enterocytes (Haegebarth et al. 2006).

1.3.3. Paneth cells

Paneth cells are located within the crypt where they complete their maturation by escaping the flow of migration toward the villus, and instead migrate downward to settle at the crypt bottom where they can persist for 2 months or more, with the oldest Paneth cells residing at the very base of the crypt (Ireland et al. 2005). Paneth cells are normally present only in the small intestine, but in some pathological conditions, characterized by intestinal metaplasia, these cells can also be found in the esophagus, in the stomach or in the colon. The necessity for the Math1 activity for their formation implies their secretory identity, and their differentiation depends on active Wnt signaling and on the Wnt target transcription factor

Sox9 as demonstrated by the depletion of this cell type in the *Sox9* knock-out mouse model (van Es et al. 2005; Bastide et al. 2007; Mori-Akiyama et al. 2007; Durand et al. 2012).

These cells possess extensive ER and Golgi network necessary to the production of their typical secretory granules. Granules are released via exocytosis in response to a variety of stimuli including bacterial surface components, acetylcholinergic and toll-like receptors agonists. The vast number of molecules belonging to the secretive granules makes Paneth cells a major player in the control of the homeostatic balance of the intestine via different functions (H. C. Clevers and Bevins 2013). Antimicrobial peptides such as lyzozyme and defensins are among the most abundant components of these granules and their characterization have elucidated the role exerted by Paneth cells in the innate immunity against enteric pathogens and in the modulation of the composition of the intestinal microbiota.

However the close association of Paneth cells with intestinal stem cells prompted researchers to investigate the functional relationship within these two populations. A number of recent findings demonstrate that Paneth cells constitute the prominent source of niche factors for the self-renewal compartment. This notion is supported by the fact that that the ablation of Paneth cells in 3 genetic models results in the progressive loss of *Lgr5*$^{+}$ intestinal stem cells in the *in vitro* organotypic culture system (Sato et al. 2011). However, the ablation of Paneth cells *in vivo* does not produce obvious changes in the stem compartment, indicating that, *in vivo*, these factors are redundantly produced by other sources (Garabedian et al. 1997; Durand et al. 2012). The development of primary *ex vivo* cultures of intestinal stem cells that can be grown into intestinal organotypic structures (further detailed later in the text) provided additional evidences for the role of Paneth cells in the maintenance of the stem compartment. Indeed, single sorted *Lgr5*-positive cells grown in matrigel rarely survive and give rise to mature intestinal organoids, whereas Paneth/stem cell doublets show a higher clonogenic efficiency, supporting the idea that these cells may provide intestinal stem cells with niche factors necessary to their identity (Sato et al. 2011; Geiser et al. 2012). Molecular arrays have shown that the gene expression profiles of these cells include the massive production of components redundant with the factors that are essential for the maintenance of intestinal organoids such as Wnt3, EGF, and the Dll1 and Dll4 Notch ligands (Sato et al. 2011).

1.3.4. Goblet cells

Goblet cells represent the most abundant secretory type in the small intestine, where they are equally distributed all along the crypt-villus axis. These cells are in charge of producing the mucins that constitute the physical barrier preventing the chemical and physical interaction between epithelial cells and the microorganism in the lumen (R. Goll and van Beelen Granlund 2015). They also produce factors involved in the organization of such a barrier, such as the trefoil factor 3 (TFF3) and they are implicated in the process of the immune Th2 response by the production of the resistin-like molecule β (RELM-β) (Y. S. Kim and Ho 2010). The SPDEF and KLF4 transcription factors are required for their terminal differentiation (Katz et al. 2002; Gregorieff et al. 2009; Noah et al. 2010; Ghaleb et al. 2011). This cell type share the expression of some markers with Paneth cells, like Spdef and Agr2, although no common precursors have been identified so far for these 2 populations.

1.3.5. Enteroendocrine cells

Enteroendocrine cells represent a rarer secretory lineage responsible for the production of hormones and peptides found in the secretory granules that are typically observed in this cell type. These molecules are released trough the basal membrane to the blood or function as signaling molecules modulating the activity of basal neurons, in order to the regulate metabolism and digestion. Enteroendocrine cells account for at least 16 different sub-types defined by distinctive molecular signatures, although a comprehensive functional classification is still lacking (May and Kaestner 2010). The commitment of all these sub-types depends on the function of the Neurogenin-3 transcription factor (Ngn3) (Jenny et al. 2002; Lee et al. 2002). The K and L subtypes are responsible for the production of peptides regulating the secretion of insulin by the β pancreatic cells, such as the gastric inhibitory peptides (GIP) and the glucagon like peptides (GLP). The enterocromaffin subtype is responsible for the massive production of serotonin hormone regulating the peristaltic intestinal movements. Ngn3 deficient mouse models display a severe impairment in the absorption of lipids absorption and regulation of glucose homeostasis (Mellitzer et al. 2010).

1.3.6. Tuft cells

Tuft cells constitute a very rare population (representing 0,3-0,4% of the epithelial cells) of cells that are homogenously distributed along the intestinal length and crypt-villus axis. These cells have also been identified in lung and pancreatic epithelia (Gerbe, Legraverend, and Jay

2012). Their typical morphology is characterized by the presence of long microvilli at the apical surface, suggesting that these cells might be involved in the sensing of the luminal content. Gerbe and collaborators identified these cells as an independent secretory lineage, since their terminal differentiation depend on the Atoh1 transcription factor but not on the activity of Ngn3, Spdef, Sox9 or Gfi1 transcription factors (Gerbe et al. 2011; Matthew Bjerknes et al. 2012). Tuft cells express Sox9 during their differentiation, but this factor is required neither for their specification nor for their survival in the adult intestine. The same authors have also identified doublecortin-kinase 1 (*Dclk1*) as the first specific marker of these cells, previously referred to as a potential marker for quiescent intestinal stem cells (Gerbe et al. 2009). However recent works have raised the possibility that this gene could also represent a marker of intestinal tumoral stem cells (Nakanishi et al. 2013; Westphalen et al. 2014a). The transcription factor Pou2f3 was recently identified as the first master gene responsible for the specification of tuft cells, since knock-out mice completely lack this cell lineage (Gerbe et al. 2016a). This recent work, together with two other publications has recently documented the first function of tuft cells that are essential to initiate the Th2 immune response against helmint parasites(Gerbe et al. 2016b; Howitt et al. 2016; von Moltke et al. 2016). *Pou2f3* deficient mice display an impaired capacity to eliminate these parasites, due to a defective production of the IL-25 alarmin cytokine (whose tuft cells represent the only epithelial source) resulting in the abrogation of the Th2 immune response activation.

The molecular profile of tuft cells indicate that these cells might exert other functions involved in the modulation of inflammatory processes, since these cells represent a unique epithelial source of opiodes, cyclo-oxygenases, and also express the hematopoietic prostaglandin D synthetase (Bezençon, le Coutre, and Damak 2007; Gerbe et al. 2011; Gerbe, Legraverend, and Jay 2012).

1.3.7. M-cells

Microfold cells reside in the epithelium that overlies specialized gut-associated lymphoid structures, the Peyer's patches(Owen and Jones 1974). Their function consists in the transport and the presentation of luminal antigens to the immune cells in the underlying stroma. Their maturation depends on the transcription factor SpiB belonging to the Ets family (Knoop et al., 2009). Indeed, *SpiB* knockout mouse models completely lack M-cells (de Lau et al. 2012). The cytokine Rank-L secreted by stromal cells was shown to be essential for the maturation of M-cells: although its receptor RANK is expressed by all epithelial cells, the addition of the

ligand to the culture medium induce the commitment of intestinal primary cultures toward the differentiation of M-cell lineage (de Lau et al. 2012).

1.4. Homeostatic dynamics of the intestinal epithelium

The rapid rate of turnover and its simple architectural organization make the intestinal epithelium a unique model to study the relationship between stem cells and their direct progeny as well as the influence played by genetic and environmental factors on this balance. Such basic biological knowledge becomes even more valuable when we consider the increased susceptibility to develop pathologies like cancer as the result of any failure in these mechanisms. The workhorse *Lgr5*^{high} intestinal stem cells constantly feed the transit amplifying (TA) compartment located just above the Paneth cell-containing stem-permissive environment. This progeny undergo 4-5 rounds of rapid (12 hours) cell divisions before they undergo to terminal differentiation and continue migrating toward the tip of the villus. Alternatively, as previously mentioned these committed daughter cells can in turn revert to stemness and replace the injured *Lgr5*$^{+}$ compartment.

Each crypt contains a constant number of about 15 *Lgr5*$^{+}$ cells, whose identity is robustly (but not exclusively) defined by the heterotypic contact with Paneth cells. The prevailing view on how adult stem cells accomplish their dual homeostatic role has long been based on an asymmetric cell division model in which daughter cells adopt divergent stem or TA fates. Short- and long-term clonal tracing results showed that equipotent stem cells rather divide symmetrically each day and are subjected to a neutral competition for the available surface of contact with surrounding Paneth cells, with none of daughter cells having a higher a priori chance to maintain stemness (Lopez-Garcia et al. 2010; Snippert et al. 2010). Such conclusion is coherent with the relatively long time needed for a newly formed crypt to become monoclonal (about 1 to 6 months), which means that at a given moment all the cells in the same crypt derive from one of those 15 stem cells. The number of stem cells is therefore tightly regulated by the presence of Paneth cells, which are in turn generated in finely controlled number and localization at the bottom of the crypt (van Es et al. 2005; Andreu et al. 2008; Farin, Van Es, and Clevers 2012). This homing was shown to be associated to the presence of EphrinB1 ligand, which is expressed by differentiated cells in a reverse villus-to-crypt gradient. Paneth cells, the prevailing epithelial source of Wnt ligands, express the Wnt target gene coding for the EphB3 receptor as a result of autocrine stimulation, so that the EphrinB1-EphB3 interaction exerts a repulsive force driving the downward migration of these

cells toward the bottom of the crypt (Batlle et al. 2002). All committed EphB3-negative cells are mechanically pushed into the crypt-to-villus flow by newly formed TA cells. Therefore EphB3 knock-out mice display defective homing of Paneth cells that tend to comigrate with the other cells. The neutral competition between stem cells to maintain the proximity to Paneth cells has been shown to be biased by genetic mutations that are typically associated with colorectal cancer initiation and progression and that confer intestinal stem cells a relatively slight clonal advantage, although their fate is not deterministic since many wild-type cells are still capable to replace the mutated ones (figure 8) (Vermeulen et al. 2013; Vermeulen and Snippert 2014). This observation represents one of the first direct proofs that the intrinsic program of the tissue contributes to the maintenance of genome integrity, which has long represented an outstanding open question on the tissue accounting for the highest turnover rate in the body. As for many types of adult stem cells, the immortal strand hypothesis was believed to represent the mechanism responsible for genome integrity in intestinal stem cells. According to the original Cairns model, segregation of the old- and the newly synthesized DNA strands occur asymmetrically at stem cell division, with the old strands retained by the daughter cell maintaining the stem identity (Cairns, 1975). In 2011 two independent works showed that this model does not apply to intestinal stem cells, which segregate their chromosomes randomly at every cell division, both in normal homeostasis and during regeneration upon injury (Escobar et al. 2011; Schepers et al. 2011).

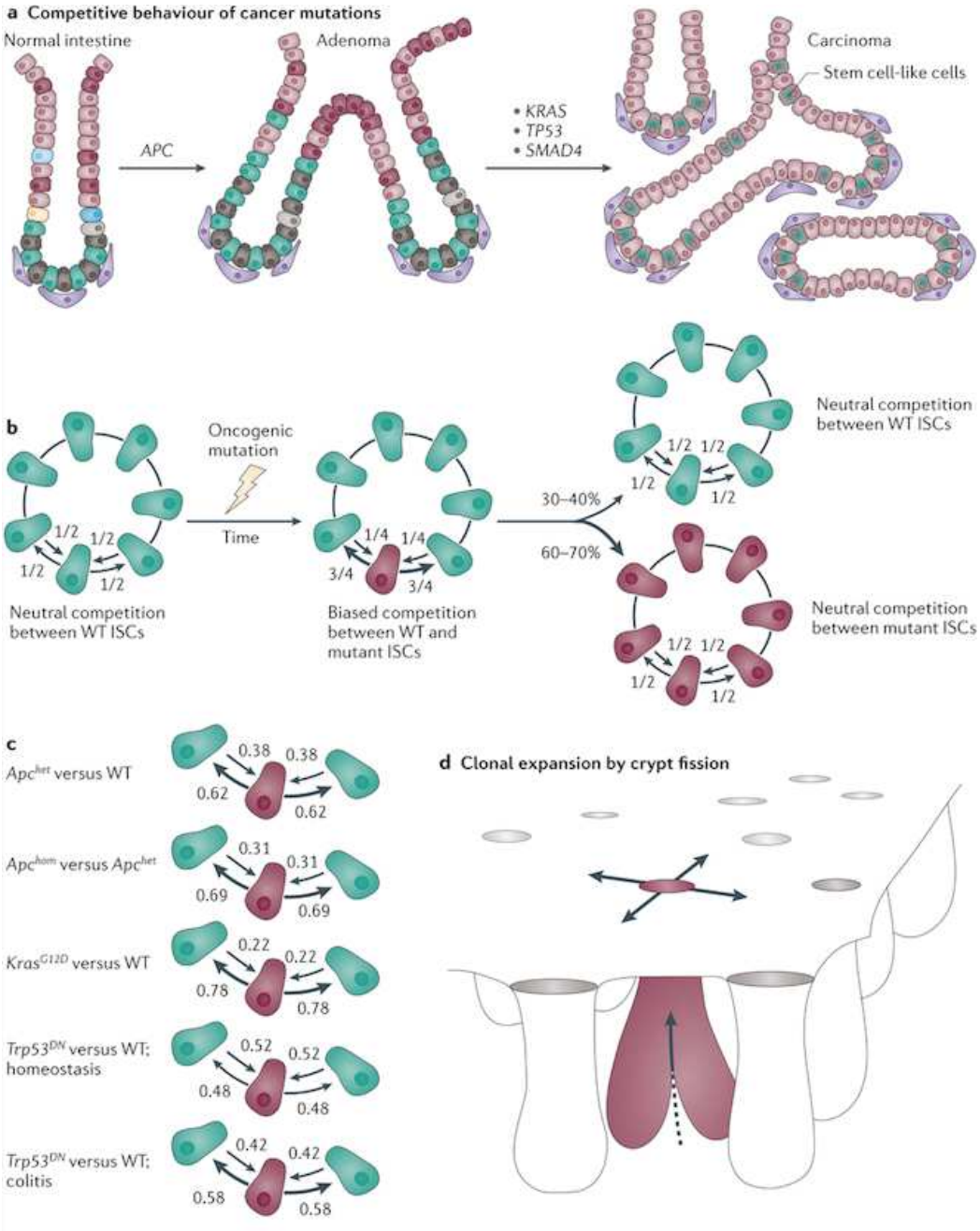

Figure 8: intestinal stem cells dynamics in intestinal homeostasis and cancer. A) Schematic representation of the adenoma to carcinoma sequence associated with the accumulation of genetic lesions. Oncogenic mutations alter the competitive fitness of intestinal stem cells. The mutation creates a bias that favor mutated cells over wild-type cells to colonize the entire crypt,s but is not deterministic since a proportion of wild-type cell can still displace mutated ones. C) Quantification of the relative competitive advantage associated to the main oncogenic mutation. D) The mutant clone expands throughout the epithelium via enhanced rate of crypt fission. (Vermeulen and Snippert 2014)

1.5. Major signaling pathways governing the epithelial homeostasis

As briefly mentioned in the previous sections, the precise architecture and cell composition of the different regions of the intestinal epithelium is orchestrated by strict gradients of soluble

molecules (morphogens) produced by different sources located at different areas of the intestine (Vanuytsel et al. 2013). The phenotypic response of each cell is therefore determined by its position within this concentration of different gradients. Morphogens involved in at least three major signaling pathways cooperate in order to establish and maintain this organization: the Wnt pathway, the BMP pathway and the Notch pathway. In this section we will illustrate the sources of the morphogens controlling the activity of these pathways, their intracellular effectors and the phenotypic outcomes as well as their role in the decision between proliferation, self-renewal and differentiation.

1.5.1. The Wnt pathway

The Wnt signaling pathway controls a myriad of biological processes throughout development and adult life of the entire animal kingdom. Most mammalian genomes, including the human genome, harbor 19 Wnt genes falling into 12 conserved subfamilies (H. Clevers and Nusse 2012). Proteins encoded by these genes act as close-range signaling morphogens by interacting with their receptors consisting in a heterodimeric complex of a Frizzled and LRP5/6 subunits (figure 9). The ten mammalian Frizzled receptors are 7-transmembrane receptors having a large extracellular N-terminal cysteine-rich domain that constitutes a hydrophobic binding platform for lipid-modified Wnt ligands (Bhanot et al. 1996; Dann et al. 2001; Janda et al. 2012). In the absence of binding of Wnt to the receptor complex, cytosolic β-Catenin is efficiently captured by the destruction complex formed the scaffold protein Axin, the casein kinase 1 (CK1) the Adenomatous Polyposis Coli protein (APC) and the glycogen synthase kinase 3β (GSK3β) (Mao et al. 2001; Zeng et al. 2005). The two kinases in the complex phosphorylate the N-ter of the β-Catenin allowing the binding of the E3 ubiquitin ligase complex followed by its degradation mediated by the proteasome (Davidson et al. 2005). The interaction between the Wnt ligands and the receptors leads to the phosphorylation of the cytoplasmatic domain of LRP5/6 and a conformational change in both LRP and Frizzled subunits allowing the sequestration of Axin which prevents proteosomal degradation of the β-Catenin and allows its translocation to the nucleus. As a result, β-Catenin interacts with T-cell/lymphoid enhancer factor (Tcf/Lef) family members by displacing Groucho repressor from the complex, thus modulating the transcription of Wnt target genes (Behrens et al. 1996; Molenaar et al. 1996). Among the first and most important Wnt target genes were cMyc and Cyclin D1 (Beier et al. 1999; Herbst et al. 2014). Nuclear localization of β-Catenin therefore represents the most common hallmark of Wnt activation. The activity of the Wnt

pathway is also enhanced by the function of the secreted the R-spondin able to enhance proliferation of intestinal epithelial cells both in vivo and in vitro (Kazanskaya et al. 2004). Lgr4, -5 and -6 were later identified as the receptors of these glycoproteins (Carmon et al. 2011; de Lau et al. 2011). Along with the cytosolic β-Catenin destruction complex the activation of the Wnt pathways is antagonized by extracellular proteins such as the Dickkopf (DKK) and secreted frizzled-related proteins (SFRP), as well as the Wnt inhibitor factor-1 (WIF-1) (Glinka et al. 1998; Bovolenta et al. 2008).

Several studies have shown the major implication of this signaling pathway in the regulation of the balance between proliferation and differentiation in the small intestine. Neonatal *Tcf4* knockout mice lack the proliferative epithelial compartment. Conditional deletion of this gene, as well as in the case of β-Catenin, showed that Wnt signaling is required for the maintenance of crypts in adult animals (Korinek et al. 1998; Pinto et al. 2003). Since Paneth cells represent the main source of Wnt ligands, the activity of the pathway is modulated in a crypt-to-villus gradient. Stem cells (and differentiated Paneth cells) residing at the bottom of the crypts are exposed to the highest concentration of Wnt factors allowing the self-renewal ability and multipotency (Sato et al. 2011). The discovery of the Wnt target gene *Lgr5* (receptor of the Wnt agonist Rspo) as a *bona fide* positive marker of intestinal stem cells provided the first direct evidence of the role played by this signaling pathway in the promotion of the intestinal stem phenotype (Barker et al. 2007). Several alterations concerning the molecular players of the Wnt pathway are associated with colorectal cancer susceptibility, initiation and progression.

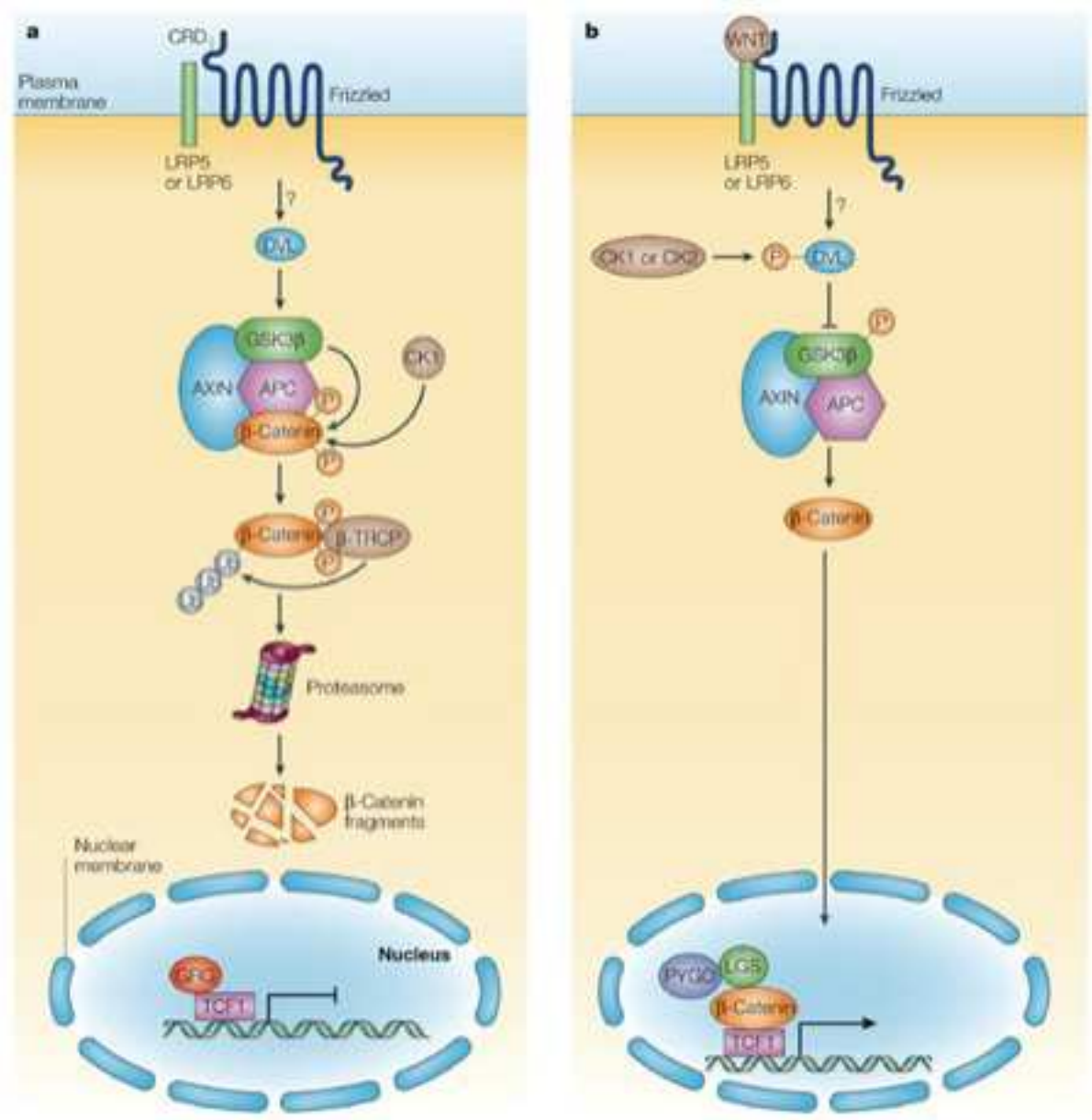

Figure 9: schematic representation of the Wnt pathway before (A) and after the binding of Wnt ligand followed by the activation of the intracellular signaling cascade leading to the modulation of the expression of Wnt target genes.

1.5.2. The TGF-β/BMP pathway

Bone Morphogenetic Proteins are soluble factors belonging to the TGF-β cytokine family known to be involved in several developmental processes as well as in adult tissue homeostasis (Vanuytsel et al. 2013). Depending on the tissue and on the cellular context BMPs were shown to regulate cell growth, differentiation and apoptosis. BMP ligands are

secreted in their active form in the extracellular environment where they form homo- or heterodimeric complexes before binding to their cognate receptors (BMPRs) (figure 10). Tight regulation of the pathway is exerted at multiple levels. Soluble antagonists are secreted to sequester them from binding to their receptors. BMPs bind to a class of Ser/Thr receptors type I/II heterodimers. There are four type I (Alk1, Alk2, Alk3 (BMPR1A), Alk6 (BMPR1B)) and three type II (BMPR-II, ActR-IIA and ActR-IIB) receptors (Zwijsen, Verschueren, and Huylebroeck 2003; Schmierer and Hill 2007). BMPRs sequences contain an N-terminal extracellular binding domain, a transmembrane domain and a Ser/Thr kinase C-terminal domain. BMPs first bind to the type I receptors, and then to the BMP/BMPR1 complex bind with high affinity the type II receptor. The proximity of type I and type II receptors allows the phosphorilation of the Gly/Ser domain in the type I receptor sequence by the type II kinase domain, converting the complex to its active form. The activated complex signals through the phosphorylation of members of the family of protein homologues of *Drosophila* gene *Mothers against decapentaplegic* (SMADs). SMAD proteins can be divided into 3 functional classes:

- Receptor associated SMADs (R-SMADs), representing the intracellular effectors of the BMP activation. R-SMADs 1, -5, -8 bind to the active BMPR and exclusively transduce BMP signaling, while R-SMADs 2, -3 belong to the TGF-β signaling pathway.
- Cooperating SMADs (Co-SMADs) 2 and 4 which form active complexes with R-SMADs. Their expression represents a supplemental layer of regulation of the signal transduction.
- Inhibitory SMADs 6 and 7 which can prevent the phosphorylation and the activity of R-SMADs by sequestering SMAD1 in an inactive SMAD1-6 complex or by preventing the phosphorylation of R-SMADs mediated by the activated BMPR.

Phosphorylated R-SMADs form heterodimeric complexes with Co-SMAD and can then efficiently translocate to the nucleus where, in combination with other transcription factors, they exert a regulation on the expression of multiple target genes. These targets include the family of *Id1-4* factors that act as dominant negative regulators by preventing the binding of other bHLH transcription factors to their targets (Jen, Weintraub, and Benezra 1992; Ogata et al. 1993; Iavarone et al. 1994; Bhatia et al. 1999). BMP can also inhibit proliferation by regulating the expression or the stability of cyclin-dependent kinase inhibitors (Yamato et al. 2001; Beck et al. 2007).

The expression of the BMP pathway components in the intestine is complex, with part of these components being expressed in both epithelial and stromal cells and others being restricted to the mesenchyme (Hardwick et al. 2004; Li et al. 2007; Haramis et al. 2004). Experimental models of reduction of the BMP signal via the knockdown of the receptor Bmpr1A or the overexpression of the Noggin inhibitor display hyperproliferation of the intestinal stem cells, formation of ectopic crypts along the villus axis and development of intestinal polyps, suggesting a role for the BMP signals as a quiescence marker (Hardwick et al. 2004). In 2004, a controversial work from He and colleagues suggested that BMPs signaling might prevent stem cell identity by antagonizing the Wnt pathway via the activation of PTEN and the suppression of nuclear β-catenin accumulation mediated by Akt (He et al. 2004). However, a more accurate examination of the *PTEN* expression pattern showed that this marker is associated with enteroendocrine cells at the bottom of the crypt rather than intestinal stem cells (Matthew Bjerknes and Cheng 2005).

The BMP extracellular inhibitors gremlin (Grem) 1 and 2 are exclusively expressed by the mesenchymal myofibroblasts surrounding the crypts, thus ensuring the inactivation of BMP ligands in the stem and proliferative compartment. Genetic duplication of a 40 kilobases region upstream the *GREM1* gene is associated with ectopic epithelial expression of the gene, an automosomal dominant human condition resulting in hereditary mixed polyposis syndrome (HMPS) characterized by the development of mixed-morphology colorectal tumors at a median age of 47 (Jaeger et al. 2012). In a recent work from Davis and colleagues, the authors showed that the aberrant expression of *Grem1* in epithelial cells leads to the formation of ectopic crypts in the villus axis (Davis et al. 2015). However these crypts lack *bona fide* $Lgr5^{+}$ stem cells. Markers of stem cells only appear in the tissue upon the constitutive activation of the Wnt pathway mediated by the loss of *Apc* function, thus reinforcing the idea that both activation of Wnt- and suppression of BMP signaling represent *conditio sine qua non* for the establishment and maintenance of stemness in the intestinal epithelium.

However, the transcriptional outcome mediated by the BMP signaling in intestinal epithelial cells is still poorly characterized. Some evidences propose that Ids can promote differentiation instead of proliferation in the small intestine since *Id2* and *Id3* were found to be upregulated in cells at the crypt-villus junction.

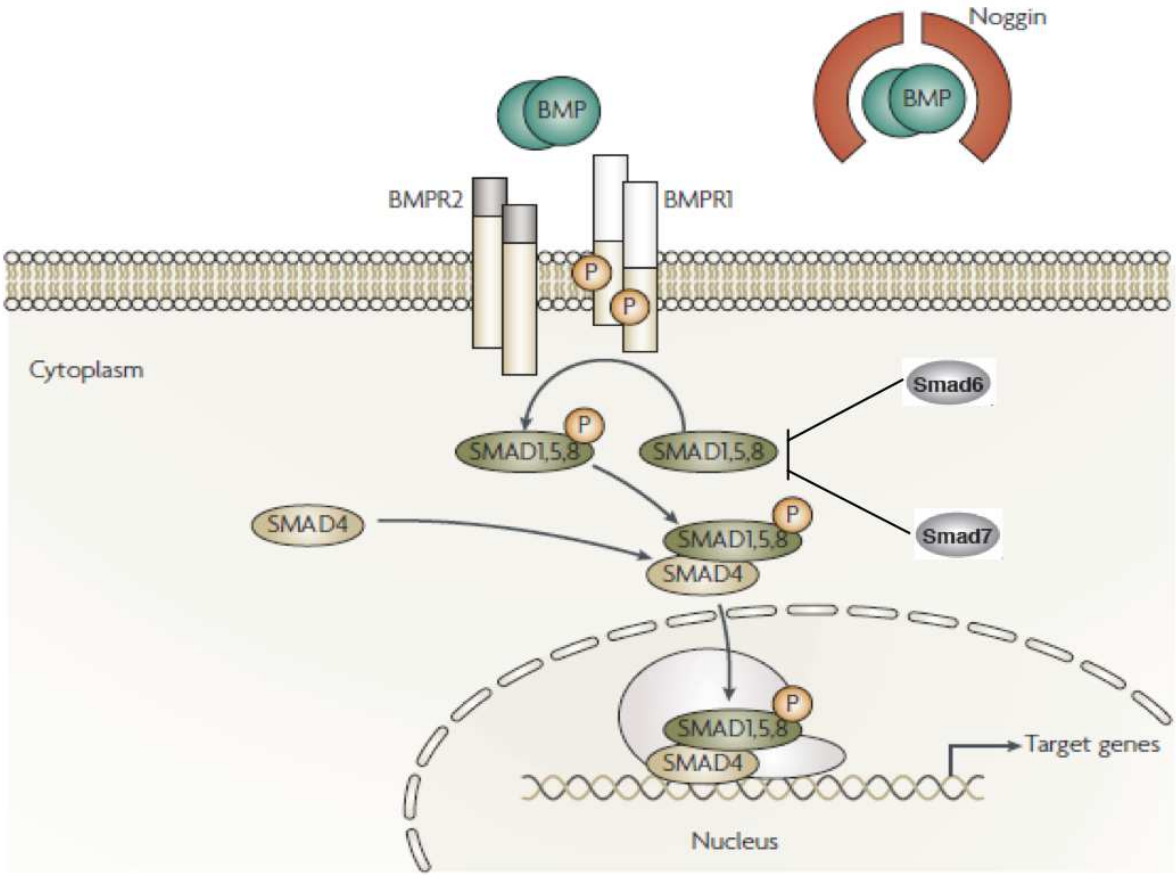

Figure 10: schematic representation of the Notch pathway signaling upon the ligand of BMPs soluble factors to the BMP receptors. BMPs ligands are sequestered by the extra cellular inhibitors (example Noggin) produced by the microenvironment.

1.5.3. The Notch pathway

The highly conserved Notch signaling pathway is responsible for cell fate decision through cell-to-cell interaction mediated by the expression of Notch-ligands and –receptors in metazoan. Four single-pass trans-membrane Notch receptors (1-4) specifically interact with 5 single-pass trans-membrane ligands Jagged1, 2, Delta-likke (Dll) 1, 3 and 4 (Chiba 2006). This interaction results in the proteolytic release of the receptor N-terminus intracellular domain (NICD) mediated by intracellular γ-protease (figure 11) (De Strooper et al. 1999). Upon release, NICD translocate to the nucleus where it binds to the transcription factor CLS inducing differential transcription of several Notch-target genes (Artavanis-Tsakonas, Rand, and Lake 1999).

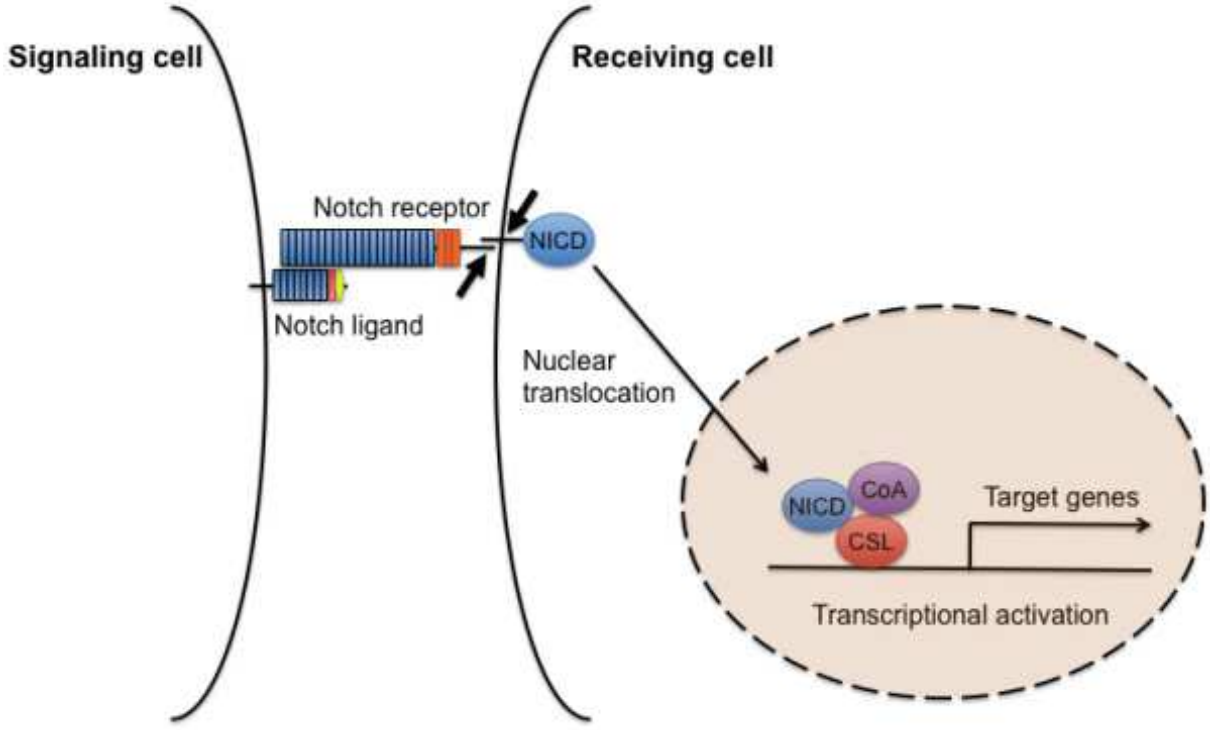

Figure 11: schematic representation of the activation of the Notch sgnalilng via the cell-cell interaction leading to the proteolitic excision and the translocation of the Notch intracellular domain (NICD).

Notch receptors and ligands are heterogeneously expressed across the different epithelial populations and loss-of-function studies have shown a certain degree of redundancy between these actors (Sander and Powell 2004; Pellegrinet et al. 2011; Fre et al. 2011). Specific intestinal deletion of *Notch1* and *2* does not result to an obvious intestinal phenotype. However, blocking both receptors leads to the conversion of proliferative cells to postmitotic goblet cells (Riccio et al. 2008). *Dll1*/*Dll4*/*Rbp*-J combined knockout animals display the loss of expression of the *bona fide* stem markers Olfm4, Ascl2 and Lgr5, which correlates with the loss of $Ki67^{+}$ proliferative cells in the crypts (Pellegrinet et al. 2011; Stamataki et al. 2011). Paneth cells express *Dll4* to maintain the undifferentiated state of adjacent intestinal stem cells (Sato et al. 2011). Importantly, lineage tracing studies have showed the expression of Notch receptors 1 and 2 and and active Notch signaling in the multipotent stem compartment. As previously mentioned, Notch activation represses the expression of Atoh1 and, to a smaller extent, Neurogenin-3 transcription factors both responsible for the maturation of secretory lineages (Fre et al. 2005). Indeed, stem cells and enterocytes progenitors express high levels of *Hes1*, while its expression is lost in all secretory cell types. Constitutive epithelial activation of the Notch signaling leads to the expansion of the proliferative compartment and to the depletion of goblet cells accompanied by a general impairment of differentiation (Fre et al., 2005). Taken together, all these observations support the formulation of a lateral inhibition model, according to which the expression of *Dll1* and *Dll4* in Paneth cells triggers the Notch signaling in all the surrounding stem cells, therefore

promoting the expression of *Hes1* and the "default" enterocyte fate program (T.-H. Kim and Shivdasani 2011; Sancho, Cremona, and Behrens 2015). Cells that exit the Paneth cell permissive zone are no longer exposed to membrane-bound Notch ligands and can stochastically shut-off the expression of Hes1, hence inducing the expression of Atoh1 and committing to the secretory fate.

1.6. In vitro organotypic cultures in the study of epithelial biology in homeostasis and disease

The identification of *Lgr5* as a robust marker of intestinal stem cells has led to a dramatic development in the understanding of their biology. One of the most outstanding achievements is represented by the establishment of protocols allowing the conditions for culturing *Lgr5*-positive cells *ex vivo*. In 2009 Sato and collaborators showed that single sorted $Lgr5^{+}$;GFP^{high} cells obtained from *Lgr5-EFGP-ires-Cre*^{ERT2} crypts can build structures that retain hallmarks of intestinal epithelium in vivo (Sato et al. 2009). When cultured in laminin-enriched matrigel mimicking the crypt base environment in the presence of EGF, the BMP inhibitor Noggin and R-spondin1, *Lgr5*-positive cells are able to give rise to organoids that recapitulate the stereotypical structure and physiology of the intestinal epithelium (figure 12). Structures consist in multiple crypt-like domains containing *Lgr5*$^{+}$ proliferating cells intermingled between Paneth cells, and villus-like domains lining the central lumen in which apoptotic cells are shed. All differentiated epithelial lineages are represented and can be identified by the expression of their typical markers. Structures can be dissociated and replated to form new organoids, without any loss of replating efficiency after several passages. Organoids remain morphologically and karyotypically indistinguishable after several successive replatings for an indefinite lapse of time. After few replatings, cultures are stroma-free and their maintenance only depends on EGF, R-spondin1 and Noggin that are added to medium. However, although all epithelial cells are exposed to the same concentration of morphogens added to the medium, only cells within the crypt display signs of active Wnt signaling such as the nuclear translocation of β-catenin. Taken together, these observations demonstrate that epithelial stem cells possess differential responsiveness to extrinsic stimuli as part of an intrinsic program allowing the self-organization of the epithelial architecture which is therefore, at least at some extent, independent on the positional cues provided by the environment *in vivo*.

The ability of intestinal stem cells to grow into structures that faithfully recapitulate the self-renewal hierarchy of the intestinal epithelium offers a wide range of approaches to investigate

several aspects related to intestinal physiopathology, regenerative medicine and drug screening. First, the requirement for a minimal well-defined culturing medium may allow the evaluation of the role played by extrinsic factors in the regulation of the homeostatic balance between proliferation, differentiation and death. Organoids can be derived from conditional genetic animal models in order to monitor the effect of genetic components on a real time basis, for instance upon the deletion of coding sequences via the activation of transgenic recombinases in culture. This model is also amenable to any experimental protocol used for cell lines, including transfection of DNA and small interfering RNA as well as retro- and lentiviral mediated transduction (Koo et al. 2012; Onuma et al. 2013).

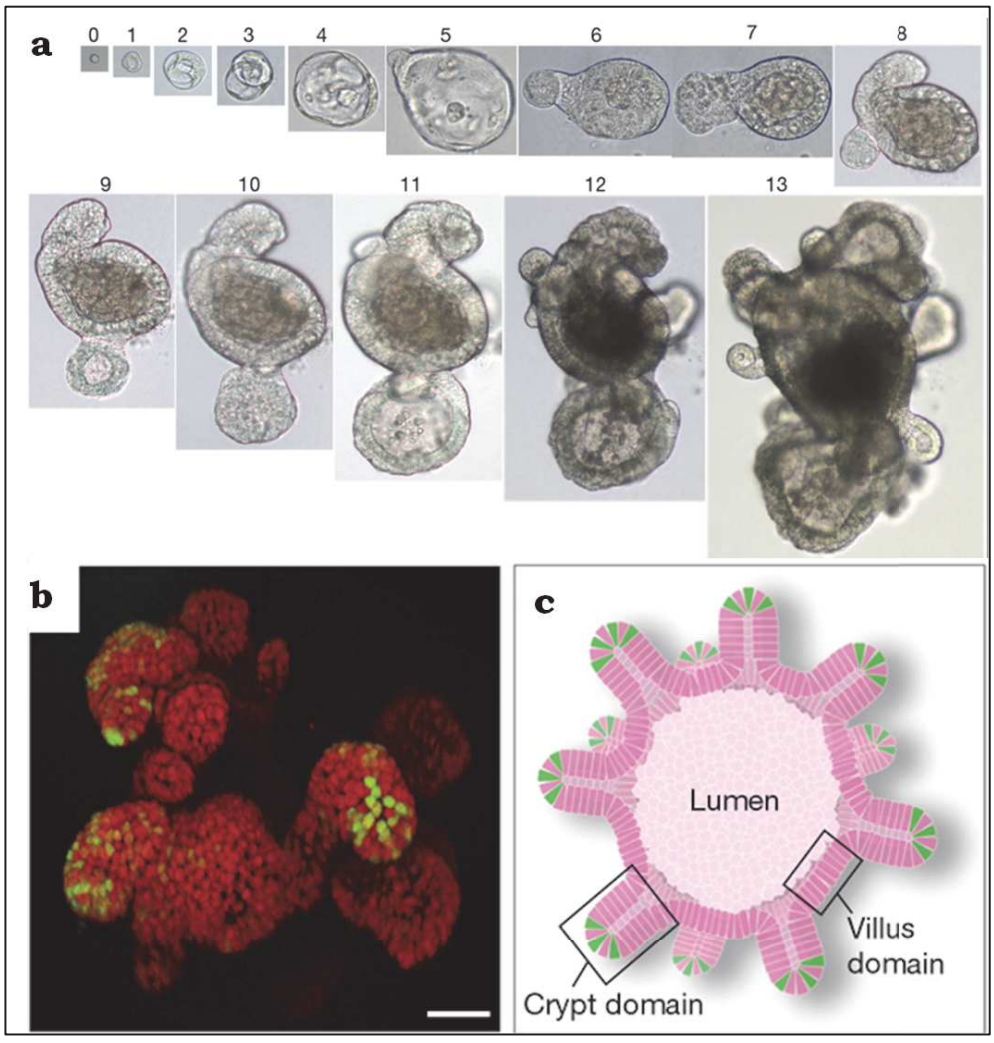

Figure 12: intestinal organotypic cultures. A) Kinetic of development from a single Lgr5+ cell plated on matrigel (day 0) to fully developed structures accounting for crypt and villus domains. B) reconstruction of confocal imaging of an epithelial organoids (nuclei are in red, Lgr5+-GFP+ cells in green are located at the bottom of the crypts.) C) schematic representation of the organotypic structure. (Sato et al. 2009).

Recently, genome-editing technologies were successfully applied in order to model the genetic basis of human diseases in organotypic cultures. In 2013 the Clevers group made use of CRISPR/Cas9 mediated homologous recombination in order to correct the mutation of the CFTR locus in intestinal organoids derived from biopsies of patients affected by cystic fibrosis and restore the function of the transmembrane conductor receptor coded by the gene (Schwank et al. 2013). The same team also recently provided formal validations of the multistep genetic model driving colorectal cancer initiation and progression (Drost et al. 2015; Matano et al. 2015). Authors were able to recapitulate the phenotypic traits of the well described adenoma to carcinoma progression by sequentially introducing genetic mutations in four of the most commonly mutated colorectal cancer genes (*APC*, *P53*, *KRAS* and *SMAD4*). This model also allows researchers to establish primary lines from human adenomas and colorectal cancer. The current challenge in public health consists in the generation of biobanks of cultures derived from patients' biopsies that can be suitable to bridge the gap between the individual molecular background data provided by deep-sequencing and the screening for the choice of personalized treatment.

2. Colorectal cancer

Cancer represents the leading cause of death in economically developed countries and the second leading cause in developing countries. The global incidence of cancer continues to increase, which is explained by the aging and growth of the world population but also by the increasing adoption of cancer-causing behaviors and by the increase of cancer-causing environmental factors in the economically developing world (Jemal et al. 2011; Globocan 2012).

Colorectal cancer (CCR) represents the third most commonly diagnosed cancer in males and the second in females. Overall, the highest incidence rate is found in economically developed countries, whereas the lowest rates are found in Africa and south-central Asia (figure 13). Rates are substantially higher in males than in females. Notably, the incidence of colorectal cancer is rapidly increasing in areas historically at low risk such as countries in Eastern Europe and Eastern Asia. These trends are likely to be associated with economical development and mutating life-style in these areas (Jemal et al. 2011). These evidences suggest that the overall incidence is largely influenced by environmental modifiable cues. Nonetheless, colorectal cancer actually represents an extremely heterogeneous group of malignancies associated with a complicated molecular classification (Müller, Ibrahim, and Arends 2016). The molecular and environmental components of the related risk are therefore variable. Interestingly, the United States is the only country in which the incidence rate has shown a statistically significant decrease in the most recent period, which largely depends on the development of screening tools for early diagnosis and effective removal of pre-cancerous lesions. The results of a multicentre randomized trial performed in the United Kingdom published in 2010 showed that the preventive one-time screening of the population aged between 55 and 64 reduced the incidence by 33% and the mortality by 43% (Hilsden and Rostom 2010).

Colorectal cancer related death is associated to invasiveness and acquisition of metastatic capacity associated to the late stages of the malignancies. Classification of patients to their clinical stage is therefore made according to the TNM (Tumor-Node-Metastasis) system, which describes the size of the primary tumor, whether the nearby lymph nodes contain cancer cells, and whether cancer has spread to a distant organ. Prognosis is very variable and correlates with the clinical stage at diagnosis. Survival rate is over 90% within the first 5 years for stage I patients, 50% for stage III patients and 5-10% for stage IV patients. Overall, these

notions indicate that the early evaluation of the individual risk and the diagnosis of the pathology at very early stages represent the most effective tools in public health management.

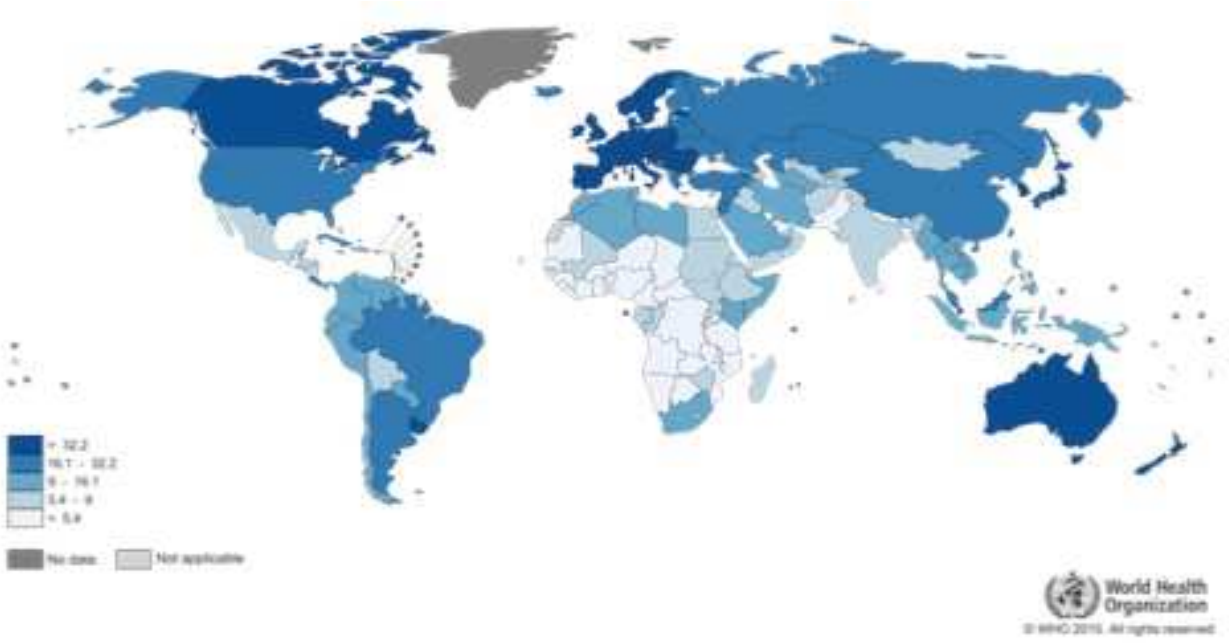

Figure 13: heat-map representing the incidence of colorectal cancer in the world represented as the number of new cases per year. Legend represents new cases in thousands. (Globocan 2012)

2.1. Genetic alterations driving initiation and progression of CRC

As mentioned, colorectal cancer represents a heterogeneous group of malignancies, and many efforts were made to provide a molecular classification of its different subtypes (Müller, Ibrahim, and Arends 2016). The majority of 70-80% CRC are sporadic, whereas around 20-30% of the cases have a hereditary component associated to genetic alterations that can be either uncommon, such as Lynch Syndrome (3-4%) patients and the familial adenomatous patients (FAP, 1-2%), or associated to low-risk rare alleles (Whiffin et al. 2014). The vast majority of sporadic cases were found to be associated to mutations in the Adenomatous polyposis coli (APC) Wnt negative regulator, while an additional 15% of patients show alterations in other components of the Wnt pathways that are either mutated or epigenetically silenced (Vogelstein et al. 1988; Morin et al. 1997; Frayling IM and Arends MJ, 2016). These evidences clearly suggested that alterations leading to the constitutive activation of the Wnt signaling play a central role in the initiation of CRC. Importantly, FAP patients carry a heterozygous germline mutation on the *APC* gene (de la Chapelle 2004). As a result of the

loss or inactivation of the second allele, these individuals invariably develop multiple adenomas by the age of 30, unless they undergo to preventive colostomy. In 1990, by examining the collection of genomic alterations most commonly associated to different stages of the malignancies, Fearon and Vogelstein proposed a schematic model summarizing the main genetic events associated to the adenoma to carcinoma progression ((Fearon and Vogelstein 1990). According to this model, the initiating loss of *APC* function results in the formation of a hyperproliferative pre-cancerous lesion. This step is typically followed by gain-of-function type mutations on the *RAS* oncogene, or other mutations resulting in the constitutive activation of the MAPK signaling that normally acts downstream the EGF. The third major event is inactivation of the *p53*, which is responsible for inactivation of the cell cycle check-points normally triggered by DNA damage in normal cells and that leads to the adenoma to carcinoma transition. The fourth main alteration in the sequence leads to the loss of TGFβ responsiveness either through the loss of the co-operating SMAD4 or the inactivation of the TGFBRII receptor. Although this model has represented a conceptual breakout in our understanding of the molecular etiology of CRC, its formal validation was only recently accomplished. Dow and collaborators have recently shown that *Apc* suppression is not only responsible for adenoma initiation, but it is also indispensable for tumor maintenance. By making use of a conditional in vivo model of doxycycline-regulated shRNA suppression of *Apc* the authors showed that restoration of *Apc* function leads to rapid regression of the tumor that eventually results in the restoration of the disrupted crypt-villus homeostasis (Dow et al. 2015). Importantly, such restoration is independent on the presence of the additional mutations (*Kras*, *p53*) that are responsible for the progression to carcinoma, proving that the constitutive activation of the Wnt pathway represents a *conditio sine qua non* for tumor maintenance at any stage of its progression. Two independent works showed that the sequential introduction of the main alterations described in the Fearon and Vogelstein model trough CRISPR/Cas9 targeted gene modification of human intestinal organoids can efficiently recapitulate the phenotypic hallmarks of carcinoma progression and invasiveness (Drost et al. 2015; Matano et al. 2015). In particular, the concomitant loss of APC and P53 leads to extensive aneuplody, a condition referred to as chromosome instability (CIN), whereas the concomitant alteration of *APC*, *KRAS*, *p53*, *SMAD4* and *PIK3CA* confer metastatic potential to epithelial cells when those cells are injected into immunosuppressed mice. In addition to this well described sequence it is estimated that about 7 to 15% of CRC may develop via a different morphological sequence, known as serrated pathway (Noffsinger, 2009). The progression via this pathway shares some characteristics with the Lynch syndrome

(hereditary non polyposis colorectal cancer, HNPCC), which is a dominant negative condition associated to mismatch repair gene mutations (mostly *MSH2* or *MLH1*) (de la Chapelle 2004). About 80-90% of serrated polyps are classified as benign hyperplastic lesions whereas a small proportion may progress to colorectal carcinoma (IJspeert et al. 2016). Tumors developing via this alternative pathway are highly heterogeneous in terms of molecular feature. However the most common initiating alteration is represented by the *BRAF V600E* mutation (Rad et al. 2013).

2.2. Toward a molecular classification of CRC

The advent of in-depth wide-range genomic and transcriptomic analyses has allowed the comprehensive characterization of the genomic features associated with CRC heterogeneity. Such analyses have been used to attempt to answer to the need for a more precise classification of patients according to their molecular profiles and propose more accurate prognostic parameters (figure 14) (Müller, Ibrahim, and Arends 2016). A major common feature of CRC is represented by genetic instability, and the mechanisms by which the accumulation of genetic lesions occurs have been successfully used to establish a classification with clinical relevance.

Two main mechanisms have been classically proposed to explain genetic instability. Chromosome instability (CIN) represents the most common phenotype (84% of tumors) characterized by gross karyotypic alterations in chromosomes copy number and various chromosomal rearrangements such as insertion/deletion and translocations (Pino and Chung 2011). This phenotype is detectable in most tumors that arise via the classic adenoma-carcinoma sequence and are associated to the loss of *APC*. However, Dross and collaborators have shown that the p53 mutation dramatically enhances the rate of chromosomal aberrations due to an increase in the percentage of mitotic errors (Bhanot et al. 1996). The second cluster of lesions is characterized by hypermutation and micro-satellite genomic instability (MSI) and accounts for about 13-16% of CRC (Vilar and Gruber 2010). These lesions frequently display a WT p53 status and a near-diploid karyotypic profile. The high mutational rate is associated to defective DNA mismatch repair (MMR) mechanisms mostly related with heterozygous dominant alteration on either *MSH2* or *MLH1* genes. A third phenotype is known and is commonly referred to as CpG islands methylation phenotype (CIMP), characterized by an enrichment of hypermetylated genomic regions corresponding to CpG islands within the promoters of genes with oncosuppressive function (Serra et al. 2014). MSI and CIMP groups

partially overlap, since in many cases the suppression of *MLH1* activity represents the result of a hypermethylation of its promoter associated to transcriptional downregulation of the gene. Two molecular classifications have been recently proposed for CRC and are based either on integrated genome-wide genomic and transcriptomic profiling, or on the stratification of transcriptomic profiling data from multiple previous studies. The cancer genome atlas (TCGA) network project account for the combined analyses of whole genome sequencing of germline and cancer samples from patients, mRNA, miRNA and DNA methylation profiling (The Cancer Genome Atlas, 2012). The results revealed that patients can be split into two major groups by mutation rate that match well the previously described MSI and CIN groups. The category with high mutational rate can be further divided into distinct subgroups accounting for high (13%) or extremely high mutation rate (3%). The integrated analyses allowed establishing lists of genes that are significantly frequently altered in the hyper- and ultra-mutated groups. The consortium molecular subtypes (CMS) defined two major categories and 4 sub-categories classified by molecular attributes and expression signatures (Guinney et al. 2015).

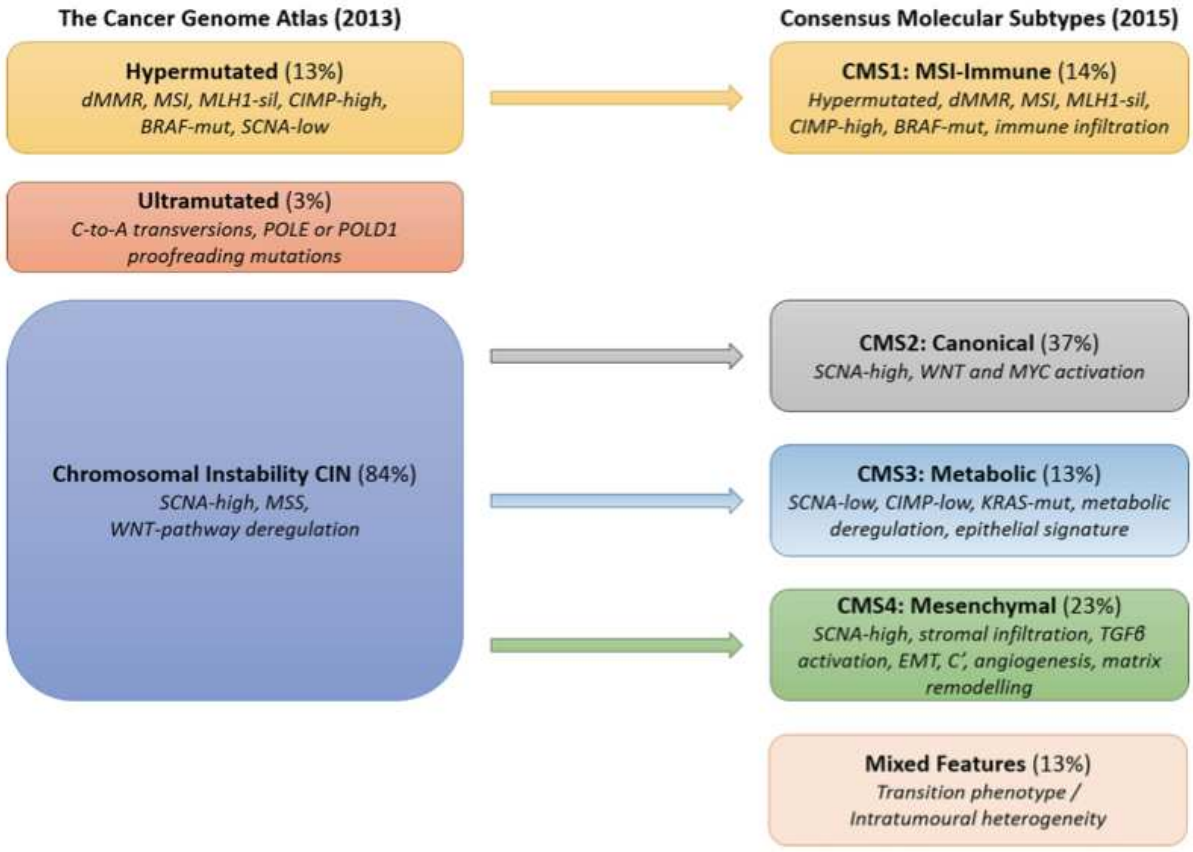

Figure 14: schematic illustration of the molecular classification of CRC types according the cancer genome atlas (TCGA) and the consensus molecular subtypes proposed by Guinney and colleagues in 2015. The illustration shows the overlap between the different groups of each classification. (Muller et al. 2016).

2.3. Intestinal tumor initiating cells

Cancer is commonly thought to initiate in a single cell after an initial oncogenic event and eventually progress through the clonal selection of additional mutations in the progeny of this cell. However, the identity and features of tumor initiating cells remain highly debated. Central to the theory of cancer initiating cells, or cancer stem cells, is the observation that not all tumor cells are equal (H. Clevers 2016). This suggests a hierarchical organization of the tumor that somehow resemble the one found in normal tissue, in which cells have different life span, with some that are long-lived and capable to self-renew. The first attempts to demonstrate the existence of cell with increased capacity to initiate the tumor consisted in xenotransplants of phenotypically different tumor cells into immunosuppresed mice (Lapidot et al. 1994; Al-Hajj et al. 2003). Only a fraction of these cells were able to efficiently give rise to newly formed tumors accounting for the same heterogeneity than the primary tumor. Acute myeloid leukemia represents a paradigmatic model in this sense: tumor initiating cells are

likely to represent the mutated counterpart of normal stem cell, since they share hierarchical maturation into progenitors and differentiated lineages.

In 2009 Barker and colleagues showed that $Lgr5^+$ cells acquire the capacity to establish and maintain intestinal tumor upon the Cre-mediated induction of *Apc* loss in *ApcLoxp/Loxp , Lgr5-EGFP-ires-CreERT2* mice (Barker et al. 2009). They also showed that the loss of *Apc* in transiently amplifying progenitor cells does not efficiently lead to tumor formation, and the rare lesions that arise in this model do not progress over the state of microadenoma. Cancer initiating cells thus represent the result of the tumor initiating mutation in the intestinal stem cell pool. However, as previously discussed, a certain degree of plasticity seems to exist in the hierarchy of the normal epithelium, and some populations are capable to reconstitute the $Lgr5^+$ compartment upon injury. $Krt19^+$ cells were shown to be able to repopulate the epithelium upon irradiation and to initiate tumors upon the deletion of *Apc* in these cells (Asfaha et al. 2015). Therefore, multiple populations with differential stem potential could be able to initiate intestinal cancer. In 2013 Schwitalla and collaborators showed for the first time that under certain conditions differentiated epithelial cells may acquire a tumorigenic potential (Schwitalla et al. 2013). Indeed, the activation of NF-κB signaling reinforces the activity of the B-Catenin and accelerates crypt transformation but also induces differentiated cells to dedifferentiation and expression of bona fide stem markers. These dedifferentiated cells gain tumor-initiating capacity. In 2012 Nakanishi and collaborators proposed Dclk1 as a possible marker of tumor initiating cells (Nakanishi et al. 2013). This marker is only expressed by differentiated tuft cells in the healthy intestine (Gerbe et al. 2009). However, lineage-tracing experiments showed that $Dclk1^+$ cells can fuel tumor growth whereas conditional ablation of these cells remarkably induces a regression of adenomas of Apc^{Min} mice. Of note, how rare and poorly proliferative tumor $Dclk1^+$ cells can populate the whole tumor within a couple of days remains difficult to understand. A contrasting work recently proposed $Dclk1^+$ tuft cells as quiescent long-lived stem cells with tumor initiating ability (Westphalen et al. 2014b), in sharp contradiction with previously published studies (Gerbe et al. 2011). According to their evidences, the authors proposed that tuft cells are important for tissue regeneration and do not initiate tumors upon conditional deletion of *Apc* unless in the case of injury experimentally induced by administration with the proinflammatory dextran sodium sulfate (DSS). Together, these works seem to support the idea that upon constitutive activation of the Wnt pathway (which constitutes the first step to cancer initiation) only cells with stem identity are able to initiate tumors with different efficiency according to their position in the hierarchy, and additional stimuli are needed to trigger tumor initiating ability in differentiated cells.

Less is known about the identity of cancer initiating cells in human. *CD133*$^{+}$ cells were first identified as potential human CRC initiating cells capable to efficiently renew the tumor after serial xenotranplants (Ricci-Vitiani et al. 2007). Later works showed that these tumor initiating cells probably form a heterogeneous population in which cells display distinct self-renewal and metastatic potential (Dieter et al. 2011). The identification of the molecular mechanisms involved in tumor initiation, self-renewal ability and heterogeneity represent a major issue for the design of tool for the effective eradication of cancer.

2.4. Genetic animal models of CRC

To better identify the alterations in the homeostatic processes associated with the initiation and progression of CRC as well as the possible targets for prevention and treatment, a number of genetic and non-genetic models have been developed (Johnson and Fleet 2013). The use of animal models allows avoiding the mutational complexity that is typically found in cancer cell lines, allowing the investigation on the impact of single genetic components. In vivo models also allow defining the role played by the microenvironment on tumor development. To be suitable for the study of the pathology these models were designed to respond to some important criteria. First, the development of cancer is limited to the intestine, in order to avoid the confounding effects exerted by neoplasia in other organs. Second, the histological and molecular features of lesions have to mimic as closely as possible those found in human cancer. To study the processes that are associated to tumor initiation, a panel of genetic models carrying a heterozygous germline mutation on the Apc gene was developed. During adult age these animals spontaneously lose the WT allele trough loss of heterozygosity and invariably develop adenomas in the small and large intestine at variable rate, recapitulating the condition of FAP patients. An important discrepancy between these models and human cancer consists in the fact that these mouse models carrying mutations on *Apc* develop tumor in the small intestine at higher rate than they do in the large intestine whereas the greatest majority of human CRC is found in the colon. This discrepancy is probably due to the inverse trend of proliferation rate that characterize human and mouse stem cells: stem cells divide more rapidly in the human colon than in the small intestine, which may explain the higher chance of biallelic loss in the colon (Sangiorgi and Capecchi, 2015). In this case the workhorse in the pre-clinical studies has been represented Apc^{Min} mouse identified from a mutagenesis screen in the the C57Bl6/J genetic background (Moser, Pitot, and Dove 1990). These mice carry a heterozygous T-to-A transversion at position 2549 which truncate the Apc

protein at amino acid 850. Other similar models were developed by homozygous recombination in the germline, as in the case of *Apc*$^{\Delta 14}$ mice (obtained through the Cre mediated germline deletion of the exon 14) that have features similar to those of *Apc*^{Min} mice but develop a higher number of intestinal adenomas at adulthood (Colnot et al. 2004). The *Apc*^{1322T} model was designed to express a 1322 amino acid Apc protein and retain one of the 20 aminoacid repeats that bind β-catenin, and was useful to examine the "just-right" hypothesis according to which the presence of at least one binding repeat represents the condition for optimal WNT signaling driving CRC initiation and progression (Albuquerque et al. 2002; Pollard et al. 2009). Other models were created to express non degradable β-catenin or defective form of the mismatch repair genes like *Msh2* (Reitmair et al. 1996). Conditional models are available to combine the expression of specific recombinase proteins to LoxP flanked sequences in order to study the immediate and/or specific effects of genetic alterations. The control of the temporal/spatial activity is conferred by the expression of the recombinase driven by a tissue or cell type related promoter. The best examples are constituted by the *Villin-Cre* mice, which allows targeting intestinal epithelial cells, the *Ah-Cre* mouse in which the expression is driven by the *P4501A1* promoter allowing the expression of the recombinase upon oral administration of mice with B-napthoflavone and the *Lgr5-EGFP-ires-Cre* mouse in which the oncogenic hit can be specifically induced in the intestinal stem cell compartment and is then inherited by its progeny (el Marjou et al. 2004; Ireland et al. 2004; Barker et al. 2007). Additional models are available to investigate the feature associated with invasiveness and metastasis. The combination of *Apc*$^{\Delta 14}$ allele and *Fabl-Cre;LSL-Kras*$^{G12D/+}$ or *Villin-Cre;LSL-Kras*$^{G12D/+}$ (i.e. in which one Kras allele is replaced by the oncogenic variant carrying a glycine residue replacing an aspartate on the chromosome 12) showed the development of more advanced tumors characterized by high-grade hyperplasia, loss of cell polarity and complete lack of terminally differentiated cells in these mice (Calcagno et al. 2008). *Apc*^{Min}*;Pten*$^{-/-}$ mice have larger more invasive tumors (Shao et al. 2007). *Smad3* knockout mice on the 129/Sv background develop aggressive carcinomas that are often accompanied by metastasis to regional lymph nodes (Zhu et al. 1998). An interesting model to screen the tumor-suppressor or oncogenic identity of genes in the intestine is constituted by the "Sleeping Beauty" system, in which the triple combination of the *Villin-cre*, *LSL-SB11 transposase* and *T2/Onc transposon* transgenes enhances transposition leading to random insertional mutagenesis in the intestinal epithelium (Starr et al. 2011).

3. Epigenetic dynamics in healthy homeostasis and cancer

According to its most popular definition, epigenetics describes the acquisition of measurable and stably heritable phenotypic traits that do not depend on changes in the DNA sequence. The genetic information contained in the DNA is packaged in the nucleus of each cell as a macromolecular complex, the chromatin, which is constituted by the interaction between DNA, proteins and RNA. Epigenetic mechanisms allow genetically identical cells to achieve diverse phenotypic characteristics by controlling the transcriptional availability of different regions of the genome through differential packaging and marking of the chromatin. Such a modulation of the information in the genetic sequence can be stably maintained, yet adapts to changing environmental or developmental needs. This dynamic adaptation is accomplished via the activity of different actors representing initiators, such as long non-coding RNA, writers, which establish the epigenetic marks, readers, which transduce the information of the epigenetic code modulating the availability of transcription factors and transcriptional machinery, remodelers, which dynamically alter the distribution of nucleosomes, and insulators that can form boundaries between the different domains in the chromatin (Shen and Laird 2013). Gene expression is modulated through a complex crosstalk between 3 main mechanisms: DNA methylation, histone modification and RNA interference (Dekker, Marti-Renom, and Mirny 2013).

Epigenetic regulation is indispensable for the control of embryonic development and adult homeostatic balance of tissues. During embryogenesis these mechanisms are well known to determine the lineage specification adopted by cells in the three germ layers. However, the precise involvement of the same mechanisms in post-natal homeostasis and in the stem cell function is less well understood in mammals and only in the recent years the development of pertinent *in vivo* models has made the information on the epigenetic control of adult stem cells accessible to investigators. Much more is known about the way these pathways are altered in cancer, since in this case the investigation benefits of the large availability of primary biopsies, animal and cellular models of many types of human cancer at different stages which can be easily compared with their non tumoral counterparts (Jones and Baylin 2002; You and Jones 2012).

The application of in-depth sequencing for the epigenomic profiling of cancer cells has led the field to the forefront of cancer biology (Ernst et al. 2011; Adams et al. 2012; ENCODE Project Consortium 2012). These *–omic* approaches have allowed scientists to focus on the

clinical relevance of global epigenetic signatures and provide novel tools with diagnostic and prognostic value.

3.1. DNA methylation

DNA methylation is a heritable epigenetic modification consisting in the covalent transfer of a methyl group to the C-5 position of the cytosine ring of DNA catalyzed by DNA methyltransferases (DNMTs). In plants, cytosine methylation occurs in asymmetrical (CHH, where H is A, C or T) and symmetrical (CH or CHG) contexts (Jones 2012). In mammals, DNA methylation occurs in every genomic context although more than 98% of DNA methylation is found in a CpG dinucleotide cotext in adult somatic cells, whereas as much as a quarter of all methylation appears in a non-CpG context in embryonic stem cells (ESCs). DNA methylation plays a role in a number of processes during development including X-chromosome inactivation, suppression of repetitive elements, regulation of transcription, transposition and genomic imprinting. Genomic imprinting is a mammalian specific epigenetic phenomenon that involves DNA methylation of precise genomic regions resulting in allele-specific methylation and parental-origin-dependent monoallelic expression. The global DNA methylation profile is erased during zygote formation and re-established in the embryo, except at imprinted regions. The methylation of DNA is regulated by a family of DNMT enzymes that use S-adenosyl-L-methionine (SAM) as a methyl donor: DNMT1, DNMT3A, DNMT3B and DNMT3L (Bestor 2000). DNMT1 preferentially interacts with hemimethylated DNA at the replication foci during the S phase of the cell cycle and is responsible for copying DNA methylation patterns to the nascent DNA strand (figure 15). DNMT1 is therefore commonly considered as a maintenance DNA methyltransferase (Probst, Dunleavy, and Almouzni 2009). *Dnmt1* knock-out mouse models display embryonic lethality at E9. In contrast to DNMT1, DNMT3A and DNMT3B have higher affinity for unmethylated CpG and perform *de novo* methylation (Okano et al. 1999; M. G. Goll and Bestor 2005). Mice lacking Dnmt3A die at about 4 weeks of age, whereas *Dnmt3B* knockout mice show embryonic lethality at E14.5 to E18.5. DNMT3L lack the methyltransferase enzymatic activity but support the activity of DNMT3A and DNMT3B by increasing their capacity to bind S-adenosyl-L-methyonine and stimulating their activity *in vivo* (Kareta et al. 2006). *Dnmt3l* homozygous-null mice are viable, but its importance in maintaining the monoallelic expression of imprinted loci was revelead in embyos of heterozygous mice derived from DNMT3L-null oocytes that die at E9 (Bourc'his et al. 2001). In mammals, nearly all CG

dinucleotides are methylated at cytosine residues especially in areas of repetitive sequences. On the contrary CpG-enriched regions, defined as CpG islands, are close to the 5' regions of the gene appear to be protected from this modification, in part by and guanine-cytosine strand asymmetry and accompanying R-loop formation and possibly also by active demethylation (Bird et al. 1985; Ginno et al. 2012). Methylation of CpGs in these regions occurs at variable extent in different cell types. Methylated cytosines are recognized and bound by methyl-CpG binding domain proteins (MBD) or zinc-finger protein (ZBTB) that are able to induce transcriptional repression by recruiting transcriptional co-repressors (Wade 2001). DNMT3A and DNMT3B each consist of an NH2—terminal regulatory domain that contain a PWWP domain, a cystein-rich domain, and a COOH-rerminal catalytic domain (Bestor 2000). The PWWP domain was shown to be required for the methylation of satellite repeats in the genome. DNA methylation at enhancers and promoters is correlated with priming and activation of lineage-specific genes at the appropriate time during embryonic and post-natal development (Bock et al. 2012; Easwaran et al. 2012). Conversely, promoters involved in stem cell gene expression become more methylated as cells commit to differentiation. Indeed, some recent functional studies showed that DNMT3A and 3B work in a redundant fashion in the *de novo* methylation of most genomic regions during adult stem cell differentiation, as demonstrated by the synergistic effect of the conditional ablation of both enzymes compared to the (Challen et al. 2014) impact of a single knock-out on the ability of adult stem-cells to self-renew and differentiate. DNMT3A is required for the methylation of imprinted loci during gametogenesis, whereas DNMT3B is not. Conversely DNMT3B is responsible for methylation of pericentromeric regions of the chromosomes. To further investigate this functional overlap and the specific genomic targets of these two enzymes, Liao and colleagues recently extensively characterized the effects of their targeted or combined CRISPR-Cas9-mediated disruption in human embryonic stem cells (hESC) (Liao et al. 2015). Double ablation of DNMT3 enzymes results in a progressive and rapid global reduction of DNA methylation, while single knockouts only display a mild phenotype, with the exception of genomic satellite sequences which appear to be more sensitive to the loss of DNMT3B. Authors found 96% of DMRs in double knock-out cells to be redundantly targeted by both DNMT3 enzymes, although regions accounting for high CpG density, like certain promoters, are more selectively targeted by one of those. This study confirmed that de novo enzymes act redundantly and are both implicated in the long-term maintenance of a pluripotent state, although a degree of differential affinity exists for a subset of genomic features.

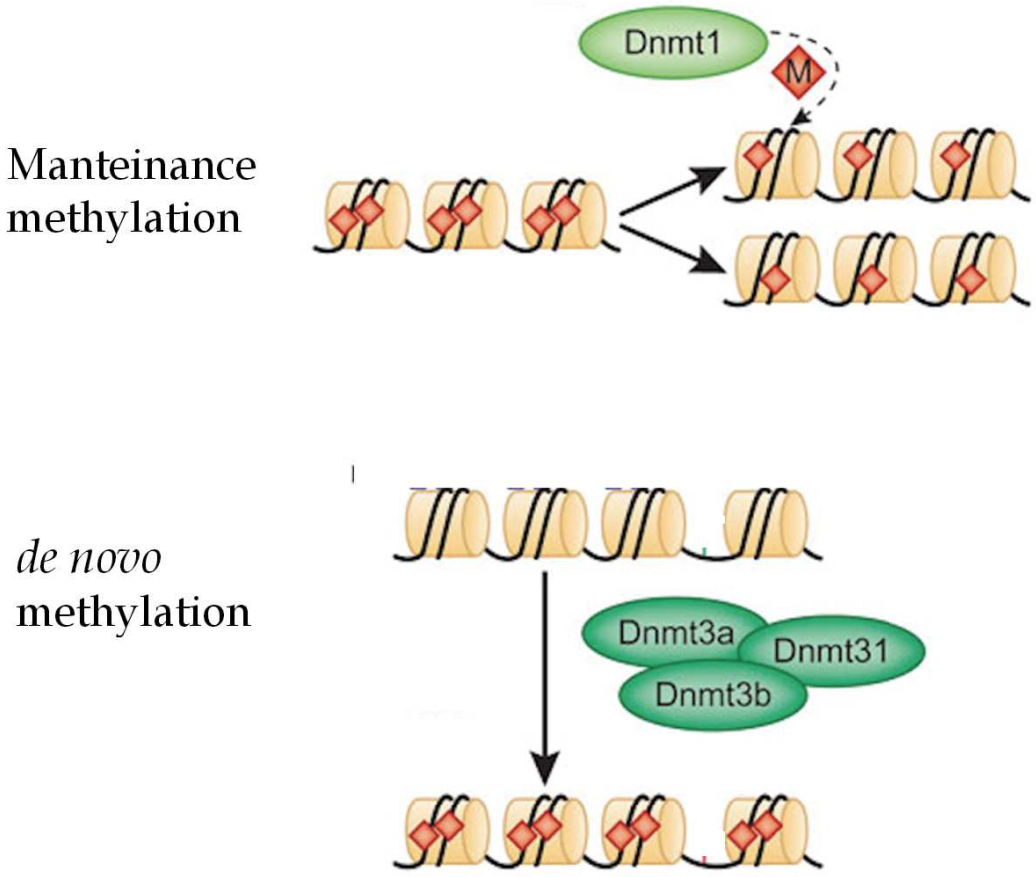

Figure 15: Schematic represantation of the involvment of the different DNMTs in mainteinance and *de novo* methylation of the DNA.

Mechanisms participating to active demethylation of the genome are way less understood. 5-methylcytosine can be further converted into 5-hydroxymethyl-22-deoxycytidine by the activity of the ten-eleven-translocation (TET) enzyme family members, eventually promoting cytosine demethylation (Tahiliani et al. 2009). However, the precise sequence of events leading to demethylation and the biological relevance of this process remains unclear, although increasing evidences show that mutations in *TET* genes are associated with various types of cancer (Rasmussen and Helin 2016).

Alterations in DNA methylation profiles represent a hallmark of cancer. In 1983 Feinberg and Vogelstein first documented that human adenocarcinoma samples are characterized by widespread genomic hypomethylation as they demonstrated by comparing tumor samples with their surrounding healthy mucosa (A. P. Feinberg and Vogelstein 1983). Several later works have extended this initial observation to many types of cancer, showing that the reduction of megabase-scale genomic domains preferentially occur in the repetitive portions of the genome and in regions overlapping with lamina-associated domains which interact with

the nuclear periphery (Berman et al. 2012). Hypomethylation of the genome is a universal feature shared by benign and malignant tumors and is therefore suspected to occur at the earliest stages of cancer development. This alteration then contributes to different aspects of cancer biology by leading to the overexpression of genes involved in tumorigenesis, to the aberrant activation to the activation of intragenic expression, genomic instability and loss of imprinting (LOI) (Aran et al. 2011; Aran and Hellman 2013; Aran, Sabato, and Hellman 2013) . On the other hand, tumor development is also accompanied by the focal hypermethylation of selective regions that often correspond to regulatory elements associated with the expression of genes with tumor-suppressive function (Wu et al. 1993; Herman and Baylin 2003; Andrew P. Feinberg and Tycko 2004; Hegi et al. 2005). The focal hypermethylation in human cancers was initially extensively documented for tumor suppressor genes such as retinoblastoma-1 (*RB1*), *MutL* protein homolog 1 (MLH1), *BRCA1*, adenomatous polyposis coli (*APC*) (Greger et al. 1989). These observations were later extended to several other genes that are specifically affected in different malignancies. In a recent attempt to describe the early alterations involved in colorectal cancer development Grimm and collaborators analyzed the methylation profiles of intestinal adenoma from $Apc^{Min/+}$ mice (Grimm et al. 2013). The authors found that a large number of alterations are produced in early adenomas although the global alteration in gene expression profiles poorly correlates with the global extent of methylation of DMRs at this stage. Importantly, they found that hypermethylation of tumor-suppressor genes occur very rarely at this stage, suggesting that in the case of colorectal cancer this mechanism should be considered as a late mechanism in tumor progression more than as early instructive step. These results also suggest that this epigenetic signature arise *de novo* and do not represent the expansion of a signature associated to any given intestinal population such as the stem compartment. Until recently, however, very little was known about the contribution of DNA methylation to the mechanisms governing the homeostatic balance of intestinal epithelium and whether the disruption of these mechanisms participates to colorectal cancer onset. A recent work showed that some important changes occur in the methylation profiles during differentiation of epithelial cells (Sheaffer et al. 2014). These changes are not often associated to regions closely associated to gene promoters and are more frequent found in active intestinal enhancers of genes. Reduction in the methylation of gene enhancers associated with intestinal lineage specification coordinates the binding of transcription factor allowing the activation of expression as cells differentiate. Conversely, enhancers of genes associated with stem identity are methylated, which allows the repression of those genes. In accordance with these results

the same work shows that conditional deletion of *Dnmt1* results in an expansion of intestinal crypts associated with an impaired differentiation of intestinal stem cells into post-mitotic lineages. Expression of the three DNA methyltransferases in the intestinal epithelium was shown to occur in a crypts-to-villus gradient, with the highest amount expressed in the stem fraction. This compartimentalization is coherent with the requirement of maintenance and de novo and methylation in actively proliferating cells that need to remodel their methylation profile as they commit to differentiate. Due to the embryonic lethality associated with mutations in these genes, there are no evidences for genetic alteration associated with colorectal cancer incidence in the population. However, upregulation of *de novo* methyltransferases expression has been reported as a feature of the colorectal adenoma-to-carcinoma sequence (Lin et al. 2006). The activity of both *de novo* enzymes is associated with the rate of intestinal tumor initiation in animal models. Transgenic over-expression of one or the other gene in $Apc^{Min/+}$ background was associated with an increase in intestinal tumor load. The overexpression of Dnmt3 enzymes correlate with increased methylation and reduced expression of precise target genes that are known to represent risk loci associated with colorectal cancer development, such as the oncosupressor *Igf2*, and the *Sfrp2* and *Sfrp4* genes coding for the Wnt pathway extracellular inhibitors (Linhart et al. 2007; Samuel et al. 2009). Analyses of the normal mucosa suggested that these few particular genes represent targets for aberrant *de novo* methylation in the pre-neoplastic tissue before the earliest oncogenic alteration occurs. DNA methylation was also shown to represent a prognostic marker for CRC. In 2011 the analysis of the transcriptomic profiling performed on cohorts of patients suggested that prognosis correlates with the extent of the expression of WNT target genes (de Sousa E Melo et al. 2011). The results described in this work confirmed the existence of a counterintuitive positive correlation between expression of WNT target genes and survival, and that reduced expression of WNT targets is associated with an increased chance for patients to progress more rapidly toward the malignant stages of the disease. Strikingly, the authors showed that the reduced expression of WNT target genes is associated with focal hypermethylation of CpG islands associated with the expression of those genes.

During the recent years, DNA methylation inhibitors have widely been proposed as possible therapeutic agents (Hatzimichael and Crook 2013). The two most frequently used DNA inhibitors are the azanucleosides 5-azacytidine and 5-aza-2-deoxycytidine), representing cytosine analogues working as demethylating agents through the covalent trapping of DNA methylatrasferases once they are incorporated into the DNA. Both of these agents received the

FDA approval for the treatment of myelodisplastic syndromes and acute leukemia (Itzykson and Fenaux 2011). Although these molecules have showed their efficacy in promoting the demethylation of tumor suppressor genes and in restoring the sensitivity to chemotherapeutics in various cancer models, their use in clinical trials provided less encouraging results in the case of solid tumors, probably due to the relatively reduced proliferative rate of these tumors. It should be noted that these agents are highly cytotoxic and non-specific, making the robust evaluation of the effectiveness of DNA methylation inhibition as a therapeutic strategy more complicated.

3.2. Histone modification and the histone code

The basic unit of chromatin, the nucleosome, consists in a 146-bp DNA loop wrapped around an octamer of core histone-proteins (two H2A/H2B dimer and H3/H4 tetramer). Histone proteins are decorated at their N- and C-terminal domains by different covalent modifications including acetylation, methylation, phopshorylation and ubiquitinylation. These post-translational modifications determine whether chromatin domains are organized in a densely compact and inactive state (heterochromatin) or in a more open and active configuration (euchromatin). Post-translational modifications of histones are coordinated by families of enzymes that are responsible for adding or removing every mark, such as acetyltransferases (HATs) and histone deacetylases (HDACs), histone methyltransferase (HMTs) and demetylases (KDMs). A list of the post-translational modification and their position on histone tails is provided in the figure 16.

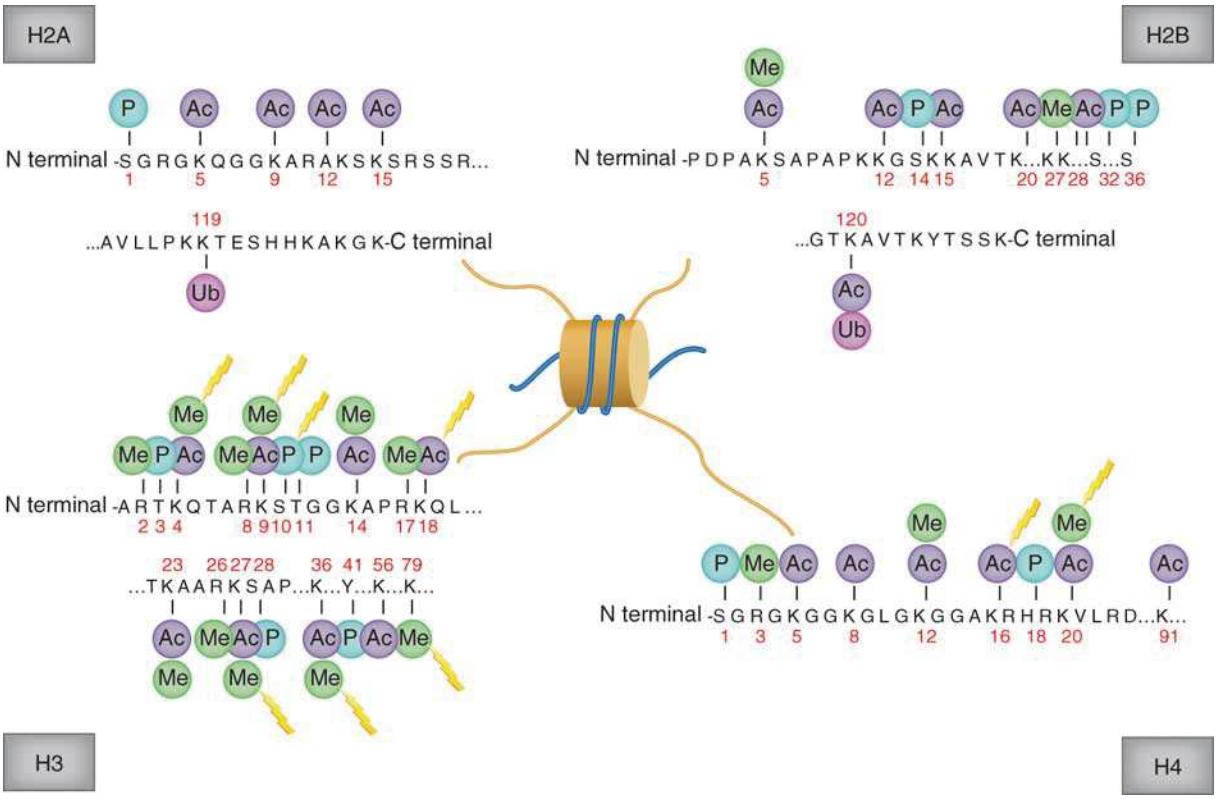

Figure 16: schematic representation of post-translational histone modifications. Covalent modification proper to each position on the histone H2A, H2B H3 and H4 are indicated. Ac: acetylation; Me: methylation; P: phosphorylation; Ub: ubiquitinylation. (Rodríguez-Paredes and Esteller 2011)

In animals, histone modifiers act in complex. Polcomb repressive complexes (PRC) 1 and 2, and the Thritorax group are guided to their targets by specific motifs in the genomic sequence (Tanay et al. 2007; Ku et al. 2008). The PRC2 complex act by catalyzing the trimethylation of the lysine 27 (H3K27me3) of the histone 3 which provide a docking site for the PRC1 complex, whose enzymatic core RING1B monoubiquitinylates the histone H2A at lysine 119 (H2K119ub1) thereby impeding the RNA polymerase II elongation (Mills 2010). The trithorax group complex, containing the MLL acetyltransferase which lays down the acetylation of the lysine 4 on the histone H3, and the KDM6A demethylase that removes the H3K27me3 mark and counteracts the repressive function of the polycomb groups (Mills 2010). Despite the extensive literature describing the role of these complexes in regulating gene transcription during embryonic stem cell differentiation and embryonic development, their roles in the biology of adult stem cells is still largely unexplored. One interesting feature of embryonic and adult stem cells consists in the existence of bivalent domains on regions corresponding to the transcription factors responsible for differentiation of specific lineages. These regions are decorated with both the activating H3K4Me3 and the suppressive

H3K27me3 marks (Bernstein et al. 2006). Upon differentiation the Trithorax group complex removes the repressive H3K27me3 allowing the transcription of specific transcription factors required for the specification into a particular lineage, whereas genes that are not required for that particular lineage lose the activating H3K4 mark and undergo spreading of the H3K27 mark that terminally represses the transcription of those genes (Hawkins et al. 2010). Gene enhancers in absorptive and secretory progenitors in the intestinal epithelium were shown to present comparable levels of H3K4me2 and H2K27ac histone marks that define an accessible permissive chromatin configuration (T.-H. Kim et al. 2014). This observation may represent an epigenetic mechanism underlying the plasticity previously described for intestinal progenitors and also represent a possible explanation for the capacity of progenitors to undergo lateral inhibition controlling the choice between absorptive and secretory fate.

The PRC1 complex was shown to actively ensure the maintenance of intestinal stem cell identity and self-renewal capacity by sustaining the activity of the Wnt pathway through the repression of members of the ZIC family transcription factors that interfere with the transcriptional activity of the β-Catenin/Tcf4 complex (Chiacchiera, Rossi, Jammula, Piunti, et al. 2016). Indeed, the conditional deletion of RING1B results in the overexpression of the Zic TF and in the displacement of β-Catenin/Tcf4 from their target promoters in intestinal *Lgr5*-positive cells, therefore altering not only the self-renewal capacity but also the β-Catenin oncogenic activity of these cells. The same group found that the PRC2 complex is involved in secretory lineage commitement by regulating specific transcription factors (Chiacchiera, Rossi, Jammula, Zanotti, et al. 2016). It was also already known that the PRC2 complex is involved in terminal differentiation of intestinal epithelial cells. Ideed the RNA-i mediated knockdown of the SUZ12 core subunit of the PRC2 complex in the Caco2/15 intestinal cell line induces the loss of H3K27me3 mark and the activation of the enterocytic differentiation program (Benoit et al. 2012). A vast and increasing literature extensively supports the mechanistic role of genetic alterations in the modulation of the histone code in cancer development. As an example, aberrant translocation of the MLL gene encoding for one of the H3K4 methyltransferases accounts for about 80% of infant leukemia. The primary mechanism in this case is attributed to the inappropriate recruitment of epigenetic factors on the MLL target genes, resulting in the disruption of the genetic silencing (Tan et al. 2011). Recent studies have revealed that some important features of cancer are defined by alterations whose nature is purely epigenetic. In 2014, the bimodal prognostic classification of children affected by ependymomas was shown to be associated with a Polycomb repressive complex target signature corresponding to a CpG island methylator phenotype of the same loci (Mack

et al. 2014). Patients affected by this malignancy are indistinguishable trough genomic analyses, which revealed the absence of genomic alterations and zero recurrent somatic nucleotide variants associated with the poor- or good-prognosis groups. However, the PRC2 binding signature and DNA methylation profiles found in the tumor samples are completely predictive of prognosis in these young patients.

3.3. MicroRNA

MicroRNA mediated interference represent an additional highly conserved epigenetic mechanism adopted throughout the animal and plant kingdoms in order to modulate the information contained in the genomic sequence (Hayes, Peruzzi, and Lawler 2014). These transcripts are encoded as single miRNA or clusters of miRNAs and processed through a conserved mechanism to their mature single-stranded form which can then associate to the RNA-induced silencing complex (RISC) (Krol, Loedige, and Filipowicz 2010). This interaction typically result in the reduced translation or deadenylation and degradation of multiple target mRNA that are recognized trough the complementarity between the mRNA and the 5' "seed" region of the miRNAs (figure 17). After their discovery in 1993, an impressively vast literature has shown the role of miRNAs in the modulation of any biological process as well as their implication in the development of pathologies. MicroRNAs dysregulation in cancer was first observed when genes encoding for Mir-15 and Mir-16 were found to be located in a genomic region that is frequently deleted in chronic lymphocytic leukemia (Calin et al. 2002). These microRNAs negatively regulate the expression of the antiapoptotic factor BCL2. Since then it has been documented that miRNAs play roles in all of the cancer hallmarks. Screening performed to examine the expression of miRNAs in CRC identified many alterations possibly implicated with cancer development as tumor suppressor or oncogenes. Mir143 and mir145 represent examples of tumor suppressive microRNA regulating cell growth and possibly stemness (Michael et al. 2003). Mir-21 has well characterized oncogenic function in many cancer types and its expression in CRC is well documented (Volinia et al. 2006; Selcuklu, Donoghue, and Spillane 2009). Several other miRNAs have been implicated in many features of CRC development, invasiveness and metastasis. However, the role of miRNAs in regulating the biology of the intestinal epithelia and their implication in the rupture of homeostasis is still poorly investigated. In a recent work a complex feedforward loop mechanism involving miR34a, Notch and the Notch inhibitor Numb was shown to regulate symmetric cell division and fate decision and to

counter excessive proliferation of intestinal stem cells under inflammatory condition (Bu et al. 2016). The authors also showed that this mechanism can induce asymmetric cell division in colorectal cancer stem cells in order to limit excessive proliferation but it is subverted but the silencing of mi-34a at later stages of cancer progression.

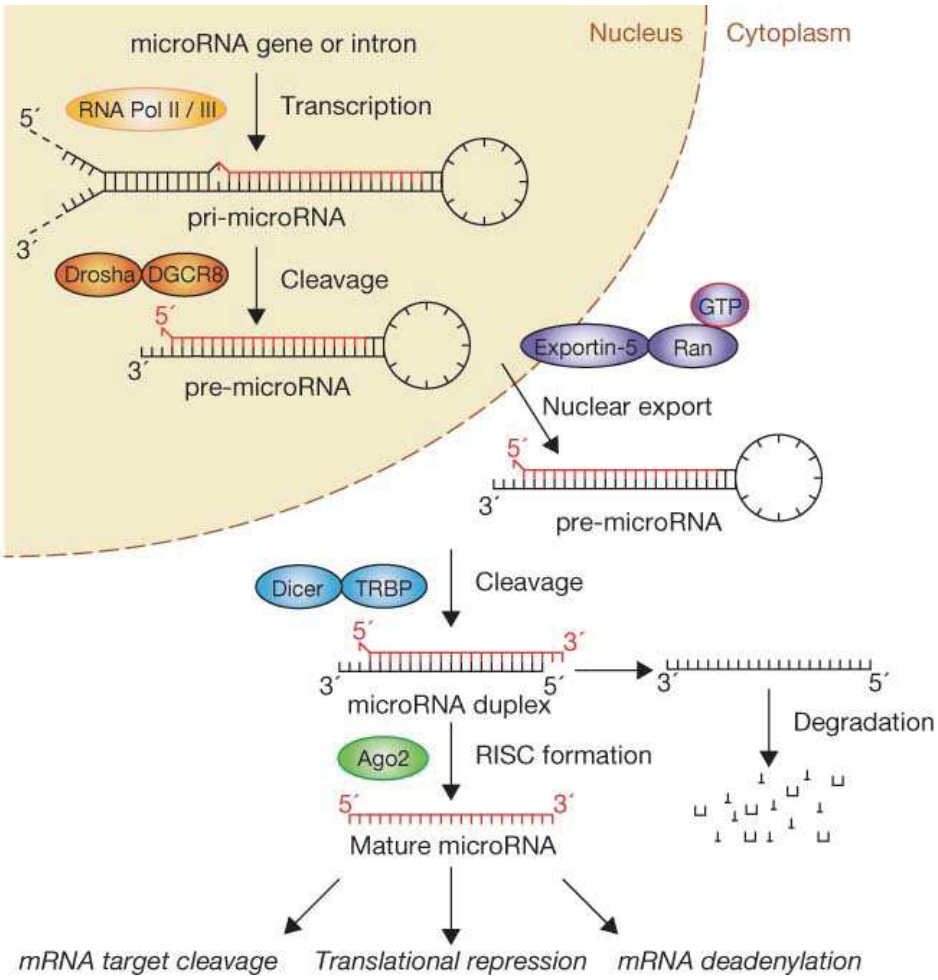

Figure 17: microRNA biogenesis and function. microRNA are produced through the transcription and processed by the Drosha complex before they are exported in the cytoplasm and additionally processed before they are included in the RISC complex. Suppression of gene expression is mediated via different mechanisms depending on the degree of complementarity with the target mRNAs. (Krol, Loedige, and Filipowicz 2010)

3.4. The epigenetic progenitor: a unifying model in cancer etiology

Although cancer cells have long been represented as the best example of the phenotypic result of genetic alterations, genomic and epigenomic analyses are increasingly revealing the widespread misregulation of epigenetic mechanisms at all steps of cancer development. The disruption of the epigenetic regulation currently represents a major focus in the study of

cancer biology. In the previous sections we summarized whether genetic and epigenetic mechanisms can influence each other and cooperatively interfere with the factors involved in the maintenance of normal homeostatic balance. These evidences have prompted the formulation of a theory known as the epigenetic progenitor origin of cancer (Andrew P. Feinberg, Ohlsson, and Henikoff 2006). According to this model, epigenetic alterations may occur in a population of healthy progenitor cells prior to the accumulation of the tumor-initiating genetic alteration. Such epigenetic disruption would result in an alteration of the balance between proliferation and differentiation or in an increased susceptibility of a subpopulation of cells to genetic alterations (figure 18). These epigenetic alterations are likely to concern genes involved in the maintenance of stemness. In this model, the stochastic or environmentally induced epigenetic imbalance of stem cells is followed by a cancer initiating mutation involving a tumor suppressor or a gatekeeper gene in the population of epigenetically disrupted progenitors. Such a mutation further increases the genetic and epigenetic plasticity of the progeny, allowing the subsequent development of distinct sub-clones responsible for tumor evolution. Multiple lines of evidences support this model. Importantly, some epigenetic features such as the global hypomethylation of the genome represent hallmarks of oncogenic transformation, which are supposed to occur very early during tumor development. In addition, hypermethylation and silencing of certain loci are retrieved in the healthy tissue of cancer patients, suggesting that these alterations may even occur prior to cancer initiation. In addition, genomic instability which is commonly used to explain rapid clonal evolution does not apply to most solid tumor types which are genomically stable yet display high plasticity. At present, however, the epigenetic progenitor cancer model remains speculative and still awaits a formal demonstration.

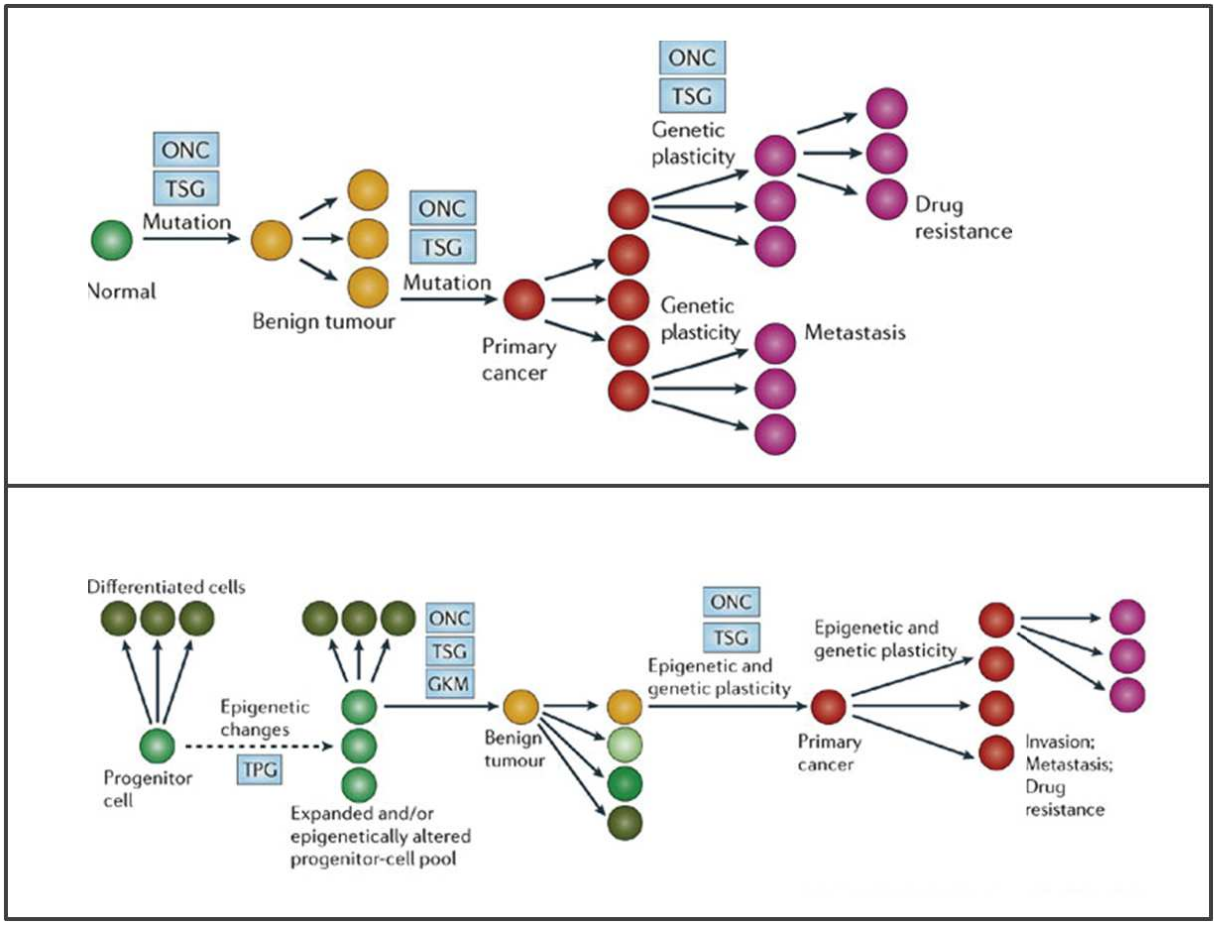

Figure 18: the epigenetic progenitor model of cancer development. A) Schematization of the classic view: upon the initiating mutation the tumor initiating cells start dividing rapidly and additional mutations clonally selected to give rise to the tumor heterogeneity responsible for different features of aggressive cancers. B) The epigenetic progenitor model: adult progenitor cells are epigenetically and become more prone to accumulate the oncogenic alteration driving tumor initiation. Further genetic and epigenetic alterations increase the plasticity of tumor cells. TSG: tumor-suppressor gene; ONC: oncogene; TPG: tumor-progenitor gene; GKM: gatekeeper mutation (Andrew P. Feinberg, Ohlsson, and Henikoff 2006)

AIMS OF THE WORK

Cancer represents nowadays one of the main concerns, if not the greatest concern, in public health management. The elucidation of the mechanisms implicated in cancer susceptibility, initiation and progression toward its latest stages has also largely contributed in promoting the basic understanding of their contribution to the control of the normal homeostatic balance in cells and tissues. The outstanding accomplishments made during the last few decades in the identification of the genetic changes involved in cancer development have been accompanied by comparable advances in the characterization of the epigenetic control of malignancies. These include (but are not limited to) the role of widespread epigenomic changes, such as the alteration of the DNA methylation profiles, the nuclear architecture and the nuclear compaction. For multiple experimental reasons, such as the relative ease to recover the biological substrate from different types of sample, DNA methylation has long represented the most well studied epigenetic modification in cancer (Kulis and Esteller 2010; Sandoval and Esteller 2012). Some alterations associated with this modification are now considered as hallmarks of cancer development and currently represent targets for the discovery of prognostic biomarkers and for the development of therapeutic strategies. General hypomethylation of the genome represented the first widespread alteration to be ubiquitously retrieved in cancer samples, independently on the stage and on the genetic pathway associated with cancer initiation (A. P. Feinberg and Vogelstein 1983). In the case of colorectal cancer, genome-wide hypomethylation is thought to occur very early, probably immediately after the first oncogenic mutation which is commonly represented (80% of sporadic CRC) by the loss of *APC*. Focal hypermethylation of regions controlling the expression of genes with tumor suppressive function also represents an interesting debated issue. Some evidences show that even this kind of change may occur very early, even prior to the genetic alteration driving oncogenic transformation, as demonstrated by the fact that hypermethylation of certain genes is found in the non-tumoral healthy tissue of animal models and in patients (Linhart et al. 2007). However a recent work raised some concerns on whether these alterations actually represent rare stochastic events subjected to clonal selection rather than a general instructive mechanism associated with intestinal tumorigenesis (Grimm et al. 2013).

In 2006 some authors speculated that epigenetic disruption of stem/progenitor cells may represent a possible common mechanism in cancer etiology (Andrew P. Feinberg, Ohlsson, and Henikoff 2006). Their model proposes that epigenetic alterations may represent the

earliest source of the impairment in the homeostatic balance occurring in multipotent cells, and that this disruption may set the stage for the subsequent accumulation of genetic alterations. Increasing evidences show that cells at the top of tumor hierarchy (i.e. tumor initiating cells and/or tumor stem cells) are reminiscent of the features describing normal stem cells, i.e. self-renewal ability and multipotency, and should therefore be considered as a mutated counterpart of these latter.

However, one main concern can be raised on the strategy used to obtain the evidences presented so far, which is intrinsically summarized in the title of the landmark work "*Hypomethylation distinguishes genes of some human cancer from their normal counterpart*" published in 1983 (A. P. Feinberg and Vogelstein 1983). Since then, the experimental strategy to investigate the epigenetic features of cancer development has always consisted in the comparison between the tumor samples and their surrounding healthy tissue. Such a comparison accounts for an intrinsic heterogeneity since cell types in cancer and healthy tissue are differentially represented, which inevitably results in a different representation of the molecular signatures associated to each of these cell types. This heterogeneity becomes confounding when we consider that each tumor arises from a single cell belonging to one precise population. In other words, the comparison of healthy and tumor samples, even in the case of very early lesions, cannot allow formulating conclusions about the timing at which epigenetic alterations actually occur and what their role is in promoting the earliest phases of cancer.

The present work aims at tackling two main questions about the epigenetic contribution to cancer initiation and to the modulation of cancer susceptibility:

1) ***How early do the epigenetic alterations occur upon the earliest genetic events in the sequence driving oncogenic transformation, and how do these changes functionally contribute to the phenotypic traits acquired by tumor cells?***

To answer this question we examined the genomic methylation and gene expression profiles of intestinal epithelial cells *in vivo* early after the loss of one or both *Apc* alleles, which represents the most common alteration associated to human CRC initiation. To do so, we made use of conditional mouse models in which the recombination of *Apc* is specifically targeted to epithelial cells, since the expression of the recombinase Cre is under the control of epithelial promoters. The initial characterization was performed on the genomic DNA and coding RNA recovered from *Lgr5*$^{+}$ intestinal stem cells, whose isolation was allowed by the use of an *Lgr5-EGFP-ires-Cre*^{ERT2} transgenic model in which none, one or both alleles of *Apc*

contain LoxP sites flanking the exon 14 of the gene (*Apc*$^{+/+}$*; Lgr5-EGFP-ires-Cre*^{ERT2}, *Apc*$^{LoxP/+}$*; Lgr5-EGFP-ires-Cre*^{ERT2}, *Apc*$^{LoxP/LoxP}$*; Lgr5-EGFP-ires-Cre*^{ERT2}). It should be noted that, at least in the context of constitutive Wnt activation as the tumor initiating event, intestinal stem cells are so far considered as the population most likely involved in tumor initiation.

The DNA methylation profiles presented in this work were obtained in collaboration with the team of Michael Weber (École Supérieure de Biotechnologie de Strasbourg) by using a reduced representation bisulfite sequencing (RRBS) approach (Meissner et al. 2005). This high-throughput analysis allows the investigation of DNA methylation profiles on a single nucleotide level. RRBS combines restriction enzyme mediated digestion and sequencing of the DNA in order to restrict the analysis on the genomic regions that have high CpG content (CpG islands, representing about 1% of the genome). These regions include the majority of promoters and repeated sequences.

Epigenetic modifications are, by definition, reversible. To challenge the possible biological impact of the signature we tried to modulate the activity of the machinery responsible *for de novo* DNA methylation and evaluate its contribution to the acquisition of the tumorigenic phenotype of intestinal epithelial cells upon the loss of *Apc*. This functional validation was performed by using *in vitro* organotypic models, which recapitulate in many ways the physiology of the intestinal epithelium. Organoids were obtained by culturing intestinal epithelial cells from a transgenic conditional model in which the expression of the recombinase Cre is driven by the epithelial *Villin* promoter (*Apc*$^{+/+}$*; Villin-Cre*^{ERT2}*;*. *Apc*$^{LoxPLoxP+}$*; Villin-Cre*^{ERT2}*).*

2) ***How does the epigenetic variability existing within a population account for the heterogeneous relative risk to develop cancer independently on the genetic heterogeneity?***

Epigenetic mechanisms modulating the extent of gene expression are of course key mediators of the biological variability. Many efforts have been spent to characterize the genomic features of patients affected by different types of cancer in order to identify genetic loci associated with increased relative risk (The Cancer Genome Atlas, 2012). However the epigenetic control may provide a supplemental layer of complexity. A work published in 2011 showed that cohorts of isogenic animals (i.e. genetically identical) display a large degree of heterogeneity in terms of the extent of DNA methylation at multiple regions of the genomes resulting in heterogeneous expression of associated genes (Andrew P. Feinberg and Irizarry

2010). The analysis of differentially methylated regions revealed that these are often associated with the expression of genes implicated in key developmental processes. These results confirm that the heterogeneity existing within a population is, at least in part, modulated by the epigenetic variability. We therefore decided to investigate the existence of a molecular signature in the healthy intestine associated with differential susceptibility to develop intestinal cancer. To do so, we made use of a constitutive inbred model consisting in isogenic mice carrying a germline heterozygous mutation on *Apc* (*Apc*$^{\Delta 14/+}$). These mice invariably develop multiple adenomas during their adult life, although the severity of the phenotype (i.e. the number of adenomas developed at a given age) is largely variable. Since these mice are genetically identical, the source of such a phenotypic heterogeneity is to be researched elsewhere. We therefore examined the molecular profiles (RRBS and transcriptomic analyses) found in the healthy (tumor-free) intestine of isogenic mice with variable degree of susceptibility, which we quantified according to the number of tumors found at the age of sixteen weeks. In order to test the capacity of these signatures to be predictive of the relative risk to develop multiple adenomas before the pathology initiate, we designed and validated in collaboration with the team of Michael Helmrath (MD, MS, director of the surgical intestinal rehabilitation research program at the Cincinnati Children Hospital) a surgical strategy according to which intestinal samples are collected in young mice before tumors have time to develop and variability becomes extensive. Animals were then let age and develop tumors in order to correlate the severity of the pathology with the molecular signature found in the previously collected tumor-free intestinal biopsies from the same individuals. However, the development of an effective surgical protocol required us a very long set-up. At the same time, we therefore decided to investigate the correlation between the molecular profiles found in the tumor-free portion of the intestine of adult mice (sixteen weeks) and their individual susceptibility (numbers of adenomas developed at sacrifice when intestinal samples are collected). This double approach allowed us to test whether the molecular signatures in the healthy intestine are informative of individual risk to develop tumors at two different stages: before tumor initiation, and after the heterogeneous development of multiple adenomas has occurred.

RESULTS

SECTION I: ALTERATIONS IN THE DNA METHYLATION AND GENE EXPRESSION PROFILES UPON THE ONCOGENIC ACTIVATION OF THE WNT PATHWAY AND THEIR FUNCTIONAL IMPACT ON EPITHELIAL HOMEOSTASIS

1. Epithelial response to the loss of *Apc*

Inactivation of *Apc* in intestinal epithelial cells results in the rapid translocation of the β-catenin and constitutive activation of the Wnt pathway, whose immediate effects consist in the impairment of cell differentiation and migration (Sansom et al. 2004). This alteration induces distinct biological responses in the proliferative and differentiated compartments, governed by the different molecular programs activated in immature and post-mitotic cells (Andreu et al. 2005).

$Apc^{LoxP/Loxp}$; $VillinCre^{ERT2}$ animals become visibly ill and have to be sacrificed at day 6 after the injection with tamoxifen. At this time point the intestinal epithelium displays the expected "crypt-like" phenotype, in which proliferating cells exceed the crypt-villus boundary and occupy the majority of the axis (figure 19). However, at day 1 post-injection the morphology of crypts appears normal or slightly hyperproliferative, and the phenotype is then acquired gradually, as shown by the progressive increase in the number of Ki-67 positive cells in the crypt compartment. The opposite trend is observed for the alkaline-phosphatase staining, indicating a progressive elimination of terminally differentiated cells in the crypt-villus axis. These observations indicate that, as expected, the loss of *Apc* does not induce a dedifferentiation of mature cells, and the crypt-like phenotype is rather associated to the renewal of the epithelium in which terminally differentiated cells are gradually replaced by actively proliferating ones.

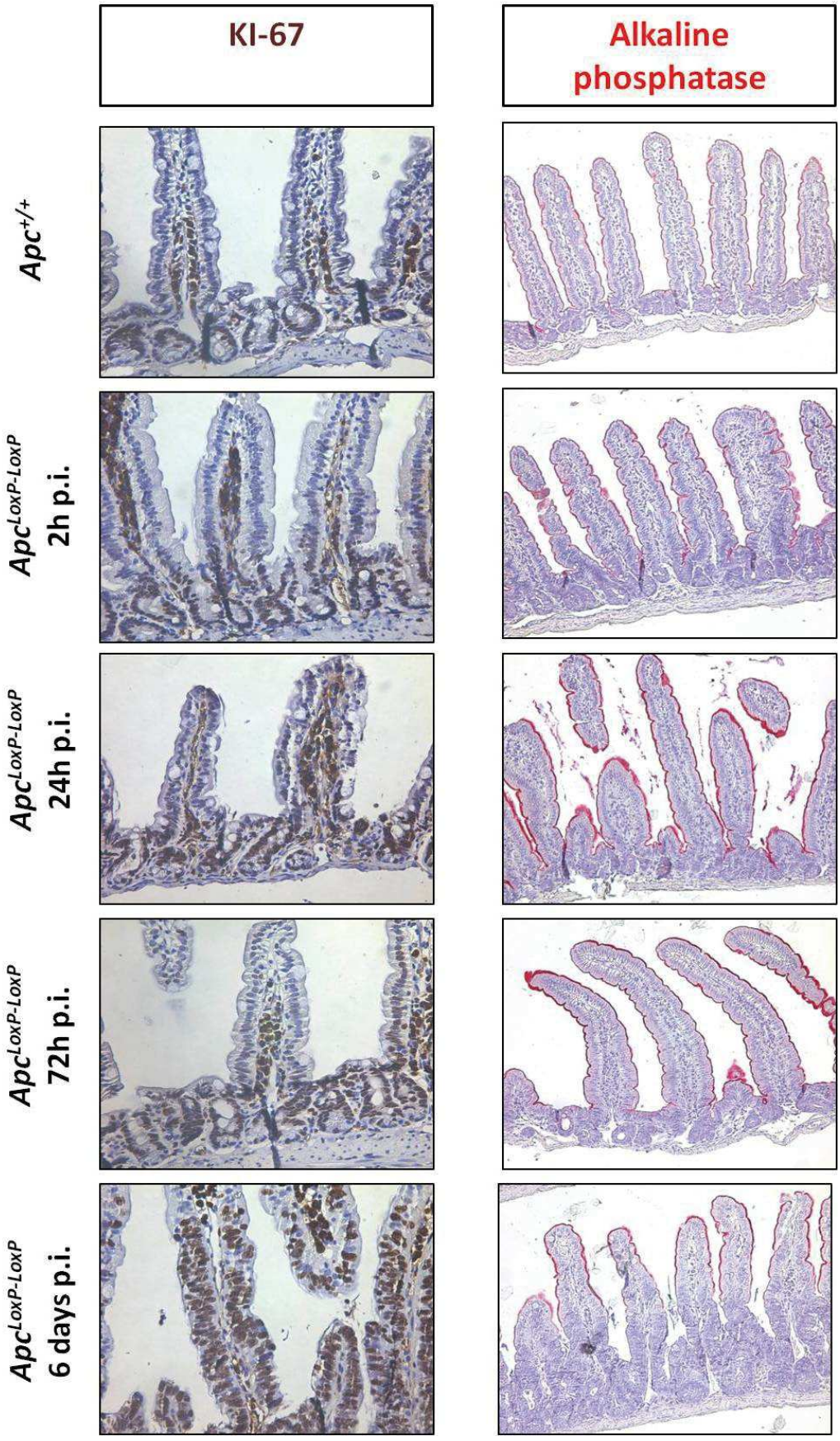

Figure 19: ***Apc*** **loss results in increased proliferation and** ***de novo*** **differentiation but not in de-differentiation of intestinal epithelial cells of** $Apc^{LoxP/LoxP}$**;** $VillinCre^{ERT2}$ **mice. Ki-67 immunostaining (left**

panels) indicates actively proliferating cells at different time points after injection with tamoxifen (40X magnification). Alkaline phosphatase staining (right panels) highlights the terminally differentiated compartment at the same time points (20x magnification).

The crypt-like phenotype is associated with a shift in the expression of some markers in the epithelium of $Apc^{Loxp/Loxp}$ mice that were selected among target genes of Wnt signaling activation (*Lgr5*, *Myc*), DNA methyltransferas (*Dnmt1*, *Dnmt3b*), and factors belonging to histone modifier complexes (*Eed*, *Ezh2*, *Bmi1*, *Hdac2*). All of these genes are up-regulated in the *Apc*-deficient epithelium. The immunostaining of Dnmt1 confirmed that six days post-injection its expression co-localizes with markers of active cell division (PCNA) and exceeds the crypt-villus junction, further demonstrating that a distinct program is maintained in the immature compartment and propagated in hypertrophic crypts (figure 20).

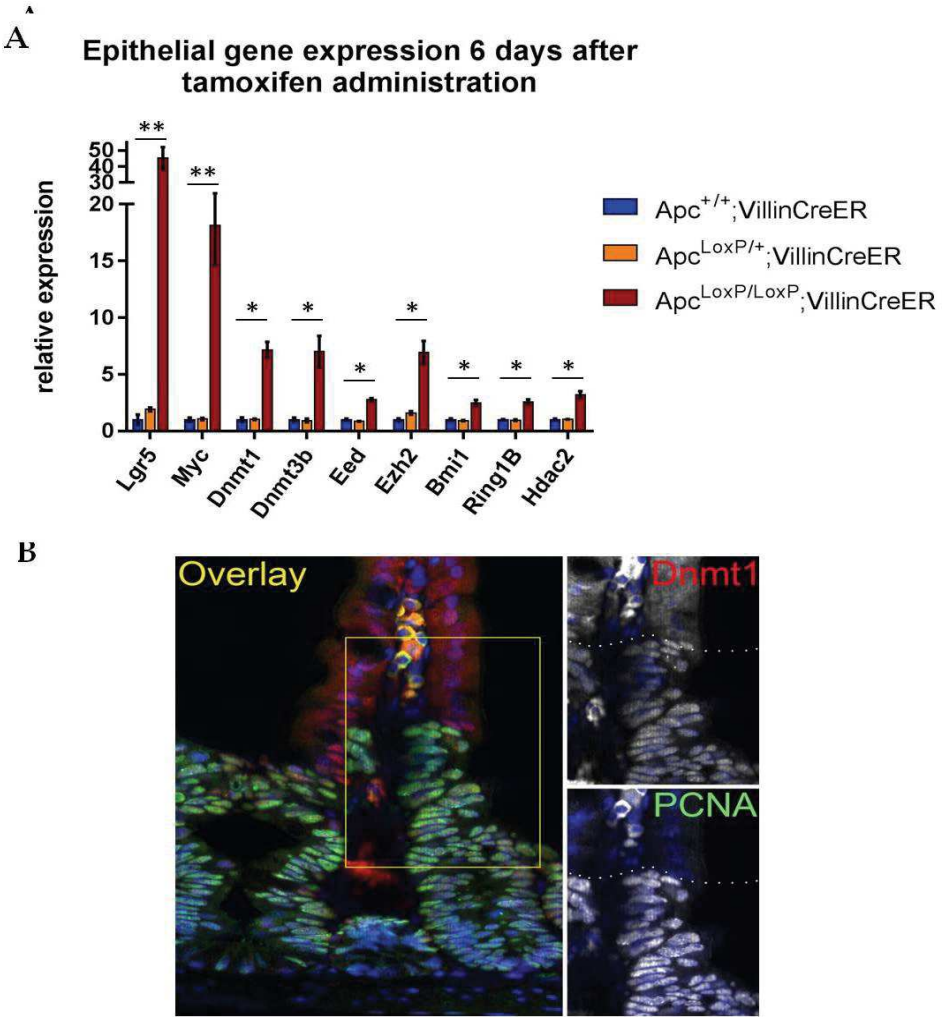

Figure 20: the hypertrophic proliferative compartment upon the deletion of *Apc* in the intestinal epithelium. A) Relative gene expression of Wnt targets (*Lgr5*, *Myc*), DNA methyltrasferases (*Dnmt1*, *Dnmt3b*) and components of the Polycomb repressive complex in the $Apc^{+/+}$, $Apc^{LoxP/+}$, $Apc^{LoxP/LoxP}$; *Villin-*

Cre^{ERT2} epithelium 6 days after the administration with tamoxifen. Results represent the average of 4 biological replicates and are normalized on the expression of the *Gapdh* and *Hprt* housekeeping genes. Error bars represent S.E.M. * represents a P-value <0.05, ** P-value<0.01 as calculated by the Mann-Whitney *U*-test. B) immunostaining showing the pattern of expression of Dnmt1 (red) and PCNA (green) in the intestinal $Apc^{LoxP/Loxp}$ epithelium 6 days after the administration of tamoxifen. Hoechst (blue) is used to stain the nuclei; 40x magnification

2. The loss of *Apc* induces an expansion of the CBC compartment and alters the cell cycle dynamics of $Lgr5^+$ cells

Given the epithelial morphologic and molecular changes associated with the loss of *Apc* in the *Villin-*Cre^{ERT2} model, we reasoned that any comparison between the Apc^{WT}, Apc^{Het} and Apc^{KO} epithelium in this model would rather reflect the impairment in the epithelial architecture and ratio of proliferating versus differentiated cells. We therefore decided to better focus the attention on the immediate outcome associated with the constitutive activation of the Wnt pathway in $Lgr5^+$ CBC cells by making use of the $Lgr5^+$*-EGFP-ires-*Cre^{ERT2} model. This model provided us with multiple advantages:

1) The variegated expression of the transgenic locus (about 1 out of 4 crypts express the recombinase, figure 21), results in a less sever phenotype, which allows the characterization of the effects of inactivation of *Apc* at later time points than in the case of the *Villin-*Cre^{ERT2} model, in which the duration of the experiment is limited by the short survival of the animals (sacrifice at day 6 days upon the first injection). We reasoned that fifteen days might represent a reasonable lapse of time for the *de novo* establishment and propagation of DNA methylation patterns within the crypt compartment.
2) The recombinase is specifically expressed by $Lgr5^+$ cells, which allows us to determine the impact exerted by the constitutive activation of the Wnt pathway on the intestinal stem cells and their immediate progeny.
3) The locus contains a reporter gene (coding for enhanced GFP), allowing us to isolate the *Lgr5*+ cell population, representing the main tumor cell-of-origin population, and monitor the progressive outcome of the recombination in this specific cell compartment.

As expected, fifteen days after the administration with tamoxifen nearly 100% of GFP-positive cells display the translocation of the β-Catenin (hallmark of the activation of the Wnt signaling) and transgenic crypts become hypertrophic (figure 20). In our experimental set-up,

however, this model may have one limitation related to the stability of the GFP. The *Lgr5* locus represents a transcriptional target of the Wnt pathway. Indeed, the GFP is expressed and accumulates more abundantly in $Lgr5^{+}$ cells upon the deletion of *Apc* than it does in $Apc^{+/+}$ $Lgr5^{+}$ cells. At day 15 post-injection this accumulation results in an expanded population of GFP-labelled progeny that is no longer confined to the bottom of the crypt. This implicates the possibility that, at this time point, some early differentiating cells in the crypt might have inherited some "leaking" GFP from their progenitors.

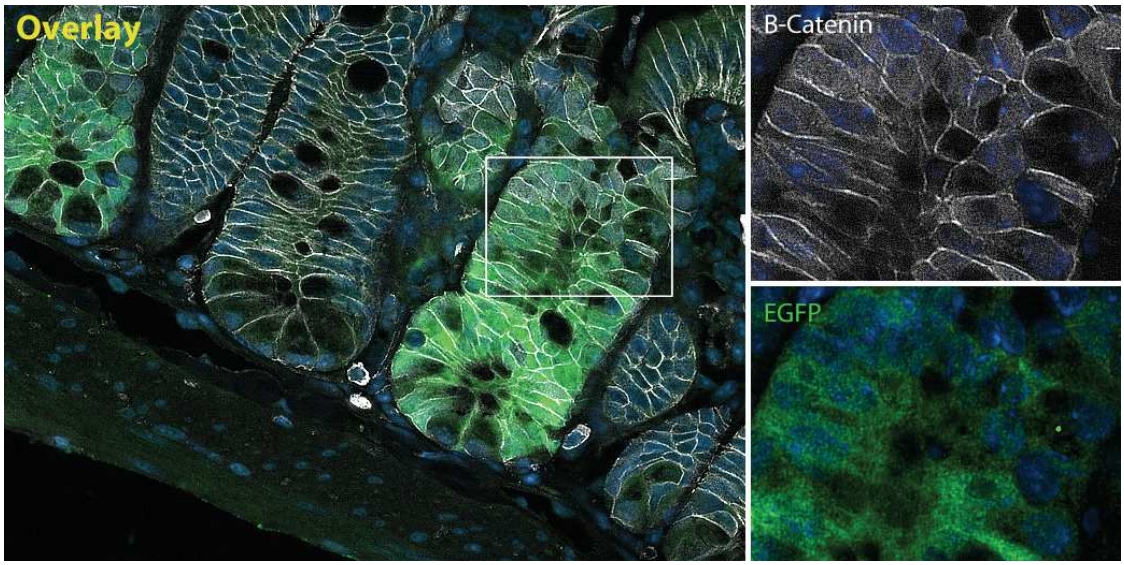

Figure 21: Wnt activation in $Lgr5^{+}$ stem cells leads to the formation of a hypertrophic GFP-positive compartment. The GFP (green) staining in the crypts expressing the transgene exceeds the normal localization of $Lgr5^{+}$ cell compartment 15 days after the activation of the Lgr5-Cre recombinase. All GFP^{+} cells show the translocation of the β-Catenin (white) within the cytoplasm and the nucleus. GFP is absent in post-mitotic Paneth cells within the same crypts.

However, when we examined the expression of markers of terminally differentiated secretory populations most commonly found at the bottom of the crypt such as tuft cells cells (Dclk1), Paneth cells (Lyzozyme) and enteroendocrine cells (Chromogranin A) we observed minimal or no co-localization with the GFP staining, suggesting that both in $Apc^{+/+}$ and $Apc^{LoxP/LoxP}$ crypts, GFP positive cells are very likely to only consist in $Lgr5^{+}$ cells and their immediate undifferentiated progeny fifteen days post-injection (figure 22).

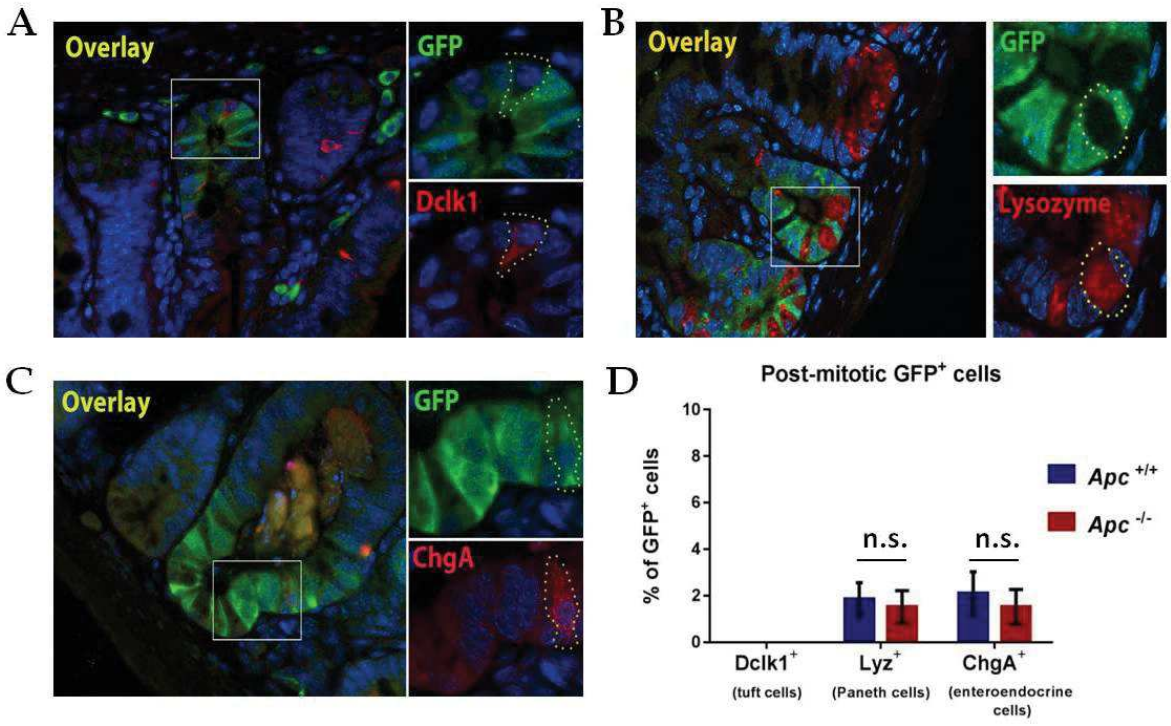

Figure 22: The GFP rarely co-localizes with markers of the post-mitotic cell populations typically found at the bottom of the crypt. A) Dclk1 (red) identifying differentiated tuft cells. B) Lyzozyme marks Paneth cells within the crypt. C) Example of the rare colocalization of the GFP with Chromogranin A expressed by enteroendocrine cells. 40x magnification. D) Quantification of the co-expression of these makers with the GFP. Results represent the average quantification of > 20 transgenic crypts found in two biological replicates of each genotype (*Apc*$^{+/+}$*; Lgr5-EGFP-ires-Cre* or *Apc*$^{LoxP/LoxP}$*; Lgr5-EGFP-ires-Cre*). Error bars represent S.E.M. Statistical significance was evaluated by two-tailed Student t-test.

To better characterize the increase of the proliferative compartment occurring upon the deletion of *Apc* in Lgr5-positive stem cells we decided to quantify the size of the stem cell compartment in the transgenic crypts. As mentioned, however, the stability of the GFP makes the reporter alone uncertain to this aim, since *Lgr5*$^{+}$ cells transfer part of their GFP content to their non-stem progeny at cell division. We therefore decided to perform a double quantification by using an anatomical criterion, the position between two Paneth cells, as well as the expression of a supplemental *bona fide* marker, Olfactomedin 4 (Olfm4), both associated with the CBC identity (van der Flier, Haegebarth, et al. 2009, 4) (figure 23 A). *Apc*$^{LoxP/LoxP}$ *Lgr5-EGFP-ires-Cre*^{ERT2} crypts display a slight but statistically significant increase in the number of *Olfm4*-expressing cells that we revealed by *in situ* hybridization of the *Olfm4* mRNA, as well as a slight significant increase in the number of GFP-positive cells intermingled between two Paneth cells fifteen days after the initial injection of mice with tamoxifen (Figure 23 B). Both strategies converged to reveal a relative increase in the number of CBC close to 15%. The increase in the number of stem cells is accompanied by a

similar raise in the number of Paneth cells in the transgenic crypts (figure 23 C). As previously described, the constitutive activation of Wnt signaling perturbs the homing of Paneth cells (Batlle et al. 2002). Indeed, we frequently observed Paneth cells aberrantly located outside their normal position. Therefore, the inactivation of *Apc* in *Lgr5*$^{+}$ cells leads to an increase in the size of the stem cell compartment including its own epithelial niche.

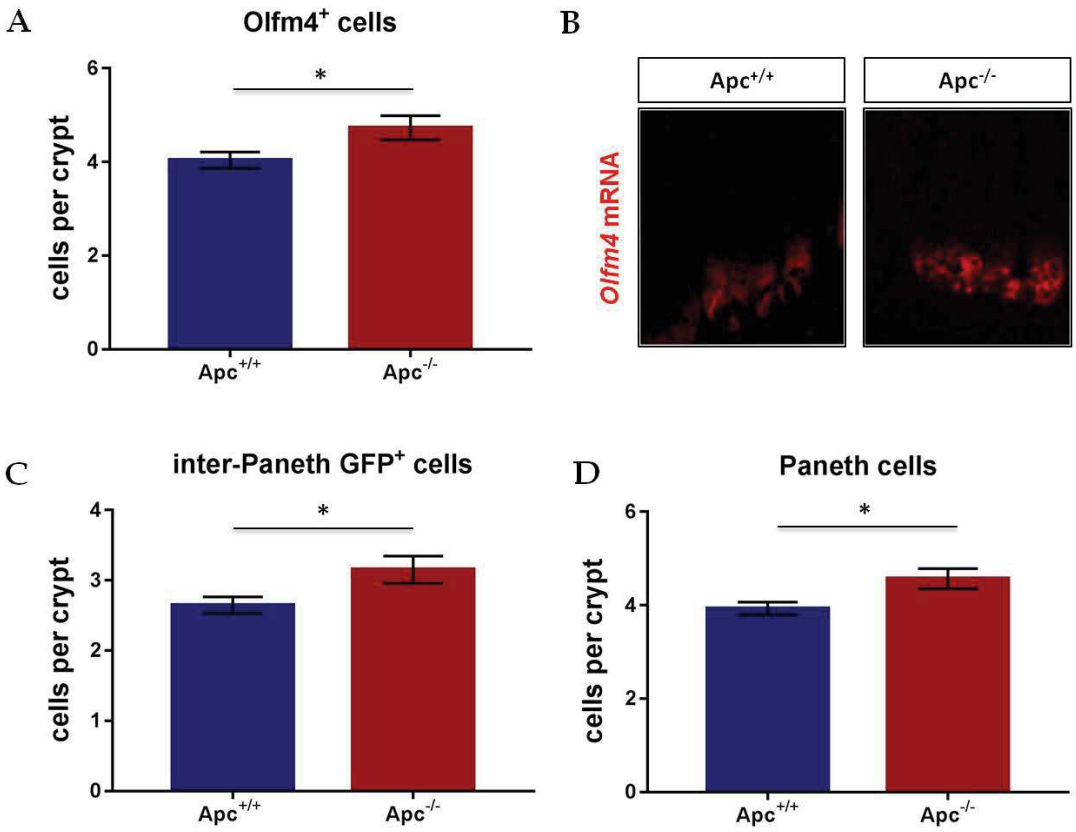

Figure 23: Expansion of the CBC stem compartment 15 days after the deletion of *Apc* in Lgr5^{+} cells. Quantification of *Olfm4*-positive cells within the GFP-positive crypts. B) Representative *Olfm4* staining obtained by *in situ* hybridization. C) Average number of GFP^{+} cells intermingled between two Paneth cells per crypt. D) Average number of Paneth cells in the GFP^{+} crypts. All the results represent the average value of > than 20 crypts in two biological replicates of each genotype (*Apc*$^{+/+}$*; Lgr5-EGFP-ires-Cre* or *Apc*$^{LoxP/LoxP}$*; Lgr5-EGFP-ires-Cre.)*. Error bars represent S.E.M. * represents a P-value<0.05 as calculated by the Mann-Whitney *U*-test.

The activation of the Wnt pathway makes intestinal stem cell independent on the secretion of Wnt stimuli provided by the niche, especially those provided by surrounding Paneth cells. However, active Wnt signaling alone is not sufficient to explain the increase in the size of the stem compartment. We reasoned that the accumulation of intestinal stem cell consequent to the deletion of *Apc* could be explained by either an alteration in the dynamics of ISC or by a

reduced responsiveness of Apc^{KO} ISC to the pro-differentiation stimuli exerted by the microenvironment outside the normal stem-permissive location.

The sequential loss of *Apc* alleles was previously shown to confer a selective advantage to ISCs, which are more likely to replace their WT counterparts (Vermeulen et al. 2013). We therefore decided to better investigate the cell cycle dynamics of GFP-positive cells 15 days after the initial injection with tamoxifen. Unexpectedly, the analyses by mean of flow cytometry on the cell cycle distribution of isolated GFP-positive cells showed a significant reduction in the number of cells in the S phase, associated with an accumulation of cells in the G0/G1 phase (Figure 24 A). This result may indicate a surprising reduction in the proliferative rate of Apc^{KO} cells, or the presence of post-mitotic cells in the GFP-positive population. As previously shown in the figure 22, we rarely observed the co-localization of the GFP with markers of terminally differentiated populations in the crypt. To ensure that the increase in proportion of G0/G1 cells does not represent the result of a bias introduced in the fluorescent-activated cells sorting of the different genotypes, we quantified the co-localization of the GFP with Siglec-F, a surface marker of post-mitotic tuft cells that are frequently found in the mouse intestinal crypts (Gerbe et al. 2016). The result of the staining shows a weak and comparable co-expression of the two markers (less than 1% of GFP-positive cells for all genotypes), making the possibility of bias due to a differential contamination with post-mitotic cells very unlikely (Figure 24 C). Together, these observations suggest an unexpected reduction in the rate of cell division of GFP^{+} cell compartment after the loss of function of a key tumor suppressor gene.

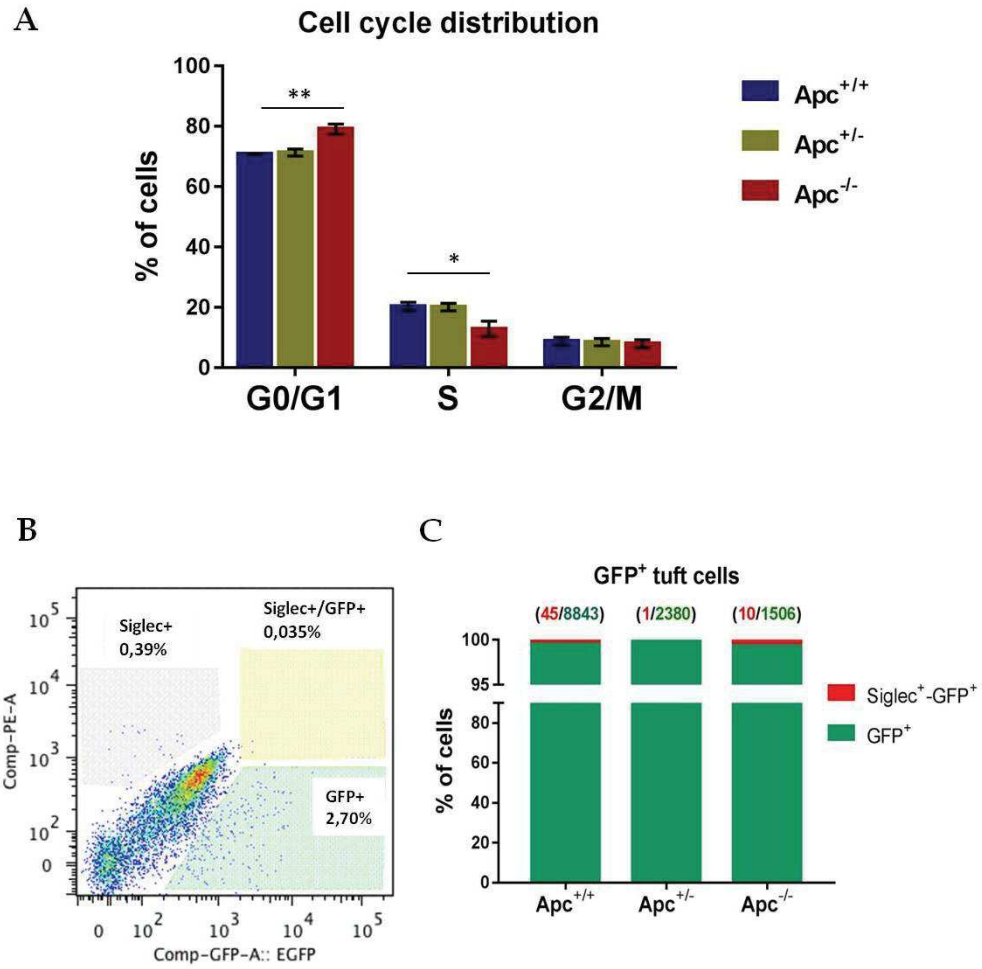

Figure 24: Alteration in the cell cycle dynamics of GFP$^+$ cells 15 days after the deletion of *Apc* in Lgr5+ cells. A) Mean percentage of cells in the different phases of the cell cycle is quantified by flow cytometry according to their DNA content after staining. Results represent the average of 3 *Apc$^{+/+}$; Lgr5-EGFP-ires-Cre*, 4 *Apc$^{LoxP-/+}$; Lgr5-EGFP-ires-*Cre and 4 *Apc$^{LoxP/LoxP}$; Lgr5-EGFP-ires-Cre* mice in which at least 7000 GFP$^+$ cells were analyzed. Error bars represent S.E.M. * represents a p-value <0.05, ** p-value<0.01 as calculated by two-tailed Student t-test. B) Example of the flow cytometry strategy to evaluate the proportion of cells expressing Siglec-F and/or the GFP. C) Representative percentage of GFP cells co-expressing the Siglec-F tuft cell marker in one individual per genotype. Records above each bar represent the real number of positive events.

3. *In vivo* molecular profiling of *Lgr5*$^+$ cells and their immediate progeny

3.1. Fluorescent-activated cell sorting strategy

To characterize the earliest impact of the sequential loss of *Apc* alleles we decided to analyze the DNA methylation and gene expression profiles found in *Lgr5*$^+$ cells and their immediate progeny (progenitors/transit amplifying cells) in *Apc^{WT}*, *Apc^{Het}* and *Apc^{KO}* GFP$^+$ cells that we isolated fifteen days after the first injection with tamoxifen. Several studies have shown that

GFP-positive cells actually account for functionally distinct populations (Barker et al., 2007; Barker et al., 2009; Munoz et al., 2012). It was shown that due to the stability of the eGFP reporter (inherited at cell division by the early *Lgr5*-negative progeny), the epithelium of these mice actually consists in 3 main populations that are distinguishable according to their brightness: the GFP^{high} (brightest fluorescence) population accounts for cells with high clonogenic capacity, whereas the GFP^{low} population accounts for actively proliferating non clonogenic cells. The GFP^{neg} population is constituted by late TA and differentiated cells (Barker et al. 2007; Sato et al. 2011; Muñoz et al. 2012).

Although the highly clonogenic population would appear as the most interesting to be examined, our *in vivo* experimental design does not allow to easily discriminate the different functional populations according to the brightness of cells in the *Apc*-deficient context as in the case of WT cells. Coherently with the previously mentioned increase in the size of the GFP^+ compartment, the $Apc^{LoxP/LoxP}$ dissociated epithelium shows a remarkable rise (6-fold) in the percentage of the GFP^+ cell fraction as well as a shift in the brightness of cells when they are excited by a 488nm laser (figure 25 B). We reasoned that any attempt to functionally classify $Apc^{-/-}$ cells according to their brightness would be over-simplistic and we therefore decided to include in the analysis all the GFP^+ cells whose brightness exceeds a severe threshold that we defined in order to minimize the risk of contamination with post-mitotic or false-positive GFP^+ cells (gates are shown in the figure 24A). Overall, this strategy allows us to focus the subsequent analyses on $Lgr5^+$ cells and their most immediate progeny, the compartment accounting for the highest plasticity and most likely involved in tumor initiation, by providing the cells with a reasonable lapse of time for epigenetic changes to be produced and propagated within the proliferative compartment.

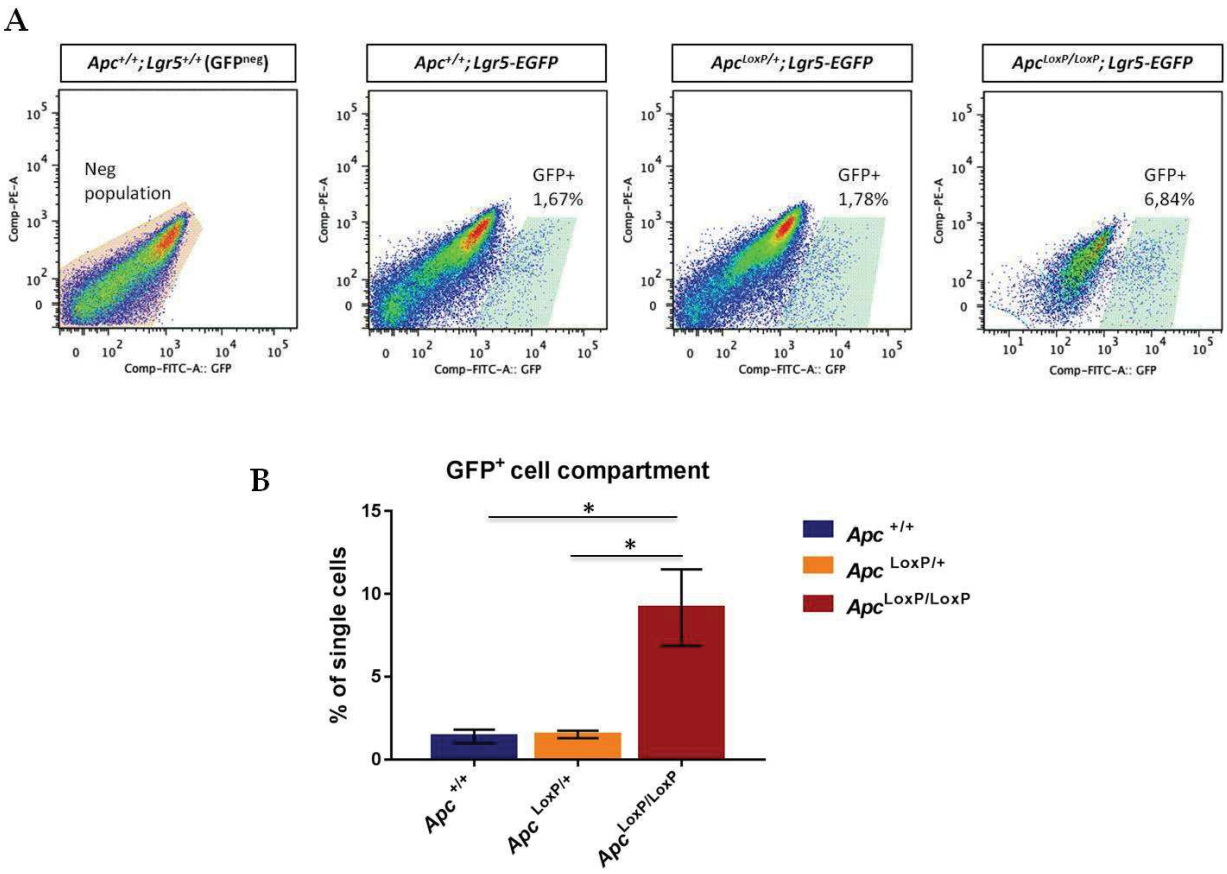

Figure 25: Fluorescent-activated cell sorting of GFP-positive cells from *Lgr5-EGFP-ires-Cre* epithelia. A) Illustration of the gating strategy. The positive gate established above the threshold of autofluorescence (orange gate) quantified in the Lgr5$^{+/+}$ control epithelium is then applied to isolate GFP-positive single live (7-AAD negative) cells from all of the three genotypes (*Apc*$^{+/+}$*; Lgr5-EGFP-ires-Cre*, *Apc*$^{LoxP-/+}$*; Lgr5-EGFP-ires*-Cre and *Apc*$^{LoxP/LoxP}$*; Lgr5-EGFP-ires-Cre*. B) Quantification of GFP^{+} cells in the three genotypes represented as the average percentage of single live cells from 5 *Apc*$^{+/+}$*; Lgr5-EGFP-ires-Cre*, 5 *Apc*$^{LoxP/+}$*; Lgr5-EGFP-ires*-Cre and 8 *Apc*$^{LoxP/LoxP}$*; Lgr5-EGFP-ires-Cre* mice. Error bars represent S.E.M. * represents a p-value <0.05 as calculated by the Mann-Whitney *U*-test.

3.2. The sequential loss of *Apc* alleles progressively alters the transcriptomic profiles of the self-renewal compartment

According to the Knudson model, the oncogenic inactivation of a gene with tumor suppressive function occurs upon the sequential alteration of both alleles (Knudson, 1971). In the case of colorectal cancer, the loss of the first *Apc* allele can either occur in the germline (as in the case of FAP patients) or somatically (sporadic CRC). The second hit occurs during the adult life, via either the disruption of the second allele or its epigenetic silencing. To investigate the molecular changes associated with this progressive sequence we performed a transcriptomic analysis on the polyadenylated transcripts (mRNA) of *Lgr5*-positive cells and their immediate progeny isolated from *Apc*$^{+/+}$, *Apc*$^{LoxP/-}$ and *Apc*$^{LoxP/LoxP}$ small intestines. The

comparison between KO and WT cells shows that the biallelic loss of *Apc* dramatically impacts on the global gene expression profiles of these cells and we found significant differential expression of 5112 out of 25797 analyzed transcripts (figure 26). Similar effects are observed by comparing the gene expression profiles of heterozygous (HET) cells with those of KO cells, confirming that most of changes occur after the abrogation of *Apc* function upon the inactivation of the second allele (complete loss of function) that in turn allows the constitutive activation of the Wtn signaling. Nevertheless, 478 transcripts were found to be differentially expressed upon the earliest genetic alteration (loss of the first allele) suggesting that the reduction in the *Apc* gene dosage impacts on the molecular phenotype of $Lgr5^{+}$ cells, although the heterozygous epithelium appears macroscopically normal and does not show any major alteration in the features considered so far in both *Villin-*Cre^{ERT2} and *Lgr5-*Cre^{ERT2} mice.

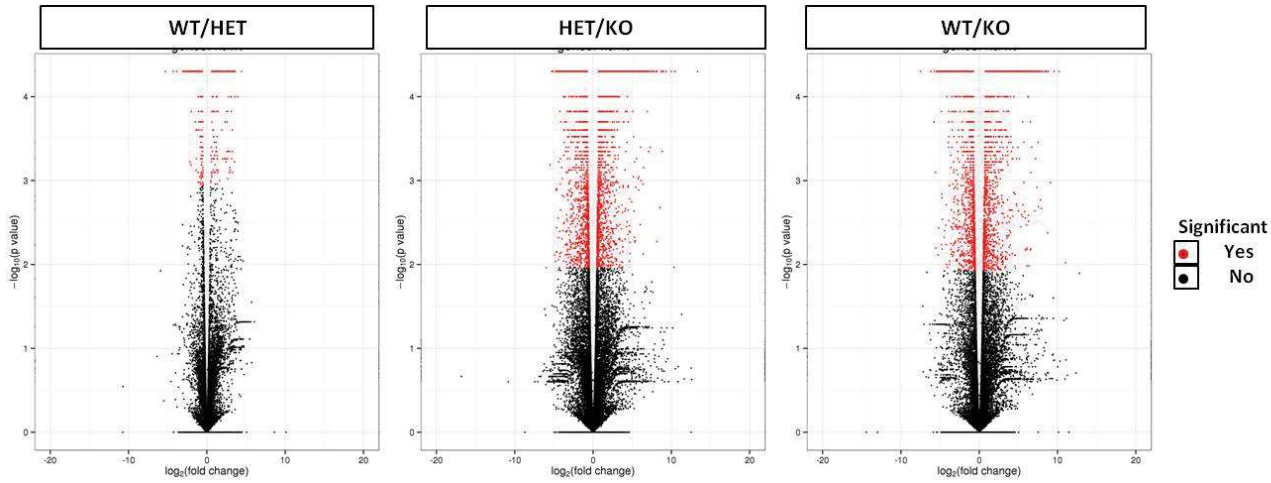

Figure 26: progressive alteration of the gene expression profile in GFP^{+} cells. Volcano plots illustrating the relative change for all the transcripts analyzed in the comparison between $Apc^{+/+}$ (WT), $Apc^{+/-}$ (HET) and $Apc^{-/-}$ (KO) *Lgr5*-positive cells and their progeny. Red dots represent transcripts whose expression is significantly altered. Gene expression analyses are performed on cohorts of 4 animals per genotype. X-axis represent the $\log_2$ relative fold change, Y-axis represents the P-value associated to each transcript.

Gene ontology (G.O.) analyses performed on the list of genes differentially expressed upon the loss of one allele show the significant overrepresentation of a number of KEGG pathways (figure 27). Interestingly, G.O. functional classes of genes associated with "xenobiotic metabolism" and "drug metabolism" are highly represented among differentially expressed genes.

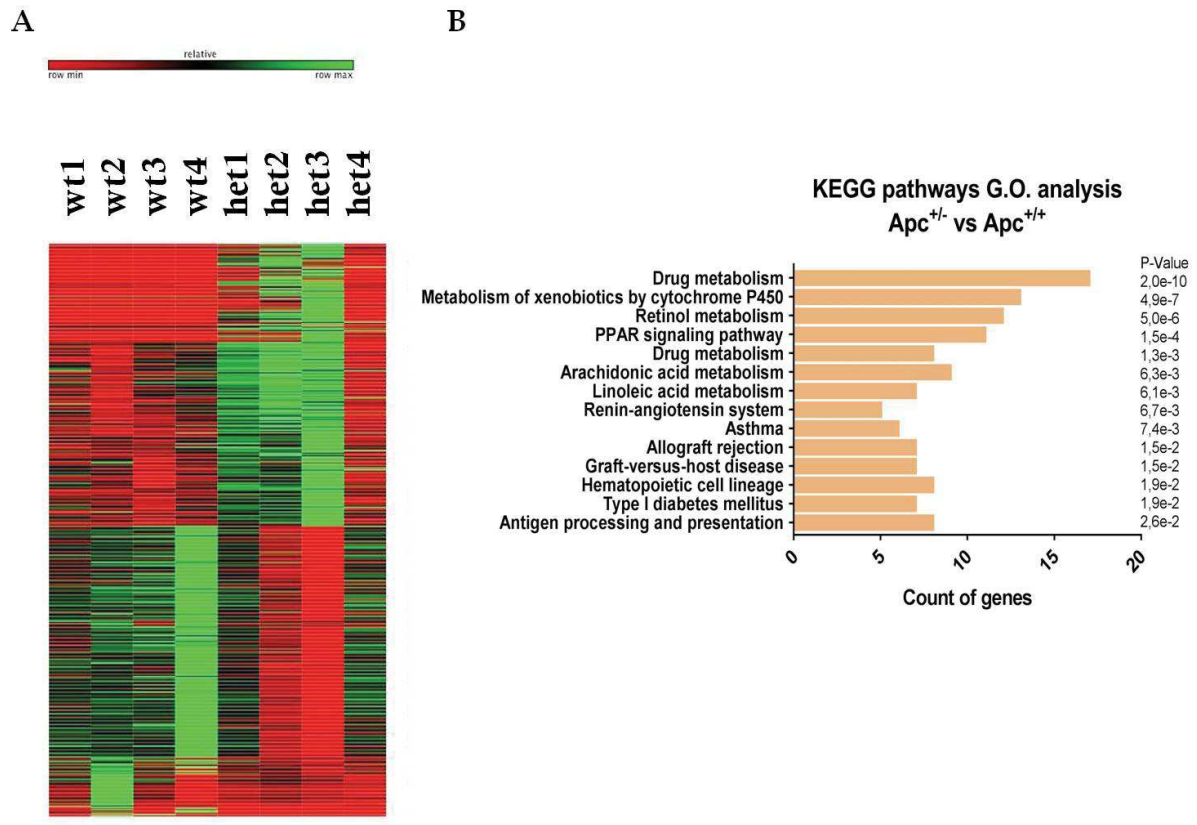

Figure 27: Altered gene expression in response to the loss of one *Apc* allele in *Lgr5*$^{+}$ cells and their immediate progeny. A) Heatmap representing the differential expression profiles of *Apc*$^{+/+}$ and *Apc*$^{+/-}$ sorted cells. B) List of the 15 most represented KEGG pathways obtained by G.O. analysis performed by using David public resource (david.ncifcrfgov). The associated P-value corrected for multiple testes is shown for each class.

The trancriptomic profiles obtained from *Apc*^{KO} GFP^{+} cells provided us with the opportunity to further investigate the molecular features associated with the accumulation of intestinal stem cells and the changes in their proliferative dynamics previously described. To this aim we decided to interrogate the gene expression profiles via gene set enrichment analyses (GSEA) (Subramanian et al. 2005). This bioinformatic tool consists in a computational method that determines whether an *a priori* defined set of genes associated with a given biological or molecular function, cell identity, developmental process or disease shows statistically significant concordant differences between two biological states (in our case represented by the presence or deletion of *Apc*). The primary result provided by the GSEA is an enrichment score (ES), which defines the extent of the positive or negative correlation of a given biological state with the specific set of genes considered. We therefore selected sets of genes representing the transcriptomic signature previously found to be up-regulated in intestinal stem cells (Muñoz et al. 2012), transit-amplifying cells (Merlos-Suárez et al. 2011)

and differentiated epithelial cells (Merlos-Suárez et al. 2011). The results show that the transcriptomic profile associated with the loss *Apc* correlates with the expression of the gene set associated to the stem identity (figure 28). Conversely, the gene set associated with intestinal differentiation show a positive correlation with the profile of expression in WT cells. None of the two states showed significant correlation with the signature associated to transit-amplifying progenitors.

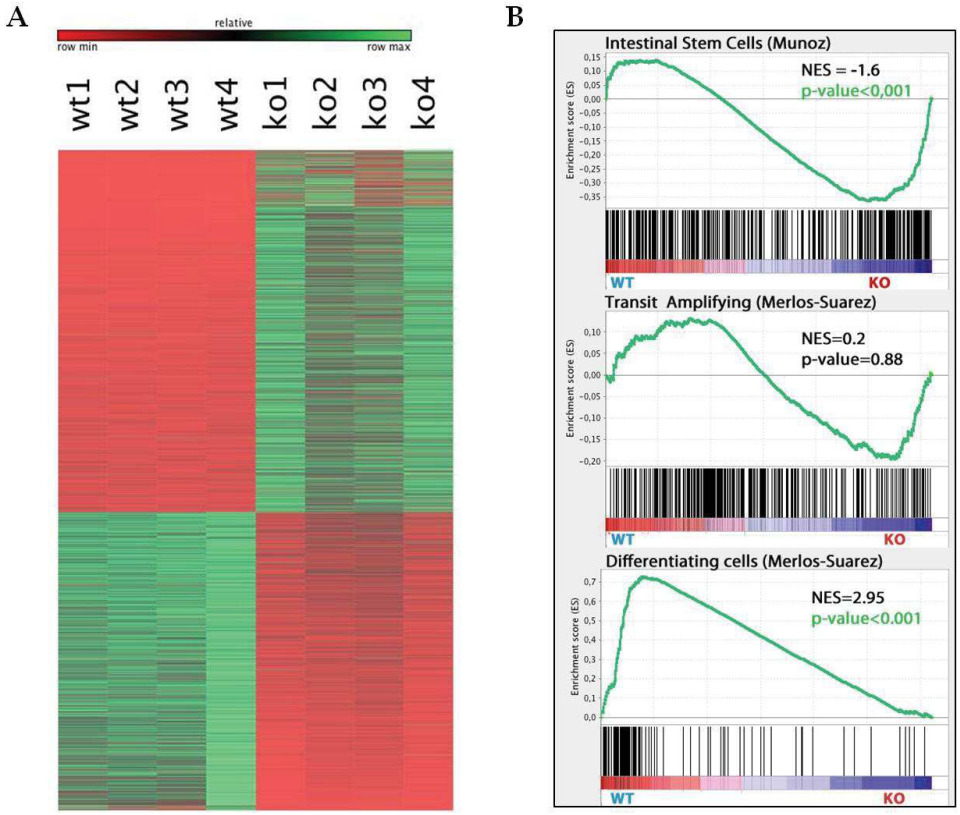

Figure 12: Altered gene expression in response to the loss of function of *Apc* in *Lgr5*$^{+}$ cells and their progeny. A) Heatmap representing the differential expression profiles of *Apc*$^{+/+}$ and *Apc*$^{-/-}$ sorted cells. B) GSEA analyses performed by evaluating the enrichment of signatures with associated with stemness (Munoz et al., 2012), transit amplifying cells (Merlos-Sauarez et al., 2011) and differentiated cells (Merlos-Suarez et al., 2011). NES represents the normalized enrichment score corrected for multiple tests calculated with 1000 permutations (Subramanian et al. 2005), and indicates the extent of the correlation with the transcriptomic profile associated with the *ApcWT* phenotype.

Indeed, when we manually inspected the list of differentially expressed genes we found that the expression of several markers commonly associated with ISC identity is up-regulated in knock-out cells, with the exception of *Olfm4,* whereas key regulators and markers of epithelial commitment toward the different mature lineages (enterocytes, enterendocrine, goblet, tuft and M-cells) are down-regulated in these cells. The Paneth cell lineage, the differentiation of

which relies on Wnt activity (van Es et al. 2005), represents the only exception in this altered fate program. We concluded that this is coherent with the proportional increase of the stem and Paneth compartment found in Apc^{KO} crypts and with previous findings on the effect of *Apc* loss on the Paneth cell compartment (Andreu et al. 2005). Table 1 provides some examples of differentially expressed genes associated with stemness and differentiation of intestinal epithelial cells.

	Gene	Fold change (log_2) KO/WT	pValue
Stemness	*Axin2*	1.23781	5,00E-05
	Hunk	1.24112	5,00E-05
	Lgr5	0.620887	0.046031
	Msi1	0.585349	0.00435
	Olfm4	-3.94049	5,00E-05
	Sox4	1.42886	5,00E-05
Differentiation	*Atoh1*	-2.13125	5,00E-05
	Neurog3	-1.18645	0.0001
	Pou2f3	-1.37836	0,00005
	Sox9	0.098655	0.231329
	Spdef	-1.17012	5,00E-05
	SpiB	-2.39898	5,00E-05
	Agr2	-1.35446	5,00E-05
	Alpi	-3.5941	5,00E-05
	Dclk1	-2.15812	0,00185
	Insm1	-1.24594	5,00E-05
	Krt20	-2.13125	5,00E-05
	Lct	-5.32423	5,00E-05
	Muc2	-3.11944	5,00E-05
	Mmp7	2.14603	5,00E-06

Table 1: Relative change in the expression of genes associated with stemness and commitment of the intestinal epithelium. "Stem" genes represent part of the signature associated with $Lgr5^{high}$ cells proposed by Munoz and collaborators (Munoz et al., 2012). *Atoh1* is the master regulator of the secretory cell fate in the intestinal epithelium. The list also contains transcription factors responsible for commitment and markers of terminal differentiation of all the intestinal cell types: enterocytes (*Alpi*, *Lct*, *Krt20*), goblet cells (*Spdef*, *Agr2*, *Muc2*), Paneth cells (*Sox9*, *Mmp7*), enteroendocrine cells (*Insm1*, *Neurog3*), tuft cells (*Pou2f3*, *Dclk1*) and M-cells (*SpiB*). Corrected P-value for multiple tests is shown for each gene.

Overall, these results confirm the key role exerted by *Apc* in controlling the balance between proliferation and differentiation via the modulation of Wnt signaling and support the observed increase of the stem compartment occurring as a result of the accumulation of stem cells at the expense of differentiation. Moreover, the raise of the transcriptional signature associated with stemness occurs in absence of any significant change in the representation of TA cell markers

in the population constituted by *Lgr5*$^{+}$ cells and their progeny, thus supporting the idea that commitment of intestinal stem cells toward differentiation occurs very early in the crypt.

3.3. Biallelilc loss of *Apc* alters the DNA methylation profiles of the self-renewal compartment

Genomic DNA samples collected from the same samples were used to examine the DNA methylation profiles associated with the sequential deletion of *Apc* copies, via reduced-representation bisulfite sequencing. We considered as differentially methylated all of the CpGs displaying a significant relative variation over a threshold of 10%.

Overall, the comparison between *Apc*^{WT} and *Apc*^{Het} cells revealed very few changes (58 DMR) associated with the first genetic hit. The cross-comparison with transcriptomic data shows a poor correlation between the methylation and gene expression, with most of the significantly differentially methylated genes being equally expressed in the GFP-positive compartment of wild type and heterozygous animals (data not shown).

The biallelic *Apc* loss, however, produced a more consistent impact, since 790 CpGs were found to be differentially methylated in *Apc*^{KO} cells (figure 29). We found 595 (75%) of these CpGs to be hypomethylated in *Apc*-deficient cells. Importantly, hierarchical clustering shows a high degree of similarity in the profiles of the biological replicates in the two groups, indicating that the loss of *Apc* produces well defined concordant changes in DNA methylation. The G.O. analysis performed on the genes associated with differentially methylated regions shows the significant overrepresentation of some KEGG pathways terms. Notably, this analysis revealed an overrepresentation of genes associated with Wnt and TGF-beta/BMP signaling, among the others.

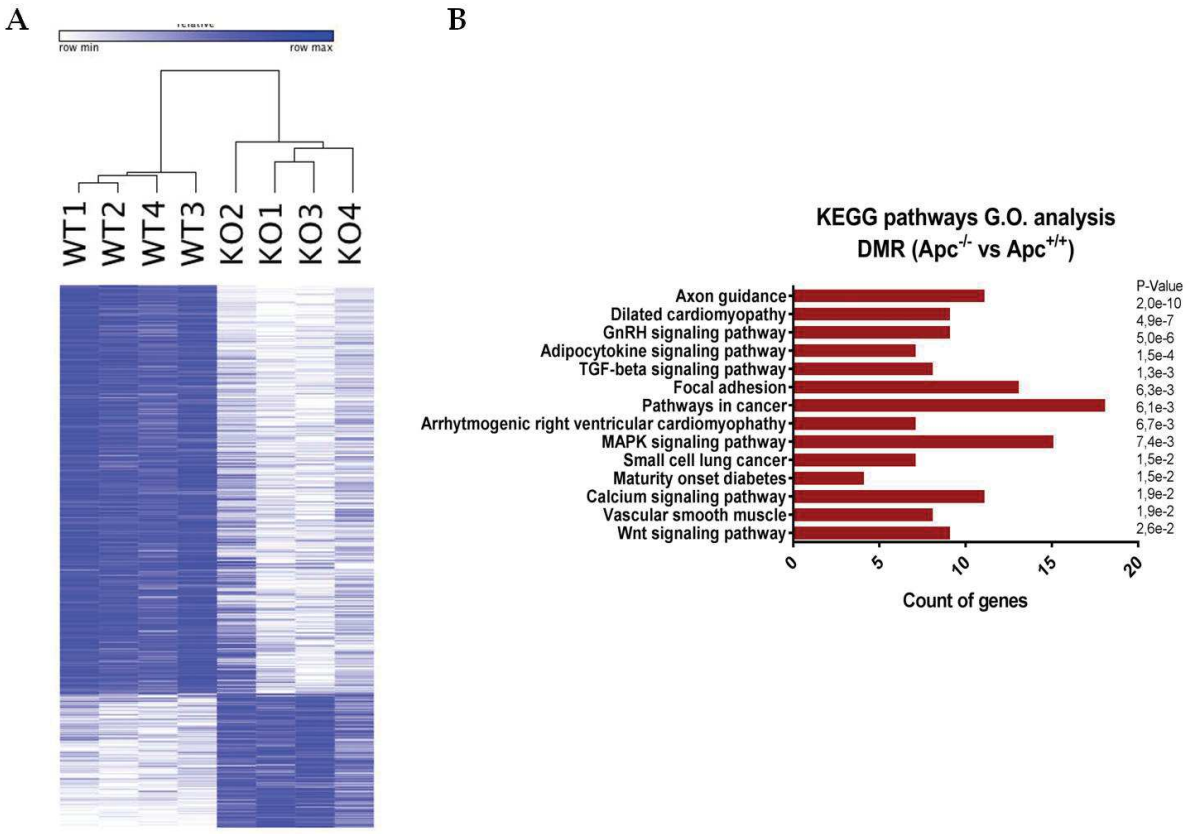

Figure 29: Differentially methylated regions in WT and KO *Lgr5*$^{+}$ cells and their immediate progeny. A) Heatmap representing the hierarchical clustering of differential methylation profiles of *Apc*$^{+/+}$ and *Apc*$^{-/-}$ sorted cells. B) List of the 15 most represented KEGG pathways obtained by the G.O. analysis performed by using David public resource. The associated corrected P-value is shown for each class.

RRBS results do not allow us to attempt any speculation on the general extent of genomic methylation, since this method only takes into account 1% of the genome consisting in CpG-rich regions. However, when we examined more closely the intracisternal A particle mobile elements (IAP), which are transposable regions severely methylated in normal cells, we did not find any significant decrease in their DNA methylation patterns on a single nucleotide scale (figure 30). This result was validated by McrBC enzymatic genomic digestion followed by region-specific qPCR analysis (for further details see material and methods), which confirmed that the high extent of CpG methylation is maintained at IAP genomic regions in *Apc*^{KO} cells. This observation suggests that hypomethylation does not necessarily occur at genome-wide scale at this initial stage of cancer development and may involve only some specific genomic features of intestinal stem cells.

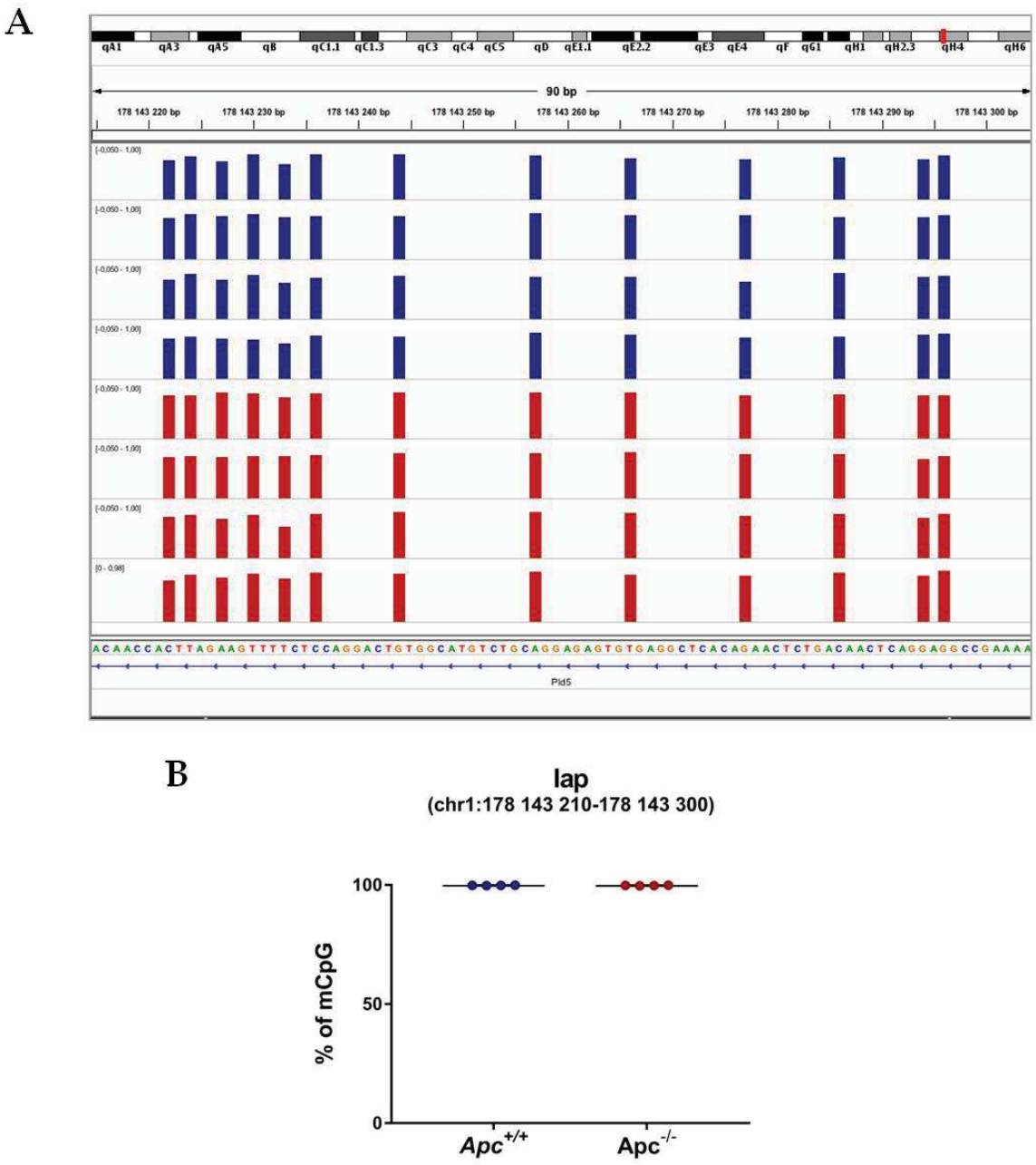

Figure 30: methylation of a representative IAP region in *Apc*$^{+/+}$ and *Apc*$^{-/-}$ *Lgr5*$^{+}$ cells and their immediate progeny. A) Integrative genomic viewer (IGV) snapshot focusing the genomic region associated to IAP element showing methylated sites. Bars represent the extent of methylation (0 to 1) in 4 biological replicates of *Apc*^{WT} (blue) and *Apc*^{KO} (red) FACS-isolated cells. B) Verification of DNA methylation extent by qPCR performed on McrBC digested genomic DNA on 4 biological replicates. The strategy used for the normalization is detailed in the material and methods.

4. Constitutive activation of the Wnt pathway in ISC is associated with reduced responsiveness to the BMP/TGF-β signaling pathway via altered DNA methylation and expression of its components

We decided to investigate whether the impairment in the cells fate associated with the constitutive activation of the Wnt signaling in ISC might correlate with the remodeling in the methylation patterns observed upon the loss of *Apc* in these cells.

As previously mentioned, the G.O. analysis on the list of differentially methylated regions revealed a significant number of genes belonging to the TGF-β/BMP signaling pathway. BMP signaling plays a crucial role in sustaining cell differentiation, and its activity is regulated in a crypt-to-villus gradient by the variable secretion of BMP ligands and their antagonists by epithelial and mesenchymal cells (Vanuytsel et al., 2013). We found that a region associated with transcription of the BMP inhibitor *Smad6* is hypomethylated in *Apc*-deficient cells (mean methylation difference of -46%), whereas the promoter of the activin receptor 1 (*Acvr1*) and the BMP2-associated kinase (*Bmp2k*) are hypermethylated (respectively 14% and 12% gain of methylation). RNAseq data show a three-fold increase in the expression of Smad6 and Smad7 BMP inhibitors, and a two-fold downregulation of BMP2k. McrBC enzymatic digestion followed by region-specific qPCR analysis confirmed the hypomethylation of the *Smad6* associated region in GFP^+ cells, and RT-PCR semiquantitative was used to validate its transcriptional upregulation in an independent biological cohort of GFP^+ cells (figure 31). We concluded that the constitutive activation of Wnt signaling provokes an alteration in the extent of DNA methylation and expression of key factors involved in the Bmp/TGF-β signaling.

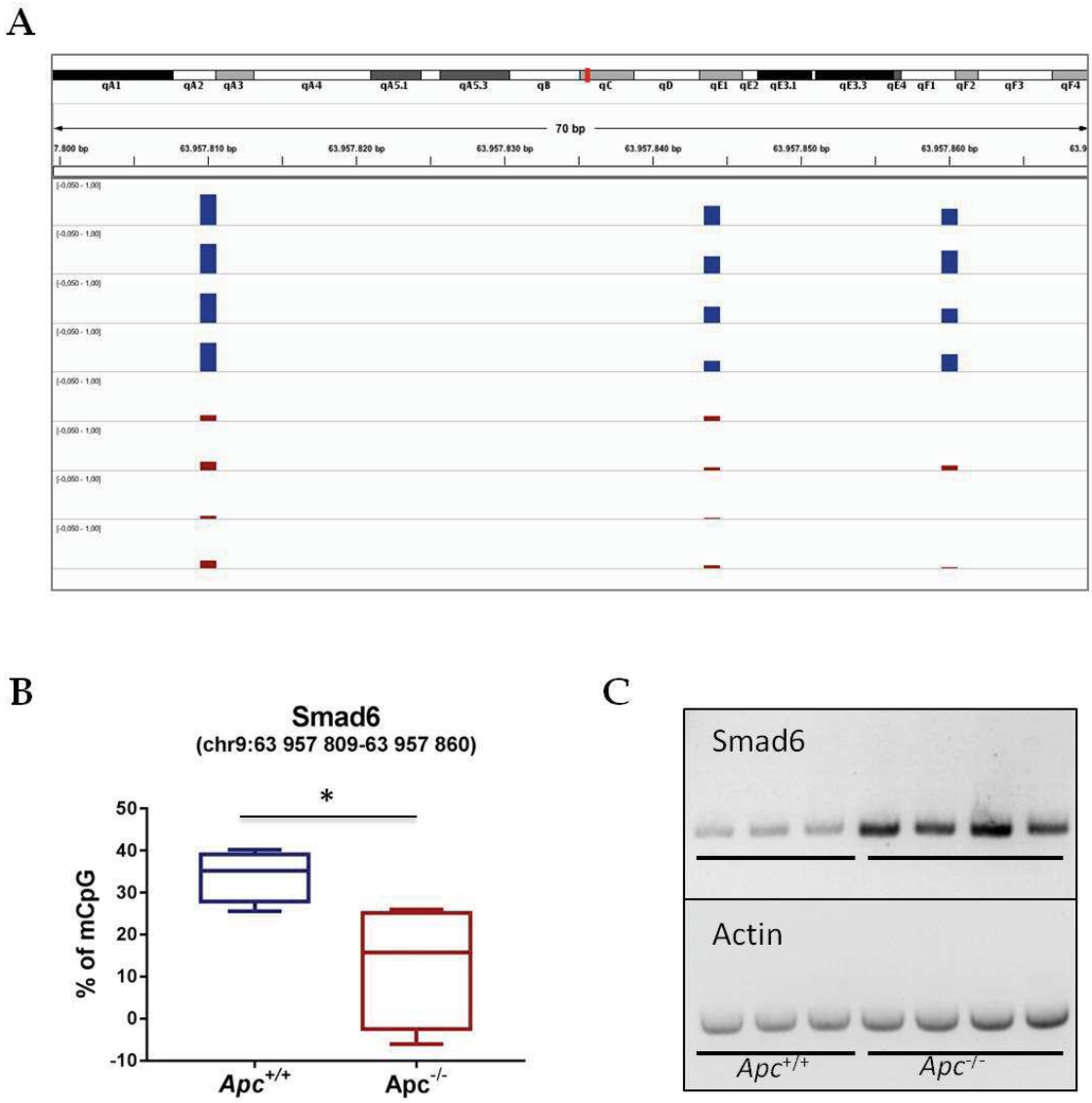

Figure 31: methylation and expression of *Smad6* in $Apc^{+/+}$ and $Apc^{-/-}$ $Lgr5^{+}$ cells and their immediate progeny. A) IGV snapshot focusing the genomic region associated to the *Smad6* promoter showing 3 differentially methylated sites. Bars represent the extent of methylation (0 to 1) in 4 biological replicates of WT (blue) and KO (red) sorted cells as quantified by RRBS. B) Verification of DNA methylation extent by qPCR performed on McrBC digested genomic DNA on 4 biological replicates. The strategy used for the normalization is detailed in the material and methods. * represents a P-value <0.05 as calculated by Mann-Whitney *U*-test C) RT-PCR showing the expression of *Smad6* in 3 $Apc^{+/+}$ and 4 $Apc^{-/-}$ biological replicates. *ActinB* is showed as an internal housekeeping control.

Since an increasing literature shows that opposite gradients of BMP and Wnt activity cooperates in the maintenance of well-defined stem, proliferative and differentiated compartments in the intestine, we reasoned that these changes could indicate a reduced responsiveness of $Lgr5^{+}$ cells and their progeny to the pro-differentiation BMP stimuli.

To test this hypothesis we analyzed the localization of the intracellular effectors of this signaling cascade in the epithelium of the small intestine of $Apc^{+/+}$; $Villin\text{-}Cre^{ERT2}$ and

Apc$^{Flox/Flox}$; *Villin-Cre*^{ERT2} mice six days after their administration with tamoxifen. As expected, in the WT epithelium we observed the phosphorylation and translocation of the Smad 1/5/8 effectors into the nuclei of differentiated cells in the villus, and in post-mitotic Paneth cells at the bottom of the crypts, whereas the proliferative crypts show a weak cytoplasmatic staining (figure 32). Strikingly, this pattern of translocation is abrogated or severely altered in the epithelium upon the deletion of *Apc*. Nuclear staining could only be observed at the tip of villi in part of the epithelium, suggesting that the progressive loss of phosphorylation/translocation occurs in the epithelium in a crypt-to-villus direction as a result of the cellular turnover after the deletion of *Apc*. The same alteration was found when we examined the patterns of translocation of the BMP2/3, which are described as effectors of the canonical TGF-β singaling in the small intestine (not shown). Together, these results indicate that the loss of *Apc* leads to an altered expression of some components of the Bmp/TGF-β signaling pathway, in part associated with the alteration in the DNA methylation profiles of these same genes. In turn, this likely results in an impaired responsiveness of the self-renewal compartment to the pro-differentiation stimuli exerted by the microenvironment.

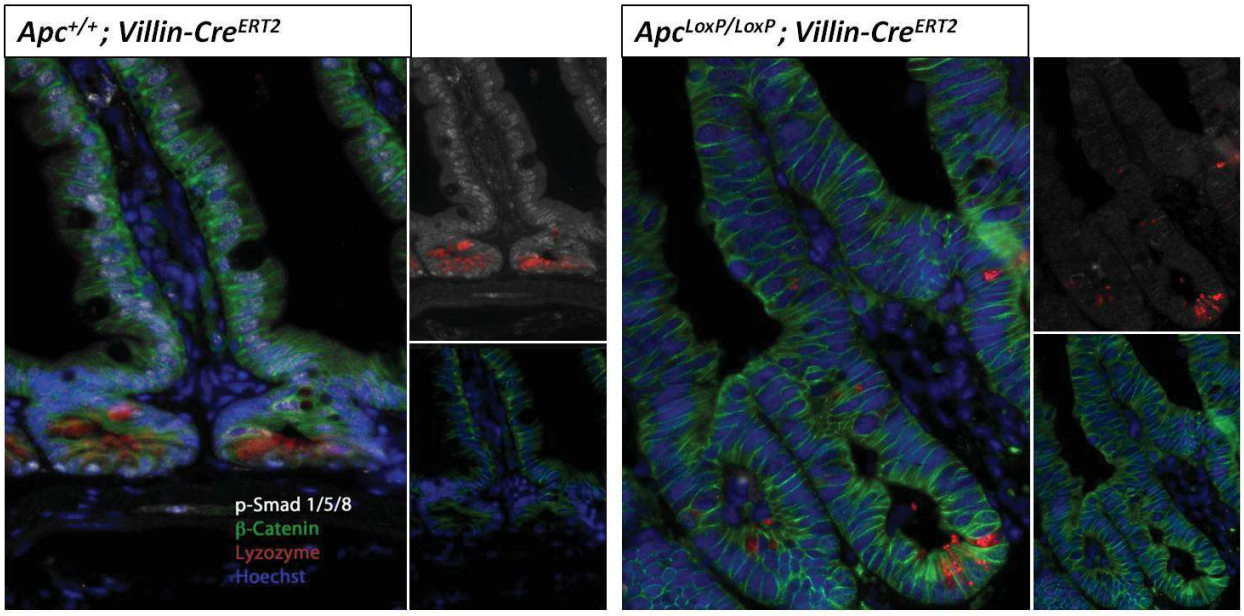

Figure 32: translocation patterns of phospho-Smad 1/5/8 effectors in the *Apc*$^{+/+}$ and *Apc*$^{LoxP/LoxP}$; *Villin-Cre*^{ERT2} at day 6 post-tamoxifen injection. p-Smad (white), Lyzozyme (Paneth cells marker) and β-catenin (green) are immunostained. 40X magnification.

5. Inhibition of the Dnmt3b *de novo* methyltransferase activity reduces the proliferative rate of *Apc*^{KO} organoids and restores the responsiveness to exogenous Bmp stimuli

The RRBS profiling shows that the loss of function of *Apc* and the subsequent constitutive activation of the Wnt pathway are accompanied by the establishment of DNA methylation patterns in the stem cell compartment that affects the activity of pathways related with stemness and fate determination of those cells. Patterns of DNA methylation are generally established *de novo* by Dnmt3a and Dnmt3b methyltransferases, and maintained at cell division by the activity of Dnmt1. Enzymatic activity of the Tet family enzymes participates in promoting demethylation. This multiplicity makes the design of a biological validation challenging, since each of these modifiers and erasers is likely to contribute in the establishment of these patterns. We reasoned that by modulating the activity of the *de novo* methyltransferases we would, at least in part, affect the capacity of stem cells to remodel their DNA methylation profile upon the loss of *Apc*. Several inhibitors of Dnmt enzymes are used to test the role of DNA methylation in tumor growth and cancer progression. However, these molecules do not show selective affinity with respect to the three enzymes participating to *de novo* and maintenance methylation, and their effectiveness is based on the progressive demethylation of the genome leading to the demethylation of hypermethylated tumor suppressors. In 2010, Kuck and collaborators showed that Nanaomycin A, an antibiotic belonging to the quinone class extracted from Streptomyces, presents selective binding affinity to the catalytic domain of human Dnmt3b (Kuck et al. 2010). This affinity was confirmed by molecular docking and *in vitro* assays. They also found that the treatment of human cell lines with this molecule reduces the general extent of DNA methylation and re-activates the expression of some genes without affecting the activity of Dnmt1. At the best of our knowledge, this was the first and only known *de novo* methyltrasferase-specific inhibitor. We therefore decided to functionally test the role of *de novo* methylation in the achievement of the tumorigenic phenotype by treating organotypic cultures prepared from the epithelium of $Apc^{LoxP/LoxP};Villin\text{-}Cre^{ERT2}$ mice with Nanaomycin A. These cells received Nanaomycin A in their medium at the same time as the pulse with 4-hydroxy-tamoxifen. The treatment was maintained all along the duration of the experiment and fresh medium was replaced every 3 days. As a control, we included wells that we treated with 5-Azacytidine, a nucleoside inhibitor that functions through unspecific enzyme covalent trapping to the DNA. Although the formation of different epithelial compartments is well recapitulated in intestinal organotypic cultures, these are, overall, fast-dividing. When we examined the proliferative rate, we found that about 60% of $Apc^{+/+};Villin\text{-}Cre^{ERT2}$ cells were Ki-67-positive, and the treatment with either Nanaomycin A or 5-azacytidine did not disturb the proliferation of live WT cells, although 5-azacytidine treatment induces extensive cell death (not shown).

Macroscopically, we did not observe any change in cell death associated with Nanaomycin A administration. Upon the administration with 4-hydroxi-tamoxifen, cells from *Apc*$^{LoxP/LoxP}$*;Villin-Cre*^{ERT2} organoids displayed, as expected, an alteration in the morphology of the structures that became cystic (epithelial spheroids), which was accompanied by an increase in their proliferative rate (78% +/- SEM of KI-67 positive cells) (figure 33 C). Strikingly, both Nanaomycin-A and 5-azacytidine significantly reduced the proliferation of knock-out organoids to extents comparable to those found in treated and untreated WT cultures (figure 33 C). Although we did not examine the DNA methylation profiles, it seems unlikely that these results could depend on cell pathways other than DNA methylation (off-target effects), since Nanaomycin A and 5-azacytidine are molecules belonging to different classes (a nucleoside and an antibiotic), which both inhibit DNA methylation via different mechanisms (substrate-catalytic domain interaction and enzyme covalent trapping respectively).

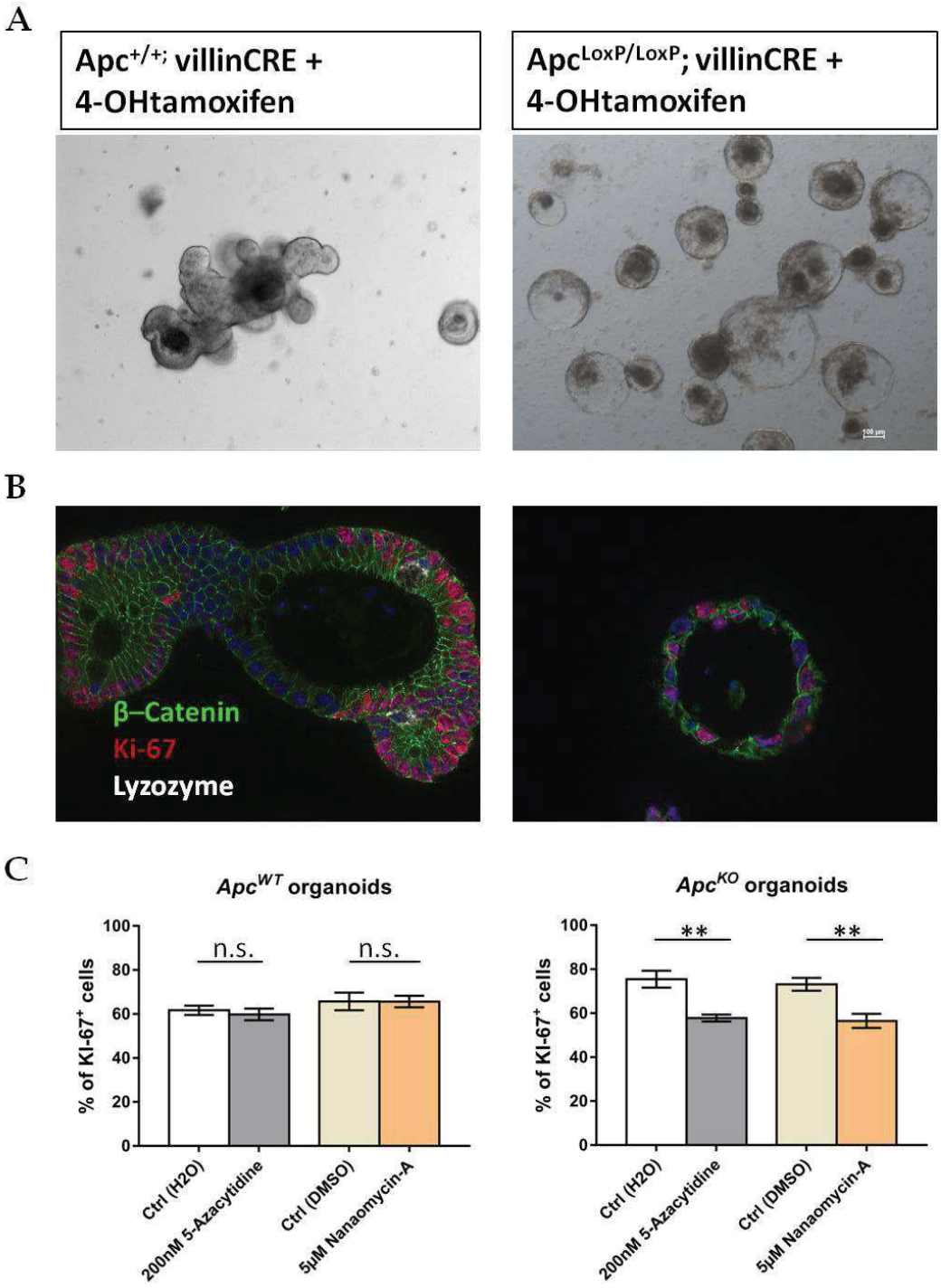

Figure 33: morphologic changes upon *Apc* deletion in intestinal organotypic cultures and effects of Dnmt3b inhibition. A) Brightfield image of $Apc^{+/+}$ and $Apc^{LoxP/LoxP}$;$Villin\text{-}Cre^{ERT2}$ organoids 3 days after the addition of 4-hydroxy-tamoxifen to the medium: the deletion of *Apc* induces the formation of spheroids. B) Ki-67 proliferative marker in $Apc^{+/+}$ and $Apc^{LoxP/LoxP}$; $Villin\text{-}Cre^{ERT2}$ organoids showing the loss of the distinct compartments after the deletion of *Apc*. C) Quantification of Ki-67-positive cells indicating the proliferation in $Apc^{+/+}$ and $Apc^{-/-}$; Villin-Cre^{ERT2} organoids in response to the addition of 5-Azacytidine or Nanaomycin A. Results represent the average of >40 structures in two biological replicates per condition. Error bars represent S.E.M. ** indicates p-value < 0.01 as calculated by Student *t*-test.

We then decided to test whether the inhibition of *de novo* methylation could reverse the immediate effects of *Apc* loss impacting on cell fate determination by monitoring the responsiveness to the BMP stimuli. One main advantage provided by organotypic cultures consists in the absence of mesenchymal cells, which allows culturing the cells in the defined presence of morphogenetic factors in the medium. The BMP inhibitor Noggin is usually added to the medium in the absence of exogenous BMP ligands, which favors the maintenance of the self-renewal ability by preventing precocious differentiation. We therefore tested the effects of the depletion of recombinant Noggin and the subsequent addition of recombinant Bmp2 in presence or absence of Nanaomycin A. Even in this case, Nanaomycin A was added to the medium at the same time of the administration with 4-hydroxi-tamoxifen. After 6 replatings (24 days) the medium of WT and KO cultures was depleted of Noggin. This did not produce consistent changes in the morphology of WT organoids, although we noticed a progressive reduction in re-plating efficiency, which is consistent with the role of Noggin in preventing precocious differentiation. In the case of Apc^{KO} cultures, the absence of Noggin induced the onset of a "dimpling" morphology in spheroids that was severely accentuated in the presence of Nanaomycin A (figure 34). When we further increased the BMP stimulation by addition of recombinant Bmp2, this result was exacerbated and we observed the progressive formation of several crypt-like structures in Apc^{KO} cultures in the presence of Nanaomycin A. We interpreted these morphological observations as an attempt of *Apc* knock-out cells to recover the formation of a differentiated compartment in the presence of Bmp signals, which is favored by the inhibitory activity of the Nanaomycin A. This result functionally confirms the implication of *de novo* methyltransferase activity in the impaired responsiveness to BMP stimuli.

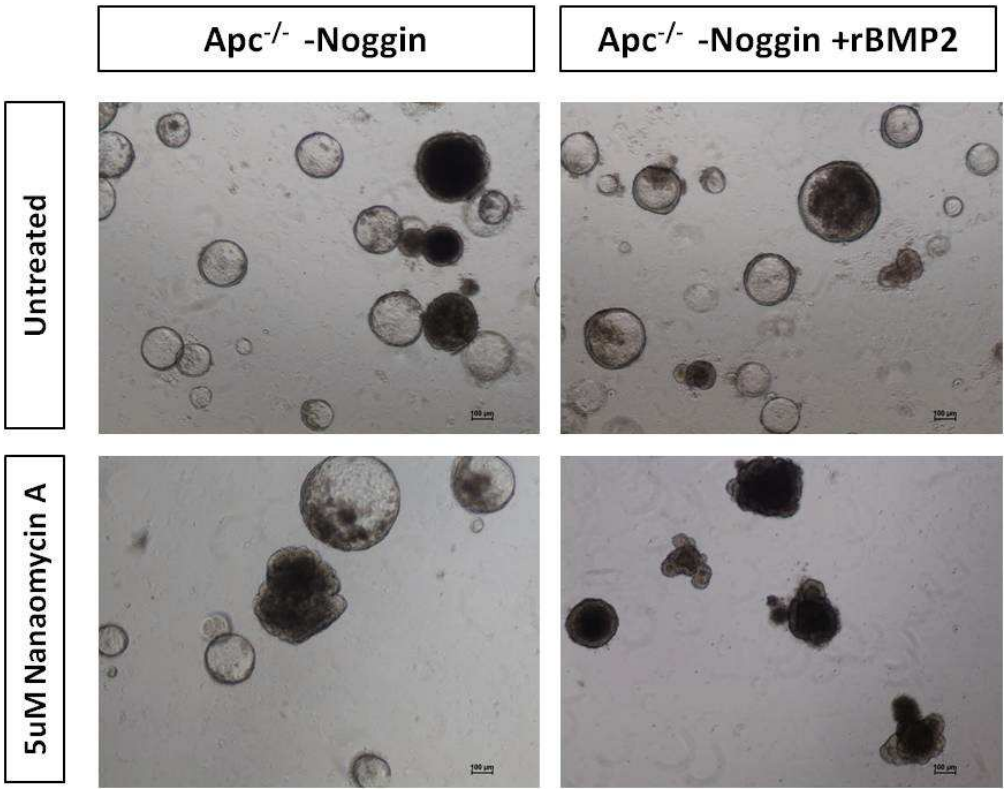

Figure 34: Dnmt3b inhibition increases the epithelial responsiveness to differentiation stimuli. Representative fields (10x magnification) show the effects of the Bmp stimulation through deprivation of recombinant Noggin and addition of recombinant Bmp2 in presence or absence of Nanaomycin A in *Apc*$^{Lox/LoxP}$; *villinCre*^{ERT2} cells treated with 4-hydroxytamoxifen to induce the recombination. Bars indicate 100 µM.

6. shRNA mediated knock-down as a stable model for the repression of *de novo* methylation in intestinal organotypic cultures

The use of a specific inhibitor seems to support our initial hypothesis concerning the functional requirement of *de novo* methylation for the establishment of the phenotype associated with the loss of *Apc* in intestinal stem cells. This approach has the clear advantage of inhibiting the methyltransferase activity of Dnmt3b without affecting its expression and its interactions within the nucleus. However it also has some limitations. First, the lack of other specific inhibitors limits the possibility to extend the investigation to Dnmt3a, whose activity and targets are not necessarily redundant with those of Dnmt3b. Second, although *de novo* DNA methylation is very likely to be the main target of this treatment, we cannot exclude that off-target effects might cooperate in modulating the stemness of primary cultures. Indeed, a recent work has shown that antibiotics may impact on the stemness of cancer cell lines, probably by differentially modulating the activity of the ribosome and translation (Relier et

al., 2016). Third, this approach makes the design of an *in vivo* pre-clinical study challenging, due to the lack of knowledge on the bioavailability of this molecule upon the administration to animals and to its possible systemic effects that may impact tumor formation and growth.

To get further insight into the contribution of *de novo* methylation to the tumorigenic potential of Apc^{KO} intestinal stem cells, we decided to establish stable models of Dnmts knockdown via the lentiviral transduction of transgenic organotypic cultures with shRNA targeting the *Dnmts* transcripts. Immunohistochemical staining shows that the knock-down occur at variable extent in different structures within the WT cultures, with heterogeneous expression of Dnmt3a and Dnmt3b (intensity of the nuclear staining ranging from absent or very weak to comparable with the intensity found in lentiviral transduced non-target control cells) (figure 35). We reasoned that such heterogeneity is probably due to the variable location and multiplicity of lentiviral integration in the stem cell genome. Indeed, since the primary cell cultures are polyclonal and form from multiple stem cells, the insertion of a single copy of the lentiviral genome can be sufficient for a given cell to acquire the resistance to the antibiotic selection without efficiently impacting the target mRNA expression, whereas multiple genomic insertions may result in more abundant expression of the shRNA and more effective knockdown.

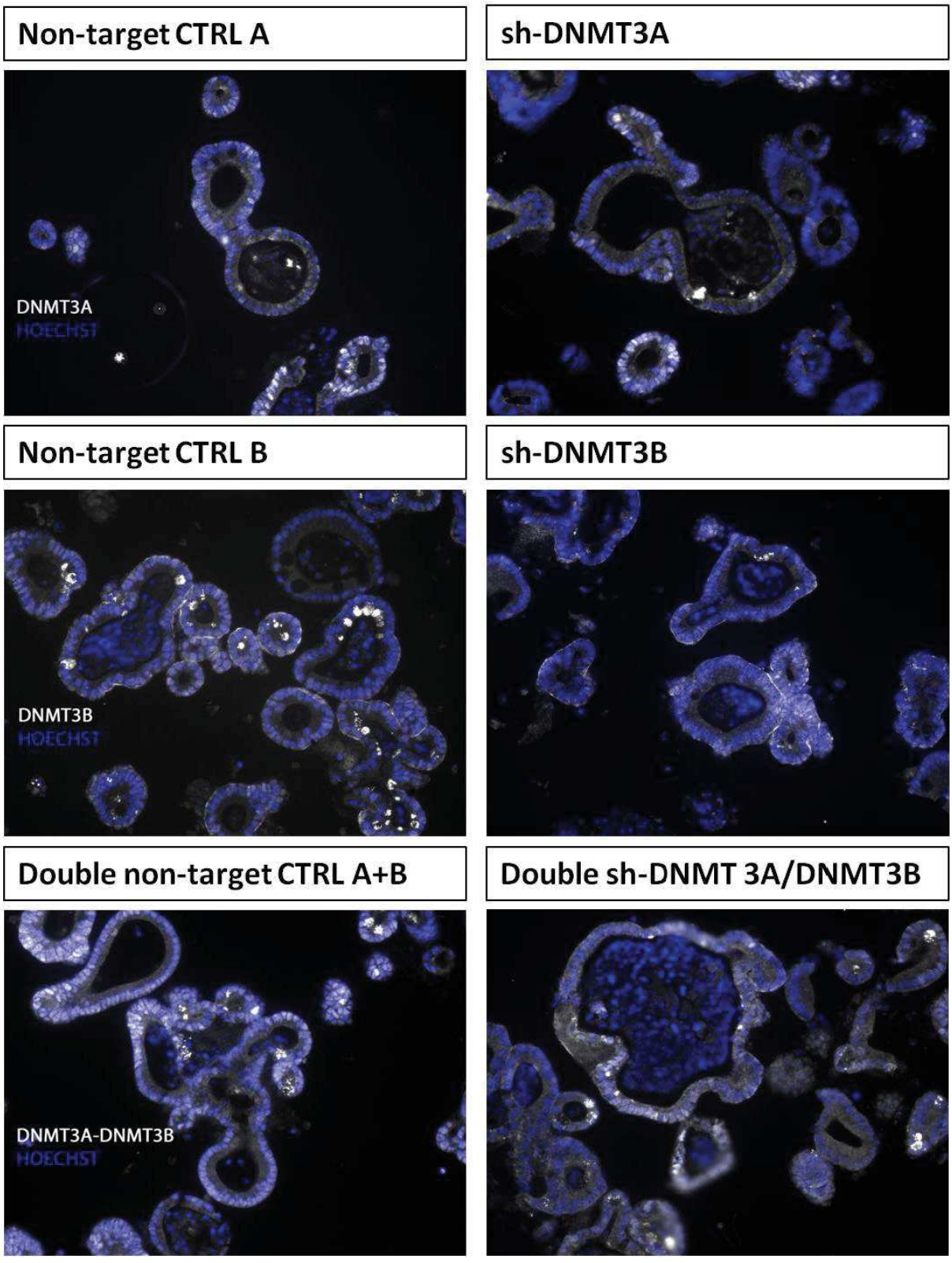

Figure 35: lentiviral-mediated tranduction of Dnmt3a and Dnmt3b specific sh-RNA results in heterogeneous knock-down in intestinal *Villin-Cre*^{ERT2} organoids. Left panels show the patterns of expression in control cells transduced with non-target lentivirus. Right panels show the patterns of expression in cells transduced with the specific shRNA or combination of both. DNA methyltrasferases are immunostained (white) and nuclei are stained with Hoechst (blue). 40X magnification.

Despite this heterogeneity, we found that upon the treatment with 4-hydroxy-tamoxifen, the general rate of cell-division was significantly reduced in Apc^{KO} cultures expressing the Dnmt3b specific shRNA, whereas the stable expression of the Dnmt3a specific shRNA did not significantly impact the proliferation (figure 36). Interestingly, the combination of both shRNA provokes a reduction in the Ki-67 expression and BrdU incorporation comparable to that found in the case of Dnmt3b knock-down. Together, these observations suggest that Dnmt3a does not critically sustain the proliferation of Apc^{KO} cells, although other important features (e.g. cell death) may be regulated by its activity, and that Dnmt3a does not takes on the role of Dnmt3b when this latter is depleted. On the other hand, Dnmt3b knock-down can phenocopy the effect obtained by treating cells with a Dnmt3b-specific inhibitor (Nanaomycin A), or a general Dnmts inhibitor (5-Azacytidine), supporting its prominent role in sustaining cell growth upon the deletion of *Apc*.

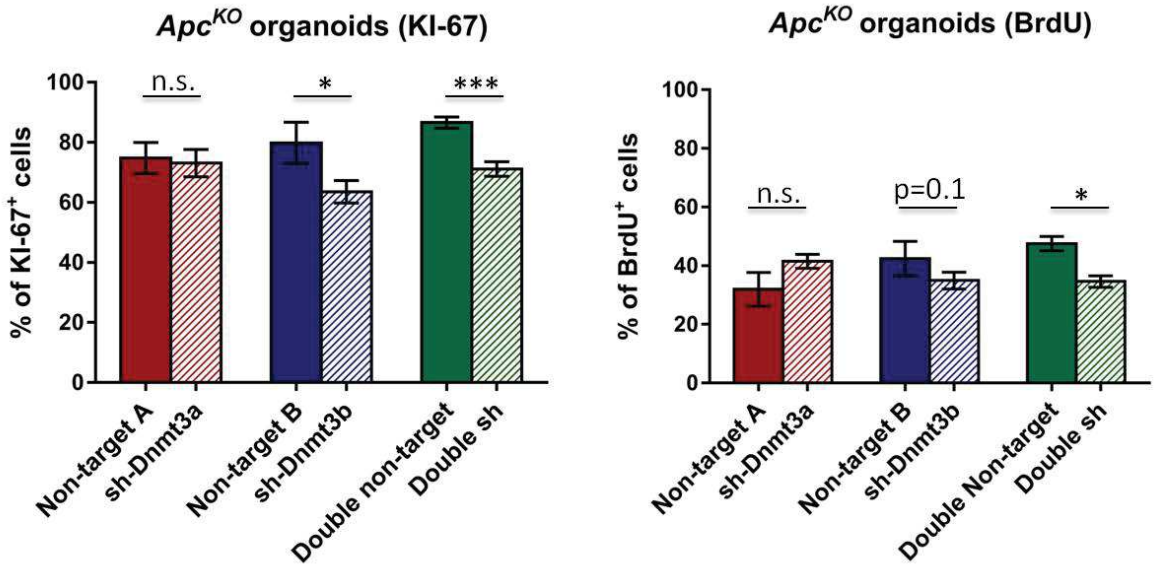

Figure 36: proliferative rate in response to Dnmt3a/Dnmt3b knockdown in organotypic $Apc^{LoxP/LoxP}$,$Villin\text{-}Cre^{ERT2}$ cultures treated with 4-hydroxy-tamoxifen. Figures show the average % of Ki-67 expressing cells and BrdU incorporation in the different conditions. Results represent the average of at least 25 individual structures. * indicates a P-value <0.05, * indicates a P-value <0.001 as calculated by Mann-Whitney *U*-test.**

SECTION II: DNA METHYLATION AND TRANSCRIPTOMIC PROFILES ASSOCIATED WITH DIFFERENTIAL SUSCEPTIBILITY TO TUMOR INITATION IN *Apc*$^{\Delta 14}$ MICE

1. Genetic and non-genetic heterogeneity governing the variable tumor initiation rate in *Apc*$^{\Delta 14}$ mice

Apc$^{\Delta 14/+}$ mice constitute a valuable model to investigate the genetic and environmental modifiers modulating the rate of tumor initiation in the gut. These mice spontaneously develop multiple intestinal adenomas with complete penetrance during their adult life as a consequence of the stochastic loss of heterozygosity (LOH) in intestinal stem cells leading to the constitutive activation of the Wnt signaling in those cells (Colnot et al., 2004). We can therefore consider the number of tumors developed at a given age as proportional to the relative susceptibility of any individual to develop intestinal neoplasia. Our team recently found that *Apc*$^{\Delta 14/+}$ mice in our inbred colony develop intestinal adenoma at highly variable rate. The highest heterogeneity in the tumor count is found at the age of sixteen weeks, when the number of intestinal adenomas varies between one and more than one hundred and twenty. This heterogeneity is remarkably more pronounced than the one originally described in *Apc*$^{\Delta 14/+}$ mice raised in specific pathogen free (SPF) conditions by Colnot and collaborators. Surprisingly, the team also found that these mice develop adenoma in a bimodal manner, and *Apc*$^{\Delta 14/+}$ individuals can be assigned to two distinct phenotypic groups according to the number of adenomas that are found in the small intestine at the age of sixteen weeks (Quesada et al., unpublished data). As shown in the figure 37, the number of visible adenomas at this age is either between one and twenty (*Apc*$^{\Delta 14/+}$ "FEW" animals) or higher than forty (*Apc*$^{\Delta 14/+}$ "MANY" animals). Mice belonging to the "MANY" group begin to die at the age of sixteen weeks with signs of rectal bleeding, anemia and splenomegaly. The formation of rectal prolapses also frequently occurs in mice developing severe polyposis in the colon. Mice belonging to the "FEW" group do not show any of these signs at sixteen weeks, and nearly 100% of those mice are alive at five months. Overall, the onset of the systemic effects associated with severe polyposis is delayed in this group (Quesada et al., unpublished).

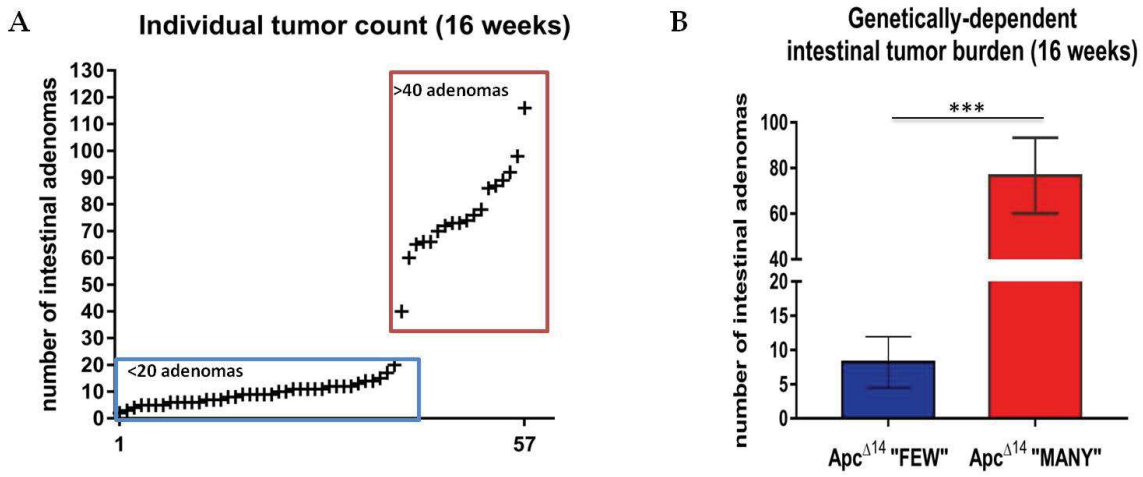

Figure 37: intestinal tumor burden in 16 weeks-old co-isogenic mice. A) Individual tumor count in a representative cohort of 57 animals. B) Genetic-dependent differential tumor burden. n= 39 *Apc*$^{\Delta 14/+}$ "FEW" + 18 *Apc*$^{\Delta 14/+}$ *MANY"). Error bars represent standard deviation, * indicates a P-value <0.001 as calculated by two-tailed Student t-test.**

As expected, the progeny of any *Apc*$^{\Delta 14/+}$ parents accounts for a mendelian proportion of 50% *Apc*$^{+/+}$ and 50% *Apc*$^{\Delta 14/+}$. However, by examining the breeding schemes used to maintain the colony, we observed that the *Apc*$^{\Delta 14/+}$ progeny of any parent having developed less than twenty adenomas accounts for 73% of *Apc*$^{\Delta 14/+}$ belonging to the same group and 27% of mice with a tumor count >40. On the other hand, the *Apc*$^{\Delta 14/+}$ progeny of any parent having developed >40 tumors at the age of 16 weeks only consists in mice with >40 adenomas at this same age, and we never observed any reversion in this mode of segregation across several generations (figure 38). Together, these evidences suggested the existence of a genetic polymorphism in an independent locus located on the chromosome 18 (where *Apc* is located) approximatively 27 centiMorgan away from the *Apc* locus (the genetic distance between two loci represents the frequency of crossing-over occurring between these two). This polymorphism exerts tumor suppressive function in the genetic substrain accounting for mice developing less than twenty tumors by sixteen weeks, while its disruption as a consequence of meiotic recombination occurring in 27% of the progeny of parents carrying the suppressive allele reverts the *Apc* phenotype to the a "MANY" status. The littermates represent therefore two co-isogenic substrains (i.e. they are genetically identical at all but one loci). This finding does not represent a unique case: genetic polymorphisms known as modifiers of *Min* (*Mom*) exert comparable tumor suppressive functions in the *Apc*^{Min} model.

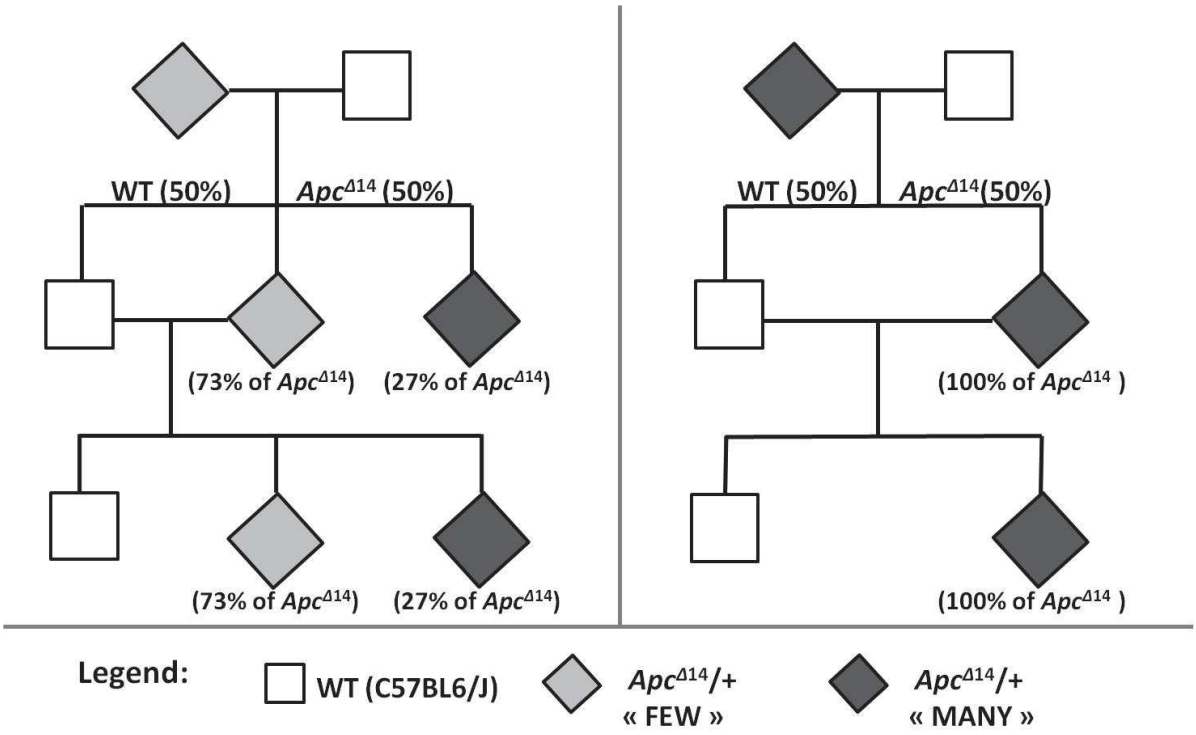

Figure 38: schematic representation of the breeding outputs showing the non-random segregation of the unknown genetic polymorphism.

When we analyzed cohorts of younger individuals we found that Apc$^{\Delta 14/+}$ mice belonging to the "FEW" substrain invariably develop less than three visible lesions at the age of six weeks, whereas *Apc$^{\Delta 14/+}$* mice in the "MANY" substrain invariably display more than twelve visible intestinal adenomas (figure 39). This confirms that this unprecedented polymorphism delays the tumor initiation in the gut of Apc$^{\Delta 14/+}$ mice rather than inducing a regression of pre-formed adenomas.

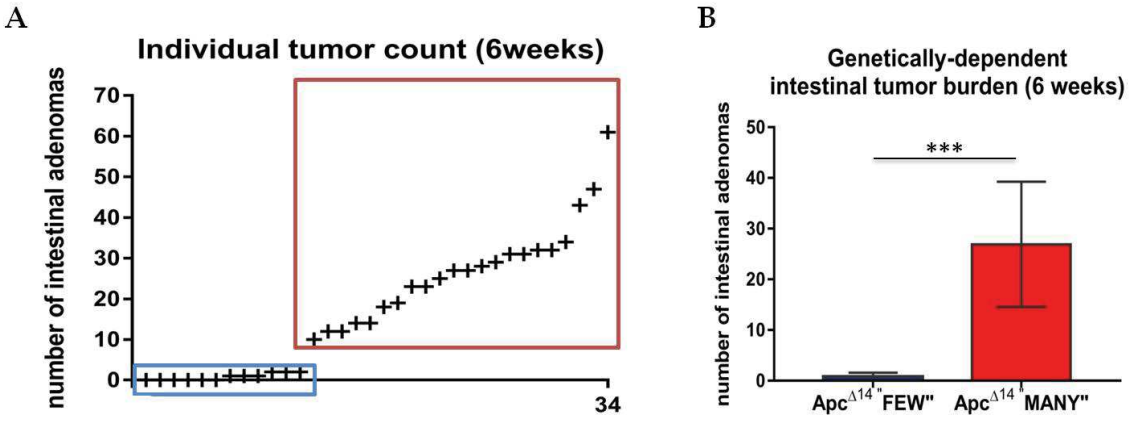

Figure 39: intestinal tumor burden in 6 week-old co-isogenic mice. A) Individual tumor count in a representative cohort of 34 animals. Blue and red boxes highlight the individuals belonging to "FEW" and

"MANY" genetic sustrain respectively. B) Genetic-dependent differential tumor burden. n= 12 *Apc*$^{\Delta 14/+}$ "FEW" + 22 *Apc*$^{\Delta 14/+}$ *MANY").* Error bars represent standard deviation. * indicates a P-value <0.001 as calculated by two-tailed Mann-Whiney *U*-test.**

The formal identification of this modifier and its functional role in intestinal homeostasis and tumorigenesis does not represent the aim of the work presented here. However, it provides a valuable example of the dramatic role played by the genetic variability in modulating the individual susceptibility to develop intestinal neoplasia. Nonetheless, both genetic substrains of *Apc*$^{\Delta 14/+}$ animals display a remarkable intra-group heterogeneity in terms of tumor initiation rate (i.e. susceptibility to develop multiple adenomas), which cannot be associated to any other major genetic change present in the *Apc*$^{\Delta 14/+}$ colony.

2. Molecular profiles associated with variable tumor initiation rate in sixteen week-old isogenic *Apc*$^{\Delta 14/+}$ mice

Epigenetic mechanisms control the expressivity of a given genotype. Furthermore, the epigenetic landscape was shown to be highly variable in cohorts of isogenic animals (Feinberg and Izarry, 2010). Both *Apc*$^{\Delta 14/+}$ substrains display an extensive variability in terms of the relative risk to develop multiple adenomas, which we consider as a surrogate of individual susceptibility.

We decided to investigate whether the heterogeneous susceptibility could be associated with distinct molecular signatures in the sixteen week-old healthy (tumor-free) intestine of mice belonging to the same genetic substrain (*Apc*$^{\Delta 14/+}$ "FEW"*),* in order to exclude the influence of the unknown genetic modifier on the heterogeneity in our colony. We therefore established arbitrary windows of poor or high susceptibility within this group of isogenic individuals, and we considered as poorly susceptible all the individuals having developed less than 6 adenomas at sixteen weeks, whereas co-aged mice having developed more than 10 adenomas were classified as highly susceptible (figure 40). Adult mice belonging to the "MANY" subtrain were not analyzed. These animals begin to develop severe polyposis very early, which in turn leads to the rapid onset of various types of systemic failure. This severity represented the main argument prompting us to select the "FEW" substrain for the subsequent analyses, in order to minimize the local and systemic effects exerted by adenomas on the surrounding non-tumoral intestinal environment.

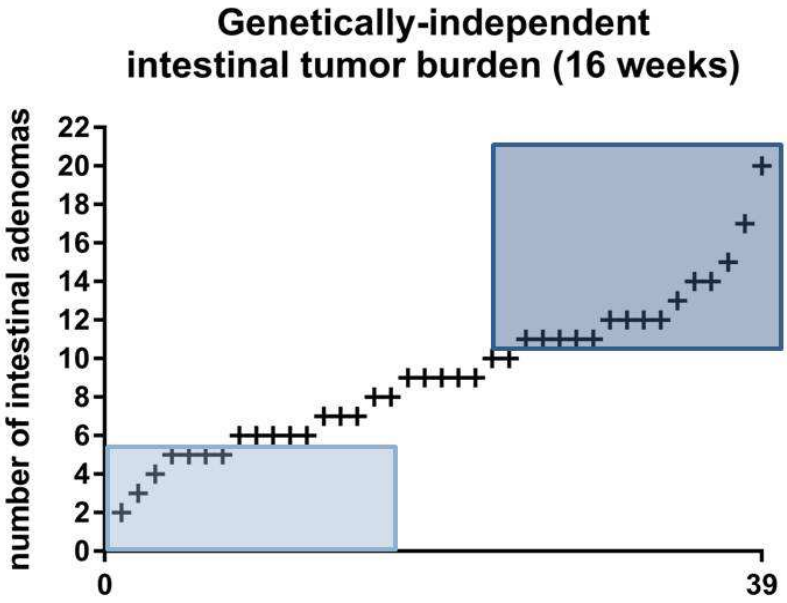

Figure 40: Non-genetic variable relative risk. The individual tumor burden is shown in a cohort of 39 16 weeks-old $Apc^{\Delta 14/+}$ "FEW" animals. Individuals with poor and high tumor initiation rate were selected for the comparison of the molecular profiles in their non-tumoral intestinal tissues. Light and dark blue boxes highlight the arbitrary poor and high susceptibility classes.

We eventually selected two groups of four individuals with either poor or high tumor initiation rate. At sacrifice, intestinal and colonic adenomas were counted and accurately removed, and the tumor-free epithelial and mesenchymal (stroma + muscle) fractions from the distal intestine of those mice were individually collected. We decided to focus the analyses on the tumor-free distal small intestine, since this is the prevalent anatomical location of adenoma development in $Apc^{\Delta 14/+}$ mice. We then verified the absence of any contamination with tumor cells by quantifying the expression of both wild-type and Δexon14 truncated alleles in the epithelial fraction. Epithelial cells forming intestinal adenomas are Apc^{KO} as a result of loss of heterozygosity (LOH). Any contamination of the tumor-free tissue with tumoral cells would alter the relative ratio of expression, which is expected to be close to 1 in the tumor-free epithelium of $Apc^{\Delta 14/+}$ mice. The results show a weak heterogeneity in the expression of both isoforms, with a ratio close to 1 for all the biological replicates in the two groups (figure 41). Furthermore, we detected similar extent in the activity of the Wnt pathway that we monitored by analyzing the expression of the Wnt target gene *Myc*. Overall, these results robustly support the absence of contamination with tumor Apc^{KO} cells in the 8 samples selected for *–omic* profiling.

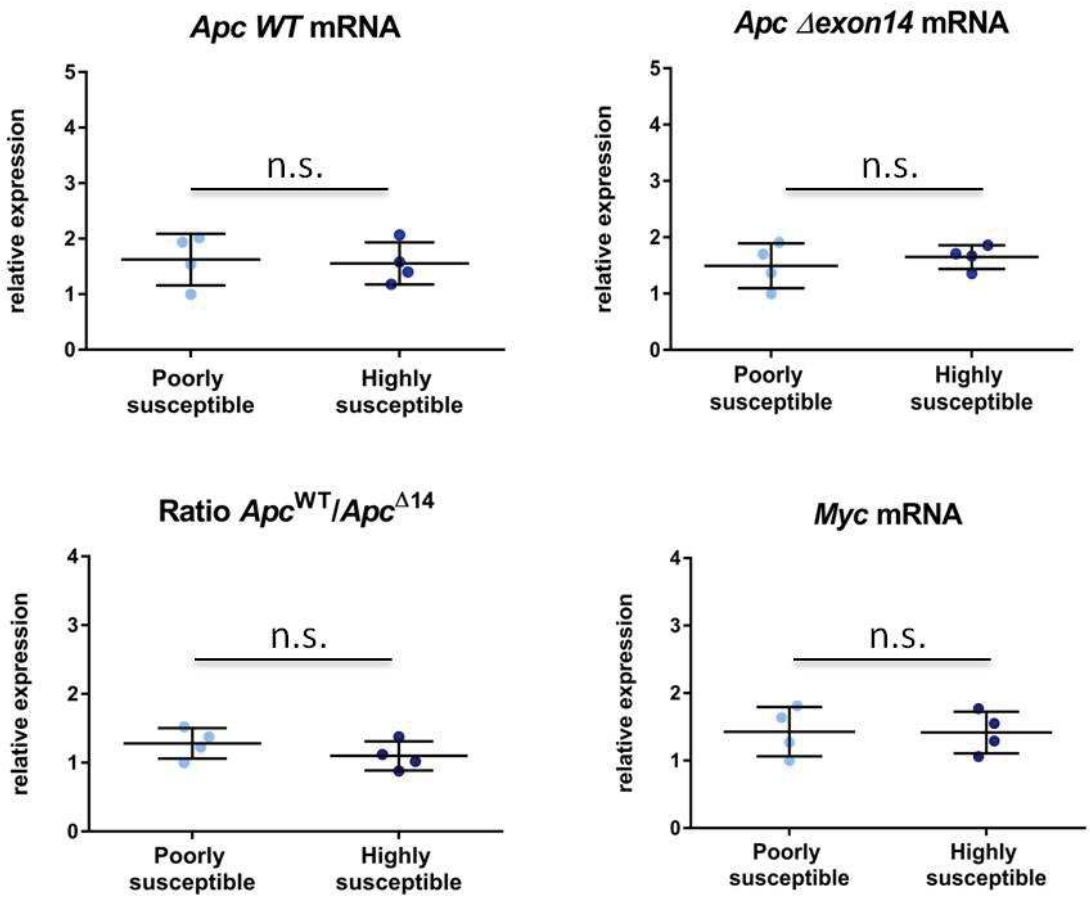

Figure 41: verification of the tumor-free samples selected for *–omic* profiling. qPCR results show comparable expression of the WT and truncated forms of *Apc* and *Myc* in $Apc^{\Delta 14/+}$ mice. Individual and average values in each of the two groups normalized on the expression of housekeeping *Gapdh* and *Hprt* genes are shown. P-value was verified to be >0.05 by Mann-Whitney *U*-test

Since the small intestine includes a myriad of non-epithelial cell types accounting for different molecular signatures, we also evaluated the enrichment of the two different fractions obtained by scraping the intestinal epithelium after incubation in 30 mM EDTA (see material and methods) to avoid any bias due to heterogeneity in the collection of the biological samples. This verification confirmed the purity of the epithelial fraction demonstrated by the reduced expression of the stromal marker Vimentin associated with a strong enrichment in the expression of the epithelial marker Epcam (figure 42). The combination of these markers also demonstrates the relative enrichment of the mesenchymal fraction. Although the results seem to suggest some contamination of this fraction with epithelial cells, the extent is comparable in all the samples.

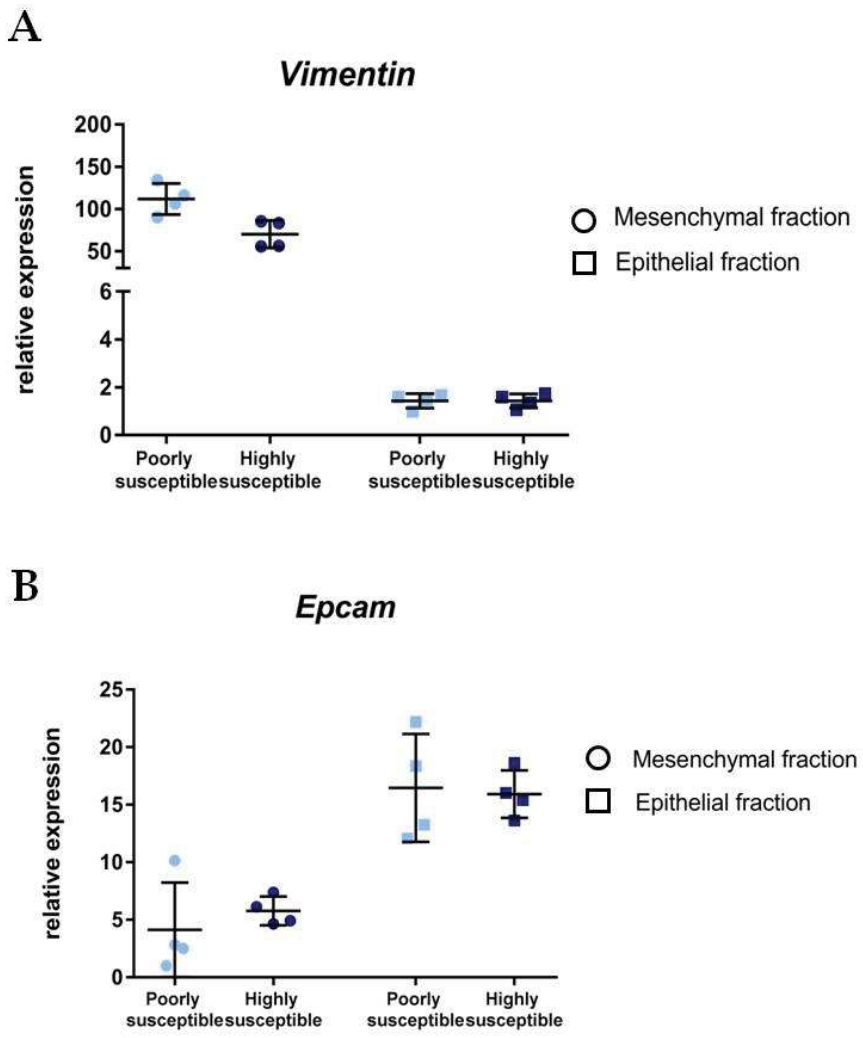

Figure 42: relative enrichment of epithelial and mesenchymal fractions. A) qPCR results showing the expression of the stromal cell marker Vimentin in the epithelial and mesenchymal fractions collected by scraping. B) qPCR results showing the expression of the epithelial marker Epcam. Individual and mean values in each of the two groups normalized on the expression of *Gapdh* and *Hprt* housekeeping genes are shown.

The RRBS profiling performed on the epithelium of poorly and highly susceptible mice revealed a limited number of significant DMR distinguishing the two groups and, overall, clustering analyses of the signatures obtained did not show increased similarity between the individuals assigned to the same class of susceptibility. Some of those 53 differentially methylated regions are associated with the promoters of interesting candidates with potential biological relevance such as the phospholipase A2 group IIA (*Pla2g2a,* also known as the first discovered modifier of *Min* gene*),* the vascular endothelial growth factor A (*VegfA*), and the transcription factor *Gata4*. For most of these regions, however, the difference in the extent of methylation is relatively poor and the two groups show an overlap. We therefore decided to

test the impact on the transcription of genes showing a consensus in their methylation profiles (i.e. no overlap between the extents of methylation of the individuals in the two groups). The differential methylation does not seem to significantly impact on the transcription of those genes, although a tendency toward down-regulation seems to exist in response to the hypermethylation in one group as in the case of *Rps5* and *Gse* (DNA methylation and gene expression are showed in figure 43

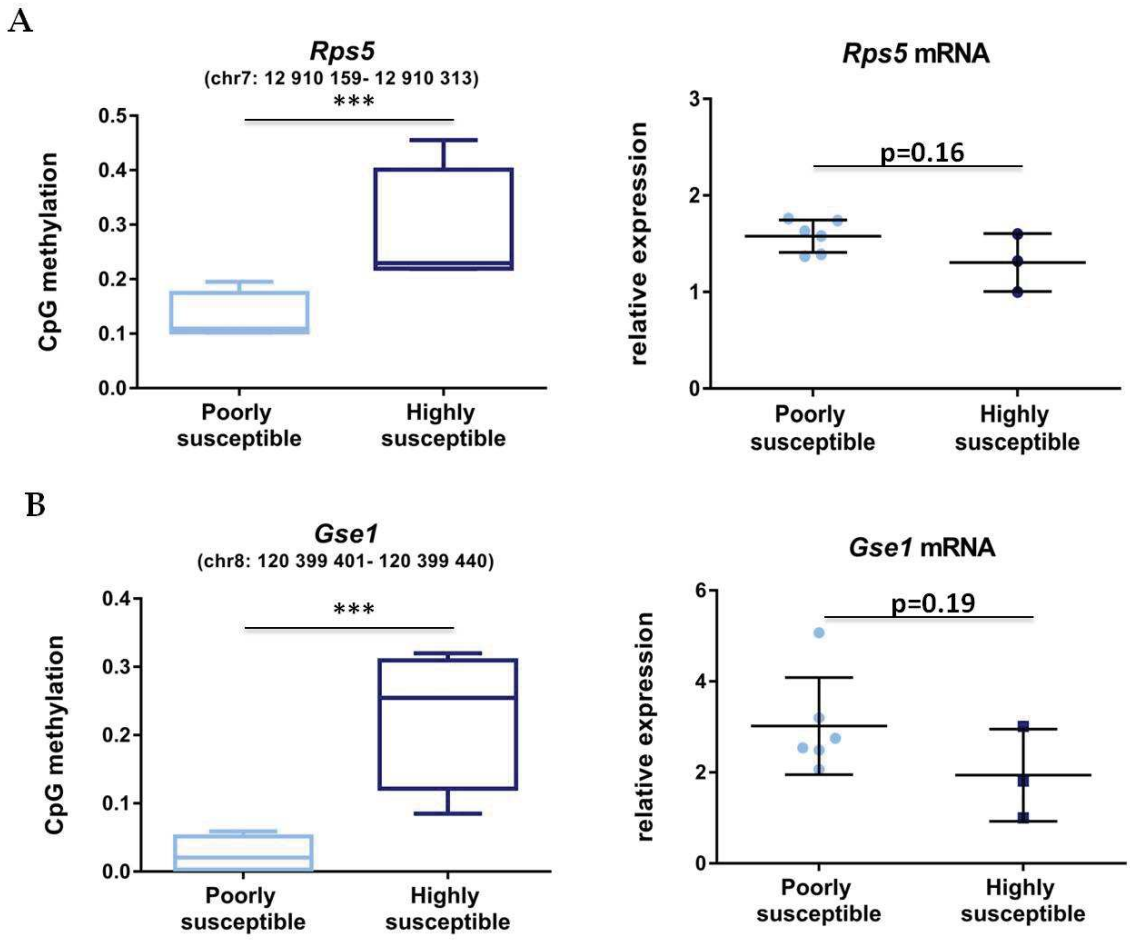

Figure 43: CpG methylation extent as quantified by RRBS (left) in regions showing a consensus (no overalp between the two groups) and qPCR quantification of the transcription of the genes in close proximity to the DMRs: A) *Rps5* and B) *Gse*. * indicates a Q-value <0.001; qPCR results show the individual and average relative expression obtained in 6 poorly susceptible and 3 highly susceptible biological replicates normalized on the expression of *Gapd* and *Hprt* housekeeping genes, together with the associated P-value as calculated by Mann-Whitney *U*-test.**

The gene expression profiles obtained in the same cohort of 4 poorly susceptible and 4 highly susceptible mice provided us with more interesting results. By applying a fold change cut-off of $\log_{1.1}$ we found 73 differentially expressed genes in the epithelial fraction (figure 44) and 780 differentially expressed genes in the mesenchymal fractions of mice belonging to the two

classes of susceptibility. Importantly, hierarchical clustering of the epithelial profiles of expression showed similarity in the biological replicates belonging to each of these classes. The same was true for mesenchymal profiles (data not shown). In other words, the analysis on the expression of coding transcripts is able to correctly determine whether any of the 8 individuals belongs to one or the other class of susceptibility.

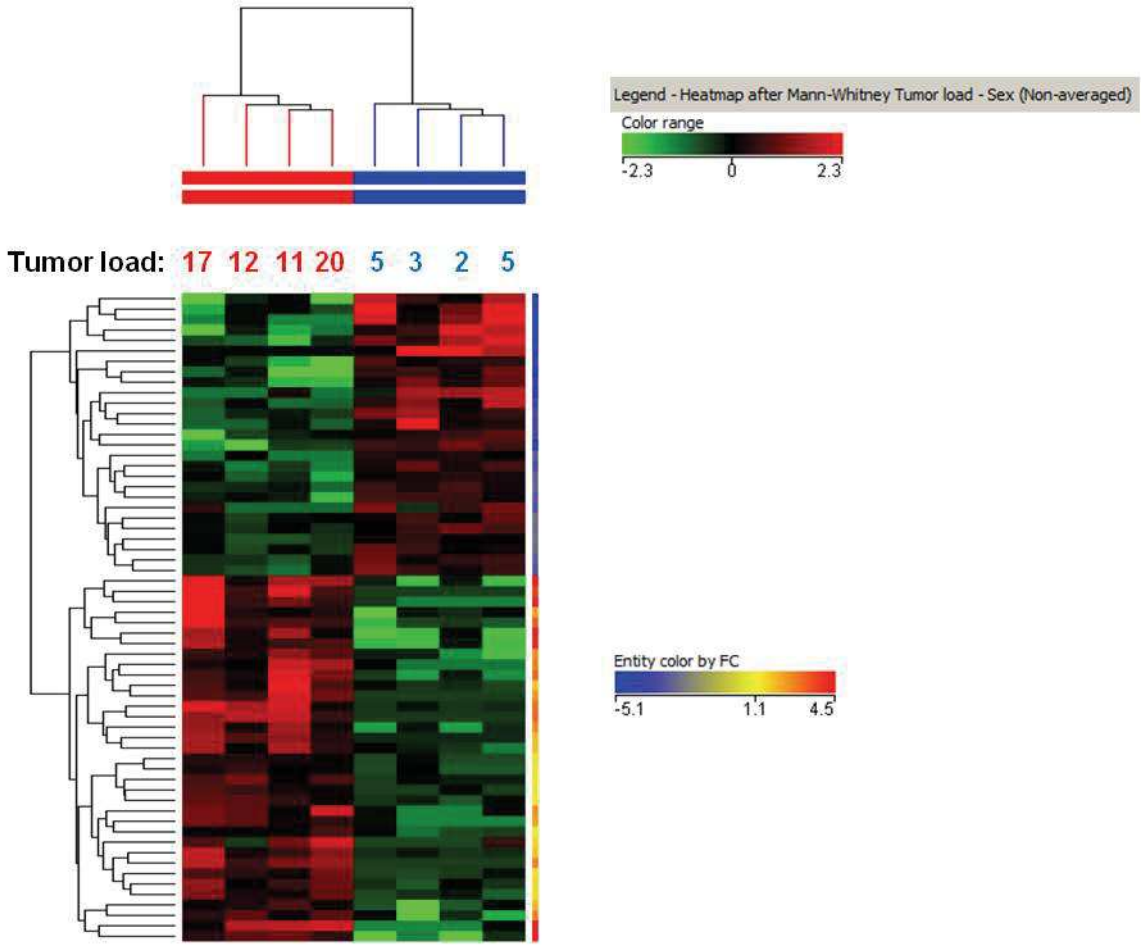

Figure 44: Heatmap and hierarchical clustering analysis of 73 differentially expressed genes in the epithelial fraction of poorly and highly susceptible adult individuals. Mann-Whitney unpaired corrected P-values cut-off=0.05

3. Evaluation of the predictive value of intestinal signatures in six weeks-old *Apc*$^{\Delta 14/+}$ isogenic mice

We also tested whether the molecular signatures found in tumor-free intestine of young individuals could be informative on the relative risk to develop multiple adenomas (i.e. the severity of the pathology) during their adult life. To do so, we collected biopsies of the distal

intestine from six weeks-old $Apc^{\Delta 14/+}$ isogenic mice belonging to the "FEW" genetic substrain (mice developing 1-20 by the age of 16 weeks). Six weeks looked to us as the reasonable age for mice to undergo intestinal anastomosis, consisting in the resection of a portion of the small intestine followed by the surgical restoration of its integrity in order for mice to survive. As previously showed in the figure 39, due to the delay associated with the presence of the unknown genetic polymorphism, mice belonging to the "FEW" group present a very limited number (0 to 2) of adenomas when they are of six week-old, whereas mice belonging to the "MANY" substrain already display an extensive variability in tumor initiation. However, the progeny of mice carrying the unknown polymorphism that determine the FEW status inevitably accounts for 27% of mice with a "MANY" status. As a result, since the observation of $Apc^{\Delta 14/+}$ mice at the age of six weeks does not provide any indication regarding their "FEW" or "MANY" status, we expected 27% of the mice undergoing to surgery to be of no use for this part of the work.

The surgical strategy and procedure were developed in collaboration with the team of Michael Helmrath (MD, MS). Out of 60 $Apc^{\Delta 14/+}$ that underwent to surgery, 48 survived until the end of the study (80% survival rate) and, according to their tumor count, 38 were found to belong to the "FEW" substrain. It took on average 16 days post-surgery for $Apc^{\Delta 14/+}$ "FEW" mice to recover their initial weight (figure 45). Their weight evolution was comparable to what we observed for control WT mice that underwent to surgery, whereas the recovery was delayed in $Apc^{\Delta 14/+}$ "MANY" mice, certainly due to increased severity of their pathology and extensive tumor development.

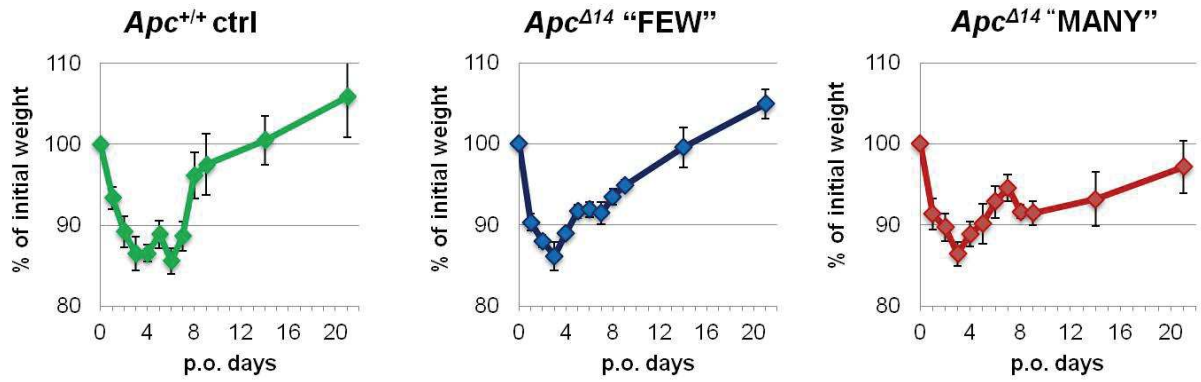

Figure 45: weight evolution after the intestinal resection. The % of the initial weight is shown at different time points post-resection performed on day 0. Results represent the average of 12 $Apc^{+/+}$, 12 $Apc^{\Delta 14/+}$ "FEW" and 12 $Apc^{\Delta 14/+}$ "MANY" mice. Error bars represent S.E.M.

The tumor burden of operated mice at 120 days spanned from 0 to 19 and from 40 to 109. Importantly, when we compared the distribution of adenomas along the small intestinal axis in a representative cohort of four operated females belonging to the "MANY" substrain with the distribution in non-operated females, we didn't observe any significant shift tumor initiation (figure 46). We therefore concluded that our surgical strategy did not majorly alter the phenotype of our $Apc^{\Delta 14/+}$ models, and any subtle variations presented in terms of tumor burden are to be attributed to the resection of two-three centimeters of the anatomical portion (the distal small intestine) in which adenomas generally initiate at elevated rate in the $Apc^{\Delta 14/+}$ model.

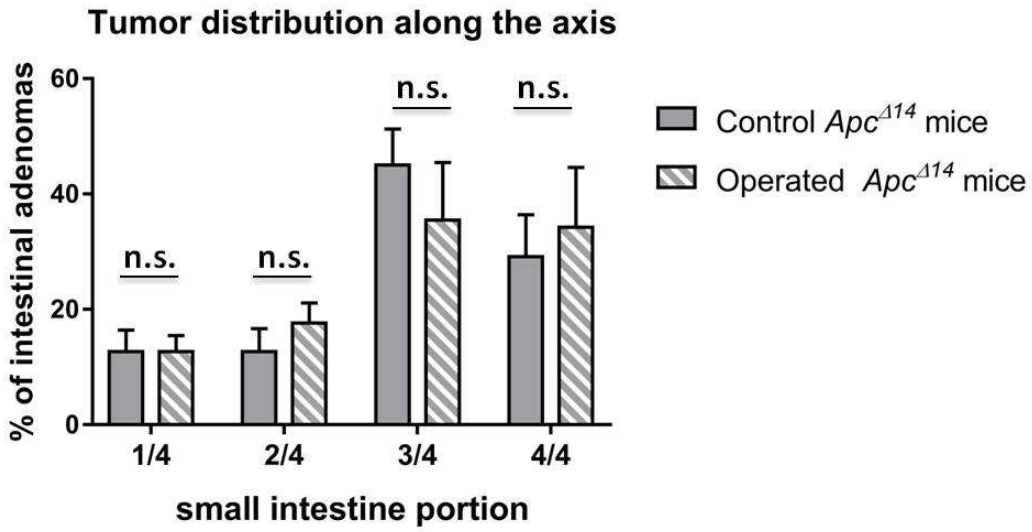

Figure 46: tumor development along the small intestine of operated and control $Apc^{\Delta 14/+}$ mice. Results represent the average % tumors found in of *4* $Apc^{\Delta 14/+}$ "MANY" females per group. The analysis was performed on the "MANY" substrain to evaluate a larger n of adenomas and obtain more informative statistics. Error bars represent SEM. P-value were calculated by the Mann-Whitney *U*-test.

We eventually assigned five individuals to each class of poor (tumor burden was 0, 1, 2, 3 and 4 respectively) and high susceptibility (15, 15, 17, 18 and 19 adenomas). To avoid any possible bias associated to epithelial scraping, we decided to analyze the methylation and gene expression profiles of the intact intestinal biopsy.

RRBS analysis of the intestinal biopsies provided us with a list of 292 differentially methylated regions. Even in this case, hierarchical clustering did not reveal preferential similarity between biological replicates belonging to the same arbitrary class of susceptibility and for most of the regions we did not find a consensus trend in the extent of methylation with an overlap between the two classes. Furthermore, differential methylation does not significantly alter the expression of genes associated with those DMRs, as we found in the case of *Arid1B* and *ApoD* (figure 47).

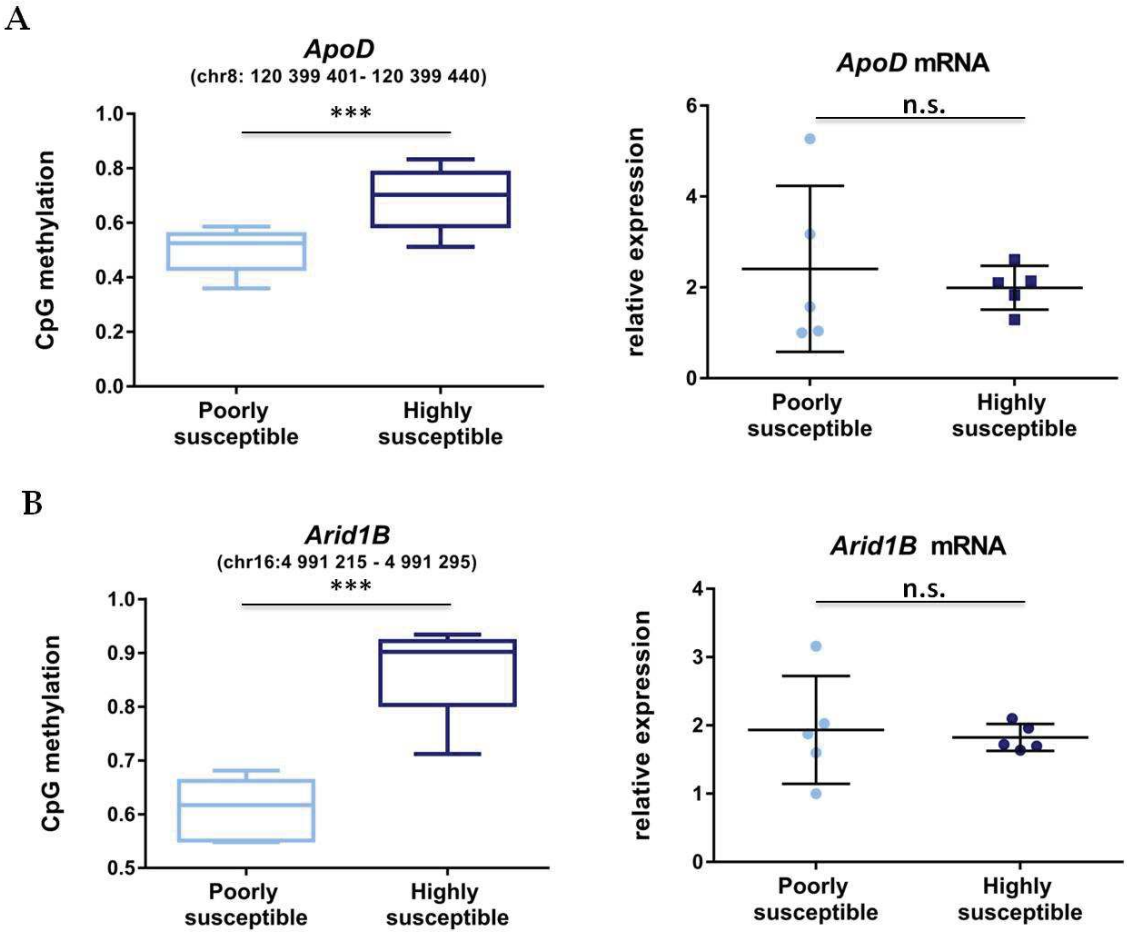

Figure 47: CpG methylation extent as quantified by RRBS (left) in regions showing a consensus (no overalp between the two groups) and qPCR quantification of the transcription of the genes in close proximity to the DMRs: A) *ApoD* and B) *Arid1B*. * indicates a Q-value <0.001. qPCR results show the individual and average relative expression obtained in 5 poorly susceptible and 5 highly susceptible biological replicates normalized on the expression of Gapd and Hprt housekeeping genes, together with the associated P-value as calculated by Mann-Whitney *U*-test.**

Once again, the analysis of the transcriptomic profiles shows that the global gene expression at six weeks correlates with the severity of the phenotype quantified as the number of visible intestinal adenomas developed by the same individuals at the age of four months (120 days) (figure 48). Indeed, isogenic individuals assigned to a particular class of susceptibility according to their tumor burden display similarity in the transcriptional profiles even before multiple adenomas had time to initiate in the intestine of those individuals. Even in this case, however, the differential expression does not depend on the extent of methylation of the promoters of those genes in the healthy intestine of the two groups of mice.

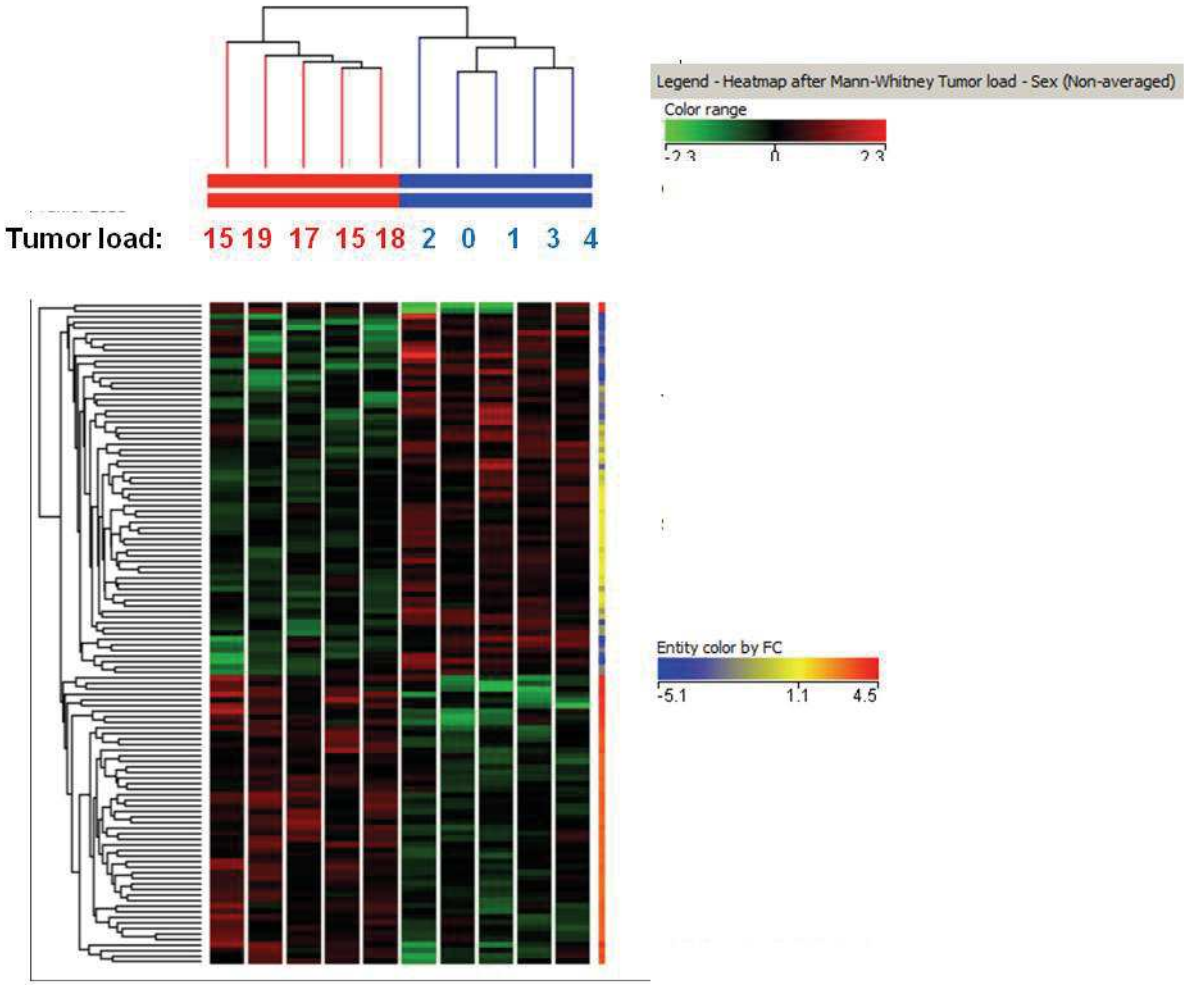

Figure 48: Heatmap of differentially expressed genes in the intestinal biopsies of six-week old poorly and highly susceptible individuals. The individual tumor load at sacrifice (120 days) is shown. Mann-Whitney unpaired corrected p-values cut-off=0.05

DISCUSSION AND PERSPECTIVES

In this work we tried to unravel the dynamics and the biological impact of the molecular signatures associated to the most precocious phases of intestinal tumorigenesis, with particular attention to the role exerted by DNA methylation and its effects on gene expression. Overall, these characterizations have allowed us to identify some novel insights into the biology of the intestinal stem cell compartment, including the perturbation of specific mechanisms controlling the balance between self-renewal and differentiation immediately after the earliest genetic alterations associated to the development of colorectal cancer. We also provided evidences suggesting the existence of a non-genetic heterogeneity associated to the variability in a complex phenotypic trait such as the relative individual risk to develop cancer.

SECTION I: ALTERATIONS IN THE DNA METHYLATION AND GENE EXPRESSION PROFILES UPON THE ONCOGENIC CONSTITUTIVE ACTIVATION OF THE WNT PATHWAY AND THEIR FUNCTIONAL IMPACT ON EPITHELIAL HOMEOSTASIS

The comparison between tumors and their surrounding healthy environment, which has long represented the common strategy for the detection of epigenetic alterations associated with cancer development, does not provide relevant information about the precise timing at which any of these alterations are produced. Moreover, the results of such comparison are somehow biased by the differential heterogeneity of the two samples (tumor and healthy tissue) in terms of representation of different cell types.

We therefore decided to focus the molecular analyses on the compartment responsible for the renewal of the intestinal epithelium, which also represents the compartment-of-origin of intestinal neoplasia. For this part of the work we took advantage of inducible transgenic models allowing us to monitor at precise timing the immediate outcomes of the loss of one or both *Apc* alleles at *–omic* and macroscopic scale. The characterization performed on the isolated *Lgr5*$^{+}$ intestinal stem cells and their immediate progeny shows that very few modifications in the methylation of CpG-rich genomic regions are associated with the earliest genetic event in cancer development, represented by the loss of one allele of *Apc*. Nonetheless, a number of changes occur in the transcriptomic profile of heterozygous intestinal stem cells involving a significant number of genes associated with mechanisms of

cellular detoxification. Although these alterations cannot to be attributed to differential DNA methylation, they might exert a relevant biological impact. We could imagine that the loss of a single copy of *Apc* may render the actively proliferating stem cells more prone to accumulate further genetic alterations due to a deficit in the detoxification of the xenobiotics that are commonly present in the environment. This hypothesis will of course require a functional validation. To this aim, we will challenge intestinal cells with common xenobiotics and we will then monitor *in vivo* or *ex vivo* the accumulation of genotoxic agents immediately after the loss of one allele and quantify the rate of accumulation of genomic damage in these cells, compared to Apc^{WT} cells. Organotypic cultures will represent a valuable model to mechanistically dissect these aspects.

We found that the most dramatic impact on the molecular phenotype is produced upon the complete loss of function of *Apc* in the self-renewal compartment of the small intestine. The transcriptomic profiling of $Lgr5^{+}$ cells and their immediate progeny indicates a deficit in the capacity to commit toward differentiation, which is accompanied by an increase in the expression of markers associated with stemness. These evidences are consistent with the role of the Wnt signaling in the modulation of the balance between stemness and differentiation (Sansom et al. 2004; Andreu et al. 2005). We also showed that a number of alterations are produced in the DNA methylation profiles of these cells. The RRBS analyses do not allow investigating the general extent of genomic methylation at this particular stage. However the fact that transposable IAP regions remain severely methylated upon the deletion of *Apc* may suggest that the general hypomethylation of the genome, described as a hallmark of oncogenic transformation, may not necessarily apply to the early phase consequent to the loss of *Apc* in the stem cell population. To validate this hypothesis we are now considering the whole-genome bisulfite sequencing (WGBS) of these cells that would provide us with more comprehensive information on regions with reduced representation of CpG (CpG shores). However, our approach allowed us to focus our attention to the regions of the genome associated with the gene promoters, and to monitor the functional impact of these alterations on gene expression. Among the most represented biological functions in our list of DMR we found the BMP/TGF-β signaling pathway, whose implication in the cell fate determination of intestinal stem cells is well documented (Vanuytsel et al. 2013). Interestingly we found that differential methylation correlates with the differential expression of some regulators of this pathway, which in turn induces an altered pattern of activation of the BMP signaling upon the loss of *Apc in vivo*. This observation by itself represents a novelty in the biology of intestinal stem cells. Although these two signaling pathways are known to cooperate in the cell fate

determination (Vanuytsel et al., 2013), we previously ignored the existence of a "cross-talk" by which the activation of the Wnt pathway would reduce the responsiveness of epithelial stem cells to the BMP stimuli. Although we did not examine any possible key factor at which these pathways can converge, we provided evidences that this reduced responsiveness is in part mediated through the differential methylation of positive and negative regulators of the BMP signaling. The characterization of the Apc^{KO} stem cell compartment confirms the reduced potential of *Apc*-deficient ISC to undergo differentiation, and indeed these cells accumulate in hypertrophic crypts (figure 49).

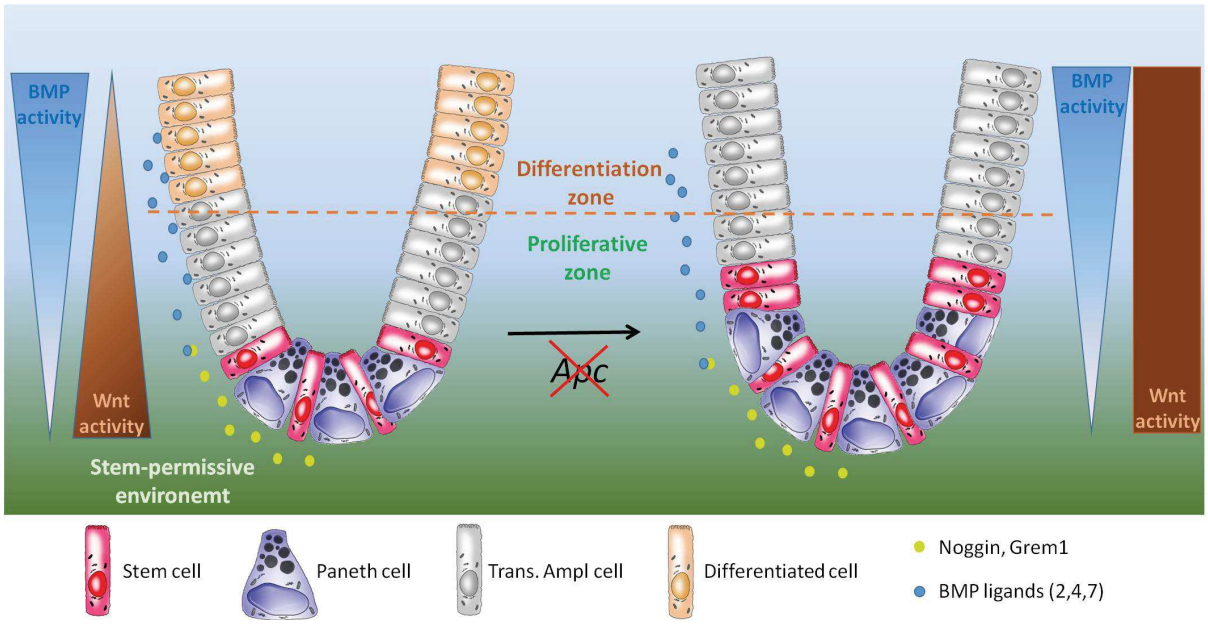

Figure 49: Schematic representation of the early effect produced by the loss of *Apc* in intestinal stem cells. The constitutive activation of the Wnt signaling makes intestinal stem cells and their immediate progeny less responsive to the gradient of BMP stimuli produced by the surrounding niche (Noggin and Grem1 represent the BMP inhibitors secreted by the mesenchyme nearby the crypt bottom). This impaired responsiveness results in an expansion of the stem and Paneth cell compartment at the expense of cell differentiation.

However, when we considered the proliferative dynamics of ISCs, we unexpectedly found that Apc^{KO} cells in the self-renewal compartment divide more slowly that their wild-type counterpart. This reduced proliferation rate may represent a mechanism adopted by *Apc*-deficient stem cells to avoid an excessive accumulation (due to the deficit in their commitment and elimination) that would probably expose them to hypoxia or other types of cellular stress.

Strikingly, we showed that the reduced responsiveness to pro-differentiation stimuli can be partially rescued by inhibiting the function of *de novo* methyltransferases. Indeed, by treating

cells with an inhibitor of Dnmt3b, we observed an increased responsiveness of *Apc*^{KO} organotypic cultures to extrinsic pro-differentiation Bmp stimuli (figure 50). This functional verification represents a proof of principle of the fact that the biological outcome of a critical genetic alteration is in part mediated by reversible epigenetic mechanisms. Aside from its importance in the basic understanding of stem cell biology, this finding may become relevant for the future design of therapeutic strategies. A recent work showed that constitutively active Wnt signaling upon *Apc* inactivation represents a *conditio sine qua non* for the establishment and maintenance of colorectal cancer (Dow et al., 2015). Indeed, this work shows that the restoration of *Apc* expression in conditional *in vivo* models is associated with tumor regression and re-establishment of the normal crypts-villus homeostatic balance via the promotion of differentiation even at late stages of the adenoma-to-carcinoma progression. We could realistically imagine that the modulation of the activity of the epigenetic mechanisms functioning downstream the loss of *Apc* would recapitulate the biological outcome obtained through its genetic restoration. This perspective is further supported by our data showing that the inhibition of the Dnmt3b enzymatic activity via the administration of Nanaomycin A as well as the shRNA-mediated knock-down of its expression both result in a drop of the proliferative rate of *Apc*^{KO} cells to extents comparable to those of wild-type cells. In order to complete this functional characterization we will soon evaluate the "stemness" of *Apc*^{KO}cells upon the inhibition of *de novo* methylation activity. In brief, this experiment will consist in treating *Apc*^{KO} organoids with BMP ligands in presence or absence of Nanaomycin A or upon the stable knockdown of *de novo* DNMTs expression. The organotypic structures obtained in the two conditions will be then dissociated, single cells will be seeded and their self-renewal ability will be tested by measuring their capacity to re-form new structures (clonogenicity assay). Since the inhibition of *de novo* methylation seems to promote the differentiation of *Apc*^{KO} cells, we would expect a reduced capacity to self-renew and form spheroids as a read-out of the *de novo* Dnmts inhibition.

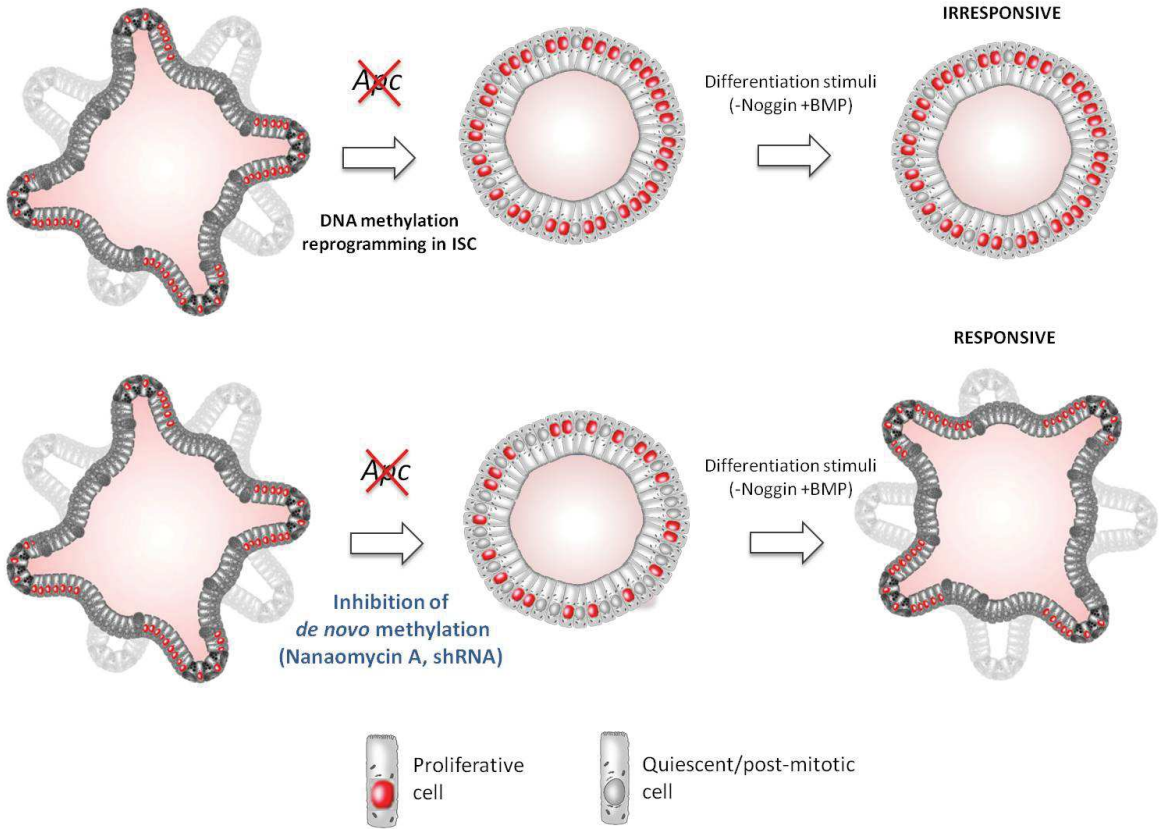

Figure 50: schematic representation of the effects of the inhibition of *de novo* methyltrasferases activity on epithelial organotypic structures in which *Apc* is deleted. Constitutive activation of Wnt signaling is accompanied by a remodeling of the methylation profiles resulting in hyperproliferation and reduced responsiveness to the pro-differentiation BMP stimuli. When the activity of the *de novo* methyltrasferases is inhibited at the same time of *Apc* inactivation via the treatment with a Dnmt3b inhibitor or via shRNA-mediated knockdown, the proliferative rate of knock-out cells is reduced (red nuclei represent actively dividing cells). Moreover, when those cells are stimulated with BMP morphogens, organoids display an increased ability to form a differentiated compartment.

The establishment of a genetic stable model of *de novo* Dnmts knockdown has also allowed us to design a pre-clinical strategy to further investigate *in vivo* the impact of the *de novo* methylation on the capacity of Apc^{KO} epithelial cells to initiate a tumor. To this aim, the shRNA and control lentiviral-transduced cells will be soon injected into the flank of Nude mice in order to monitor the establishment and outgrowth of adenomas. We recently tested the capacity of $Apc^{LoxP/LoxP}$; $VillinCre^{ERT2}$ treated with 4-hydroxy-tamoxifen to initiate tumors after the allo-transplant in these mice, and we found that these cells form tumors at elevated rate, whereas, as expected, $Apc^{+/+}$; $VillinCre^{ERT2}$ control cells do not display any tumorigenic potential. This strategy will provide us with the outstanding possibility to compare the *in vivo* read-out with the molecular profiling obtained from the same cell-cultures. However, the heterogeneous effectiveness of shRNA transduction found in our cultures have so far

represented a limitation, since cells accounting for the most effective knock-down are likely to undergo a negative selection. To overcome this limitation we recently established clonal cultures in order to select clones accounting for the most effective knock-down and avoid any negative selection during *in vitro* expansion and tumor formation. Together with the establishment of a shRNA-mediated knock-down model, we are also currently establishing organotypic models of *de novo* Dnmts abrogation by mean of CRISPR-Cas9 gene editing. Supplemental pre-clinical read-out will be obtained by using the existing conditional *in vivo* models (*Dnmt3a*$^{LoxP/LoxP}$; *Dnmt3b*$^{LoxP/LoxP}$) that are not currently available in the team. The conditional deletion of these genes in the intestinal epithelium will be used to further investigate their impact on the rate of spontaneous tumor initiation in *Apc*$^{\Delta 14}$ mice, focusing the analysis to the self-renewal compartment by using the *Lgr5-EGFP-ires-Cre*^{ERT2} reporter transgenic model.

The characterization we initiated does not take in account any epigenetic modification other than DNA methylation. It should be noted that it is still unclear whether DNA methylation represents a superior instructive mechanism serving as a template for other epigenetic modifications (e.g. histone marks) or a subordinate mark in the regulation of the chromatin status. Therefore, a better comprehension of the epigenetic mechanisms regulating the acquisition of the tumorigenic potential in intestinal stem cell would certainly benefit of an extensive investigation on the dynamics of histone modifications.

SECTION II: DNA METHYLATION AND TRANSCRIPTOMIC PROFILES ASSOCIATED WITH DIFFERENTIAL SUSCEPTIBILITY TO TUMOR INITATION IN *Apc*$^{\Delta 14}$ MICE

Unraveling the mechanisms modulating the relative susceptibility to develop cancer probably represented the most conceptual and technically challenging part of the work. The results provided us with some interesting information. Indeed, although genetic polymorphisms play a major role in determining the severity of the pathology, we showed that an extensive degree of variability exists in two genetic substrains of *Apc*$^{\Delta 14}$ mice. Isogenic mice belonging to each substrain are challenged by identical housing conditions and fed with the same diet. As full inbreeding is impossible, minimal residual segregation should be taken into account. However, the genetic heterogeneity due to novel mutations corresponds to 8-12 single-nucleotide polymorphisms across the entire genome (Bailey, 1982). Inbred mice can also vary with respect to variable number of tandem repeats and transposon insertion (Julier et al. 1990; Lathe 2004). Some other sources of initial individuality should be considered, such as

intrauterine position, imprinting errors, maternal stress, and post-natal handling. However, the heterogeneity in complex phenotypic traits in inbred mice is already documented in the literature. Recently, Freund and collaborators showed that genetically identical mice develop heterogeneous exploratory behavior correlating with individual difference in adult hippocampal neurogenesis (Julia Freund et al. 2013; J. Freund et al. 2015). Furthermore, several studies in the medical literature describe the concept of epigenetic individuality of human homozygotic twins (Bell and Spector 2011).

Here we examined the possible correlation between differential individual risk and heterogeneous molecular states, by analyzing DNA methylation and gene expression of isogenic mice belonging to the same genetic strain. Our characterization via reduced-representation bisulfite sequencing can only partially tackle the question regarding the involvement on DNA methylation, and a more comprehensive investigation by WGBS would be required. However, our data suggest that the methylation of CpG-rich sequences (accounting for promoter regions involved in the regulation of gene expression) in the pre-tumoral healthy tissue does not significantly correlate with the relative susceptibility to initiate intestinal tumors. We cannot exclude the possibility that the differential methylation of other genomic features (e.g. gene bodies and CpG shores) could impact on this trait. It should also be mentioned that the analysis of tissues made up of several cells types represents a limitation in this part of the work, since the remodeling of the epigenetic profiles is likely to occur in the most plastic compartments like the self-renewal epithelial stem/progenitor compartment. However, the use of transgenic reporter models (e.g. the *Lgr5-EGFP-ires-CRE*^{ERT2}) would introduce a source of genetic heterogeneity, since mice are not in a pure genetic background.

On the other hand, gene expression profiles in the healthy tissue of differentially susceptible mice revealed an interesting correlation with the tumor initiation rate. Importantly, this result was confirmed in intestinal biopsies of young mice before they had time to develop multiple adenomas, suggesting that global transcriptomic profiles may have a predictive value in the evaluation of the individual risk. In the immediate future these results will require an attentive validation that was so far impeded by the limited size of our biological cohorts especially in the case of surgical biopsies, in order to identify a minimal core signature associated with increased susceptibility to tumor initiation. Such signature could be then compared by mean of bioinformatic analysis with the data obtained in cohorts of patients in order to evaluate whether this may be predictive on the severity and the recurrence of the human pathology. To test the biological relevance of the differential gene expression, the most significant

candidates could be chosen to evaluate the influence of their dosage on the rate of tumor initiation. In 2010 Alimonti and colleagues showed that gene dosage impacts tumor development and tumor growth by using a hypomorphic model of expression of *Pten,* which revealed an increased susceptibility to CRC consequent to the downregulation of this gene (Alimonti et al. 2010). We could imagine adopting the same strategy and testing whether the downregulation or overexpression of certain genes in our signatures may modify the average tumor burden in cohorts of $Apc^{\Delta 14}$ mice. However, we suspect that the combinatorial effect of the signature rather than single candidates can influence the susceptibility at the population scale.

Epigenetic signatures other than DNA methylation (e.g. the polycomb repressive complex binding landscape) could constitute an instructive mechanism and the investigation on these epigenetic signatures may therefore provide an interesting tool to decipher and evaluate the individual risk. To this aim, the transcriptomic profiles will be examined via gene set enrichment analyses, in order to evaluate *in silico* the enrichment of pre-established epigenetic signatures that would be then further investigated by molecular biology and in-depth sequencing in the already existing cohorts of biological samples.

METHODS

1. Animal models in this work

Apc$^{LoxP/+}$*; Villin-Cre*^{ERT2} mice were generated by crossing *Apc*$^{LoxP/LoxP}$ (Colnot et al., 2004) mice with *Villin-Cre*^{ERT2} mice (El Marjou et al., 2004), and siblings were then bred to maintain the colony constituted by *Apc*$^{LoxP/LoxP}$, *Apc*$^{LoxP/+}$ or *Apc*$^{+/+}$; *Villin-Cre*^{ERT2} animals. For the conditional deletion of the exon 14 (inducing a frameshit mutation at AA580 position), all mice (including *Apc*$^{+/+}$*; Villin-Cre*^{ERT2} controls) were injected at day 0 with 1 milligram of Tamoxifen (Sigma-Aldrich) reconstituted in a solution of 9 volumes of sunflower oil and 1 volume of 70% Ethanol, and fed with tamoxifen-rich diet (Harlan) for no longer than five consecutive days before sacrifice at different time-points (2h-24h-72h and 6 days post-injection).

The same breeding strategy was used to generate and maintain the colony of *Lgr5-EGFP-ires-Cre*^{ERT2} (Barker et al., 2007) containing the conditional LoxP sites flanking the exon 14 of one, both or none *Apc* alleles. Even in this case, activation of the Cre recombinase was obtained by a single injection with Tamoxifen followed by five consecutive day of tamoxifen-rich diet. Mice were generally sacrificed at day 15 post injection.

The *Apc*$^{\Delta 14/+}$ model was generated by Colnot and collaborators (Colnot et al. 2004). Briefly, *Apc*$^{LoxP/+}$ males were crossed with *Meu3Cre40* (germline Cre) females to obtain the constitutive heterozygous deletion of the exon 14. The *Apc*$^{\Delta 14/+}$ colony ("FEW" and "MANY" substrains) was maintained by breeding *Apc*$^{\Delta 14/+}$ males with C57BL6/J females (Charles Rivers laboratories).

All mice were housed at the Institut de Génomique Humaine animal facility in specific pathogen free (SPF) conditions. Experimental procedures were performed in accordance with the French government regulation for animal experimentation (Ministère de l'agriculture, de l'agroalimentaire et de la forêt).

The genotype of all mice was analyzed by PCR on tail-tip genomic DNA, using the primers listed in the table below.

Primer (Forward-Reverse)	Sequence	Amplicon size
Apc.Int13S	CTAGTACTTTTCAGACGTTCATG	$Apc^{\Delta 14}$ = 240 bp
Apc.Int14a	CAATATAATGAGCTCTGGGCC	
ApcFlox F	CTGTTCTGCAGTATGTTATCA	WT = 180 bp
ApcFlox R	CTATGAGTCAACACAGGATTA	KO = 250 bp
Villin-Cre F	CAAGCCTGGCTCGACGGCC	Tg = 280 bp
Villin-Cre R	CGCGAACATCTTCAGGTTCT	
Lgr5-EGFP-ires-Cre F	GCAGAAGAACGGCATCAAG	Tg = 138
Lgr5-EGFP-ires-Cre R	GCTCAGGTAGTGGTTGTCG	

Table 2: list of primers used for animal genotyping. The expected amplicon size is provided. In the *$Apc^{\Delta 14/+}$*, *Villin-CreERT2* and *Lgr5-EGFP-ires-CreERT2,* the presence of PCR product indicates the deletion (*$Apc^{\Delta 14/+}$*) or the presence of the transgene, whereas WT genotypes do not produce any amplicon.

2. Epithelial and mesenchymal samples preparation.

After sacrifice, *$Apc^{\Delta 14}$* intestines were everted and washed with 1x PBS. The selected intestinal portion (indicated in the results) was then opened longitudinally on an ice-cold plate. Tumors in this portion were counted under a stereomicroscope (Nikon SMZ1000, Nikon Instruments), carefully removed, collected and snap-frozen in liquid nitrogen. The surrounding tumor-free environment was then incubated in 30mM EDTA (Sigma-Aldrich) in HBSS pH 7.4 (Gibco) on ice and the epithelium was scraped by mean of two thin needles, collected and snapfrozen in liquid nitrogen. The remaining portion (muscle + submucosa) was further checked under to eliminate any remaining epithelium, collected and snapfrozen. Representative images of the two isolated fractions are shown in figure 51.

Epithelial samples from *$Apc^{+/+}$*, *$Apc^{LoxP/+}$* and *$Apc^{LoxP/LoxP}$*; *Villin-Cre^{ERT2}* mice injected with tamoxifen were scraped as described above, snap-frozen and stored at -80°C.

All frozen intestinal samples were subsequently submerged in liquid-nitrogen and underwent to mechanical dry pulverization. Powder samples were then aliquoted and stored at -80°C until subsequent gDNA and RNA extraction.

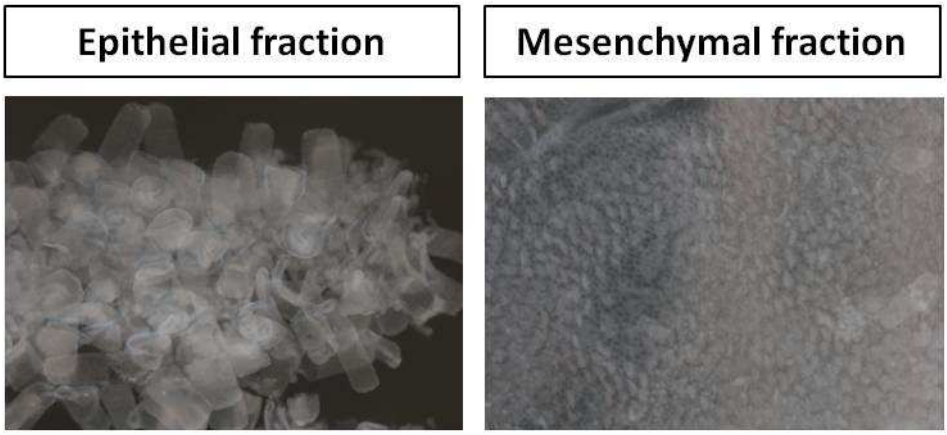

Figure 51: Example of epithelial and mesenchymal fractions obtained by epithelial scraping after 30mM EDTA incubation.

3. Intestinal biopsy collection by ileo-ileal resection

A trained operator performed intestinal microsurgery on six week-old $Apc^{\Delta 14}$ mice. 48 hours prior to surgery mice were switched to liquid isotonic diet (Jevity 1 Cal, Abbot Nutrition) and provided with water *ad libitum*. Mice were anesthetized with 1.5-2.5% isoflurane (IsoFlo, Axience) administered by aerosol. Surgery was performed on a warm plate (37°C) using a stereomicroscope (Nikon SMZ1000, Nikon Instruments) equipped with a camera (Nikon Instruments). The peritoneal cavity was irrigated with Zosyn (Tazocilline) antibiotic solution (200 mg/ml Piperacillin, 25mg/ml Tazobactam). The 2-3 cm long ileal portion to be collected was selected according to the anatomical vascular organization in order to avoid the resection of arteries and vessels and maintain the normal intestinal blood supply. After the resection, the integrity of the gut was surgically restored using a non-absorbable 9-0 ethilon suture (Ethicon). The peritoneal cavity was sutured with a 4-0 absorbable ethilon suture (ethicon). After completion of the surgery, mice were maintained in a recovery room at 32°C until awakening, when they were injected with 0.05 mg/kg Buprenorphine solution (Vetergesic multidose) and returned to their cages, where they were fed with liquid isotonic diet during seven days post-surgery. They were then switched to standard solid diet, housed in a 12-hour light/dark cycle, and weight evolution was monitored twice a week until sacrifice.

4. Tumors count in the $Apc^{\Delta 14/+}$ intestine

After sacrifice, intestines were everted and washed with 1X PBS before they were fixed with 10% buffered formalin during 4 hours at room temperature or over-night at 4°C.

Intestines were then washed twice with 1X PBS, opened longitudinally and tumors were counted using a stereomicroscope (Nikon SMZ1000, Nikon Instruments) and registered. Intestines were then processed as "swiss-rolls" as described in the section "histology and immunohistochemistry".

5. Epithelial dissociation, fluorescent activated cell sorting and flow cytometry analysis of the cell cycle.

Freshly isolated small intestines mice were opened along their length and washed with PBS. Tissue from the most proximal third of the intestinal length was then incubated for 15' in 30mM EDTA (Sigma) in HBSS pH 7.4 (Gibco) on ice, 10' in the same solution at 37°C and transferred in DMEM (Life Technologies) supplemented with 10% FBS (Sigma-Aldrich). Vigorous shaking yelded the epithelial fraction that was then resuspended and incubated in 100ul of Dispase (Becton Dickinson) in 10 ml of HBSS, supplemented with 100 ul of DNAse (Sigma-Aldrich). To investigate the co-localization of GFP with markers of mature tuft cells, single cell preparation obtained by filtration on a 30 μM mesh was incubated with a Phycoerythrin Rat anti-mouse Siglec-F antibody *(*BD pharmigen 552126*)* for 30 minutes at 4°C*,* washed with HBSS and resuspendend in an appropriate volume of HBSS pH 7.4 supplemented with 5% FBS. To exclude dead cells from the analysis and sorting, 7-Amino-Actinomycin D (7-AAD, Life Technologies) was added to the mix at a concentration of 2μl/ml, 30' prior to the analysis. GFP^{+}/$Siglec\text{-}F^{-}$/$7\text{-}AAD^{-}$ cells were sorted directly in RLT+ lysis buffer (Qiagen) supplemented with β-mercaptoethanol (Sigma-Aldrich) for subsequent gDNA/RNA extraction using a FACSAria *(*Becton Dickinson) at the IRMB imaging platform of Montpellier. An $Lgr5^{+/+}$ (GFP^{neg}) epithelial sample was systematically used as a control to establish the autofluorescence threshold and create a positive GFP-positive gate.

In the case of cell cycle analysis, after cell sorting GFP^{+} cells were incubated for 20' at 4°C in a solution containing 50 μg/ml propidium iodide (PI, Interchim), 2,4 mg/ml bovine pancreas RNAse (to avoid intracellular RNA staining, Sigma Aldrich), 0,5% W/V sodium citrate dehydrate (Sigma), 0,5% triton (Sigma-Aldrich) in distilled water. DNA content was then analyzed by mean of a GALLIOS cytometer (Beckman Coulter) at the IRMB imaging facility of Montpellier. Data analysis was performed using FlowJo flow-cytometry software.

6. Crypt isolation, organotypic culture and lentiviral-mediated transduction

For organotypic cultures, the most proximal third of the small intestine of $Apc^{+/+}$ or $Apc^{LoxP/LoxP}$; $Villin\text{-}Cre^{ERT2}$ mice is everted, opened longitudinally and washed with a 1% mix solution of antibiotics (Ampicillin, Streptomycin) in 1X PBS, and then incubated in the same solution for 15' at 4°C, twice. Intestine is then cut in small pieces (0.5 cm) and incubated in 2mM EDTA (Sigma) in HBSS pH 7.4 (Gibco) for 30' on ice. After vigorous pipetting, crypts are isolated by filtration on a 70 µM mesh and resuspended in DMEM/F12 (Gibco) supplemented with 1% antibiotics mix, 10mM Hepes and 2mM L-Glutamyne. Crypts are then counted 2000 crypts are mixed with an equivalent volume of Matrigel (Corning), and plated in presence of DMEM supplemented with N-2 supplement (Gibco), B-27 supplement (Gibco), 1,25mM N-acetylcystein, 50 ng/ml EGF (Peprotech), 100 ng/ml Noggin (R&D system), 500 ng/ml R-spondin (R&D system) and 10 µM Y-27632 (Sigma Aldrich). Cultures were replated every five days. Briefly, cells are resuspended in 500ul of DMEM/F12, mechanically dissociated by mean of a 27G needle, and approximatively ¼ of cells are resuspended in DMEM/F12 and mixed with a volume of Matrigel, and plated in presence of DMEM/F12 supplemented with growth factors.

To induce the Cre-mediated recombination of *Apc in vitro,* cells are cultured in a medium supplemented with 200 ng/ml of 4-hydroxytamoxifen resuspended in absolute ethanol during 3 days. The deletion of *Apc* knock-out organoids is then selected by removing R-Spondin from the medium. To inhibit the Dnmt3b activity, 5µM Nanaomycin A reconstituted in DMSO is added at the same time than 4-hydroxytamoxifen treatment and maintained all along the culture. Alternatively, medium is supplemented with 200 nM 5-Azacytidine in aqueous solution.

To test the Bmp responsiveness, after 4-hydroxytamoxifen and Nanaomycin A administration, organoids were seeded in absence of recombinant Noggin in the medium and recombinant Bmp2 (RD systems) reconstituted in 4mM HCl was added at the following re-plating at 200 ng/ml

For lentiviral-mediated transduction, we slightly modified the protocol described by Onuma and collaborators (Onuma et al., 2012). Briefly, organoids are single-cell dissociated with Tryple reagent (Gibco) supplemented with 10mM Y-27632 (Sigma-Aldrich). Single cells are diluted in DMEM/F12, counted and infected with Dnmt3a (clone TRCN0000039035), Dnmt3b (clone TRCN0000071068) or equivalent non-target shRNA-containing lentivirus (MISSION shRNA, Sigma-Aldrich) at M.O.I.=10 and single cells are seeded on a layer of a

solidified mix of one volume DMEM/F12 and one volume Matrigel in presence of DMEM/F12 supplemented with 2,5 uM CHIR99021 (Sigma-Aldrich) and growth factors, in which however R-Spondin is added at 1 ug/ml (instead of 500ng/ml). Virus-containing medium is removed 18 hours later and a supplemental layer of DMEMF12/matrigel is added over the cells in presence of the standard medium supplemented with growth factors. Antibiotic selection was performed 48 hours post-infection by adding puromycin at 1ug/ml or G418 400 ug/ml, and stopped one week later. Double infection with both Dnmt3a/Dnmt3b or non-target/non-target shRNA-containing lentivirus and antibiotic selection were performed sequentially.

To evaluate the rate of cell division, BrdU is added to the medium at 10 μM two hours prior to cells harvesting. Part of the cells were harvested in RLT+ lysis buffer (Qiagen) supplemented with β-mercaptoethanol and stored -80°C for further gDNA and RNA extraction.

7. Immunofluorescence, immunohistochemistry and *in-situ* hybridization

After sacrifice, intestines were everted and washed with 1X PBS before they were fixed in 10% neutral buffered formalin during 4 hours at room temperature or over-night at 4°C. Intestines were then washed twice with 1X PBS, opened longitudinally and histological samples were prepared as "swiss-rolls", dehydrated through successive baths of ethanol at increasing concentration (70-100%) and xylene and embedded in paraffine. 3-5 μM-thin sections were cut using a microtome (Leica) and rehydrated through successive baths of xylene and alcohol at decreasing concentration (100-70%). Organotypic cultures were fixed in 1neutral buffered formalin over night at 4°C, embedded in histogel (Thermo scientist) and further processed in the same manner. Epitope unmasking was systematically performed in a boiling solution of 10 mM sodium citrate dehydrate (Sigma-Aldrich) pH 6.4 for 20', and sections were let cool-down for 40' before blocking buffer solution (5% milk or 3% Donkey serum in 0,1% TBS triton) was applied for one hour at room-temperature. Primary antibodies were appropriately diluted in blocking buffer and incubation with primary antibody was performed over-night at 4°C. The list of primary antibodies used in this work is provided in table 2. Sections were then washed with two serial baths of TBS or PBS 0.1% Tween (Sigma-Aldrich). Fluorescent signal was developed by incubating with secondary antibodies coupled with AlexaFluor 488, cyanine3 or cyanine 5.5 dyes (Jackson immunology) for one hour at room temperature in the dark, and Hoechst was added at 1g/ml to stain the nuclei. Sections

were then washed twice with TBS or PBS 0,1% Tween and mounted with fluoromount aqueous mounting medium (Sigma-Aldrich). Anti-mouse/rabbit universal immuno-peroxidase polymer (N-histofine) was used for bright-field imaging. In this case, signal development was obtained by applying the SIGMAFAST 3,3'-diamino-benzidine substrate (Sigma-Aldrich). Nuclei were then stained with hematoxylin, sections were dehydrated through successive baths of ethanol and xylene, and samples were mounted with PERTEX (Histolab).

In situ hybridization was performed to detect *Olfm4*-expressing cells in transgenic (GFP^+) crypts. Briefly, GFP^+ crypts were identified by conventional immunohistochemistry and *in-situ* hybridization was performed on adjacent sections. $Olfm4^+$ cells were only counted in GFP^+ crypts found on adjacent sections. Sections were rehydrated and permeabilization was performed by applying 0,2N HCl during 15', which was followed by treatment with 3 µg/ml proteinase-K solution for 20' at 37°C. Sections were then fixed 10' with 10% neutral buffered formalin, and acetylation was performed applying a fresh a 0,1 M triethanolamine, 0,02 N HCl, 0,25% (v/v) acetic anhydre solution in sterile water during 5' at 58°C. Pre-hybridization solution (20X SSL, 500nM EDTA pH8, Dehart buffer, tRNA) was applied 2 hours at 58°C. Hybridization with 2 µg/ml *Olfm4* RNA digoxygenin-coupled probes was then performed over-night at 58°C. Sections were then washed and incubated with anti-digoxigenin alkaline-phosphatase coupled antibody (Roche) for 2 hours at room temperature. Signal was developed using SIGMAFAST FastRed TR/Naphthol (Sigma-Aldrich) for 2 hours at room temperature.

All fluorescent pictures were acquired at room temperature on a Axioimager Z1 microscope (Carl Zeiss, Inc.) equipped with a camera (AxioCam MRm; Carl Zeiss, Inc.). Bright-field immunohistochemistry pictures were taken at room temperature on an Eclipse 80i microscope (Nikon) equipped with a digital camera (Q-imaging Retiga2000R with a Q-imaging RGB slider).

Antibody	Reference	Host	Concentration
α-B-Catenin	BD biosciences 610154	Mouse	1:800
α-BrdU	Hybridoma bank G3GA	Mouse	1:600
α-Chromogranin A	SantaCruz 1488	Goat	1:800
α-Dclk1	Abcam 31704	Rabbit	1:1000
α-Digoxigenin-AP Fab	Sigma-Aldrich 11093274910		
α-Dnmt1	Abcam 19905	Rabbit	1:400
α-Dnmt3a	Abcam 23565	Rabbit	1:400
α-Dnmt3b	Abcam 2851	Rabbit	1:400
α-Lyzozyme	Santa Cruz 27958	Goat	1:400
α-GFP	Life Technologies A6455	Rabbit	1:1000
α-Ki-67	Abcam 16667	Mouse	1:1000
α-PhosphoSmad 1/5/8	Cell signalling 9511S	Rabbit	1 :200
α-PhosphoSmad 2/3	Cell signalling 8828S	Rabbit	1 :200

Table 3: primary antibodies used for immunofluorescence and immuhistochemistry in this work.

8. gDNA and RNA extraction

For nucleic acid extraction from intestinal fractions, dry powder samples were homogenized in RLT+ buffer (Qiagen) supplemented with β-mercaptoethanol. gDNA and total RNA extraction was then performed by using the AllPrep DNA/RNA/miRNA universal kit (Qiagen) following the manufacturer instructions. The integrity of RNA samples used for RNA-sequencing and qPCR analyses presented in this work was evaluated with a Bioanalyzer and the RNA integrity number was confirmed to be higher than 6 for all selected samples. Extraction of gDNA and RNA from FACS-isolated GFP-positive cells was performed by using the AllPrep DNA/RNA micro KIT following manufacturer instructions with the only exception that 80% ethanol was replaced by 70% ethanol to increase the RNA yeld. The integrity of RNA samples used for RNA-sequencing was evaluated with a Bioanalyzer and the RNA integrity number was confirmed to be higher than 6 for all of the twelve selected samples.

9. RT-PCR, semi-quantitative RT-PCR, RT-qPCR and DNA methylation quantification by qPCR on McrBC-digested genomic DNA.

Reverse transcription of RNA samples was performed by using the Transcriptor First strand cDNA synthesis KIT (Roche) following manufacturer instructions. Both random hexamer and oligodT primers were used for reverse transcription.

In the case of semi-quantitative PCR, 10 ng of cDNA prepared from GFP^+ cells RNA template were used for amplification with a thermocycler (Eppendorf). Primers used for semi-quantitative PCR are listed below.

Gene symbol	Gene name	Forward primer	Reverse primer	Amplicon size
Smad6	*Mothers against decapentaplegic 6*	AAGCCACTGGATCTGTCCGA	GGGAGTTGACGAAGATGGGG	379
Actb	*Actin beta*	AGCTCAGTAACAGTCCGCCT	CCAGCCTTCCTTCTTGGGTATG	360

Tableau 4: Primers for semiquantitative PCR performed on cDNA samples from FACS-isolated GFP^+ cells.

Real-time PCR quantification of gene expression was systematically performed in triplicate on 5 ng of cDNA by using the LightCycler 480 SYBR Green I Master (Roche) on a LightCycler 480 detection system (Roche). The efficiency of the primers used for real-time quantification (listed in the table below) was evaluated relatively to the slope obtained by the quantification of a standard curve, and the presence of a single amplicon at the expected size was checked on an 2% agarose gel. Results were normalized on the average of the expression of *Gapdh* and *Hprt* housekeeping genes and the relative quantification was obtained by applying the $^-\Delta\Delta Ct$ method described by Pfaffl (Pfaffl 2001):

$$\text{Relative expression} = \text{Efficiency}^{-\Delta\Delta Cp}$$

Gene symbol	Official gene name	Forward primer	Reverse primer	Amplicon size	Efficiency
Apc∆ex14	*Adenomatous Polyposis Coli*	TGGAAGTTAAAAAGGCAAATCC	CACAAGGCTTCCTGGTCTTT	151	1.96
Apc WT	*Adenomatous Polyposis Coli*	TTGGAAGTTAAAAAGGAATCAACC	CCATCCACAGCACAGATGTC	104	2.01
ApoD	*Apolipoprotein-D*	TCACCACAGCCAAAGGACAAA	CGTTCTTCCATCAGCGAGTAGT	171	2.01
Arid1B	*AT-rich interactive domain-containing protein 1B*	GCAGATCCCAGGGCAGC	CTGGGAGTGGGGGTGAGTA	83	1.94
Bmi1	*Polycomb complex protein Bmi-1*	CCAGCAAGTATTGTCCTATTTGTGA	TTGAAGAGTTTTATCTGAACCCTTATGTT	152	1.95
Dnmt1	*DNA methyltransferase 1*	TTTTCTGTTAAGCCATCTCTTTCC	AACAGCTCCAGCCCGAGT	105	1.98
Dnmt3b	*DNA methyltransferase 3B*	CAGGAGCCACCCAAGTTATA	AGCACCAAGTACCCCGTTG	101	1.98
Eed	*Embryonic ectoderm development*	GTATGTTTGGGATTTAGAAGTAGAAGA	CTACTGAAACTGGTTTGTCGAA	102	1.93
Epcam	*Epithelial cell adhesion molecule*	GCGGCTCAGAGAGACTGTG	CCAAGCATTTAGACGCCAGTTT	139	2.05
Ezh2	*Enhancer of zhest 2*	AGGATACAGCCTGTGCACATCATGA	GATCCAGAACTTCATCCCCCATAT	205	2.04
Gapdh	*Glyceraldehyde-3-phopshate deydrogenase*	GGAGCGAGACCCCACTAACA	ACATACTCAGCACCGGCCTC	51	1.98
Gse1	*Genetic suppressor element 1*	GGACATTTTGAGCGCGTG	ATGGCTCATTGCCTGGTAAGT		1.8
Hdac2	*Histone deacetylase 2*	GCGTACAGTCAAGGAGGCGG	GCTTCATGGGATGACCCTGGC	94	1.93
Hprt	*Hypoxanthine guanine phosphoribosyl transferase*	GCAGTACAGCCCCAAAATGG	GGTCCTTTTCACCAGCAAGCT	52	1.98
Lgr5	*Leucine-reach repeat containing G-protein coupled receptor 5*	TCTCCTACATCGCCTCTGCT	TCTAGGCGCAGGGATTGAAG	186	2.1
Myc	*Myelocytomatosis oncogene*	GCCCGCGATCAGCTCTCCTGA	CGTGGCTGTCTGCGGGGTTT	89	2
Ring1B	*Ring finger protein 1B*	AGTTACAACGAACACCTCAG	TCCAAACAAATTGGGCACAT	100	1.97
Rps5	*Ribosomal protein S5*	GTCGAGTGAATCAGGCCATCT	AGCTCATCTGCAGGGCACTC	97	1.94
Vimentin	*Vimentin*	CGGCTGCGAGAGAAATTGC	CCACTTTCCGTTCAAGGTCAAG	124	1.92

Table 5: Primers used for real-time PCR mRNA expression quantification. Expected size of the amplicon and efficiency calculated on a standard curve are indicated.

qPCR quantification of DNA methylation of selected genomic regions was performed on genomic DNA samples after digestion (16 hours at 37°C) with methylation sensitive McrBC restriction enzyme (New England Biolabs) performed by adding 400 ng of gDNA to a mix of 4 µl of NEB buffer, 0,4 µl of BSA, µl of GTP, 2 µl of McrBC enzyme and water to a final volume of 37 µl. Undigested controls are obtained by replacing the enzyme with an equivalent volume of water. Reaction was stopped by incubating the samples for 20' at 65°C. Real-time PCR quantification was then performed in triplicate on 1.39 ng of the digestion product, using specific primers designed to flank target genomic regions. Results were normalized on the average Cp of three unmethylated control regions (*Col1A2*, *Col3a1* and *Col9A2*) and the $2^{-\Delta\Delta Ct}$ value was calculated. The extent of methylation is then calculated by using the formula:

$$\% \text{ of methylation} = 100 \times \left(1 - \frac{2^{-\Delta\Delta Cp \text{ digested}}}{2^{-\Delta\Delta Cp \text{ undigested}}}\right)$$

The primers used for real-time PCR quantification of the DNA methylation extent are listed in the table below.

Genomic locus name	Forward primer	Reverse primer
Col1A2	AAAGAGAAGGATTGGTCAGAGCAGT	GCCAAGGGAGGAGACTTAGTTG
Col3a1	TTGCTGTTTCAACCACCCAATA	CATTGAGACATTTTGAAGTTGGAATT
Col9A2	CTCTGGACTTATTTTTATTGGGTATCTTTT	CAGGGAAGATGGATGTTTAAATACTG
Iap	TATGCCGAGGGTGGTTCTCTA	TGCGGCAAAACTTTATTGCTT
Smad6	GGCAAGCTTCTCCATGTACC	TTCTAGAGAGTCCAACAGTTGGC

Table 6: Primers used for real-time PCR quantification of DNA methylation in genomic samples digested with McrBC restriction enzyme.

10. Tanscriptomic analyses by Next Generation Sequencing

The transcriptomic profiling presented in this work were performed by Next Generation Sequencing on two different platforms. The RNA-seq data from *Lgr5*$^{+}$ cells were collected by GATC-biotech (European Genome and Diagnostic Centre, Konstanz-Germany) on an Illumina HiSeq 2500 (Illumina). After poly-A selection, strand specific DNA libraries were built for sequencing performed on 125 bp paired-end reads with sequencing depth of 30 million read pairs. The RNA-seq reads were aligned to the reference genome (mm10) using Bowtie alignment. TopHat identified the potential exon-exon splice junctions of the initial alignment. Then Cufflinks identified and quantified the transcripts from the pre-processed RNA-seq alignment. After this, Cuffmerge merged the identified transcript pieces to full length transcripts and annotates the transcripts based on the given annotations. Finally, merged transcripts from samples/conditions were compared using Cuffdiff to determine the expression levels (quantified as fragment per kilobase per million mapped reads, FPKM) at transcript level including in each biological sample. Combined expression data were generated by merging all the sample of each condition into one table, the differential expression values are expressed as fold-change and a measure of significance (P-value) between conditions is provided.

The RNA-seq data from *Apc*$^{\Delta 14/+}$ intestinal samples and biopsies were collected by Cincinnati Children's Hospital Medical Center NGS platform (European Cicinnati, USA) on an Illumina HiSeq 2500 (Illumina). In this case, after poly-A selection, strand specific DNA libraries were built for sequencing performed on 75 bp paired-end reads with sequencing depth of 20 million read pairs. Gene expression analyses were performed as described above.

11. Reduced representation bisulfite sequencing

RRBS were performed on gDNA samples extracted from *Apc*$^{\Delta 14}$ intestinal surgical biopsies, tumor-free epithelial fraction from sixteen week-old *Apc*$^{\Delta 14}$ mice and *Apc*$^{+/+}$, *Apc*$^{+/-}$ and *Apc*$^{-/-}$ GFP^{+} FACS-isolated cells. RRBS libraries were produced as previously described (Auclair et al. 2014). Briefly, we digested 100 ng of genomic DNA 5 hours with MspI (Thermo Scientific), performed end-repair and A-tailing (with 5 U Klenow-fragment, Thermo Scientific), and ligated to methylated adapters (with 30 U T4 DNA ligase, Thermo Scientific) in Tango 1× buffer. Fragments between 150 and 400 bp were excised from a 3%agarose 0.5× TBE gel with the MinElute gel extraction kit (Qiagen) and bisulfite-converted with the EpiTect bisulfite kit (Qiagen) with two consecutive rounds of conversion. Final RRBS ibraries were amplified by PCR with the PfUTurbo Cx hotstart DNA polymerase (Agilent)

using the following PCR conditions: 2 min at 95°C; 16 cycles of 30 sec at 95°C, 30 sec at 65°C, and 45 sec at 72°C; and 7 min at 72°C. We purified the libraries with AMPure magnetic beads (Beckman Coulter) and performed pairedend sequencing (0032 × 75 bp) on an Illumina HiSeq 2500 at Integragen SA. RRBS was performed with 100 ng starting DNA and 14 cycles for the final PCR. We cleaned the sequencing reads with Trim Galore (v0.2.1, parameters –rrbs –paired -r1 30 -r2 30 -q 20 –length 20 –retain_unpaired, http://www.bioinformatics.babraham.ac.uk/projects/trim_galore/) and aligned to the mm10genome with BSMAP (v2.74, parameters -v 2 -w 100 –r 1 -x 400 -m 30 -D C-CGG -n 1) (Xi and Li 2009). Percentage of methylation values were calculated as the ratio of the number of Cs over the total number of Cs and Ts with methratio.py in BSMAP (parameters -z -u -g). The bisulfite conversion efficiency was estimated by calculating the C-to-T conversion in non-CpG sites. For all data analysis, we filtered CpGs to have a minimum sequencing depth of 8× and visualized methylation values with the IGV browser (Robinson et al. 2011).

12. Statistical analysis

The Prism software was used for descriptive statistical analyses. As normal distribution was not met, a two-tailed Mann-Whitney *U*-test was used to calculate the P-value. For histological data quantification, sample (n) was defined as the number of cell per crypt or crypt-villus unit. Unless otherwise stated, 20 cypts, crypt-villus axes or organotypic structures were counted per histological per histological section of each genotype and condition. According to the central limit theorem, in the case of n>30, data comparison was achieved with a two-tailed Student's *t*-test. Results shown as histograms represent means, and error values are represented as SEM or standard deviation as indicated in each figure.

BIBLIOGRAPHY

Adams, David, Lucia Altucci, Stylianos E. Antonarakis, Juan Ballesteros, Stephan Beck, Adrian Bird, Christoph Bock, et al. 2012. "BLUEPRINT to Decode the Epigenetic Signature Written in Blood." *Nature Biotechnology* 30 (3): 224–26. doi:10.1038/nbt.2153.

Albuquerque, Cristina, Cor Breukel, Rob van der Luijt, Paulo Fidalgo, Pedro Lage, Frederik J. M. Slors, C. Nobre Leitão, Riccardo Fodde, and Ron Smits. 2002. "The 'Just-Right' Signaling Model: APC Somatic Mutations Are Selected Based on a Specific Level of Activation of the Beta-Catenin Signaling Cascade." *Human Molecular Genetics* 11 (13): 1549–60.

Al-Hajj, Muhammad, Max S. Wicha, Adalberto Benito-Hernandez, Sean J. Morrison, and Michael F. Clarke. 2003. "Prospective Identification of Tumorigenic Breast Cancer Cells." *Proceedings of the National Academy of Sciences of the United States of America* 100 (7): 3983–88. doi:10.1073/pnas.0530291100.

Alimonti, Andrea, Arkaitz Carracedo, John G. Clohessy, Lloyd C. Trotman, Caterina Nardella, Ainara Egia, Leonardo Salmena, et al. 2010. "Subtle Variations in Pten Dose Determine Cancer Susceptibility." *Nature Genetics* 42 (5): 454–58. doi:10.1038/ng.556.

Andreu, Pauline, Sabine Colnot, Cécile Godard, Sophie Gad, Philippe Chafey, Michiko Niwa-Kawakita, Pierre Laurent-Puig, et al. 2005. "Crypt-Restricted Proliferation and Commitment to the Paneth Cell Lineage Following Apc Loss in the Mouse Intestine." *Development (Cambridge, England)* 132 (6): 1443–51. doi:10.1242/dev.01700.

Andreu, Pauline, Grégory Peignon, Christian Slomianny, Makoto M. Taketo, Sabine Colnot, Sylvie Robine, Dominique Lamarque, Pierre Laurent-Puig, Christine Perret, and Béatrice Romagnolo. 2008. "A Genetic Study of the Role of the Wnt/Beta-Catenin Signalling in Paneth Cell Differentiation." *Developmental Biology* 324 (2): 288–96. doi:10.1016/j.ydbio.2008.09.027.

Aran, Dvir, and Asaf Hellman. 2013. "DNA Methylation of Transcriptional Enhancers and Cancer Predisposition." *Cell* 154 (1): 11–13. doi:10.1016/j.cell.2013.06.018.

Aran, Dvir, Sivan Sabato, and Asaf Hellman. 2013. "DNA Methylation of Distal Regulatory Sites Characterizes Dysregulation of Cancer Genes." *Genome Biology* 14 (3): R21. doi:10.1186/gb-2013-14-3-r21.

Aran, Dvir, Gidon Toperoff, Michael Rosenberg, and Asaf Hellman. 2011. "Replication Timing-Related and Gene Body-Specific Methylation of Active Human Genes." *Human Molecular Genetics* 20 (4): 670–80. doi:10.1093/hmg/ddq513.

Artavanis-Tsakonas, S., M. D. Rand, and R. J. Lake. 1999. "Notch Signaling: Cell Fate Control and Signal Integration in Development." *Science (New York, N.Y.)* 284 (5415): 770–76.

Asfaha, Samuel, Yoku Hayakawa, Ashlesha Muley, Sarah Stokes, Trevor A. Graham, Russell E. Ericksen, Christoph B. Westphalen, et al. 2015. "Krt19(+)/Lgr5(-) Cells Are Radioresistant Cancer-Initiating Stem Cells in the Colon and Intestine." *Cell Stem Cell* 16 (6): 627–38. doi:10.1016/j.stem.2015.04.013.

Auclair, Ghislain, Sylvain Guibert, Ambre Bender, and Michael Weber. 2014. "Ontogeny of CpG

Island Methylation and Specificity of DNMT3 Methyltransferases during Embryonic Development in the Mouse." *Genome Biology* 15 (12): 545. doi:10.1186/s13059-014-0545-5.

Barker, Nick, Johan H. van Es, Jeroen Kuipers, Pekka Kujala, Maaike van den Born, Miranda Cozijnsen, Andrea Haegebarth, et al. 2007. "Identification of Stem Cells in Small Intestine and Colon by Marker Gene Lgr5." *Nature* 449 (7165): 1003–7. doi:10.1038/nature06196.

Barker, Nick, Rachel A. Ridgway, Johan H. van Es, Marc van de Wetering, Harry Begthel, Maaike van den Born, Esther Danenberg, Alan R. Clarke, Owen J. Sansom, and Hans Clevers. 2009. "Crypt Stem Cells as the Cells-of-Origin of Intestinal Cancer." *Nature* 457 (7229): 608–11. doi:10.1038/nature07602.

Bastide, Pauline, Charbel Darido, Julie Pannequin, Ralf Kist, Sylvie Robine, Christiane Marty-Double, Frédéric Bibeau, et al. 2007. "Sox9 Regulates Cell Proliferation and Is Required for Paneth Cell Differentiation in the Intestinal Epithelium." *The Journal of Cell Biology* 178 (4): 635–48. doi:10.1083/jcb.200704152.

Batlle, Eduard, Jeffrey T. Henderson, Harry Beghtel, Maaike M. W. van den Born, Elena Sancho, Gerwin Huls, Jan Meeldijk, et al. 2002. "Beta-Catenin and TCF Mediate Cell Positioning in the Intestinal Epithelium by Controlling the Expression of EphB/ephrinB." *Cell* 111 (2): 251–63.

Beck, Stayce E., Barbara H. Jung, Eunice Del Rosario, Jessica Gomez, and John M. Carethers. 2007. "BMP-Induced Growth Suppression in Colon Cancer Cells Is Mediated by p21WAF1 Stabilization and Modulated by RAS/ERK." *Cellular Signalling* 19 (7): 1465–72. doi:10.1016/j.cellsig.2007.01.017.

Behnsen, Judith, Stefan Jellbauer, Christina P. Wong, Robert A. Edwards, Michael D. George, Wenjun Ouyang, and Manuela Raffatellu. 2014. "The Cytokine IL-22 Promotes Pathogen Colonization by Suppressing Related Commensal Bacteria." *Immunity* 40 (2): 262–73. doi:10.1016/j.immuni.2014.01.003.

Behrens, J., J. P. von Kries, M. Kühl, L. Bruhn, D. Wedlich, R. Grosschedl, and W. Birchmeier. 1996. "Functional Interaction of Beta-Catenin with the Transcription Factor LEF-1." *Nature* 382 (6592): 638–42. doi:10.1038/382638a0.

Beier, Frank, Richard J. Lee, Allison C. Taylor, Richard G. Pestell, and Phyllis LuValle. 1999. "Identification of the Cyclin D1 Gene as a Target of Activating Transcription Factor 2 in Chondrocytes." *Proceedings of the National Academy of Sciences of the United States of America* 96 (4): 1433–38.

Bell, Jordana T., and Tim D. Spector. 2011. "A Twin Approach to Unraveling Epigenetics." *Trends in Genetics: TIG* 27 (3): 116–25. doi:10.1016/j.tig.2010.12.005.

Benoit, Yannick D., Manon B. Lepage, Taoufik Khalfaoui, Eric Tremblay, Nuria Basora, Julie C. Carrier, Lorraine J. Gudas, and Jean-François Beaulieu. 2012. "Polycomb Repressive Complex 2 Impedes Intestinal Cell Terminal Differentiation." *Journal of Cell Science* 125 (Pt 14): 3454–63. doi:10.1242/jcs.102061.

Berman, Benjamin P., Daniel J. Weisenberger, Joseph F. Aman, Toshinori Hinoue, Zachary Ramjan, Yaping Liu, Houtan Noushmehr, et al. 2012. "Regions of Focal DNA Hypermethylation and Long-Range Hypomethylation in Colorectal Cancer Coincide with Nuclear Lamina-Associated Domains."

Nature Genetics 44 (1): 40–46. doi:10.1038/ng.969.

Bernstein, Bradley E., Tarjei S. Mikkelsen, Xiaohui Xie, Michael Kamal, Dana J. Huebert, James Cuff, Ben Fry, et al. 2006. "A Bivalent Chromatin Structure Marks Key Developmental Genes in Embryonic Stem Cells." *Cell* 125 (2): 315–26. doi:10.1016/j.cell.2006.02.041.

Bestor, T. H. 2000. "The DNA Methyltransferases of Mammals." *Human Molecular Genetics* 9 (16): 2395–2402.

Bezençon, Carole, Johannes le Coutre, and Sami Damak. 2007. "Taste-Signaling Proteins Are Coexpressed in Solitary Intestinal Epithelial Cells." *Chemical Senses* 32 (1): 41–49. doi:10.1093/chemse/bjl034.

Bhanot, P., M. Brink, C. H. Samos, J. C. Hsieh, Y. Wang, J. P. Macke, D. Andrew, J. Nathans, and R. Nusse. 1996. "A New Member of the Frizzled Family from Drosophila Functions as a Wingless Receptor." *Nature* 382 (6588): 225–30. doi:10.1038/382225a0.

Bhatia, M., D. Bonnet, D. Wu, B. Murdoch, J. Wrana, L. Gallacher, and J. E. Dick. 1999. "Bone Morphogenetic Proteins Regulate the Developmental Program of Human Hematopoietic Stem Cells." *The Journal of Experimental Medicine* 189 (7): 1139–48.

Bird, A., M. Taggart, M. Frommer, O. J. Miller, and D. Macleod. 1985. "A Fraction of the Mouse Genome That Is Derived from Islands of Nonmethylated, CpG-Rich DNA." *Cell* 40 (1): 91–99.

Bjerknes, M., and H. Cheng. 1981. "The Stem-Cell Zone of the Small Intestinal Epithelium. V. Evidence for Controls over Orientation of Boundaries between the Stem-Cell Zone, Proliferative Zone, and the Maturation Zone." *The American Journal of Anatomy* 160 (1): 105–12. doi:10.1002/aja.1001600109.

Bjerknes, Matthew, and Hazel Cheng. 2005. "Re-Examination of P-PTEN Staining Patterns in the Intestinal Crypt." *Nature Genetics* 37 (10): 1016-1017-1018. doi:10.1038/ng1005-1016.

Bjerknes, Matthew, Cyrus Khandanpour, Tarik Möröy, Tomoyuki Fujiyama, Mikio Hoshino, Tiemo J. Klisch, Qian Ding, et al. 2012. "Origin of the Brush Cell Lineage in the Mouse Intestinal Epithelium." *Developmental Biology* 362 (2): 194–218. doi:10.1016/j.ydbio.2011.12.009.

Bock, Christoph, Isabel Beerman, Wen-Hui Lien, Zachary D. Smith, Hongcang Gu, Patrick Boyle, Andreas Gnirke, Elaine Fuchs, Derrick J. Rossi, and Alexander Meissner. 2012. "DNA Methylation Dynamics during in Vivo Differentiation of Blood and Skin Stem Cells." *Molecular Cell* 47 (4): 633–47. doi:10.1016/j.molcel.2012.06.019.

Bourc'his, D., G. L. Xu, C. S. Lin, B. Bollman, and T. H. Bestor. 2001. "Dnmt3L and the Establishment of Maternal Genomic Imprints." *Science (New York, N.Y.)* 294 (5551): 2536–39. doi:10.1126/science.1065848.

Bovolenta, Paola, Pilar Esteve, Jose Maria Ruiz, Elsa Cisneros, and Javier Lopez-Rios. 2008. "Beyond Wnt Inhibition: New Functions of Secreted Frizzled-Related Proteins in Development and Disease." *Journal of Cell Science* 121 (Pt 6): 737–46. doi:10.1242/jcs.026096.

Bu, Pengcheng, Lihua Wang, Kai-Yuan Chen, Tara Srinivasan, Preetish Kadur Lakshminarasimha Murthy, Kuei-Ling Tung, Anastasia Kristine Varanko, et al. 2016. "A miR-34a-Numb Feedforward Loop Triggered by Inflammation Regulates Asymmetric Stem Cell Division in Intestine and Colon

Cancer." *Cell Stem Cell* 18 (2): 189–202. doi:10.1016/j.stem.2016.01.006.

Buczacki, Simon J. A., Heather Ireland Zecchini, Anna M. Nicholson, Roslin Russell, Louis Vermeulen, Richard Kemp, and Douglas J. Winton. 2013. "Intestinal Label-Retaining Cells Are Secretory Precursors Expressing Lgr5." *Nature* 495 (7439): 65–69. doi:10.1038/nature11965.

Calcagno, Shelly R., Shuhua Li, Migdalisel Colon, Pamela A. Kreinest, E. Aubrey Thompson, Alan P. Fields, and Nicole R. Murray. 2008. "Oncogenic K-Ras Promotes Early Carcinogenesis in the Mouse Proximal Colon." *International Journal of Cancer* 122 (11): 2462–70. doi:10.1002/ijc.23383.

Calin, George Adrian, Calin Dan Dumitru, Masayoshi Shimizu, Roberta Bichi, Simona Zupo, Evan Noch, Hansjuerg Aldler, et al. 2002. "Frequent Deletions and down-Regulation of Micro- RNA Genes miR15 and miR16 at 13q14 in Chronic Lymphocytic Leukemia." *Proceedings of the National Academy of Sciences of the United States of America* 99 (24): 15524–29. doi:10.1073/pnas.242606799.

Carmon, Kendra S., Xing Gong, Qiushi Lin, Anthony Thomas, and Qingyun Liu. 2011. "R-Spondins Function as Ligands of the Orphan Receptors LGR4 and LGR5 to Regulate Wnt/Beta-Catenin Signaling." *Proceedings of the National Academy of Sciences of the United States of America* 108 (28): 11452–57. doi:10.1073/pnas.1106083108.

Cerutti, Andrea, and Maria Rescigno. 2008. "The Biology of Intestinal Immunoglobulin A Responses." *Immunity* 28 (6): 740–50. doi:10.1016/j.immuni.2008.05.001.

Challen, Grant A., Deqiang Sun, Allison Mayle, Mira Jeong, Min Luo, Benjamin Rodriguez, Cates Mallaney, et al. 2014. "Dnmt3a and Dnmt3b Have Overlapping and Distinct Functions in Hematopoietic Stem Cells." *Cell Stem Cell* 15 (3): 350–64. doi:10.1016/j.stem.2014.06.018.

Chapelle, Albert de la. 2004. "Genetic Predisposition to Colorectal Cancer." *Nature Reviews. Cancer* 4 (10): 769–80. doi:10.1038/nrc1453.

Chiacchiera, Fulvio, Alessandra Rossi, SriGanesh Jammula, Andrea Piunti, Andrea Scelfo, Paloma Ordóñez-Morán, Joerg Huelsken, Haruhiko Koseki, and Diego Pasini. 2016. "Polycomb Complex PRC1 Preserves Intestinal Stem Cell Identity by Sustaining Wnt/β-Catenin Transcriptional Activity." *Cell Stem Cell* 18 (1): 91–103. doi:10.1016/j.stem.2015.09.019.

Chiacchiera, Fulvio, Alessandra Rossi, SriGanesh Jammula, Marika Zanotti, and Diego Pasini. 2016. "PRC2 Preserves Intestinal Progenitors and Restricts Secretory Lineage Commitment." *The EMBO Journal*, September. doi:10.15252/embj.201694550.

Chiba, Shigeru. 2006. "Notch Signaling in Stem Cell Systems." *Stem Cells (Dayton, Ohio)* 24 (11): 2437–47. doi:10.1634/stemcells.2005-0661.

Clevers, Hans. 2013. "The Intestinal Crypt, a Prototype Stem Cell Compartment." *Cell* 154 (2): 274–84. doi:10.1016/j.cell.2013.07.004.

———. 2016. "Cancer Therapy: Defining Stemness." *Nature* 534 (7606): 176–77. doi:10.1038/534176a.

Clevers, Hans C., and Charles L. Bevins. 2013. "Paneth Cells: Maestros of the Small Intestinal Crypts." *Annual Review of Physiology* 75: 289–311. doi:10.1146/annurev-physiol-030212-183744.

Clevers, Hans, and Roel Nusse. 2012. “Wnt/β-Catenin Signaling and Disease.” *Cell* 149 (6): 1192–1205. doi:10.1016/j.cell.2012.05.012.

Colnot, Sabine, Michiko Niwa-Kawakita, Ghislaine Hamard, Cécile Godard, Servane Le Plenier, Christophe Houbron, Béatrice Romagnolo, Dominique Berrebi, Marco Giovannini, and Christine Perret. 2004. “Colorectal Cancers in a New Mouse Model of Familial Adenomatous Polyposis: Influence of Genetic and Environmental Modifiers.” *Laboratory Investigation; a Journal of Technical Methods and Pathology* 84 (12): 1619–30. doi:10.1038/labinvest.3700180.

Dann, C. E., J. C. Hsieh, A. Rattner, D. Sharma, J. Nathans, and D. J. Leahy. 2001. “Insights into Wnt Binding and Signalling from the Structures of Two Frizzled Cysteine-Rich Domains.” *Nature* 412 (6842): 86–90. doi:10.1038/35083601.

Davidson, Gary, Wei Wu, Jinlong Shen, Josipa Bilic, Ursula Fenger, Peter Stannek, Andrei Glinka, and Christof Niehrs. 2005. “Casein Kinase 1 Gamma Couples Wnt Receptor Activation to Cytoplasmic Signal Transduction.” *Nature* 438 (7069): 867–72. doi:10.1038/nature04170.

Davis, Hayley, Shazia Irshad, Mukesh Bansal, Hannah Rafferty, Tatjana Boitsova, Chiara Bardella, Emma Jaeger, et al. 2015. “Aberrant Epithelial GREM1 Expression Initiates Colonic Tumorigenesis from Cells Outside the Stem Cell Niche.” *Nature Medicine* 21 (1): 62–70. doi:10.1038/nm.3750.

De Strooper, B., W. Annaert, P. Cupers, P. Saftig, K. Craessaerts, J. S. Mumm, E. H. Schroeter, et al. 1999. “A Presenilin-1-Dependent Gamma-Secretase-like Protease Mediates Release of Notch Intracellular Domain.” *Nature* 398 (6727): 518–22. doi:10.1038/19083.

Dekker, Job, Marc A. Marti-Renom, and Leonid A. Mirny. 2013. “Exploring the Three-Dimensional Organization of Genomes: Interpreting Chromatin Interaction Data.” *Nature Reviews. Genetics* 14 (6): 390–403. doi:10.1038/nrg3454.

Dieter, Sebastian M., Claudia R. Ball, Christopher M. Hoffmann, Ali Nowrouzi, Friederike Herbst, Oksana Zavidij, Ulrich Abel, et al. 2011. “Distinct Types of Tumor-Initiating Cells Form Human Colon Cancer Tumors and Metastases.” *Cell Stem Cell* 9 (4): 357–65. doi:10.1016/j.stem.2011.08.010.

Dow, Lukas E., Kevin P. O’Rourke, Janelle Simon, Darjus F. Tschaharganeh, Johan H. van Es, Hans Clevers, and Scott W. Lowe. 2015. “Apc Restoration Promotes Cellular Differentiation and Reestablishes Crypt Homeostasis in Colorectal Cancer.” *Cell* 161 (7): 1539–52. doi:10.1016/j.cell.2015.05.033.

Drost, Jarno, Richard H. van Jaarsveld, Bas Ponsioen, Cheryl Zimberlin, Ruben van Boxtel, Arjan Buijs, Norman Sachs, et al. 2015. “Sequential Cancer Mutations in Cultured Human Intestinal Stem Cells.” *Nature* 521 (7550): 43–47. doi:10.1038/nature14415.

Durand, Aurélie, Bridgitte Donahue, Grégory Peignon, Franck Letourneur, Nicolas Cagnard, Christian Slomianny, Christine Perret, Noah F. Shroyer, and Béatrice Romagnolo. 2012. “Functional Intestinal Stem Cells after Paneth Cell Ablation Induced by the Loss of Transcription Factor Math1 (Atoh1).” *Proceedings of the National Academy of Sciences of the United States of America* 109 (23): 8965–70. doi:10.1073/pnas.1201652109.

Easwaran, Hariharan, Sarah E. Johnstone, Leander Van Neste, Joyce Ohm, Tim Mosbruger, Qiuju Wang, Martin J. Aryee, et al. 2012. “A DNA Hypermethylation Module for the Stem/Progenitor Cell Signature of Cancer.” *Genome Research* 22 (5): 837–49. doi:10.1101/gr.131169.111.

ENCODE Project Consortium. 2012. “An Integrated Encyclopedia of DNA Elements in the Human Genome.” *Nature* 489 (7414): 57–74. doi:10.1038/nature11247.

Ernst, Jason, Pouya Kheradpour, Tarjei S. Mikkelsen, Noam Shoresh, Lucas D. Ward, Charles B. Epstein, Xiaolan Zhang, et al. 2011. “Mapping and Analysis of Chromatin State Dynamics in Nine Human Cell Types.” *Nature* 473 (7345): 43–49. doi:10.1038/nature09906.

Es, Johan H. van, Philippe Jay, Alex Gregorieff, Marielle E. van Gijn, Suzanne Jonkheer, Pantelis Hatzis, Andrea Thiele, et al. 2005. “Wnt Signalling Induces Maturation of Paneth Cells in Intestinal Crypts.” *Nature Cell Biology* 7 (4): 381–86. doi:10.1038/ncb1240.

Es, Johan H. van, Toshiro Sato, Marc van de Wetering, Anna Lyubimova, Annie Ng Yee Nee, Alex Gregorieff, Nobuo Sasaki, et al. 2012. “Dll1+ Secretory Progenitor Cells Revert to Stem Cells upon Crypt Damage.” *Nature Cell Biology* 14 (10): 1099–1104. doi:10.1038/ncb2581.

Escobar, Marion, Pierre Nicolas, Fatiha Sangar, Sabine Laurent-Chabalier, Philippe Clair, Dominique Joubert, Philippe Jay, and Catherine Legraverend. 2011. “Intestinal Epithelial Stem Cells Do Not Protect Their Genome by Asymmetric Chromosome Segregation.” *Nature Communications* 2: 258. doi:10.1038/ncomms1260.

Farin, Henner F., Johan H. Van Es, and Hans Clevers. 2012. “Redundant Sources of Wnt Regulate Intestinal Stem Cells and Promote Formation of Paneth Cells.” *Gastroenterology* 143 (6): 1518–1529.e7. doi:10.1053/j.gastro.2012.08.031.

Fearon, E. R., and B. Vogelstein. 1990. “A Genetic Model for Colorectal Tumorigenesis.” *Cell* 61 (5): 759–67.

Feinberg, A. P., and B. Vogelstein. 1983. “Hypomethylation Distinguishes Genes of Some Human Cancers from Their Normal Counterparts.” *Nature* 301 (5895): 89–92.

Feinberg, Andrew P., and Rafael A. Irizarry. 2010. “Evolution in Health and Medicine Sackler Colloquium: Stochastic Epigenetic Variation as a Driving Force of Development, Evolutionary Adaptation, and Disease.” *Proceedings of the National Academy of Sciences of the United States of America* 107 Suppl 1 (January): 1757–64. doi:10.1073/pnas.0906183107.

Feinberg, Andrew P., Rolf Ohlsson, and Steven Henikoff. 2006. “The Epigenetic Progenitor Origin of Human Cancer.” *Nature Reviews. Genetics* 7 (1): 21–33. doi:10.1038/nrg1748.

Feinberg, Andrew P., and Benjamin Tycko. 2004. “The History of Cancer Epigenetics.” *Nature Reviews. Cancer* 4 (2): 143–53. doi:10.1038/nrc1279.

Flier, Laurens G. van der, and Hans Clevers. 2009. “Stem Cells, Self-Renewal, and Differentiation in the Intestinal Epithelium.” *Annual Review of Physiology* 71: 241–60. doi:10.1146/annurev.physiol.010908.163145.

Flier, Laurens G. van der, Marielle E. van Gijn, Pantelis Hatzis, Pekka Kujala, Andrea Haegebarth, Daniel E. Stange, Harry Begthel, et al. 2009. “Transcription Factor Achaete Scute-like 2 Controls Intestinal Stem Cell Fate.” *Cell* 136 (5): 903–12. doi:10.1016/j.cell.2009.01.031.

Flier, Laurens G. van der, Andrea Haegebarth, Daniel E. Stange, Marc van de Wetering, and Hans Clevers. 2009. “OLFM4 Is a Robust Marker for Stem Cells in Human Intestine and Marks a Subset of Colorectal Cancer Cells.” *Gastroenterology* 137 (1): 15–17. doi:10.1053/j.gastro.2009.05.035.

"Frayling IM and Arends MJ, Adenomatous Polyposis Coli. In: Stanley Maloy and Kelly Hughes, Editors. Brenner's Encyclopedia of Genetics 2nd Edition, Vol 1. San Diego: Academic Press; 2013. P. 27–29." 2016. Accessed September 10. http://www.academia.edu/18500575/Frayling_IM_and_Arends_MJ_Adenomatous_Polyposis_Coli._In_Stanley_Maloy_and_Kelly_Hughes_editors._Brenner_s_Encyclopedia_of_Genetics_2nd_edition_Vol_1._San_Diego_Academic_Press_2013._p._27_29.

Fre, Silvia, Edouard Hannezo, Sanja Sale, Mathilde Huyghe, Daniel Lafkas, Holger Kissel, Angeliki Louvi, Jeffrey Greve, Daniel Louvard, and Spyros Artavanis-Tsakonas. 2011. "Notch Lineages and Activity in Intestinal Stem Cells Determined by a New Set of Knock-in Mice." *PloS One* 6 (10): e25785. doi:10.1371/journal.pone.0025785.

Fre, Silvia, Mathilde Huyghe, Philippos Mourikis, Sylvie Robine, Daniel Louvard, and Spyros Artavanis-Tsakonas. 2005. "Notch Signals Control the Fate of Immature Progenitor Cells in the Intestine." *Nature* 435 (7044): 964–68. doi:10.1038/nature03589.

Freund, J., A. M. Brandmaier, L. Lewejohann, I. Kirste, M. Kritzler, A. Krüger, N. Sachser, U. Lindenberger, and G. Kempermann. 2015. "Association between Exploratory Activity and Social Individuality in Genetically Identical Mice Living in the Same Enriched Environment." *Neuroscience* 309 (November): 140–52. doi:10.1016/j.neuroscience.2015.05.027.

Freund, Julia, Andreas M. Brandmaier, Lars Lewejohann, Imke Kirste, Mareike Kritzler, Antonio Krüger, Norbert Sachser, Ulman Lindenberger, and Gerd Kempermann. 2013. "Emergence of Individuality in Genetically Identical Mice." *Science (New York, N.Y.)* 340 (6133): 756–59. doi:10.1126/science.1235294.

Garabedian, E. M., L. J. Roberts, M. S. McNevin, and J. I. Gordon. 1997. "Examining the Role of Paneth Cells in the Small Intestine by Lineage Ablation in Transgenic Mice." *The Journal of Biological Chemistry* 272 (38): 23729–40.

Geiser, Jim, Koen J. T. Venken, Robert C. De Lisle, and Glen K. Andrews. 2012. "A Mouse Model of Acrodermatitis Enteropathica: Loss of Intestine Zinc Transporter ZIP4 (Slc39a4) Disrupts the Stem Cell Niche and Intestine Integrity." *PLoS Genetics* 8 (6): e1002766. doi:10.1371/journal.pgen.1002766.

Gerbe, François, Bénédicte Brulin, Leila Makrini, Catherine Legraverend, and Philippe Jay. 2009. "DCAMKL-1 Expression Identifies Tuft Cells rather than Stem Cells in the Adult Mouse Intestinal Epithelium." *Gastroenterology* 137 (6): 2179-2180-2181. doi:10.1053/j.gastro.2009.06.072.

Gerbe, François, Johan H. van Es, Leila Makrini, Bénédicte Brulin, Georg Mellitzer, Sylvie Robine, Béatrice Romagnolo, et al. 2011. "Distinct ATOH1 and Neurog3 Requirements Define Tuft Cells as a New Secretory Cell Type in the Intestinal Epithelium." *The Journal of Cell Biology* 192 (5): 767–80. doi:10.1083/jcb.201010127.

Gerbe, François, Catherine Legraverend, and Philippe Jay. 2012. "The Intestinal Epithelium Tuft Cells: Specification and Function." *Cellular and Molecular Life Sciences: CMLS* 69 (17): 2907–17. doi:10.1007/s00018-012-0984-7.

Gerbe, François, Emmanuelle Sidot, Danielle J. Smyth, Makoto Ohmoto, Ichiro Matsumoto, Valérie Dardalhon, Pierre Cesses, et al. 2016a. "Intestinal Epithelial Tuft Cells Initiate Type 2 Mucosal Immunity to Helminth Parasites." *Nature* 529 (7585): 226–30. doi:10.1038/nature16527.

Ghaleb, Amr M., Beth B. McConnell, Klaus H. Kaestner, and Vincent W. Yang. 2011. “Altered Intestinal Epithelial Homeostasis in Mice with Intestine-Specific Deletion of the Krüppel-like Factor 4 Gene.” *Developmental Biology* 349 (2): 310–20. doi:10.1016/j.ydbio.2010.11.001.

Ginno, Paul A., Paul L. Lott, Holly C. Christensen, Ian Korf, and Frédéric Chédin. 2012. “R-Loop Formation Is a Distinctive Characteristic of Unmethylated Human CpG Island Promoters.” *Molecular Cell* 45 (6): 814–25. doi:10.1016/j.molcel.2012.01.017.

Glinka, A., W. Wu, H. Delius, A. P. Monaghan, C. Blumenstock, and C. Niehrs. 1998. “Dickkopf-1 Is a Member of a New Family of Secreted Proteins and Functions in Head Induction.” *Nature* 391 (6665): 357–62. doi:10.1038/34848.

“Globocan 2012 - Home.” 2016. Accessed September 10. http://globocan.iarc.fr/Default.aspx.

Goll, Mary Grace, and Timothy H. Bestor. 2005. “Eukaryotic Cytosine Methyltransferases.” *Annual Review of Biochemistry* 74: 481–514. doi:10.1146/annurev.biochem.74.010904.153721.

Goll, Rasmus, and Atle van Beelen Granlund. 2015. “Intestinal Barrier Homeostasis in Inflammatory Bowel Disease.” *Scandinavian Journal of Gastroenterology* 50 (1): 3–12. doi:10.3109/00365521.2014.971425.

Greger, V., E. Passarge, W. Höpping, E. Messmer, and B. Horsthemke. 1989. “Epigenetic Changes May Contribute to the Formation and Spontaneous Regression of Retinoblastoma.” *Human Genetics* 83 (2): 155–58.

Gregorieff, Alex, Daniel E. Stange, Pekka Kujala, Harry Begthel, Maaike van den Born, Jeroen Korving, Peter J. Peters, and Hans Clevers. 2009. “The Ets-Domain Transcription Factor Spdef Promotes Maturation of Goblet and Paneth Cells in the Intestinal Epithelium.” *Gastroenterology* 137 (4): 1333-1345-3. doi:10.1053/j.gastro.2009.06.044.

Grimm, Christina, Lukas Chavez, Mireia Vilardell, Alexandra L. Farrall, Sascha Tierling, Julia W. Böhm, Phillip Grote, et al. 2013. “DNA-Methylome Analysis of Mouse Intestinal Adenoma Identifies a Tumour-Specific Signature That Is Partly Conserved in Human Colon Cancer.” *PLoS Genetics* 9 (2): e1003250. doi:10.1371/journal.pgen.1003250.

Grün, Dominic, Anna Lyubimova, Lennart Kester, Kay Wiebrands, Onur Basak, Nobuo Sasaki, Hans Clevers, and Alexander van Oudenaarden. 2015. “Single-Cell Messenger RNA Sequencing Reveals Rare Intestinal Cell Types.” *Nature* 525 (7568): 251–55. doi:10.1038/nature14966.

Guinney, Justin, Rodrigo Dienstmann, Xin Wang, Aurélien de Reyniès, Andreas Schlicker, Charlotte Soneson, Laetitia Marisa, et al. 2015. “The Consensus Molecular Subtypes of Colorectal Cancer.” *Nature Medicine* 21 (11): 1350–56. doi:10.1038/nm.3967.

Haegebarth, Andrea, Wenjun Bie, Ruyan Yang, Susan E. Crawford, Valeri Vasioukhin, Elaine Fuchs, and Angela L. Tyner. 2006. “Protein Tyrosine Kinase 6 Negatively Regulates Growth and Promotes Enterocyte Differentiation in the Small Intestine.” *Molecular and Cellular Biology* 26 (13): 4949–57. doi:10.1128/MCB.01901-05.

Haramis, Anna-Pavlina G., Harry Begthel, Maaike van den Born, Johan van Es, Suzanne Jonkheer, G. Johan A. Offerhaus, and Hans Clevers. 2004. “De Novo Crypt Formation and Juvenile Polyposis on BMP Inhibition in Mouse Intestine.” *Science (New York, N.Y.)* 303 (5664): 1684–86. doi:10.1126/science.1093587.

Hardwick, James C. H., Gijs R. Van Den Brink, Sylvia A. Bleuming, Isabel Ballester, Jan M. H. Van Den Brande, Josbert J. Keller, G. Johan A. Offerhaus, Sander J. H. Van Deventer, and Maikel P. Peppelenbosch. 2004. "Bone Morphogenetic Protein 2 Is Expressed By, and Acts Upon, Mature Epithelial Cells in the Colon." *Gastroenterology* 126 (1): 111–21.

Hatzimichael, Eleftheria, and Tim Crook. 2013. "Cancer Epigenetics: New Therapies and New Challenges." *Journal of Drug Delivery* 2013: 529312. doi:10.1155/2013/529312.

Hawkins, R. David, Gary C. Hon, Leonard K. Lee, Queminh Ngo, Ryan Lister, Mattia Pelizzola, Lee E. Edsall, et al. 2010. "Distinct Epigenomic Landscapes of Pluripotent and Lineage-Committed Human Cells." *Cell Stem Cell* 6 (5): 479–91. doi:10.1016/j.stem.2010.03.018.

Hayes, Josie, Pier Paolo Peruzzi, and Sean Lawler. 2014. "MicroRNAs in Cancer: Biomarkers, Functions and Therapy." *Trends in Molecular Medicine* 20 (8): 460–69. doi:10.1016/j.molmed.2014.06.005.

He, Xi C., Jiwang Zhang, Wei-Gang Tong, Ossama Tawfik, Jason Ross, David H. Scoville, Qiang Tian, et al. 2004. "BMP Signaling Inhibits Intestinal Stem Cell Self-Renewal through Suppression of Wnt-Beta-Catenin Signaling." *Nature Genetics* 36 (10): 1117–21. doi:10.1038/ng1430.

Hegi, Monika E., Annie-Claire Diserens, Thierry Gorlia, Marie-France Hamou, Nicolas de Tribolet, Michael Weller, Johan M. Kros, et al. 2005. "MGMT Gene Silencing and Benefit from Temozolomide in Glioblastoma." *The New England Journal of Medicine* 352 (10): 997–1003. doi:10.1056/NEJMoa043331.

Herbst, Andreas, Vindi Jurinovic, Stefan Krebs, Susanne E. Thieme, Helmut Blum, Burkhard Göke, and Frank T. Kolligs. 2014. "Comprehensive Analysis of β-Catenin Target Genes in Colorectal Carcinoma Cell Lines with Deregulated Wnt/β-Catenin Signaling." *BMC Genomics* 15: 74. doi:10.1186/1471-2164-15-74.

Herman, James G., and Stephen B. Baylin. 2003. "Gene Silencing in Cancer in Association with Promoter Hypermethylation." *The New England Journal of Medicine* 349 (21): 2042–54. doi:10.1056/NEJMra023075.

Hilsden, Robert J., and Alaa Rostom. 2010. "Colorectal Cancer Screening Using Flexible Sigmoidoscopy: United Kingdom Study Demonstrates Significant Incidence and Mortality Benefit." *Canadian Journal of Gastroenterology = Journal Canadien De Gastroenterologie* 24 (8): 479–80.

Howitt, Michael R., Sydney Lavoie, Monia Michaud, Arthur M. Blum, Sara V. Tran, Joel V. Weinstock, Carey Ann Gallini, et al. 2016. "Tuft Cells, Taste-Chemosensory Cells, Orchestrate Parasite Type 2 Immunity in the Gut." *Science (New York, N.Y.)* 351 (6279): 1329–33. doi:10.1126/science.aaf1648.

Iavarone, A., P. Garg, A. Lasorella, J. Hsu, and M. A. Israel. 1994. "The Helix-Loop-Helix Protein Id-2 Enhances Cell Proliferation and Binds to the Retinoblastoma Protein." *Genes & Development* 8 (11): 1270–84.

IJspeert, Joep E. G., Koos de Wit, Manon van der Vlugt, Barbara A. J. Bastiaansen, Paul Fockens, and Evelien Dekker. 2016. "Prevalence, Distribution and Risk of Sessile Serrated Adenomas/Polyps at a Center with a High Adenoma Detection Rate and Experienced Pathologists." *Endoscopy* 48 (8): 740–46. doi:10.1055/s-0042-105436.

Ireland, Heather, Carol Houghton, Louise Howard, and Douglas J. Winton. 2005. “Cellular Inheritance of a Cre-Activated Reporter Gene to Determine Paneth Cell Longevity in the Murine Small Intestine.” *Developmental Dynamics: An Official Publication of the American Association of Anatomists* 233 (4): 1332–36. doi:10.1002/dvdy.20446.

Ireland, Heather, Richard Kemp, Carol Houghton, Louise Howard, Alan R. Clarke, Owen J. Sansom, and Douglas J. Winton. 2004. “Inducible Cre-Mediated Control of Gene Expression in the Murine Gastrointestinal Tract: Effect of Loss of Beta-Catenin.” *Gastroenterology* 126 (5): 1236–46.

Itzykson, Raphael, and Pierre Fenaux. 2011. “[Hypomethylating agents for the treatment of myelodysplastic syndromes].” *Bulletin Du Cancer* 98 (8): 927–34. doi:10.1684/bdc.2011.1411.

Jaeger, Emma, Simon Leedham, Annabelle Lewis, Stefania Segditsas, Martin Becker, Pedro Rodenas Cuadrado, Hayley Davis, et al. 2012. “Hereditary Mixed Polyposis Syndrome Is Caused by a 40-Kb Upstream Duplication That Leads to Increased and Ectopic Expression of the BMP Antagonist GREM1.” *Nature Genetics* 44 (6): 699–703. doi:10.1038/ng.2263.

Janda, Claudia Y., Deepa Waghray, Aron M. Levin, Christoph Thomas, and K. Christopher Garcia. 2012. “Structural Basis of Wnt Recognition by Frizzled.” *Science (New York, N.Y.)* 337 (6090): 59–64. doi:10.1126/science.1222879.

Jemal, Ahmedin, Freddie Bray, Melissa M. Center, Jacques Ferlay, Elizabeth Ward, and David Forman. 2011. “Global Cancer Statistics.” *CA: A Cancer Journal for Clinicians* 61 (2): 69–90. doi:10.3322/caac.20107.

Jen, Y., H. Weintraub, and R. Benezra. 1992. “Overexpression of Id Protein Inhibits the Muscle Differentiation Program: In Vivo Association of Id with E2A Proteins.” *Genes & Development* 6 (8): 1466–79.

Jenny, Marjorie, Céline Uhl, Colette Roche, Isabelle Duluc, Valérie Guillermin, Francois Guillemot, Jan Jensen, Michèle Kedinger, and Gérard Gradwohl. 2002. “Neurogenin3 Is Differentially Required for Endocrine Cell Fate Specification in the Intestinal and Gastric Epithelium.” *The EMBO Journal* 21 (23): 6338–47.

Jensen, J., E. E. Pedersen, P. Galante, J. Hald, R. S. Heller, M. Ishibashi, R. Kageyama, F. Guillemot, P. Serup, and O. D. Madsen. 2000. “Control of Endodermal Endocrine Development by Hes-1.” *Nature Genetics* 24 (1): 36–44. doi:10.1038/71657.

Johnson, Robert L., and James C. Fleet. 2013. “Animal Models of Colorectal Cancer.” *Cancer Metastasis Reviews* 32 (1–2): 39–61. doi:10.1007/s10555-012-9404-6.

Jones, Peter A. 2012. “Functions of DNA Methylation: Islands, Start Sites, Gene Bodies and beyond.” *Nature Reviews. Genetics* 13 (7): 484–92. doi:10.1038/nrg3230.

Jones, Peter A., and Stephen B. Baylin. 2002. “The Fundamental Role of Epigenetic Events in Cancer.” *Nature Reviews. Genetics* 3 (6): 415–28. doi:10.1038/nrg816.

Julier, C., B. de Gouyon, M. Georges, J. L. Guénet, Y. Nakamura, P. Avner, and G. M. Lathrop. 1990. “Minisatellite Linkage Maps in the Mouse by Cross-Hybridization with Human Probes Containing Tandem Repeats.” *Proceedings of the National Academy of Sciences of the United States of America* 87 (12): 4585–89.

Kareta, Michael S., Zaida M. Botello, Joshua J. Ennis, Christina Chou, and Frédéric Chédin. 2006. "Reconstitution and Mechanism of the Stimulation of de Novo Methylation by Human DNMT3L." *The Journal of Biological Chemistry* 281 (36): 25893–902. doi:10.1074/jbc.M603140200.

Katz, Jonathan P., Nathalie Perreault, Bree G. Goldstein, Catherine S. Lee, Patricia A. Labosky, Vincent W. Yang, and Klaus H. Kaestner. 2002. "The Zinc-Finger Transcription Factor Klf4 Is Required for Terminal Differentiation of Goblet Cells in the Colon." *Development (Cambridge, England)* 129 (11): 2619–28.

Kazanjian, Avedis, Taeko Noah, Douglas Brown, Jarred Burkart, and Noah F. Shroyer. 2010. "Atonal Homolog 1 Is Required for Growth and Differentiation Effects of Notch/Gamma-Secretase Inhibitors on Normal and Cancerous Intestinal Epithelial Cells." *Gastroenterology* 139 (3): 918–28, 928-6. doi:10.1053/j.gastro.2010.05.081.

Kazanskaya, Olga, Andrei Glinka, Ivan del Barco Barrantes, Peter Stannek, Christof Niehrs, and Wei Wu. 2004. "R-Spondin2 Is a Secreted Activator of Wnt/Beta-Catenin Signaling and Is Required for Xenopus Myogenesis." *Developmental Cell* 7 (4): 525–34. doi:10.1016/j.devcel.2004.07.019.

Kim, Tae-Hee, Fugen Li, Isabel Ferreiro-Neira, Li-Lun Ho, Annouck Luyten, Kodandaramireddy Nalapareddy, Henry Long, Michael Verzi, and Ramesh A. Shivdasani. 2014. "Broadly Permissive Intestinal Chromatin Underlies Lateral Inhibition and Cell Plasticity." *Nature* 506 (7489): 511–15. doi:10.1038/nature12903.

Kim, Tae-Hee, and Ramesh A. Shivdasani. 2011. "Genetic Evidence That Intestinal Notch Functions Vary Regionally and Operate through a Common Mechanism of Math1 Repression." *The Journal of Biological Chemistry* 286 (13): 11427–33. doi:10.1074/jbc.M110.188797.

Kim, Young S., and Samuel B. Ho. 2010. "Intestinal Goblet Cells and Mucins in Health and Disease: Recent Insights and Progress." *Current Gastroenterology Reports* 12 (5): 319–30. doi:10.1007/s11894-010-0131-2.

Koo, Bon-Kyoung, Daniel E. Stange, Toshiro Sato, Wouter Karthaus, Henner F. Farin, Meritxell Huch, Johan H. van Es, and Hans Clevers. 2012. "Controlled Gene Expression in Primary Lgr5 Organoid Cultures." *Nature Methods* 9 (1): 81–83. doi:10.1038/nmeth.1802.

Korinek, V., N. Barker, K. Willert, M. Molenaar, J. Roose, G. Wagenaar, M. Markman, W. Lamers, O. Destree, and H. Clevers. 1998. "Two Members of the Tcf Family Implicated in Wnt/Beta-Catenin Signaling during Embryogenesis in the Mouse." *Molecular and Cellular Biology* 18 (3): 1248–56.

Krol, Jacek, Inga Loedige, and Witold Filipowicz. 2010. "The Widespread Regulation of microRNA Biogenesis, Function and Decay." *Nature Reviews. Genetics* 11 (9): 597–610. doi:10.1038/nrg2843.

Ku, Manching, Richard P. Koche, Esther Rheinbay, Eric M. Mendenhall, Mitsuhiro Endoh, Tarjei S. Mikkelsen, Aviva Presser, et al. 2008. "Genomewide Analysis of PRC1 and PRC2 Occupancy Identifies Two Classes of Bivalent Domains." *PLoS Genetics* 4 (10): e1000242. doi:10.1371/journal.pgen.1000242.

Kuck, Dirk, Thomas Caulfield, Frank Lyko, and Jose L. Medina-Franco. 2010. "Nanaomycin A Selectively Inhibits DNMT3B and Reactivates Silenced Tumor Suppressor Genes in Human Cancer Cells." *Molecular Cancer Therapeutics* 9 (11): 3015–23. doi:10.1158/1535-7163.MCT-10-0609.

Kulis, Marta, and Manel Esteller. 2010. "DNA Methylation and Cancer." *Advances in Genetics* 70:

27–56. doi:10.1016/B978-0-12-380866-0.60002-2.

Lapidot, T., C. Sirard, J. Vormoor, B. Murdoch, T. Hoang, J. Caceres-Cortes, M. Minden, B. Paterson, M. A. Caligiuri, and J. E. Dick. 1994. “A Cell Initiating Human Acute Myeloid Leukaemia after Transplantation into SCID Mice.” *Nature* 367 (6464): 645–48. doi:10.1038/367645a0.

Lathe, R. 2004. “The Individuality of Mice.” *Genes, Brain, and Behavior* 3 (6): 317–27. doi:10.1111/j.1601-183X.2004.00083.x.

Lau, Wim de, Nick Barker, Teck Y. Low, Bon-Kyoung Koo, Vivian S. W. Li, Hans Teunissen, Pekka Kujala, et al. 2011. “Lgr5 Homologues Associate with Wnt Receptors and Mediate R-Spondin Signalling.” *Nature* 476 (7360): 293–97. doi:10.1038/nature10337.

Lau, Wim de, Pekka Kujala, Kerstin Schneeberger, Sabine Middendorp, Vivian S. W. Li, Nick Barker, Anton Martens, et al. 2012. “Peyer’s Patch M Cells Derived from Lgr5(+) Stem Cells Require SpiB and Are Induced by RankL in Cultured ‘miniguts.’” *Molecular and Cellular Biology* 32 (18): 3639–47. doi:10.1128/MCB.00434-12.

Leblond, C. P., and C. E. Stevens. 1948. “The Constant Renewal of the Intestinal Epithelium in the Albino Rat.” *The Anatomical Record* 100 (3): 357–77.

Lee, Catherine S., Nathalie Perreault, John E. Brestelli, and Klaus H. Kaestner. 2002. “Neurogenin 3 Is Essential for the Proper Specification of Gastric Enteroendocrine Cells and the Maintenance of Gastric Epithelial Cell Identity.” *Genes & Development* 16 (12): 1488–97. doi:10.1101/gad.985002.

Li, Xing, Blair B. Madison, William Zacharias, Asa Kolterud, David States, and Deborah L. Gumucio. 2007. “Deconvoluting the Intestine: Molecular Evidence for a Major Role of the Mesenchyme in the Modulation of Signaling Cross Talk.” *Physiological Genomics* 29 (3): 290–301. doi:10.1152/physiolgenomics.00269.2006.

Liao, Jing, Rahul Karnik, Hongcang Gu, Michael J. Ziller, Kendell Clement, Alexander M. Tsankov, Veronika Akopian, et al. 2015. “Targeted Disruption of DNMT1, DNMT3A and DNMT3B in Human Embryonic Stem Cells.” *Nature Genetics* 47 (5): 469–78. doi:10.1038/ng.3258.

Lin, Haijiang, Yasuhiro Yamada, Suzanne Nguyen, Heinz Linhart, Laurie Jackson-Grusby, Alexander Meissner, Konstantinos Meletis, Grace Lo, and Rudolf Jaenisch. 2006. “Suppression of Intestinal Neoplasia by Deletion of Dnmt3b.” *Molecular and Cellular Biology* 26 (8): 2976–83. doi:10.1128/MCB.26.8.2976-2983.2006.

Linhart, Heinz G., Haijiang Lin, Yasuhiro Yamada, Eva Moran, Eveline J. Steine, Sumita Gokhale, Grace Lo, et al. 2007. “Dnmt3b Promotes Tumorigenesis in Vivo by Gene-Specific de Novo Methylation and Transcriptional Silencing.” *Genes & Development* 21 (23): 3110–22. doi:10.1101/gad.1594007.

Lopez-Garcia, Carlos, Allon M. Klein, Benjamin D. Simons, and Douglas J. Winton. 2010. “Intestinal Stem Cell Replacement Follows a Pattern of Neutral Drift.” *Science (New York, N.Y.)* 330 (6005): 822–25. doi:10.1126/science.1196236.

Mack, S. C., H. Witt, R. M. Piro, L. Gu, S. Zuyderduyn, A. M. Stütz, X. Wang, et al. 2014. “Epigenomic Alterations Define Lethal CIMP-Positive Ependymomas of Infancy.” *Nature* 506 (7489): 445–50. doi:10.1038/nature13108.

Mao, J., J. Wang, B. Liu, W. Pan, G. H. Farr, C. Flynn, H. Yuan, et al. 2001. “Low-Density Lipoprotein Receptor-Related Protein-5 Binds to Axin and Regulates the Canonical Wnt Signaling Pathway.” *Molecular Cell* 7 (4): 801–9.

Marjou, Fatima el, Klaus-Peter Janssen, Benny Hung-Junn Chang, Mei Li, Valérie Hindie, Lawrence Chan, Daniel Louvard, Pierre Chambon, Daniel Metzger, and Sylvie Robine. 2004. “Tissue-Specific and Inducible Cre-Mediated Recombination in the Gut Epithelium.” *Genesis (New York, N.Y.: 2000)* 39 (3): 186–93. doi:10.1002/gene.20042.

Matano, Mami, Shoichi Date, Mariko Shimokawa, Ai Takano, Masayuki Fujii, Yuki Ohta, Toshiaki Watanabe, Takanori Kanai, and Toshiro Sato. 2015. “Modeling Colorectal Cancer Using CRISPR-Cas9-Mediated Engineering of Human Intestinal Organoids.” *Nature Medicine* 21 (3): 256–62. doi:10.1038/nm.3802.

May, Catherine Lee, and Klaus H. Kaestner. 2010. “Gut Endocrine Cell Development.” *Molecular and Cellular Endocrinology* 323 (1): 70–75. doi:10.1016/j.mce.2009.12.009.

McPherson, Michael, Bo Wei, Olga Turovskaya, Daisuke Fujiwara, Sarah Brewer, and Jonathan Braun. 2008. “Colitis Immunoregulation by CD8+ T Cell Requires T Cell Cytotoxicity and B Cell Peptide Antigen Presentation.” *American Journal of Physiology. Gastrointestinal and Liver Physiology* 295 (3): G485-492. doi:10.1152/ajpgi.90221.2008.

Meissner, Alexander, Andreas Gnirke, George W. Bell, Bernard Ramsahoye, Eric S. Lander, and Rudolf Jaenisch. 2005. “Reduced Representation Bisulfite Sequencing for Comparative High-Resolution DNA Methylation Analysis.” *Nucleic Acids Research* 33 (18): 5868–77. doi:10.1093/nar/gki901.

Mellitzer, Georg, Anthony Beucher, Viviane Lobstein, Pascal Michel, Sylvie Robine, Michèle Kedinger, and Gérard Gradwohl. 2010. “Loss of Enteroendocrine Cells in Mice Alters Lipid Absorption and Glucose Homeostasis and Impairs Postnatal Survival.” *The Journal of Clinical Investigation* 120 (5): 1708–21. doi:10.1172/JCI40794.

Merlos-Suárez, Anna, Francisco M. Barriga, Peter Jung, Mar Iglesias, María Virtudes Céspedes, David Rossell, Marta Sevillano, et al. 2011. “The Intestinal Stem Cell Signature Identifies Colorectal Cancer Stem Cells and Predicts Disease Relapse.” *Cell Stem Cell* 8 (5): 511–24. doi:10.1016/j.stem.2011.02.020.

Michael, Michael Z., Susan M. O’ Connor, Nicholas G. van Holst Pellekaan, Graeme P. Young, and Robert J. James. 2003. “Reduced Accumulation of Specific microRNAs in Colorectal Neoplasia.” *Molecular Cancer Research: MCR* 1 (12): 882–91.

Mills, Alea A. 2010. “Throwing the Cancer Switch: Reciprocal Roles of Polycomb and Trithorax Proteins.” *Nature Reviews. Cancer* 10 (10): 669–82. doi:10.1038/nrc2931.

Molenaar, M., M. van de Wetering, M. Oosterwegel, J. Peterson-Maduro, S. Godsave, V. Korinek, J. Roose, O. Destrée, and H. Clevers. 1996. “XTcf-3 Transcription Factor Mediates Beta-Catenin-Induced Axis Formation in Xenopus Embryos.” *Cell* 86 (3): 391–99.

Moltke, Jakob von, Ming Ji, Hong-Erh Liang, and Richard M. Locksley. 2016. “Tuft-Cell-Derived IL-25 Regulates an Intestinal ILC2-Epithelial Response Circuit.” *Nature* 529 (7585): 221–25. doi:10.1038/nature16161.

Mori-Akiyama, Yuko, Maaike van den Born, Johan H. van Es, Stanley R. Hamilton, Henry P. Adams, Jiexin Zhang, Hans Clevers, and Benoit de Crombrugghe. 2007. “SOX9 Is Required for the Differentiation of Paneth Cells in the Intestinal Epithelium.” *Gastroenterology* 133 (2): 539–46. doi:10.1053/j.gastro.2007.05.020.

Morin, P. J., A. B. Sparks, V. Korinek, N. Barker, H. Clevers, B. Vogelstein, and K. W. Kinzler. 1997. “Activation of Beta-Catenin-Tcf Signaling in Colon Cancer by Mutations in Beta-Catenin or APC.” *Science (New York, N.Y.)* 275 (5307): 1787–90.

Moser, A. R., H. C. Pitot, and W. F. Dove. 1990. “A Dominant Mutation That Predisposes to Multiple Intestinal Neoplasia in the Mouse.” *Science (New York, N.Y.)* 247 (4940): 322–24.

Müller, Mike F., Ashraf E. K. Ibrahim, and Mark J. Arends. 2016. “Molecular Pathological Classification of Colorectal Cancer.” *Virchows Archiv: An International Journal of Pathology* 469 (2): 125–34. doi:10.1007/s00428-016-1956-3.

Muñoz, Javier, Daniel E. Stange, Arnout G. Schepers, Marc van de Wetering, Bon-Kyoung Koo, Shalev Itzkovitz, Richard Volckmann, et al. 2012a. “The Lgr5 Intestinal Stem Cell Signature: Robust Expression of Proposed Quiescent ‘+4’ Cell Markers.” *The EMBO Journal* 31 (14): 3079–91. doi:10.1038/emboj.2012.166.

———. 2012b. “The Lgr5 Intestinal Stem Cell Signature: Robust Expression of Proposed Quiescent ‘+4’ Cell Markers.” *The EMBO Journal* 31 (14): 3079–91. doi:10.1038/emboj.2012.166.

Nakanishi, Yuki, Hiroshi Seno, Ayumi Fukuoka, Taro Ueo, Yuichi Yamaga, Takahisa Maruno, Naoko Nakanishi, et al. 2013. “Dclk1 Distinguishes between Tumor and Normal Stem Cells in the Intestine.” *Nature Genetics* 45 (1): 98–103. doi:10.1038/ng.2481.

Noah, Taeko K., Avedis Kazanjian, Jeffrey Whitsett, and Noah F. Shroyer. 2010. “SAM Pointed Domain ETS Factor (SPDEF) Regulates Terminal Differentiation and Maturation of Intestinal Goblet Cells.” *Experimental Cell Research* 316 (3): 452–65. doi:10.1016/j.yexcr.2009.09.020.

Ogata, T., J. M. Wozney, R. Benezra, and M. Noda. 1993. “Bone Morphogenetic Protein 2 Transiently Enhances Expression of a Gene, Id (Inhibitor of Differentiation), Encoding a Helix-Loop-Helix Molecule in Osteoblast-like Cells.” *Proceedings of the National Academy of Sciences of the United States of America* 90 (19): 9219–22.

Okano, M., D. W. Bell, D. A. Haber, and E. Li. 1999. “DNA Methyltransferases Dnmt3a and Dnmt3b Are Essential for de Novo Methylation and Mammalian Development.” *Cell* 99 (3): 247–57.

Onuma, Kunishige, Masako Ochiai, Kaoru Orihashi, Mami Takahashi, Toshio Imai, Hitoshi Nakagama, and Yoshitaka Hippo. 2013. “Genetic Reconstitution of Tumorigenesis in Primary Intestinal Cells.” *Proceedings of the National Academy of Sciences of the United States of America* 110 (27): 11127–32. doi:10.1073/pnas.1221926110.

Owen, R. L., and A. L. Jones. 1974. “Epithelial Cell Specialization within Human Peyer’s Patches: An Ultrastructural Study of Intestinal Lymphoid Follicles.” *Gastroenterology* 66 (2): 189–203.

Pellegrinet, Luca, Veronica Rodilla, Zhenyi Liu, Shuang Chen, Ute Koch, Lluis Espinosa, Klaus H. Kaestner, Raphael Kopan, Julian Lewis, and Freddy Radtke. 2011. “Dll1- and dll4-Mediated Notch Signaling Are Required for Homeostasis of Intestinal Stem Cells.” *Gastroenterology* 140 (4): 1230-1240-7. doi:10.1053/j.gastro.2011.01.005.

Perez-Lopez, Araceli, Judith Behnsen, Sean-Paul Nuccio, and Manuela Raffatellu. 2016. “Mucosal Immunity to Pathogenic Intestinal Bacteria.” *Nature Reviews. Immunology* 16 (3): 135–48. doi:10.1038/nri.2015.17.

Pfaffl, M. W. 2001. “A New Mathematical Model for Relative Quantification in Real-Time RT-PCR.” *Nucleic Acids Research* 29 (9): e45.

Pino, Maria S., and Daniel C. Chung. 2011. “Microsatellite Instability in the Management of Colorectal Cancer.” *Expert Review of Gastroenterology & Hepatology* 5 (3): 385–99. doi:10.1586/egh.11.25.

Pinto, Daniel, Alex Gregorieff, Harry Begthel, and Hans Clevers. 2003. “Canonical Wnt Signals Are Essential for Homeostasis of the Intestinal Epithelium.” *Genes & Development* 17 (14): 1709–13. doi:10.1101/gad.267103.

Pollard, Patrick, Maesha Deheragoda, Stefania Segditsas, Annabelle Lewis, Andrew Rowan, Kimberley Howarth, Lisa Willis, et al. 2009. “The Apc 1322T Mouse Develops Severe Polyposis Associated with Submaximal Nuclear Beta-Catenin Expression.” *Gastroenterology* 136 (7): 2204-2213-13. doi:10.1053/j.gastro.2009.02.058.

Probst, Aline V., Elaine Dunleavy, and Geneviève Almouzni. 2009. “Epigenetic Inheritance during the Cell Cycle.” *Nature Reviews. Molecular Cell Biology* 10 (3): 192–206. doi:10.1038/nrm2640.

Rad, Roland, Juan Cadiñanos, Lena Rad, Ignacio Varela, Alexander Strong, Lydia Kriegl, Fernando Constantino-Casas, et al. 2013. “A Genetic Progression Model of Braf(V600E)-Induced Intestinal Tumorigenesis Reveals Targets for Therapeutic Intervention.” *Cancer Cell* 24 (1): 15–29. doi:10.1016/j.ccr.2013.05.014.

Rasmussen, Kasper Dindler, and Kristian Helin. 2016. “Role of TET Enzymes in DNA Methylation, Development, and Cancer.” *Genes & Development* 30 (7): 733–50. doi:10.1101/gad.276568.115.

Reitmair, A. H., M. Redston, J. C. Cai, T. C. Chuang, M. Bjerknes, H. Cheng, K. Hay, S. Gallinger, B. Bapat, and T. W. Mak. 1996. “Spontaneous Intestinal Carcinomas and Skin Neoplasms in Msh2-Deficient Mice.” *Cancer Research* 56 (16): 3842–49.

Riccio, Orbicia, Marielle E. van Gijn, April C. Bezdek, Luca Pellegrinet, Johan H. van Es, Ursula Zimber-Strobl, Lothar J. Strobl, Tasuku Honjo, Hans Clevers, and Freddy Radtke. 2008. “Loss of Intestinal Crypt Progenitor Cells Owing to Inactivation of Both Notch1 and Notch2 Is Accompanied by Derepression of CDK Inhibitors p27Kip1 and p57Kip2.” *EMBO Reports* 9 (4): 377–83. doi:10.1038/embor.2008.7.

Ricci-Vitiani, Lucia, Dario G. Lombardi, Emanuela Pilozzi, Mauro Biffoni, Matilde Todaro, Cesare Peschle, and Ruggero De Maria. 2007. “Identification and Expansion of Human Colon-Cancer-Initiating Cells.” *Nature* 445 (7123): 111–15. doi:10.1038/nature05384.

Rodríguez-Paredes, Manuel, and Manel Esteller. 2011. “Cancer Epigenetics Reaches Mainstream Oncology.” *Nature Medicine* 17 (3): 330–39. doi:10.1038/nm.2305.

Samuel, Michael S., Hiromu Suzuki, Michael Buchert, Tracy L. Putoczki, Niall C. Tebbutt, Therése Lundgren-May, Aliki Christou, et al. 2009. “Elevated Dnmt3a Activity Promotes Polyposis in Apc(Min) Mice by Relaxing Extracellular Restraints on Wnt Signaling.” *Gastroenterology* 137 (3): 902–13, 913-11. doi:10.1053/j.gastro.2009.05.042.

Sancho, Rocio, Catherine A. Cremona, and Axel Behrens. 2015. “Stem Cell and Progenitor Fate in the Mammalian Intestine: Notch and Lateral Inhibition in Homeostasis and Disease.” *EMBO Reports* 16 (5): 571–81. doi:10.15252/embr.201540188.

Sander, Guy R., and Barry C. Powell. 2004. “Expression of Notch Receptors and Ligands in the Adult Gut.” *The Journal of Histochemistry and Cytochemistry: Official Journal of the Histochemistry Society* 52 (4): 509–16.

Sandoval, Juan, and Manel Esteller. 2012. “Cancer Epigenomics: Beyond Genomics.” *Current Opinion in Genetics & Development* 22 (1): 50–55. doi:10.1016/j.gde.2012.02.008.

Sangiorgi, Eugenio, and Mario R. Capecchi. 2008. “Bmi1 Is Expressed in Vivo in Intestinal Stem Cells.” *Nature Genetics* 40 (7): 915–20. doi:10.1038/ng.165.

Sansom, Owen J., Karen R. Reed, Anthony J. Hayes, Heather Ireland, Hannah Brinkmann, Ian P. Newton, Eduard Batlle, et al. 2004. “Loss of Apc in Vivo Immediately Perturbs Wnt Signaling, Differentiation, and Migration.” *Genes & Development* 18 (12): 1385–90. doi:10.1101/gad.287404.

Sato, Toshiro, Johan H. van Es, Hugo J. Snippert, Daniel E. Stange, Robert G. Vries, Maaike van den Born, Nick Barker, Noah F. Shroyer, Marc van de Wetering, and Hans Clevers. 2011. “Paneth Cells Constitute the Niche for Lgr5 Stem Cells in Intestinal Crypts.” *Nature* 469 (7330): 415–18. doi:10.1038/nature09637.

Sato, Toshiro, Robert G. Vries, Hugo J. Snippert, Marc van de Wetering, Nick Barker, Daniel E. Stange, Johan H. van Es, et al. 2009. “Single Lgr5 Stem Cells Build Crypt-Villus Structures in Vitro without a Mesenchymal Niche.” *Nature* 459 (7244): 262–65. doi:10.1038/nature07935.

Schepers, Arnout G., Robert Vries, Maaike van den Born, Marc van de Wetering, and Hans Clevers. 2011. “Lgr5 Intestinal Stem Cells Have High Telomerase Activity and Randomly Segregate Their Chromosomes.” *The EMBO Journal* 30 (6): 1104–9. doi:10.1038/emboj.2011.26.

Schmierer, Bernhard, and Caroline S. Hill. 2007. “TGFbeta-SMAD Signal Transduction: Molecular Specificity and Functional Flexibility.” *Nature Reviews. Molecular Cell Biology* 8 (12): 970–82. doi:10.1038/nrm2297.

Schwank, Gerald, Bon-Kyoung Koo, Valentina Sasselli, Johanna F. Dekkers, Inha Heo, Turan Demircan, Nobuo Sasaki, et al. 2013. “Functional Repair of CFTR by CRISPR/Cas9 in Intestinal Stem Cell Organoids of Cystic Fibrosis Patients.” *Cell Stem Cell* 13 (6): 653–58. doi:10.1016/j.stem.2013.11.002.

Schwitalla, Sarah, Alexander A. Fingerle, Patrizia Cammareri, Tim Nebelsiek, Serkan I. Göktuna, Paul K. Ziegler, Ozge Canli, et al. 2013. “Intestinal Tumorigenesis Initiated by Dedifferentiation and Acquisition of Stem-Cell-like Properties.” *Cell* 152 (1–2): 25–38. doi:10.1016/j.cell.2012.12.012.

Selcuklu, S. Duygu, Mark T. A. Donoghue, and Charles Spillane. 2009. “miR-21 as a Key Regulator of Oncogenic Processes.” *Biochemical Society Transactions* 37 (Pt 4): 918–25. doi:10.1042/BST0370918.

Serra, Ryan W., Minggang Fang, Sung Mi Park, Lloyd Hutchinson, and Michael R. Green. 2014. “A KRAS-Directed Transcriptional Silencing Pathway That Mediates the CpG Island Methylator Phenotype.” *eLife* 3: e02313. doi:10.7554/eLife.02313.

Shao, Jinyi, M. Kay Washington, Romil Saxena, and Hongmiao Sheng. 2007. “Heterozygous Disruption of the PTEN Promotes Intestinal Neoplasia in APCmin/+ Mouse: Roles of Osteopontin.” *Carcinogenesis* 28 (12): 2476–83. doi:10.1093/carcin/bgm186.

Sheaffer, Karyn L., Rinho Kim, Reina Aoki, Ellen N. Elliott, Jonathan Schug, Lukas Burger, Dirk Schübeler, and Klaus H. Kaestner. 2014. “DNA Methylation Is Required for the Control of Stem Cell Differentiation in the Small Intestine.” *Genes & Development* 28 (6): 652–64. doi:10.1101/gad.230318.113.

Shen, Hui, and Peter W. Laird. 2013. “Interplay between the Cancer Genome and Epigenome.” *Cell* 153 (1): 38–55. doi:10.1016/j.cell.2013.03.008.

Shroyer, Noah F., Michael A. Helmrath, Vincent Y.-C. Wang, Barbara Antalffy, Susan J. Henning, and Huda Y. Zoghbi. 2007. “Intestine-Specific Ablation of Mouse Atonal Homolog 1 (Math1) Reveals a Role in Cellular Homeostasis.” *Gastroenterology* 132 (7): 2478–88. doi:10.1053/j.gastro.2007.03.047.

Snippert, Hugo J., Laurens G. van der Flier, Toshiro Sato, Johan H. van Es, Maaike van den Born, Carla Kroon-Veenboer, Nick Barker, et al. 2010. “Intestinal Crypt Homeostasis Results from Neutral Competition between Symmetrically Dividing Lgr5 Stem Cells.” *Cell* 143 (1): 134–44. doi:10.1016/j.cell.2010.09.016.

Sousa E Melo, Felipe de, Selcuk Colak, Joyce Buikhuisen, Jan Koster, Kate Cameron, Joan H. de Jong, Jurriaan B. Tuynman, et al. 2011. “Methylation of Cancer-Stem-Cell-Associated Wnt Target Genes Predicts Poor Prognosis in Colorectal Cancer Patients.” *Cell Stem Cell* 9 (5): 476–85. doi:10.1016/j.stem.2011.10.008.

Stamataki, Despina, Maxine Holder, Christine Hodgetts, Rosemary Jeffery, Emma Nye, Bradley Spencer-Dene, Douglas J. Winton, and Julian Lewis. 2011. “Delta1 Expression, Cell Cycle Exit, and Commitment to a Specific Secretory Fate Coincide within a Few Hours in the Mouse Intestinal Stem Cell System.” *PloS One* 6 (9): e24484. doi:10.1371/journal.pone.0024484.

Starr, Timothy K., Patricia M. Scott, Benjamin M. Marsh, Lei Zhao, Bich L. N. Than, M. Gerard O’Sullivan, Aaron L. Sarver, Adam J. Dupuy, David A. Largaespada, and Robert T. Cormier. 2011. “A Sleeping Beauty Transposon-Mediated Screen Identifies Murine Susceptibility Genes for Adenomatous Polyposis Coli (Apc)-Dependent Intestinal Tumorigenesis.” *Proceedings of the National Academy of Sciences of the United States of America* 108 (14): 5765–70. doi:10.1073/pnas.1018012108.

Subramanian, Aravind, Pablo Tamayo, Vamsi K. Mootha, Sayan Mukherjee, Benjamin L. Ebert, Michael A. Gillette, Amanda Paulovich, et al. 2005. “Gene Set Enrichment Analysis: A Knowledge-Based Approach for Interpreting Genome-Wide Expression Profiles.” *Proceedings of the National Academy of Sciences of the United States of America* 102 (43): 15545–50. doi:10.1073/pnas.0506580102.

Tahiliani, Mamta, Kian Peng Koh, Yinghua Shen, William A. Pastor, Hozefa Bandukwala, Yevgeny Brudno, Suneet Agarwal, et al. 2009. “Conversion of 5-Methylcytosine to 5-Hydroxymethylcytosine in Mammalian DNA by MLL Partner TET1.” *Science (New York, N.Y.)* 324 (5929): 930–35. doi:10.1126/science.1170116.

Tan, Jiaying, Morgan Jones, Haruhiko Koseki, Manabu Nakayama, Andrew G. Muntean, Ivan

Maillard, and Jay L. Hess. 2011. “CBX8, a Polycomb Group Protein, Is Essential for MLL-AF9-Induced Leukemogenesis.” *Cancer Cell* 20 (5): 563–75. doi:10.1016/j.ccr.2011.09.008.

Tanay, Amos, Anne H. O’Donnell, Marc Damelin, and Timothy H. Bestor. 2007. “Hyperconserved CpG Domains Underlie Polycomb-Binding Sites.” *Proceedings of the National Academy of Sciences of the United States of America* 104 (13): 5521–26. doi:10.1073/pnas.0609746104.

Tian, Hua, Brian Biehs, Søren Warming, Kevin G. Leong, Linda Rangell, Ophir D. Klein, and Frederic J. de Sauvage. 2011. “A Reserve Stem Cell Population in Small Intestine Renders Lgr5-Positive Cells Dispensable.” *Nature* 478 (7368): 255–59. doi:10.1038/nature10408.

Tsukita, S., M. Furuse, and M. Itoh. 2001. “Multifunctional Strands in Tight Junctions.” *Nature Reviews. Molecular Cell Biology* 2 (4): 285–93. doi:10.1038/35067088.

VanDussen, Kelli L., and Linda C. Samuelson. 2010. “Mouse Atonal Homolog 1 Directs Intestinal Progenitors to Secretory Cell rather than Absorptive Cell Fate.” *Developmental Biology* 346 (2): 215–23. doi:10.1016/j.ydbio.2010.07.026.

Vanuytsel, Tim, Stefania Senger, Alessio Fasano, and Terez Shea-Donohue. 2013. “Major Signaling Pathways in Intestinal Stem Cells.” *Biochimica Et Biophysica Acta* 1830 (2): 2410–26. doi:10.1016/j.bbagen.2012.08.006.

Vermeulen, Louis, Edward Morrissey, Maartje van der Heijden, Anna M. Nicholson, Andrea Sottoriva, Simon Buczacki, Richard Kemp, Simon Tavaré, and Douglas J. Winton. 2013. “Defining Stem Cell Dynamics in Models of Intestinal Tumor Initiation.” *Science (New York, N.Y.)* 342 (6161): 995–98. doi:10.1126/science.1243148.

Vermeulen, Louis, and Hugo J. Snippert. 2014. “Stem Cell Dynamics in Homeostasis and Cancer of the Intestine.” *Nature Reviews. Cancer* 14 (7): 468–80. doi:10.1038/nrc3744.

Vilar, Eduardo, and Stephen B. Gruber. 2010. “Microsatellite Instability in Colorectal Cancer-the Stable Evidence.” *Nature Reviews. Clinical Oncology* 7 (3): 153–62. doi:10.1038/nrclinonc.2009.237.

Vogelstein, B., E. R. Fearon, S. R. Hamilton, S. E. Kern, A. C. Preisinger, M. Leppert, Y. Nakamura, R. White, A. M. Smits, and J. L. Bos. 1988. “Genetic Alterations during Colorectal-Tumor Development.” *The New England Journal of Medicine* 319 (9): 525–32. doi:10.1056/NEJM198809013190901.

Volinia, Stefano, George A. Calin, Chang-Gong Liu, Stefan Ambs, Amelia Cimmino, Fabio Petrocca, Rosa Visone, et al. 2006. “A microRNA Expression Signature of Human Solid Tumors Defines Cancer Gene Targets.” *Proceedings of the National Academy of Sciences of the United States of America* 103 (7): 2257–61. doi:10.1073/pnas.0510565103.

Wade, P. A. 2001. “Methyl CpG-Binding Proteins and Transcriptional Repression.” *BioEssays: News and Reviews in Molecular, Cellular and Developmental Biology* 23 (12): 1131–37. doi:10.1002/bies.10008.

Westphalen, C. Benedikt, Samuel Asfaha, Yoku Hayakawa, Yoshihiro Takemoto, Dana J. Lukin, Andreas H. Nuber, Anna Brandtner, et al. 2014a. “Long-Lived Intestinal Tuft Cells Serve as Colon Cancer-Initiating Cells.” *The Journal of Clinical Investigation* 124 (3): 1283–95. doi:10.1172/JCI73434.

Whiffin, Nicola, Fay J. Hosking, Susan M. Farrington, Claire Palles, Sara E. Dobbins, Lina Zgaga, Amy Lloyd, et al. 2014. “Identification of Susceptibility Loci for Colorectal Cancer in a Genome-Wide Meta-Analysis.” *Human Molecular Genetics* 23 (17): 4729–37. doi:10.1093/hmg/ddu177.

Wu, J., J. P. Issa, J. Herman, D. E. Bassett, B. D. Nelkin, and S. B. Baylin. 1993. “Expression of an Exogenous Eukaryotic DNA Methyltransferase Gene Induces Transformation of NIH 3T3 Cells.” *Proceedings of the National Academy of Sciences of the United States of America* 90 (19): 8891–95.

Yamato, K., S. Hashimoto, T. Imamura, H. Uchida, N. Okahashi, T. Koseki, A. Ishisaki, et al. 2001. “Activation of the p21(CIP1/WAF1) Promoter by Bone Morphogenetic Protein-2 in Mouse B Lineage Cells.” *Oncogene* 20 (32): 4383–92.

Yang, Q., N. A. Bermingham, M. J. Finegold, and H. Y. Zoghbi. 2001. “Requirement of Math1 for Secretory Cell Lineage Commitment in the Mouse Intestine.” *Science (New York, N.Y.)* 294 (5549): 2155–58. doi:10.1126/science.1065718.

You, Jueng Soo, and Peter A. Jones. 2012. “Cancer Genetics and Epigenetics: Two Sides of the Same Coin?” *Cancer Cell* 22 (1): 9–20. doi:10.1016/j.ccr.2012.06.008.

Zeng, Xin, Keiko Tamai, Brad Doble, Shitao Li, He Huang, Raymond Habas, Heidi Okamura, Jim Woodgett, and Xi He. 2005. “A Dual-Kinase Mechanism for Wnt Co-Receptor Phosphorylation and Activation.” *Nature* 438 (7069): 873–77. doi:10.1038/nature04185.

Zheng, Yan, Patricia A. Valdez, Dimitry M. Danilenko, Yan Hu, Susan M. Sa, Qian Gong, Alexander R. Abbas, et al. 2008. “Interleukin-22 Mediates Early Host Defense against Attaching and Effacing Bacterial Pathogens.” *Nature Medicine* 14 (3): 282–89. doi:10.1038/nm1720.

Zhu, Y., J. A. Richardson, L. F. Parada, and J. M. Graff. 1998. “Smad3 Mutant Mice Develop Metastatic Colorectal Cancer.” *Cell* 94 (6): 703–14.

Zwijsen, An, Kristin Verschueren, and Danny Huylebroeck. 2003. “New Intracellular Components of Bone Morphogenetic Protein/Smad Signaling Cascades.” *FEBS Letters* 546 (1): 133–39.

TABLE OF CONTENTS

FIGURES:

17. **MicroRNA biogenesis and function.**

18. **The epigenetic progenitor model of cancer development.**

19. ***Apc* loss results in increased proliferation and *de novo* differentiation but not in de-differentiation of intestinal epithelial cells of $Apc^{LoxP/LoxP}$; $VillinCre^{ERT2}$ mice.**

20. **The hypertrophic proliferative compartment upon the deletion of *Apc* in the intestinal epithelium.**

21. **Wnt activation in $Lgr5^{+}$ stem cells leads to the formation of a hypertrophic GFP-positive compartment.**

22. **The GFP rarely co-localizes with markers of the post-mitotic cell populations typically found at the bottom of the crypt.**

23. **Expansion of the CBC stem compartment 15 days after the deletion of *Apc* in $Lgr5^{+}$ cells.**

24. **Alteration in the cell cycle dynamics of GFP^{+} cells 15 days after the deletion of *Apc* in Lgr5+ cells.**

25. **Fluorescent-activated cell sorting of GFP-positive cells from *Lgr5-EGFP-ires-Cre* epithelia.**

26. **Progressive alteration of the gene expression profiles in GFP^{+} cells.**

27. **Altered gene expression in response to the loss of one *Apc* allele in $Lgr5^{+}$ cells and their immediate progeny.**

28. **Differentially methylated regions in WT and KO $Lgr5^{+}$ cells and their immediate progeny.**

29. **Altered gene expression in response to the loss of function of *Apc* in $Lgr5^{+}$ cells and their progeny.**

30. **Methylation of a representative IAP region in $Apc^{+/+}$ and $Apc^{-/-}$ $Lgr5^{+}$ cells and their immediate progeny.**

31. **Methylation and expression of *Smad6* in $Apc^{+/+}$ and $Apc^{-/-}$ $Lgr5^{+}$ cells and their immediate progeny.**

32. **Translocation patterns of phospho-Smad 1/5/8 effectors in the *Apc*$^{+/+}$ and *Apc*$^{LoxP/LoxP}$; *Villin-Cre*^{ERT2} at day 6 post-tamoxifen injection.**

33. **morphologic changes upon *Apc* deletion in intestinal organotypic cultures and effects of Dnmt3b inhibition.**

34. **Dnmt3b inhibition increases the epithelial responsiveness to differentiation stimuli.**

35. **Lentiviral-mediated tranduction of Dnmt3a and Dnmt3b specific sh-RNA results in heterogeneous knock-down in intestinal *Villin-Cre*^{ERT2} organoids.**

36. **Proliferative rate in response to Dnmt3a/Dnmt3b knockdown in organotypic *Apc*$^{LoxP/LoxP}$,*Villin-Cre*^{ERT2} cultures treated with 4-hydroxy-tamoxifen.**

37. **Intestinal tumor burden in 16 weeks-old co-isogenic mice.**

38. **Schematic representation of the breeding outputs showing the non-random segregation of the unknown genetic polymorphism.**

39. **Intestinal tumor burden in 6 week-old co-isogenic mice.**

40. **Non-genetic variable relative risk.**

41. **verification of the tumor-free samples selected for *–omic* profiling. qPCR results show comparable expression of the WT and truncated forms of *Apc* and *Myc* in *Apc*$^{\Delta 14/+}$ mice.**

42. **Relative enrichment of epithelial and mesenchymal fractions.**

43. **CpG methylation extent as quantified by RRBS (left) in regions showing a consensus (no overalp between the two groups) and qPCR quantification of the transcription of the genes in close proximity to the DMRs (16 weeks).**

44. **Heatmap and hierarchical clustering analysis of 73 differentially expressed genes in the epithelial fraction of poorly and highly susceptible adult individuals.**

45. **Weight evolution after the intestinal resection. The % of the initial weight is shown at different time points post-resection performed on day 0.**

TABLES:

LIST OF ABBREVIATIONS

5-Aza: 5-azacytidine

7-AAD: 7-Amino-Actinomycin.

BMP: bone morphogenetic factor.

bp: base pair.

BrdU: Bromodeoxyuridine.

CBC: crypt base columnar cells.

CIMP: CpG island methylator phenotype.

CIN: chromosome instability.

CMS: consortium molecular subtypes.

CpG: CpG dinucleotide.

CRC: colorectal cancer.

DMEM: Dulbecco's modified eagle medium.

DNA: deoxyribonucleic acid.

DNMT: DNA methyltransferase

EGF: epidermal growth factor.

EDTA: Ethylenediaminetetraacetic acid.

FDA: food and drugs administration.

GFP: green fluorescent protein.

GLP: glucagon-like peptide.

GIP: gastric-inhibitory peptide.

GO: gene ontology.

GSEA: gene set enrichment analysis.

HAT: histone acetylase transferase.

HBSS: Hank's balanced salt solution.

HCl: hydrochloric acid.

HDAC: histone acetyltransferase.

HET: heterozygous.

HNPCC: hereditary non polyposis colorectal cancer

ISC: intestinal stem cell.

Kb: kilobase.

KI: knock-in.

KO: knock-out.

LOH: loss of heterozygosity.

LOI: loss of imprinting.

lncRNA: long non-coding RNA

mRNA: messanger RNA

miRNA: micro-RNA

MMR: mismatch repair.

MSI: micro-satellite instability.

NGS: next generation sequencing.

NICD: Notch intracellular domain.

NLRs: NOD-like receptors.

PAMPs: pathogen-associated molecular patterns.

PBS: phosphate buffered saline.

PCR: polymerase chain reaction

PE: phycoerythrin.

PRRs: pattern recognition receptors.

PI: propidium iodide.

RELM: Resistin-like molecule.

RNA: ribonucleic acid.

RNA-i: RNA interference

RNA-seq: RNA sequencening.

RRBS: reduced representation bisulfite sequencing.

RT: reverse transcription

SEM: standard error of the mean.

shRNA: short-hairpin RNA.

TF: transcription factor.

TG: transgenic.

TGF-β: transforming growth factor beta

TCGA: the cancer genome atlas.

TLRs: toll-like receptors.

WNT: Wingless-related integration site.

WGBS: whole genome bisulfite sequencing.

WT: wild-type.

Dynamique de la méthylation d'ADN et sa caractérisation fonctionnelle durant les phases précoces de la tumorigénèse intestinale

Le cancer colorectal représente la deuxième cause de mortalité par cancer en France. Dans l'intestin, l'initiation et la progression tumorale sont corrélées à l'accumulation séquentielle de mutations génétiques et épigénétiques au niveau du compartiment de renouvellement de l'épithélium. Ces altérations ont pour conséquence une croissance incontrôlée de l'épithélium et, à terme, la formation de lésions cancéreuses. En tenant compte du nombre croissant de cas de cancers colorectaux, la découverte de facteurs de prédisposition de cette pathologie reste d'un intérêt majeur. Les données de séquençage du génome humain ne suffisant pas à expliquer la prévalence de la maladie à l'échelle de la population, nous nous intéressons aux mécanismes permettant le contrôle de l'expression de certains gènes : les mécanismes épigénétiques. Dans notre équipe nous disposons de modèles animaux génétiquement modifiés nous permettant d'étudier, dans des conditions proches de la pathologie humaine, les phases précoces de l'initiation tumorale. Ces souris, bien que génétiquement identiques, développeront pourtant un nombre de tumeurs intestinales très variables. En comparant les profils moléculaires de souris développant peu ou beaucoup de tumeurs intestinales, nous souhaitons mettre en évidence les facteurs épigénétiques mis en jeu pour expliquer cette différence de susceptibilité à la tumorigenèse. Pour ce faire, nous avons mis en place une stratégie visant à prélever un échantillon intestinal, par chirurgie, sur de jeunes souris qui ont ensuite été suivies jusqu'à l'âge adulte et à l'apparition des tumeurs. Cette stratégie innovante nous a permis de corréler les profils d'expression et de methylation d'ADN d'intestins développant peu ou beaucoup de tumeurs, ouvrant la possibilité de disposer de nouveaux marqueurs prédictifs quant aux chances de développer un cancer. Ces données sont complétées par une étude sur les conséquences de la perte du gène suppresseur de tumeur Apc, un gène couramment muté dans les cancers colorectaux humain. À l'aide de modèles de souris d'invalidation inductible, nous avons déterminé les conséquences de la perte d'Apc sur les profils de méthylation de l'ADN des cellules souches intestinales, et leur capacité à initier une tumeur. L'ensemble de ces différents projets développés dans le cadre de ma thèse nous ont permis de mieux comprendre les mécanismes cellulaires liés à la prédisposition et à l'initiation tumorale et de proposer des nouvelles stratégies diagnostiques et d'évaluation du risque individuel.

DNA methylation dynamics and its functional impact during the early stages of intestinal tumorigenesis

Cancer initiation and progression represent the outcome of the progressive accumulation of genetic and epigenetic alterations. Global changes in the epigenome are now considered as a common hallmark of malignancies. However, most of our present knowledge represents the result of the comparison between fully established malignancies and their surrounding healthy tissue. Such comparison is not informative about the epigenetic contribution to the very early steps of cancer onset. By performing DNA methylation and gene expression profiling of the intestinal epithelium of relevant in vivo models we aim at shedding light on the correlation between the interindividual epigenetic polymorphisms within the population and the relative risk to develop malignancies, and establish the existence of a molecular signature associated with an increased susceptibility to develop intestinal cancer. Our results confirm that a considerable degree in the variability associated to cancer susceptibility cannot be ascribed to major genetic changes and that such heterogeneity seems to correlate with distinct molecular profiles associated to classes of poorly or highly susceptible isogenic animals.